Determining the effects of peatland restoration on carbon dioxide exchange and potential for climate change mitigation

Submitted by Naomi Le Feuvre Gatis to the University of Exeter

as a thesis for the degree of

Doctor of Philosophy in Geography

In March 2015

I certify that all material in this thesis which is not my own work has been identified and that no material has previously been submitted and approved for the award of a degree by this or any other University

Signature:…….

ACKNOWLEDGEMENTS

I would like to thank my supervisors who have provided guidance and support sharing their knowledge whenever it has been needed; Karen Anderson for her enthusiasm and ability to help me tease out the important themes from a jumbled mess of ideas; Iain Hartley whose attention to detail and in-depth knowledge have pushed me to attain the highest standards of scientific rigour; Richard Brazier for reminding me of the bigger picture and David Smith for his extensive knowledge of Exmoor and peatland restoration.

I would also like to thank my fellow postgraduate research students and associate research fellows, in particular Josie Ashe, Mike Bell, Pia Benaud, Andrew Cunliffe, Emilie Grand-Clement, Dave Luscombe and Alan Puttock. The help, both intellectual and physical, support and friendship provided by this group of people has lessened the burden (in more ways than one) and provided many good memories.

This thesis would not have been possible without the funding provided by South West Water as part of the Exmoor and Dartmoor Mires Projects and for that I am grateful. Working as part of a larger project I have been lucky enough to receive knowledge and support from colleagues working for the Exmoor Mires Project, Dartmoor Mires Project, Environment Agency, Natural England, English Heritage, Exmoor National Park and Dartmoor National Park.

Finally, I would like to thank James and my family without whom it would have been impossible.

ABSTRACT

Over the last millennium peatlands have accumulated significant carbon stores. Drainage for agricultural use has been widespread and has altered the functioning of these mires: shifting them towards carbon release. Recently, in recognition of the range of ecosystem services derived from these landscapes peatland restoration projects have been initiated. Carbon storage is often cited amongst the aims of these projects, especially since the inclusion of rewetting wetlands in the Kyoto Protocol. However, little is known about the effects of ditch blocking on CO_2 fluxes, particularly in *Molinia caerulea* dominated peatlands, a species common on degraded peatlands which tolerates a range of water table depths.

This thesis aims firstly to quantify CO_2 fluxes from a drained *Molinia caerulea* dominated blanket bog and to improve understanding of the temporal and spatial controls on these fluxes and secondly, to quantify the immediate effects of ditch blocking. Closed chamber measurements of net ecosystem exchange and partitioned below-ground respiration from control-restored paired sites were collected over the growing seasons immediately pre- (2012) and post-restoration (2013/2014). These flux data were coupled with remotely sensed data quantifying vegetation phenology and structure with a fine resolution (daily/cm) over large extents (annual/catchment).

Although temporal variation in water table depth was not related to CO_2 fluxes, the seasonal average related to vegetation composition suggesting raising water tables may promote a change in vegetation composition within these species-poor ecosystems. The distribution of water table depths, vegetation composition and CO_2 fluxes did not vary with proximity to drainage ditches despite their prominence. An empirical model suggests in a drained state these peatlands are CO_2 sources, indicating carbon previously accumulated is gradually being lost.

Data suggest restoration does not always significantly affect water tables and consequently CO_2 fluxes in the short-term. Where shallower water tables were maintained during dry conditions photosynthesis decreased and heterotrophic

respiration increased: enhancing carbon release. Research undertaken during atypical weather has been unable to determine if restoration will be able to raise water tables sufficiently to protect the existing peat store and promote the vegetation change required to reinstate CO_2 sequestration in the longer-term.

CONTENTS

Acknowledgements 3

Abstract 5

Contents 7

List of Tables 13

List Of Figures 18

List of Accompanying Material 30

1 Introduction and Rationale 33

1.1 Thesis Structure 35

1.1.1 Theme 1: Temporal and Spatial Controls on CO_2 Fluxes in a Drained *Molinia caerulea* Dominated Peatland 35

1.1.2 Theme 2: Short-term Effects of Ditch Blocking on CO_2 Fluxes in a Drained *Molinia caerulea* Dominated Peatland 37

1.1.3 Hypotheses 39

1.2 Statement of Contribution 40

2 Literature Review 45

2.1 Peat and Peatlands 45

2.1.1 What is Peat? 45

2.1.2 Peatlands 46

2.1.3 Ombrotrophic Blanket Bogs 48

2.1.4 *Sphagnum* Peat: Structure and Function of a Layered System 50

2.1.5 Damaged *Sphagnum* Peat: Structure and Function of a Haplotelmic Bog 51

2.1.6 *Sphagnum* Cycle and Vascular Plant Cycle 52

2.1.7 Global Warming Potential 53

2.2 Peatland Structure 54

2.2.1 Spatial Hierarchy 54

2.2.2 Microtope of a Damaged Peatland 57

2.3 Peat: a Valuable but Vulnerable Carbon Store 59

2.4 Current Knowledge on the Effects of Drainage and Ditch-Blocking on Water Table Depths, Vegetation Composition and CO_2 Fluxes 61
2.4.1 Drainage 61
2.4.2 Ditch Blocking 64
2.5 Monitoring Approaches 68
2.5.1 Carbon Dioxide Fluxes in the Field 68
2.5.2 Vegetation Phenology, Biomass, Structure and Composition 73
2.6 Summary 80
3 Site Description and Overview of Experimental Design 83
3.1 Catchment Selection and Location 83
3.2 Within-Site Selection and Experimental Design 86
3.3 Summary 98
4 MODIS Vegetation Products; useful measures of vegetation phenology and peatland CO_2 exchange 99
4.1 Abstract 99
4.2 Highlights 100
4.3 Key Words 101
4.4 Introduction 101
4.5 Materials and Methods 103
4.5.1 Site Description 103
4.5.2 Digital Camera 103
4.5.3 Terra MODIS 106
4.5.4 Ancillary measurements 110
4.5.5 Analysis 110
4.6 Results 112
4.6.1 Phenology of 2013 112
4.6.2 Comparing Vegetation Products to Carbon Dioxide Fluxes 120
4.7 Discussion 121
4.7.1 MODIS Vegetation Products as Measures of Phenology 121
4.7.2 Vegetation Products as Proxies for Net Ecosystem Exchange 126

4.8 Conclusion 128
4.9 Acknowledgements 129
5 Temporal variability in growing season CO_2 fluxes in a drained *Molinia caerulea* dominated peatland. 131
5.1 Abstract 131
5.2 Introduction 132
5.3 Method 133
5.3.1 Study Sites 133
5.3.2 Gas Flux Measurements 136
5.3.3 Vegetation Phenology Proxy 138
5.3.4 Statistical Analysis 139
5.3.5 Net Ecosystem Exchange Modelling 140
5.4 Results 141
5.4.1 Environmental Variables 141
5.4.2 Seasonality 144
5.4.3 Drivers of Temporal Variation 148
5.4.4 Modelled Net Ecosystem Exchange 155
5.5 Discussion 157
5.5.1 Seasonal Variation 157
5.5.2 Drivers of Temporal Variation in CO_2 Fluxes 162
5.6 Conclusion 169
5.7 Acknowledgments 170
6 The effect of drainage ditches on vegetation diversity and CO_2 fluxes in a *Molinia caerulea* dominated peatland. 171
6.1 Abstract 171
6.2 Keywords 172
6.3 Introduction 172
6.4 Study Sites 173
6.5 Method 177
6.5.1 Net Ecosystem Exchange Measurements 177

6.5.2 Vegetation Greenness 177
6.5.3 CO_2 Exchange Measurements and Modelling 178
6.5.4 Soil CO_2 Efflux Measurements 179
6.5.5 Vegetation Composition and Primary Productivity 181
6.5.6 Statistical Analysis 182
6.6 Results 183
6.6.1 Spatial Variation with Distance from a Drainage Ditch 183
6.6.2 Spatial Variation between Sites 189
6.6.3 Drivers of Spatial Variability 190
6.7 Discussion 193
6.7.1 Drainage Ditches, Water Table Depths and Vegetation 193
6.7.2 Site, Water Table Depths and Vegetation 194
6.7.3 Spatial Variability of CO_2 Fluxes 195
6.8 Conclusion 199
6.9 Acknowledgements 200
7 A new cost- and time-effective method for measuring fine scale vegetation structure in complex landscapes using ground and UAV based digital images 201
7.1 Abstract 201
7.2 Keywords 202
7.3 Introduction 202
7.3.1 Vegetation Structure at a Plot and Landscape Scale 202
7.3.2 Vegetation Structure and Its Environment 204
7.4 Materials and Methods 205
7.4.1 Study Site 205
7.4.2 Plot Scale Image Collection 207
7.4.3 Plot Scale Image Processing 209
7.4.4 Landscape Scale Image Collection and Processing 210
7.4.5 Ground Validation 212
7.4.6 Linking Structural Characteristics to Environmental Conditions and CO_2 Fluxes 213

7.5 Results 214
7.5.1 The Effect of the Number of Photographs on the Data Content of Plot Scale Point Clouds derived using SfM 214
7.5.2 Plot Scale Digital Surface Models of Tussock Structure 220
7.5.3 The Effect of Number of Photographs on the Coverage of SfM Derived Point Clouds at a Landscape Extent 221
7.5.4 Landscape Scale Digital Surface Models Derived from UAV Images 224
7.5.5 Structural Characteristics at a Landscape Extent Derived from UAV-Based Images 230
7.5.6 Relationship Between Vegetation Structure and Environmental Conditions 232
7.6 Discussion 235
7.6.1 Plot Scale Digital Surface Models Derived using Ground Based images and SfM 235
7.6.2 Plot Scale Structural Characteristics Derived using SfM 237
7.6.3 Landscape Extent Digital Surface Models Derived using UAV-based images and SfM 238
7.6.4 Fine Scale Structural Characteristics at a Landscape Extent 242
7.6.5 Tussock Structure and its Environment 244
7.7 Conclusion 246
7.8 Acknowledgements 248
8 Short-term effects of ecohydrological restoration on CO_2 fluxes in a drained *Molinia caerulea* dominated peatland 249
8.1 Abstract 249
8.2 Keywords 250
8.3 Introduction 250
8.4 Method 254
8.4.1 Study Sites 254
8.4.2 Experimental Design 255
8.4.3 Measurements and Data Analysis 256
8.4.4 Gas Flux Measurements 256

8.4.5 Vegetation Measurements 258
8.4.6 Ancillary Data 259
8.4.7 Statistical Analysis 260
8.5 Results 261
8.5.1 Hypothesis 1: The Effect of Restoration on Water Table Depths through Time 262
8.5.2 Hypothesis 2: The Effect of Restoration on CO_2 Fluxes through Time . 266
8.5.3 Hypothesis 3: The Spatial Effect of Restoration on Water Table Depths 273
8.5.4 Hypothesis 4: The Spatial Effect of Restoration on CO_2 Fluxes 277
8.6 Discussion 280
8.6.1 Hypothesis 1: The Effect of Restoration on Water Table Depths through Time 280
8.6.2 Hypothesis 2: The Effect of Restoration on CO_2 Fluxes through Time . 281
8.6.3 Hypothesis 3: The Spatial Effect of Restoration on Water Table Depths 285
8.6.4 Hypothesis 4: The Spatial Effect of Restoration on CO_2 Fluxes 286
8.7 Conclusion 288
8.8 Acknowledgments 289
9 General Discussion 291
9.1 Remote Sensing of Vegetation Phenology and Structure 292
9.2 Spatial and Temporal Controls on CO_2 Fluxes in a Degraded Peatland 295
9.3 Effect of Restoration on CO_2 Fluxes 299
9.4 Landscape Management Implications 302
9.5 Limitations 304
9.6 Further Work 307
10 Conclusion 311
11 Supplementary Material 313
12 Bibliography 335

LIST OF TABLES

Table 3.1 Timeline of key milestones related to this project. 97

Table 4.1 Spatial and temporal resolution of the MODIS products downloaded and the number of time-steps available between 1st Jan 2012 and 24th Oct 2013. 107

Table 4.2 Effect of data processing of Green Red Vegetation Index thresholds derived from the time-lapse camera. 114

Table 4.3. Summary of phenological measures, day of year for start, peak and end of growth and length of season. Number in brackets indicate the number of days difference between phenological measures, measured with Green-Red Vegetation Index derived from the digital camera estimated using the half-maximum method (first number) and the zero threshold method (second number) and those estimated using MODIS vegetation products. Days Out is the average number of days difference for start, peak and end of growth. Pearson's correlation coefficient between GRVI and the other vegetation products is shown ($p<0.001$) n=187. 119

Table 5.1 Site properties of experimental sites at Aclands and Spooners..... 136

Table 5.2 Comparison between seasonal and annual mean temperature (°C), total rainfall (mm) and sunshine (hours) for 2012, 2013, 2014 and the 30 year regional (Southwest England) mean (1982-2011) (UK Meteorological Office 2015)..... 142

Table 5.3 Input variables and results for a stepwise multiple linear regression with photosynthesis at 600 µmol Photons m^{-2} s^{-1} (P_{G600}) and ecosystem respiration (µgC m^{-2} s^{-1}) at Aclands and Spooners catchments. Variable is the one selected for the model. No significant two-variable models occurred. The proportion of variance (r^2) and the significance of the relationships (p) are shown. All relationships were positive. 151

Table 5.4 Seasonal Q_{10} and mean respiration at 10 °C (µmol m^{-2} s^{-1}) (R_{10}) values for total, heterotrophic and autotrophic respiration at each site. Regression coefficient (r^2) and significance (p) of exponential relationships between soil temperature at 5 cm (°C) and total,

heterotrophic and autotrophic respiration at each site. n is the number of sample days. 152

Table 5.5 Relationships between total, heterotrophic and autotrophic respiration as measured and corrected to 10 °C and environmental variables (soil temperature at 5 cm (°C) (T5), water table depth (cm below surface) (WTD), fraction of photosynthetically active radiation absorbed (fPAR) and normalised difference vegetation index (NDVI)). Regression coefficient (r^2) and significance (p) of quadratic, (Quad), exponential (Exp) or linear (Lin) relationships. Only relationships with $p<0.050$ are shown. + indicates a positive relationship, – a negative relationship. 153

Table 5.6 Coefficient estimates and standard errors of coefficients used in annual net ecosystem exchange model (Equation 5.5) 156

Table 5.7 Modelled annual net ecosystem exchange and maximum monthly CO_2 uptake and release, the month is indicated. Values in brackets are the 95 % confidence intervals..... 157

Table 6.1 Site properties of experimental sites at Aclands and Spooners..... 175

Table 6.2 Mean and standard error (in brackets) distance from the ditch (m)water table depth (cm below surface), percentage coverage of *Molinia caerulea*, leaf litter and non-*Molinia* species, annual net primary productivity (ANPP), species richness and Inverse Simpson diversity index for different sites and proportional distances from the ditch. 184

Table 6.3 Two-way ANOVA for mean water table depth, vegetation indices, peat depth and modelled ecosystem respiration (R_{Eco}) and photosynthesis at 600 µmol Photons $m^{-2}s^{-1}$ (P_{G600}) (µgC m^{-2} s^{-1}) at all locations (n=36) with site, proportional distance from the ditch (Plot) and proportional distance from the ditch nested within site as between subject variables. SS is sum of squares, df degrees of freedom, MS mean sum of squares, F the F-ratio and p the significance. Shaded dark grey where $p<0.050$. 186

Table 6.4 Repeated measures ANOVA results for total, heterotrophic and autotrophic respiration adjusted to 10 °C. Proportional distance from

the ditch (Plot) and site were between subject effects and sample round (Time) was a within subject effect. SS is sum of squares, df degrees of freedom, MS mean sum of squares, F the F-ratio and p the significance. Shaded dark grey where p<0.050. 187

Table 6.5 Regression coefficients (r^2) and significance (in brackets) of linear regression between water table depth (cm below-ground surface) and annual net primary productivity (ANPP), peat thickness and vegetation indices. Regression coefficients (r^2) and significance (in brackets) of linear regression between modelled photosynthesis at 600 µmol Photons m^{-2} s^{-1} (P_{G600}), modelled ecosystem respiration (R_{Eco}), total (R_{Tot}), heterotrophic (R_{Het}) and autotrophic (R_{Aut}) below-ground respiration at 10 °C and water table depth, annual net primary productivity (ANPP), peat thickness and vegetation indices (n=36). Shaded dark grey where p<0.050. + positive covariance – negative covariance. 192

Table 7.1 Description of images and number of images input in each VisualSfM run for plot S3R1 and resultant outcomes 216

Table 7.2 Images collected for each vegetated plot, number of images used to make point clouds by VisualSfM, root mean square error (RMSE) of georectified point cloud and average density of points within the area of interest. Locations shaded gravy where less than 120 images input..... 219

Table 7.3 Root mean squared errors (RMSE), Pearson Correlation Coefficients and significance (p) between elevation (meters above sea level) measured using a DGPS and modelled using 0.5 m resolution LiDAR data, 0.02, 0.05, 0.10 and 0.275 m resolution DSMs derived from digital images using VisualSfM. A total of 71 tussock tops and 284 inter tussock locations were measured..... 228

Table 7.4 Comparison between mean tussock height (m), standard deviation from mean (Stdev) (m) and root mean square error (RMSE) between tussock heights derived from UAV digital images at 0.02, 0.05, 0.1 and 0.275 m grid resolution and measured tussock heights. Percentage of tussocks where the height was overestimated, Pearson's Correlation coefficient and significance (p). n=71. 231

Table 7.5 Comparison between ecosystem respiration (µgC m^{-2} s^{-1}) estimated from tussock heights derived from UAV digital images at 0.02, 0.05, 0.10 and 0.275 m grid resolution and validation data modelled for a temperature of 12 °C based on empirically derived parameters. RMSE is the root mean square error. 235

Table 8.1 Significance of T-tests between pre- and post-restoration at Aclands and ANOVA between pre-, 1 year post and 2 years post-restoration at Spooners within proportional distances (⅛, ¼, ½) from the ditch in each catchment. Shaded dark grey where p<0.050. 278

Table 8.2 Average and standard error (in brackets) of species coverage (percent) by site and proportional distance from the ditch (plot). # coverage of 1 % at one location. 279

Table 11.1 Number of sample locations and number of net ecosystem exchange measurements collected in dark and light (full and shaded) condition at Aclands and Spooners on a given date and sample round. # Excluded as only three out of nine locations sampled. * excluded when focussing on growing season. 315

Table 11.2 Number of sample locations where clipped (2 replicates) and clipped and trenched (2 replicates) measurements were collected at Aclands and Spooners on a given date and sample round. # data excluded as treatment effects apparent. *Data excluded as levels of detection less than uncertainty within a plot. 316

Table 11.3 Reported photosynthesis and ecosystem respiration values (µgC m^{-2} s^{-1}). Results from this study are shaded grey. CC closed chamber, EC eddy covariance 317

Table 11.4 Reported total and heterotrophic below-ground respiration rates (µmol m^{-2} s^{-1}). Results from this study are shaded grey. 319

Table 11.5 Reported net ecosystem exchange values (tonnes ha^{-1} yr^{-1}), positive values indicate a source of CO_2 to the atmosphere, negative values a sink. Results from this study are shaded grey 321

Table 11.6 Location specific empirically derived coefficients for R_{Eco} and P_{G600} models. Regression coefficient (r^2), number of data points (n) parameters: P1 (µgC m^{-2} s^{-1}), K1 (µmol Photons m^{-2} s^{-1}), a

(dimensionless), b ($°C^{-1}$), c (dimensionless), d ($°C^{-1}$), e (dimensionless), T_{Opt} (°C) and T_{Tol} (°C). 324
Table 11.7 Seasonal Q_{10} and mean respiration at 10 °C (R_{10}) values for total, heterotrophic and autotrophic respiration at each site. Regression coefficient (r_2) and significance (p) of exponential relationships between soil temperature at 5 cm (°C) and total, heterotrophic and autotrophic respiration at each site. n is the number of sample days. 326
Table 11.8 Average vegetation composition (% coverage) and standard errors (in brackets) by proportional distance from the ditch and site. Overall mean, minimum (min), maximum (max) and number of occurrences (n). # cover of 1 % at a single location..... 327

LIST OF FIGURES

Figure 2.1 Global distribution of mires, mangroves and wetlands in bays and lagoons (Lappalainen 1996). 47

Figure 2.2. Distribution of peat and peaty soils in the UK (JNCC 2011). 49

Figure 2.3. The structure and function model for peatlands. Water table represented by the dashed line. Adapted from (Clymo 1992). 50

Figure 2.4. Peatlands as hierarchical complex systems. State, flux and forcing variables are arranged in order of increasing temporal scale and spatial extent. Boxes identify the spatial hierarchy of landforms. Solid arrows denote boundary conditions (constraints) and dashed arrows internal driving variables and external forcing at particular temporal scales (Belyea and Baird 2006). 55

Figure 2.5 The effect of a falling water table and drying acrotelm on the microtope and vegetation composition of a blanket mire. First the microtope becomes smooth with the loss of hollows and associated species (green area). Then hummock species (red area) (e.g. *Sphagnum capillifolim)* become dominant and form a smooth carpet underlying dwarf shrubs. Finally *Sphagnum* species are completely replaced by non-*Sphagnum* mosses, dwarf shrubs and tussock forming graminoids (Lindsay 2010). 58

Figure 2.6 Vegetation profiles of wet-heath (a), drier Molinietum (b) and wetter Molinietum (c) (Rutter 1955). 59

Figure 3.1 Location of study areas within Southwest England (a). Aclands lies to the west and Spooners to the east (b). (Ordnance Survey 2008a, d). 84

Figure 3.2 Location of control and restored paired sites within a, Aclands and b, Spooners. Plots were located ⅛, ¼ and ½ the distance between adjacent ditches. (Ordnance Survey 2008b, c) 87

Figure 3.3 Aclands catchment in July 2012, pre-restoration. Looking north from site A1R across the main drainage channel towards sites A2R, A3R and A3C. The water table depth, flow and quality monitoring equipment can also be seen. Of note is the dominance of *Molinia caerulea* across the catchment. 88

Figure 3.4 Spooners catchment in May 2012, pre-restoration. Looking northeast from site S3R towards sites S2 and S1. Again note the dominance of *Molinia caerulea* across the catchment and the volume of leaf litter and dormant vegetation. 89
Figure 3.5 Looking up-gradient along a straight, down-slope hand-dug ditch at site A2C prior to equipment installation (March 2012). The ditch is 38 cm wide and 24 cm deep but not easily visible within the landscape apart from in late winter when the vegetation is dormant and flattened by winter rain and wind. 89
Figure 3.6 Visible aerial photograph collected from a QuestUAV fixed wing aircraft at approximately 100 m altitude over Aclands catchment in March 2012. a, Straight hand-dug up-slope ditches (typically <50 cm) running from top left to bottom right. Patches of green *Juncus sp*. typical of more nutrient rich flushes can be seen. b, Shallower (15-20 cm) Herringbone hand-dug ditches and a mauve patch of wet heath species on the watershed dominated by *Calluna vulgaris* and *Erica tetralix* with some *Sphagnum sp. and Eriophorum vaginatum.* 90
Figure 3.7 Visible aerial photograph collected from a QuestUAV fixed wing aircraft at approximately 100 m altitude over Spooners catchment in March 2012. Straight hand-dug up-slope ditches (typically <50 cm) and rectangular peat cuttings can be seen. 91
Figure 3.8 Arrangement of plots at ⅛, ¼ and ½ the distance between adjacent ditches perpendicular to the ditch at site A1C following installation in March 2012 looking away from the ditch. 92
Figure 3.9 Equipment permanently installed at each location in March 2012… 93
Figure 3.10 Full-light net ecosystem exchange measurement in progress (shade cloths not shown) September 2014. 94
Figure 3.11 Measurement of below-ground heterotrophic respiration from a trenched and clipped soil collar (a) and below-ground total respiration from a clipped soil collar (b), September 2014. 94
Figure 3.12 Tripod set up for downward facing images used to derive greenness excess index between 20/06/2012 and 25/10/2012..... 95
Figure 3.13 Photograph of Brinno TLC time-lapse camera *in situ* at Spooners, installed in April 2013. 95

Figure 3.14 One week following restoration at Spooners site S2R. The peat dams can be seen with small pools of water up-gradient. 96
Figure 3.15 Visible aerial photograph collected from a QuestUAV fixed wing aircraft at approximately 100 m altitude over Spooners catchment in November 2014. The pattern of regular ditch blocks using peat dams can be seen. The approximate location of site S2R is marked 96
Figure 4.1 a, Location of study site within the UK and Exmoor National Park (inset). Location of time-lapse camera and extent of the 250 m, 500 m and 1000 m MODIS pixels. b, Aerial photo of the pixel extent. 1:25000 Ordnance Survey Map (Ordnance Survey 2008d)..... 105
Figure 4.2 Series of images of the Region of Interest used to calculate average red and green digital numbers taken with a digital camera. Images are from 32, 24, 16, 8 and 0 days before and after the start, peak and end of growth estimated using the half-maximum and zero-threshold methods. Day of Year indicated on each image. 112
Figure 4.3 GRVI Data Processing. Third order Fourier Series fitted to raw Green Red Vegetation Index (GRVI) data, points outside the 95% confidence interval were excluded (a). Data gaps were filled by linear interpolation and an 8-day moving average calculated (b). Comparison of 8-day moving average calculated from raw GRVI data, raw data with points outside the 95 % confidence interval excluded and data with gaps filled by linear interpolation (c)..... 113
Figure 4.4 MODIS Data Processing. Third order Fourier series with 99 % confidence interval fitted to weighted MODIS fPAR data, good quality data weighted 1 and poor quality data weighted 0 (a). Data outside the 99 % confidence interval was excluded from further analysis. Third order Fourier series fitted to non-weighted MODIS fPAR8 data (b). 115
Figure 4.5 Temporal variation in eight day average Green Red Vegetation Index (GRVI) and air temperature over the 2013 growing season. A total of 190 north facing images taken at solar noon were collected between 23 Apr 2013 and 29 Oct 2013, 23 of these images were excluded as outliers and replaced by linear interpolation prior to averaging. 116

Figure 4.6 Time series of digital camera measured Green Red Vegetation Index and MODIS derived Vegetation Products scaled to percentage of maximum value to allow for direct comparison. 118

Figure 4.7 Relationship between Net Ecosystem Exchange (NEE) at 600 µmol Photons m^{-2} s^{-1} (µgC m^{-2} s^{-1}) and digital camera Green Red Vegetation Index, MODIS derived Vegetation Products and air temperature (° C). Linear correlations shown are with solid lines where p<0.050 and dashed lines where p<0.099. Error bars show 95 % confidence intervals. 121

Figure 5.1 Location of Aclands and Spooners catchments (b) within the southwest of England (a). Location of study sites within Aclands (c) and Spooners (d) study catchments. Man-made drainage ditches and "natural" streams are shown in light blue. Coastline shapefile (Ordnance Survey 2008a), 1:50 000 Ordnance Survey Map (Ordnance Survey 2008e) 1:10000 Ordnance Survey map (Ordnance Survey 2008b, c). 135

Figure 5.2 Temporal variation in a, soil temperature at 15 cm (°C) at S2R2, b, photosynthetically active radiation (µmol Photons m^{-2} s^{-1}), c, total daily precipitation at Spooners (mm) and d, water table depth (cm below surface). Error bars are one standard error. 143

Figure 5.3 Temporal variation in a, photosynthesis at 600 µmol Photons m^{-2} s^{-1} (P_{G600}) (µgC m^{-2} s^{-1}) b, ecosystem respiration (R_{Eco}) (µgC m^{-2} s^{-1}) (not temperature corrected), c, photosynthesis at full light (µgC m^{-2} s^{-1}) and d, net ecosystem exchange at full light (µgC m^{-2} s^{-1}) at Aclands (black diamonds) and Spooners (white boxes) (n=9). Error bars are one standard error. 145

Figure 5.4 Seasonal variation in below-ground respiration rates as measured. Total (white), heterotrophic (black) and autotrophic (grey) mean respiration rates measured at a, Aclands and b, Spooners Error bars are one standard error. 146

Figure 5.5 Seasonal variation in the proportional contribution of heterotrophic (black) and autotrophic (grey) respiration to total below-ground respiration at a, Aclands and b, Spooners. 147

Figure 5.6 Relationship between photosynthesis at 600 µmol Photons m^{-2} s^{-1} (P_{G600}) (µg C m^{-2} s^{-1}) and water table depth (cm below ground surface) (a, b & c), soil temperature at a depth of 5 cm (°C) (d, e & f), fraction of photosynthetically active radiation absorbed (fPAR) (g, h & i) and normalised difference vegetation index (NDVI) (j, k & l)) at Aclands (a, d, g & j), Spooners (b, e, h & k) and both catchments together (c, f, i & l). Error bars are one standard error. 149

Figure 5.7 Relationship between ecosystem respiration (µgC m^{-2} s^{-1}) and water table depth (cm below ground surface) (a, b & c), soil temperature at a depth of 5 cm (°C) (d, e & f), fraction of photosynthetically active radiation absorbed (fPAR) (g, h & i) and normalised difference vegetation index (NDVI) (j, k & l) at Aclands (a, d, g & j), and Spooners (b, e, h & k) and both catchments together (c, f, i & l). Error bars are one standard error. 150

Figure 5.8 Relationship between below-ground respiration (µmol m^{-2} s^{-1}) as measured (a, b & c) and corrected to 10 °C (d, e & f) and water table depth (cm below ground surface) with total (a & d), heterotrophic (b & e) and autotrophic (c & f) at Aclands (black diamonds) and Spooners (white squares, dashed lines) and across both catchments (solid lines). Regressions drawn where $p<0.050$ for significant see Table 5.5. 154

Figure 5.9 Modelled average monthly net ecosystem exchange (NEE) (gC m^{-2}). Positive values indicate a release of CO_2 to the atmosphere. Vertical lines indicate start and end of annual flux calculation periods. Error bars indicate 95 % confidence intervals for modelled NEE fluxes. 156

Figure 5.10 Comparison of photosynthesis and ecosystem respiration rates (µgC m^{-1} s^{-1}) measured in this study to those reported in other studies. More details in Supplementary Material Table 11.3 159

Figure 6.1 Location of Aclands and Spooners study catchments (b) within the southwest of England (a). Location of study sites within Aclands (c) and Spooners (d) study catchments. Coastline shapefile (Ordnance Survey 2008a), 1:50 000 Ordnance Survey Map (Ordnance Survey

2008e) 1:10 000 Ordnance Survey Map (Ordnance Survey 2008b, c). 176

Figure 6.2 Variation with proportional distance from the ditch in a, water table depth (cm below ground surface), b, Ellenberg's Moisture Indicator Values, c, peat thickness (cm), d, Inverse Simpson Diversity Index, e, percentage coverage of Non-*Molinia* species, f, species richness, g, percentage coverage of *Molinia caerulea*, h, percentage coverage of leaf litter and i, annual net primary productivity (ANPP) (g m^{-2}). n=12. Error bars are one standard error. 185

Figure 6.3 Variation in modelled photosynthesis (P_{G600}) (µgC m^{-2} s^{-1}) and ecosystem respiration (R_{Eco}) (µgC m^{-2} s^{-1}) with a, proportional distance from the ditch and b, site. Error bars are one standard error. Letters denote statistically significant groups p=0.012. 188

Figure 6.4 Variation in total, heterotrophic and autotrophic respiration at 10 °C (µmol m^{-2} s^{-1}) with a, proportional distance from the ditch and b, site. Error bars are one standard error. Letters denote statistically significant groups p=0.018. 189

Figure 7.1 Location of Spooners study catchment (b) within the southwest of England (a). Location of vegetated plots where plots scale images were collected (diamonds), validation vegetated plots (triangles), area of interest used to compare digital surface models (DSMs) (square) and extent of point cloud (shading). (Ordnance Survey 2008a, b, e). 206

Figure 7.2 Distribution of images used by VisualSfM at S3R1 to create model (194 images used of 204 collected) demonstrating the multiple heights and distances at which photographs were taken. 208

Figure 7.3 Typical placement of solid static objects with distinct colours around the vegetated plot to increase the probability of keypoint identification. 208

Figure 7.4 Flight paths for Unmanned Aerial Vehicle. Approximately 100 m altitude, 60 % along track overlap and 30 % across track overlap. The second flight path was at an oblique angle to the first, but still flying up-wind, to increase overlap. 211

Figure 7.5 Point clouds resulting from 180, 140, 80 and 40 images input. 40a and b included the same 20 images plus a further 20 from either 1 m (40b) or 2 m distance (40a). An image taken from approximately the same view is also shown. Colours represent relative elevation. Stakes are approximately 50 cm tall. 217

Figure 7.6 Variation in processing time (hundreds of seconds) (a), average point cloud density (thousands of points m^{-2}) (b), point cloud variance (m) (c), point cloud elevation range (m) (d), number of cells in 0.02 m resolution digital surface model (DSM) (e) and DSM elevation range (m) with number of images input to VisualSfM software for 0.55 x 0.55 m plot (S3R1). 218

Figure 7.7 Digital Surface Models (DSM) of S3R1 created using VisualSfM showing mean (a) and natural break (b) thresholds (grey surfaces) between area classed as tussock and area classed as soil . Areal extent of plot is 0.53 x 0.59 m. DSM aligned with image in Figure 7.5. 220

Figure 7.8 Comparison of tussock height (m), tussock area (%) and tussock volume (m^3) estimated for 14 plots using VisualSfM and the mean threshold (mean), natural breaks threshold (NB) and ground validation data (GV) measured using a DGPS (n=71). Error bars reach the maximum and minimum recorded values. The vertical box extends from the 25^{th} to the 75^{th} percentile with a horizontal line at the 50^{th} percentile. 221

Figure 7.9 Point clouds created using VisualSfM from all images (532) (a) and a subset of 203 images focused in the centre of the catchment (b). Coloured by red, green and blue values associated with each point. Both images are in the same arbitrary scale and co-ordination prior to georectification. Approximate scale and north direction given. 223

Figure 7.10 Digital Surface Models for the catchment from UAV-based images with a cell resolution of 0.05 m (a) and from a 0.5 m resolution LiDAR. Lines indicate locations of cross-sections in Figure 7.11. 225

Figure 7.11 Cross-sections of elevation along lines A, B, C, D & E (Figure 7.10) for UAV-based image VisualSfM digital surface model (DSM) (0.05 m

resolution) and LiDAR DSM (0.5 m resolution). Note Line A is 200 m long whilst the others are 100 m long. Vertically exaggerated..... 226
Figure 7.12 Difference in elevation (m) between LiDAR digital surface model (DSM) and UAV-based image VisualSfM DSM. The elevation of the LiDAR is greater than the UAV-SfM DSM in the green areas and lower in the red areas. 227
Figure 7.13 Relationship between tussock (black diamond) and inter tussock (grey cross) elevations (meters above sea level) as measured using DGPS and estimated from the digital surface models (DSMs) derived using LiDAR and digital images from a UAV at a range of grid sizes. 229
Figure 7.14 Semi-variograms of UAV image and LiDAR derived digital surface models for a 14 x 14 m area of interest. 231
Figure 7.15 Variation in water table depth (m below ground surface) (a and e), species richness (b and f), ecosystem respiration (R_{Eco}) (µgC m^{-2} s^{-1}) (c and g) and photosynthesis (P_{G600}) (µgC m^{-2} s^{-1}) (d and h) with tussock volume (m^3) (a, b, c and d) and maximum tussock height (m). R_{Eco} and P_{G600} derived from an empirical model) at a temperature of 12 °C, GEI of 60 and PAR of 600 (see section 6.5) based on flux chamber measurements. Tussock height and volume were derived using VisualSfM and the mean threshold (grey squares and dashed lines) and natural break threshold (black diamonds and solid lines). Pearson correlation coefficient (r) and significance (p) values are shown..... 234
Figure 8.1 Location of Aclands and Spooners catchments (b) within the southwest of England (a). Location of control (C) and restored (R) study sites within Aclands (c) and Spooners (d) study catchments. The three plots within each study site were located ⅛, ¼ and ½ the distance between adjacent ditches. Coastline shapefile (Ordnance Survey 2008a), 1:50 000 Ordnance Survey Map (Ordnance Survey 2008e) 1:10 000 Ordnance Survey map (Ordnance Survey 2008b, c). 255

Figure 8.2 Deviation of the regional (Southwest England) seasonal rainfall (mm) and mean air temperatures (°C) during 2012, 2013 and 2014 from the 100 year mean (UK Meteorological Office 2015)..... 262

Figure 8.3 Average water table depth at the control and restored locations pre-, 1-year and 2-years post restoration (a). Difference in water table depth between the control and restored locations (DiffWTD) pre-, 1-year and 2-years post-restoration (b). Error bars are one standard error. n>36..... 263

Figure 8.4 a, Depth to water table (cm) at the control location at Aclands (white diamonds) (n=7) and Spooners (grey squares) (n=4). Error bars are one standard error. b, Difference in water table depth between the control and restored locations at Aclands and Spooners . Vertical dashed lines indicate the start and finish of restoration at Spooners (March-April 2013) and Aclands (April 2014)..... 264

Figure 8.5 Variation in the difference in water table depth between the control and restored locations (DiffWTD) (cm) with variation in water table depth at the control locations (cm) at Aclands (diamonds) and Spooners (squares) catchments pre-(grey) and post-restoration (black)..... 265

Figure 8.6 Average photosynthesis at 600 µmol Photons m^{-2} s^{-1} (a) and ecosystem respiration (b) at the control and restored locations pre-, 1-year and 2-years post-restoration (µgC m^{-2} s^{-1}). Average photosynthesis at 600 µmol Photons m^{-2} s^{-1} ($PG_{R/C}$) (c) and ecosystem respiration ($REco_{R/C}$) (d) at the restored location as a proportion of the variable at the controlled location pre-, 1-year and 2-years post- restoration. Error bars are one standard error. 267

Figure 8.7 Average difference in photosynthesis at 600 µmol Photons m^{-2} s^{-1} (P_{G600}) and ecosystem respiration (R_{Eco}) (µgC m^{-2} s^{-1}) between control and restored locations pre-, 1-year and 2-years post-restoration at Aclands and Spooners catchments. A positive value indicates restored locations released more CO_2 i.e. more respiration or less photosynthesis. Error bars are one standard error..... 268

Figure 8.8 Temporal variation in photosynthesis at 600 µmol Photons m^{-2} s^{-1} (P_{G600}) and ecosystem respiration (R_{Eco}) at the control and restored

locations (μgC m^{-2} s^{-1}) at Aclands (a) and Spooners (b). Vertical dashed line indicates timing of restoration. Error bars are one standard error. 269
Figure 8.10 Average total, heterotrophic and autotrophic respiration at 10 °C at control and restored locations pre-, 1-year and 2-years post-restoration (a). Average total, heterotrophic and autotrophic respiration at the restored location as a proportion of respiration at the control location pre-, 1-year and 2-years post- restoration (b). Error bars are one standard error. 271
Figure 8.11 Temporal variation in the difference in water table depth (cm), heterotrophic and autotrophic respiration (μmol m^{-2} s^{-1}) between control and restored locations in Aclands (a) and Spooners (b) catchments. Vertical dashed line indicates timing of restoration. Error bars are one standard error. 272
Figure 8.12 Spatial variation in a, difference in water table depth between control and restored locations (DiffWTD) (cm), b, photosynthesis at 600 μmol Photons m^{-2} s^{-1} ($PG_{R/C}$), c, ecosystem respiration ($REco_{R/C}$), and d, total ($RTot_{R/C}$), e, heterotrophic ($RHet_{R/C}$) and f, autotrophic below-ground respiration ($RAut_{R/C}$) at the restored location as a proportion of the variable at the controlled location at different proportional distances from the ditch at Aclands and Spooners, pre- (2012) and 1-year (2013 at Spooners, 2014 at Aclands) and 2-years (2014 at Spooners) post- restoration. Error bars are one standard error. Letters denote statistically significant groups ($p<0.050$). Higher values indicate depth to water table or CO_2 flux from restored location greater than depth to water table or flux from control location. 275
Figure 8.13 Spatial variation in the difference in water table depths between control and restored locations (DiffWTD) with average peat thickness of the control and restored pairs (cm) (a) and water table depth at the control location (WTD_C) (cm) (b) pre- and 1-year post restoration. Global models with the same slope but different intercepts drawn for pre- and post-restoration. 276

Figure 9.1 Functioning of a deep actively forming *Sphagnum* peatland (a & b) and a shallow degraded *Molinia caerulea*-dominated peatland (c & d) under high (a & c) and low (b & d) water tables. 296
Figure 9.2 Processes observed (red) following restoration and predicted (green) should decreased photosynthesis bring about a dramatic change in vegetation composition. 301
Figure 11.1 Time series of an 8-day moving average relative brightness (Equation 2) of (a) red, (b) green and (c) blue for the 2013 growing season. Time series of and 8-day moving average (d) greenness excess index (Equation 1) and (e) green-red vegetation index (Equation 3), (f) photosynthetically active radiation (PAR) (μmol.Photons.$m^{-2}s^{-1}$) and (g) air temperature (°C) for the 2013 growing season. 313
Figure 11.2 Factor weightings for the first (PCA1) and second (PCA2) principal axis from principal component analysis of species present in vegetation composition analysis 314
Figure 11.4 Variation in a, water table depth (cm), b, percentage coverage of non-*Molinia* species, c, Inverse Simpson Diversity Index, d, modelled photosynthesis (P_{G600}) (μgC m^{-2} s^{-1}) and ecosystem respiration (R_{Eco}) (μgC m^{-2} s^{-1}) and e, total, heterotrophic and autotrophic respiration at 10 °C (μmol m^{-2} s^{-1})..... 328
Figure 11.5 Temporal variation in total (a), heterotrophic (b) and autotrophic (c) respiration (μmol m^{-2} s^{-1}) at 10 °C at control and restored locations within Aclands catchment. Error bars are one standard error..... 329
Figure 11.6 Temporal variation in total (a), heterotrophic (b) and autotrophic (c) respiration (μmol m^{-2} s^{-1}) at 10 °C at control and restored locations within Spooners catchment. Error bars are one standard error. ... 330
Figure 11.7 Water table depth (cm) at the control and restored locations averaged by proportional distance from the ditch within each catchment, pre- 1-year and 2-years post-restoration. Error bars are one standard error. 331
Figure 11.8 Photosynthesis at 600 μmol Photons m^{-2} s^{-1} (a) and ecosystem respiration (b) at the control and restored locations pre-, 1-year and

2-years post restoration (µgC m^{-2} s^{-1}). Error bars are one standard error. 332
Figure 11.9 Total (a), heterotrophic (b) and autotrophic (c) respiration at 10 °C at the control and restored locations pre-, 1-year and 2-years post restoration (µmol m^{-2} s^{-1}). Error bars are one standard error. 333

LIST OF ACCOMPANYING MATERIAL

Table 11.1 Number of sample locations and number of net ecosystem exchange measurements collected in dark and light (full and shaded) condition at Aclands and Spooners on a given date and sample round. # Excluded as only three out of nine locations sampled. * excluded when focussing on growing season. 315

Table 11.2 Number of sample locations where clipped (2 replicates) and clipped and trenched (2 replicates) measurements were collected at Aclands and Spooners on a given date and sample round. # data excluded as treatment effects apparent. *Data excluded as levels of detection less than uncertainty within a plot. 316

Table 11.3 Reported photosynthesis and ecosystem respiration values (µgC m^{-2} s^{-1}). Results from this study are shaded grey. CC closed chamber, EC eddy covariance 317

Table 11.4 Reported total and heterotrophic below-ground respiration rates (µmol m^{-2} s^{-1}). Results from this study are shaded grey. 319

Table 11.5 Reported net ecosystem exchange values (tonnes ha^{-1} yr^{-1}), positive values indicate a source of CO_2 to the atmosphere, negative values a sink. Results from this study are shaded grey 321

Table 11.6 Location specific empirically derived coefficients for R_{Eco} and P_{G600} models. Regression coefficient (r^2), number of data points (n) parameters: P1 (µgC m^{-2} s^{-1}), K1 (µmol Photons m^{-2} s^{-1}), a (dimensionless), b ($°C^{-1}$), c (dimensionless), d ($°C^{-1}$), e (dimensionless), T_{Opt} (°C) and T_{Tol} (°C). 324

Table 11.7 Seasonal Q_{10} and mean respiration at 10 °C (R_{10}) values for total, heterotrophic and autotrophic respiration at each site. Regression coefficient (r_2) and significance (p) of exponential relationships between soil temperature at 5 cm (°C) and total, heterotrophic and autotrophic respiration at each site. n is the number of sample days. 326

Table 11.8 Average vegetation composition (% coverage) and standard errors (in brackets) by proportional distance from the ditch and site. Overall

mean, minimum (min), maximum (max) and number of occurrences (n). # cover of 1 % at a single location..... 327
Figure 11.1 Time series of an 8-day moving average relative brightness (Equation 2) of (a) red, (b) green and (c) blue for the 2013 growing season. Time series of and 8-day moving average (d) greenness excess index (Equation 1) and (e) green-red vegetation index (Equation 3), (f) photosynthetically active radiation (PAR) (μmol.Photons.$m^{-2}s^{-1}$) and (g) air temperature (°C) for the 2013 growing season. 313
Figure 11.2 Factor weightings for the first (PCA1) and second (PCA2) principal axis from principal component analysis of species present in vegetation composition analysis 314
Figure 11.4 Variation in a, water table depth (cm), b, percentage coverage of non-*Molinia* species, c, Inverse Simpson Diversity Index, d, modelled photosynthesis (P_{G600}) (μgC m^{-2} s^{-1}) and ecosystem respiration (R_{Eco}) (μgC m^{-2} s^{-1}) and e, total, heterotrophic and autotrophic respiration at 10 °C (μmol m^{-2} s^{-1})..... 328
Figure 11.5 Temporal variation in total (a), heterotrophic (b) and autotrophic (c) respiration (μmol m^{-2} s^{-1}) at 10 °C at control and restored locations within Aclands catchment. Error bars are one standard error..... 329
Figure 11.6 Temporal variation in total (a), heterotrophic (b) and autotrophic (c) respiration (μmol m^{-2} s^{-1}) at 10 °C at control and restored locations within Spooners catchment. Error bars are one standard error. ... 330
Figure 11.7 Water table depth (cm) at the control and restored locations averaged by proportional distance from the ditch within each catchment, pre- 1-year and 2-years post-restoration. Error bars are one standard error. 331
Figure 11.8 Photosynthesis at 600 μmol Photons m^{-2} s^{-1} (a) and ecosystem respiration (b) at the control and restored locations pre-, 1-year and 2-years post restoration (μgC m^{-2} s^{-1}). Error bars are one standard error. 332

Figure 11.9 Total (a), heterotrophic (b) and autotrophic (c) respiration at 10 °C at the control and restored locations pre-, 1-year and 2-years post restoration (μmol m^{-2} s^{-1}). Error bars are one standard error. 333

1 INTRODUCTION AND RATIONALE

In their natural state peatlands act as significant carbon stores (Yu *et al.* 2010), and the amount stored has accumulated gradually under waterlogged conditions since the last ice age. Inappropriate management including drainage (Holden *et al.* 2004), burning (Yallop *et al.* 2006), grazing (Tucker 2003), peat cutting (Tomlinson 2010) and commercial extraction (Soini *et al.* 2010) has put these stores at risk. A small change in the balance between primary production and decomposition can shift a peatland from carbon sequestration towards carbon release. As peatland restoration has been identified as one of the most cost-effective measures to mitigate against climate change (Bain 2011) carbon markets may provide funding for peatland restoration (Bonn *et al.* 2014). These require a means of estimating emissions from a degraded peatland and emissions savings due to restoration, most commonly species assemblages are used as a proxy for emissions (Couwenberg *et al.* 2011). At present there are no suitable emissions factors for drained *Molinia caerulea* dominated peatlands (Birkin *et al.* 2011) revealing a need to quantify CO_2 fluxes in these ecosystems.

The peatlands of Exmoor have been subject to extensive drainage (Mills *et al.* 2010) resulting in shallow peats, typically <30 cm (Bowes 2006), underlain by thin (~15 cm) silty-clayey palaeosols (Carey 2015). Although historically present on Exmoor, the current dominance of *Molinia caerulea* resulting from drainage intensified by over-grazing and burning is unprecedented (Chambers *et al.* 1999, Fyfe *et al.* 2014) resulting in a loss of the peat-forming *Sphagnum* layer across large extents. It is unlikely these heavily degraded peatlands are actively sequestering CO_2 at present, however, peat formation has been restarted in other degraded peatlands through appropriate management (Komulainen *et al.* 1999, Samaritani *et al.* 2011) indicating the potential to maintain existing, albeit marginal, peat stores and possibly resume carbon sequestration across Exmoor. Located in the southwest of England the Exmoor peatlands lie at the southern limit of the blanket bog forming bioclimatic space (Clark *et al.* 2010), as such these ecosystems are particularly vulnerable to climate change. It is vital that peat forming conditions are re-established whilst

they lie within the bioclimatic space in order to increase their resilience to future climate change.

Although *Molinia caerulea* has encroached on degraded peatlands across Western Europe, including British upland blanket bogs (Bunce and Barr 1988, Taylor *et al.* 2001), studies on the effects of drainage (Oechel *et al.* 1998, Chimner and Cooper 2003, Strack *et al.* 2006, Jaatinen *et al.* 2007) and restoration (Silvola *et al.* 1996a, Komulainen *et al.* 1999, Urbanová *et al.* 2012) have been focused in *Sphagnum* dominated peatlands and/or deeper peats. *Molinia caerulea* dominated peatlands are most likely to be restored to a more diverse, carbon accumulating plant community by ditch blocking where the current dominance of *M. caerulea* was solely due to drainage. In areas where burning and/or grazing enhanced the spread of *M. caerulea,* rewetting alone may not be sufficient to initiate a change in vegetation. It is currently unknown how restoration will affect *Molinia caerulea*, a plant that has evolved to tolerate waterlogging and favours fluctuating water levels (Taylor *et al.* 2001).

Direct measurements of CO_2 fluxes are challenging and expensive. By understanding the temporal and spatial processes controlling CO_2 fluxes (including water table depth and vegetation composition) and their response to restoration, knowledge gained in this study should be more readily transferred to other sites. In addition by linking CO_2 fluxes to vegetation composition and/or structure measureable using remote sensing methods it may be possible to upscale measurements to whole ecosystem extents. A combination of gas flux chambers and soil collars enables the measurement of CO_2 fluxes at a scale that is directly attributable to processes (Tuittila *et al.* 1999). Locating chambers and collars at discrete distances from drainage ditches along transects, allows the role of these critical spatial features to be assessed. This study is unique because partitioned (heterotrophic and autotrophic) below-ground respiration will be measured alongside ecosystem respiration and photosynthesis. Partitioning below-ground respiration enables heterotrophic decomposition of the peat store to be separated from larger, more dynamic respiration dominated by the vegetation component.

This study aims firstly to quantify CO_2 fluxes from a shallow, drained *Molinia caerulea* dominated peatland and to understand the temporal and spatial controls on these fluxes. Once this baseline has been established this study aims to quantify the spatial and temporal effects of ditch blocking on water table depths and CO_2 fluxes in the first and second growing seasons following restoration.

1.1 THESIS STRUCTURE

The next chapter presents a brief review of relevant literature to provide context for the primary research in chapters 4 to 8. Further site specific methodological and experimental context for the subsequent chapters is given in chapter 3.

The primary research content of this thesis is presented as a series of self-contained papers which firstly assess the temporal (chapter 5) and spatial (chapters 6) controls on CO_2 fluxes from two drained *Molinia caerulea* dominated catchments described in chapter 3. Then the short-term (< 2 years) effect of ecohydrological restoration on these catchments is evaluated (chapter 8). The papers constituting chapters 4 and 7 describe methodological development undertaken to support the aforementioned chapters.

1.1.1 Theme 1: Temporal and Spatial Controls on CO_2 Fluxes in a Drained *Molinia caerulea* Dominated Peatland.

Molinia caerulea has encroached on damaged peatlands so that it is now widespread across Europe including the British uplands (Bunce and Barr 1988, Taylor *et al.* 2001). It is known that vascular plants grow and decay differently to peat forming species such as *Sphagnum* (Coulson and Butterfield 1978, Otieno *et al.* 2009, Ward *et al.* 2009). However, there is limited understanding of the controls on CO_2 fluxes from peatlands currently dominated by this vegetation type. Studies from a degraded lowland raised bog in the Netherlands (Nieveen and Jacobs 2002) and a drained upland ombrotrophic bog in the Czech republic (Urbanová *et al.* 2012) both provide an insight into the temporal controls on *Molinia caerulea* within these peatlands. Chapter 5 builds on this work by assessing the effects of temporal variation in vegetation

phenology, soil temperature and water table depths on CO_2 fluxes within an upland, shallow, maritime peatland.

Having hypothesised that CO_2 fluxes would be driven by vegetation phenology a method was required to measure this. Traditional methods (e.g. date of first leaf appearance) are very labour intensive, subjective and site and species specific. Due to the remote nature of the sites a method was required that enabled measurement of green leaf phenology over the whole landscape with minimal site visits but at an approximately weekly temporal resolution. In chapter 4 daily repeat digital images from an *in situ* time-lapse camera are used to validate the use of satellite based Moderate resolution Imaging Spectroradiometer (MODIS) Normalised Difference Vegetation Index as a measure of green leaf phenology in these upland deciduous grass ecosystems.

Peatland drainage has been widespread across Europe for agricultural improvement and forestry (Sjörs 1980). Within these peatlands, drainage ditches are often the primary spatial features governing ecohydrological processes. Despite this, research aimed at understanding the broad effects of drainage have compared "pristine" to drained areas within northern peatlands (Silvola *et al.* 1996a, Alm *et al.* 1999a, Makiranta *et al.* 2008, Straková *et al.*). Conditions in these peatlands are cooler and the growing season shorter (Lund *et al.* 2015) altering the timing and controls on plant growth and CO_2 fluxes compared to the maritime peatlands of Britain. Where studies have explicitly examined the spatial controls on CO_2 fluxes they have compared microforms (Komulainen *et al.* 1999), natural hydrological gradients (Laine *et al.* 2007) or been focused on large (up to 3 m deep and wide) erosional gullies in the *Calluna vulgaris* dominated deeper peats of northern England (McNamara *et al.* 2008, Clay *et al.* 2012, Dixon *et al.* 2013, Rowson *et al.* 2013). Chapter 6 asks whether there is spatial variation in CO_2 fluxes in these shallow, maritime *Molinia caerulea* dominated peatlands and if so is there a relationship with the spatial distribution of drainage ditches and their influence on water table depth, vegetation composition and primary productivity? It aims to answer this question by measuring CO_2 fluxes in closed chambers along transects perpendicular to drainage ditches. Uniquely this study has measured ecosystem respiration and

photosynthesis as well as partitioned below-ground respiration. This enables heterotrophic decomposition of the peat store to be separated from the larger more dynamic fluxes associated with the vegetation component.

Plot scale measurements provide information on the processes driving variation in CO_2 fluxes but an ability to upscale these measurements to a landscape scale is desirable to support carbon trading schemes and policy decisions. Chapter 7 explores the use of ground- and Unmanned Aerial Vehicle-based digital remote sensing images together with Structure from Motion (SfM) computer vision techniques to measure vegetation structure at the plot and landscape scale. It then examines whether relationships between tussock structure and water table depth, vegetation community and carbon fluxes can be used to derive spatially distributed measures of these variables at a landscape extent.

Having established baseline conditions this thesis goes on to investigate the short-term (< 2 year) effects of ditch blocking on CO_2 fluxes. The experimental design of this thesis, using control and restored pairs, is such that climatic inter-annual variability can be accounted for. In addition the baseline and control-restored pairs design allows for continued or intermittent future monitoring to establish the longer-term impacts of ditch blocking on CO_2 fluxes and vegetation composition.

1.1.2 Theme 2: Short-term Effects of Ditch Blocking on CO_2 Fluxes in a Drained *Molinia caerulea* Dominated Peatland

Initially research on the effect of ditch blocking was focused on vegetation composition (Haapalehto *et al.* 2010, Bellamy *et al.* 2012), hydrology, (Wilson *et al.* 2010, Holden *et al.* 2011) and water quality (Wilson *et al.* 2011) reflecting the aims of restoration, to maintain/improve biodiversity, raise water tables and reduce water treatments costs (Parry *et al.* 2014). Increasingly carbon sequestration is stated amongst the aims of peatland restoration, particularly since compliance and voluntary carbon markets offer potential funding sources and re-wetting of wetlands has been included in the Kyoto Protocol (IPCC 2014).

Studies on the effect of drainage ditch blocking on CO_2 fluxes have focused on areas representative of different microtopography and vegetation cover (Komulainen *et al.* 1999, Urbanová *et al.* 2012). Urbanová *et al.* (2012) compared “pristine”, drained and rewetted bogs but as there was no baseline monitoring it is not possible to determine how much of the variation in vegetation composition and CO_2 flux was due to restoration and how much to other factors. Although Komulainen *et al.* (1999) had both baseline monitoring and a control their study was in a low-sedge bog in southern Finland. This difference in vegetation composition and climate makes it difficult to transfer results to the shallow, *M. caerulea* dominated peatlands of Exmoor. The spatially distributed effects of erosional gully blocking has been investigated in the deeper peats of northern England (Clay *et al.* 2012, Dixon *et al.* 2013) however, the greater size of these gullies compared to drainage ditches of Exmoor and the presence of exposed peat make these a challenging comparator.

Chapter 8 aims to quantify the spatial and temporal effects of ditch blocking on water table depths and CO_2 fluxes. It was not anticipated that significant changes in vegetation composition would occur in response to restoration over the duration of this study (Haapalehto *et al.* 2010). Instead changes to photosynthesis and autotrophic respiration were expected to indicate if restoration effects the *Molinia caerulea*, a species adapted to live where water table depths fluctuate (Jefferies 1915), and therefore whether future vegetation change, required to promote carbon sequestration (Lunt *et al.* 2010), is probable. By measuring heterotrophic respiration it was possible to investigate whether restoration encourages conservation of the peat store, the first step towards reinstating carbon sequestration.

1.1.3 Hypotheses

To address the two themes outlined above in a robust way, using a strategic scientific method the flowing hypotheses were tested.

Theme 1: Temporal and spatial controls on CO_2 fluxes (ecosystem respiration; gross photosynthesis; total below-ground respiration; heterotrophic respiration of soil organic matter and below-ground autotrophic respiration including root respiration and microbial respiration of root exudates) in a drained *Molinia caerulea* dominated peatland.

- MODIS derived vegetation products (NDVI, LAI, fPAR, EVI and GPP) can be used to model vegetation phenology as measured by an on-site time-lapse camera,
- Both time-lapse camera and MODIS derived vegetation products correlate with temporal variations in CO_2; making them useful measures of vegetation phenology for peatland CO_2 budgets,
- Temporal variation in CO_2 fluxes will primarily be driven by vegetation phenology and temperature due to the deciduous nature of the vegetation,
- Water table depth will have no effect on temporal variation in CO_2 fluxes as *Molinia caerulea* has evolved to live in environments with fluctuating water table depths (Taylor *et al.* 2001),
- There will be spatial variation in CO_2 fluxes related to drainage ditches and their influence on water table depth, vegetation composition and primary productivity,
- Ground-based and UAV-based digital photographs and Structure from Motion models can be used to derive quantitative structural measures of *Molinia caerulea* tussocks at a plot and landscape scale,
- Water table depth, vegetation composition and CO_2 fluxes are related to structural measures of *Molinia caerulea* tussocks which can be used to estimate the spatial distribution of water table depth, vegetation composition and/or CO_2 fluxes at a landscape extent.

Theme 2: Short-term effects of ditch blocking on CO_2 fluxes in a drained *Molinia caerulea* dominated peatland

- Restoration will raise water tables with the greatest effect:
    a. during dry conditions when water tables are expected to fall at the control locations but be maintained at the restored locations by pools up-gradient of the peat dams,
    b. closest to the ditch, nearer the pools formed up-gradient of the peat dams,
    c. where peat is thicker and therefore the potential to prevent deeper water tables during dry conditions is greater.
- Restoration will reduce CO_2 fluxes with the greatest effect:
    a. during dry conditions when the difference in water table depth between control and restored locations will be greatest,
    b. closest to the ditch, controlled by water table depth, primary productivity and vegetation composition,
    c. where peat is thickest, controlled by water table depth, primary productivity and vegetation composition.
- Overall restoration will have a greater effect on ecosystem respiration and below-ground heterotrophic respiration compared to photosynthesis, as raised water levels reduce aerobic respiration rates, thereby shifting the balance of CO_2 exchange towards carbon sequestration.

1.2 STATEMENT OF CONTRIBUTION

I confirm that I am the primary decision maker on experimental design, author, data collector and data analyst for all five of the papers included. Chapters 4 and 6 are currently in review with Remote Sensing of Environment and Ecohydrology respectively. Further work (chapters 5, 6 and 7) is due to be submitted to the journals Ecosystems, Methods in Ecology and Evolution and

Ecological Engineering respectively after completion of the thesis. The papers have multiple co-authors as the research has been supported by other members of the research group, particularly aiding me in equipment installation and fieldwork but also providing insightful comments on my initial drafts.

I have also been included as co-author on papers arising from the Exmoor Mires project. Although these papers do not directly form part of the thesis they provide a more holistic understanding of the peatlands and demonstrate my contribution to the wider Exmoor Mires project. All publications and citations for conference proceedings/papers stemming from this research are also listed below.

Peer-reviewed publications arising from work undertaken for the thesis.

- Gatis, N., Anderson, K., Grand-Clement, E., Luscombe, D.J., Hartley, I.P., Smith, D. & Brazier., R.E. (In Review) MODIS Vegetation Products; useful measures of vegetation phenology for peatland CO_2 budgets. *Remote Sensing of Environment*.

- Gatis, N., Luscombe, D.J., Grand-Clement, E., Hartley, I.P., Anderson, K., Smith, D. & Brazier, R.E. (2015) The effect of drainage ditches on vegetation diversity and CO_2 fluxes in a *Molinia caerulea* dominated peatland. *Ecohydrology* DOI: 10.1002/eco.1643.

- Gatis N, Anderson K, DeBell L, Benaud P, Luscombe DJ, Grand-Clement E, Hartley IP, Smith D, Brazier RE. (In Review) Measuring vegetation structure in complex ecosystems using ground- and UAV-based photography with SfM: an example from a tussock grassland. *Methods in Ecology and Evolution.*

Co-authored publications not included in this thesis, but which are cited in the text;

- Grand-Clement, E., Anderson, K., Smith, D., Luscombe, D., Gatis, N., Ross, M. & Brazier, R.E. (2013). Evaluating ecosystem goods and services after restoration of marginal upland peatlands in South-West England. *Journal of Applied Ecology, 50*, 324-334.

- Grand-Clement, E., Luscombe, D.J., Anderson, K., Gatis, N., Benaud, P. & Brazier, R.E. (2014). Antecedent conditions control carbon loss and downstream water quality from shallow, damaged peatlands. *Science of The Total Environment, 493*, 961-973

- Luscombe, D.J., Anderson, K., Gatis, N., Grand-Clement, E. & Brazier, R.E. (2014). Using thermal airborne imagery to measure near surface hydrology in upland ecosystems. *Hydrological Processes*

- Luscombe, D.J., Anderson, K., Gatis, N., Wetherelt, A., Grand-Clement, E. & Brazier, R.E. (2014). What does airborne LiDAR really measure in upland ecosystems? *Ecohydrology*

- Grand-Clement, E., Anderson, K., Smith, D., Angus, M., Luscombe, D.J., Gatis, N., Bray, L.S. & Brazier, R.E. (2015). New Approaches to the Restoration of Shallow Marginal Peatlands. *Journal of Environmental Management.DOI*i.org/10.1016/j.jenvman.2015.06.023.

- Luscombe, D.J., Anderson, K., Grand-Clement, E., Gatis, N., Ashe, J., Benaud, P., Smith, D. & Brazier, R.E. (In Prep). Understanding the hydrology of shallow, drained and marginal peatlands: Temporal Variability. *Hydrological Processes*.

- Luscombe, D.J., Anderson, K., Grand-Clement, E., Gatis, N., Ashe, J., Benaud, P., Smith, D. & Brazier, R.E. (In Prep). Understanding the hydrology of shallow drained and marginal peatlands: Spatial Variability

Conference proceedings stemming directly from research included in this thesis;

- Le Feuvre, N., Hartley, I.P., Anderson, K., Luscombe, D.J., Grand-Clement, E., Smith, D. & Brazier, R.E., Will blocking historical drainage ditches increase carbon sequestration in upland blanket mires of Southwest England? 2012 *EGU General Assembly Conference, Vienna* Abstracts 14, 704

- Gatis, N. Hartley, I.P., Anderson, K., Luscombe, D.J., Grand-Clement, E., Smith, D., Benaud, P. & Brazier, R.E. Will blocking historical drainage ditches increase carbon sequestration in upland blanket mires of Southwest England? 2012 British Ecological Society Conference, Bangor

- Gatis, N., Luscombe, D.J., Grand-Clement, E., Hartley, I.P., Anderson, K. & Brazier, R.E., The short-term effects of ecological restoration on carbon dioxide fluxes from a *Molinia caerulea* dominated marginal upland blanket bog. 2014 *EGU General Assembly Conference, Vienna* Abstracts 16, 6686

- Gatis, N., Luscombe, D.J., Grand-Clement, E., Hartley, I.P., Anderson, K., Smith, D. & Brazier, R.E., Does ditch blocking affect CO_2 fluxes from a *Molinia caerulea* dominated bog in the short-term? 2014 *IUCN Peatland Programme Annual Conference, Inverness*

- Gatis, N., Luscombe, D.J., Grand-Clement, E. Benaud, P., Ashe. J., Hartley, I.P., Anderson, K., & Brazier, R.E. Carbon dioxide fluxes from a drained *Molinia caerulea* dominated bog – how damaged was it, and has ditch blocking made a difference? 2015 *Exmoor Mires Project Conference, Dulverton*

2 LITERATURE REVIEW

2.1 PEAT AND PEATLANDS

2.1.1 What is Peat?

Peat is comprised of undecomposed or partially decomposed remains of vegetation that has accumulated *in situ* and contains between 30 % and nearly 100 % organic matter (Lindsay 2010) dependent on the conventions being used. Peat accumulates where primary productivity is (marginally) greater than decomposition over time (Clymo 1984), this occurs where a positive water balance maintains water tables near the surface thus restricting decay by reducing oxygen availability. The properties of peat, such as bulk density, hydraulic conductivity, pH and water, organic carbon and gas content vary depending on the dominant plant material (e.g. *Sphagnum*, sedge, mangrove) and the degree of humification, ranging from course fibrous to amorphous (Hobbs 1986). Consequentially the properties of the accumulated peat vary spatially, both vertically and horizontally, responding to changes in the water balance.

There is little agreement about how thick an organic rich superficial deposit must be to be mapped as peat. Joosten and Clarke (2002) found peatlands were defined as having a minimum of 20, 30, 45, 50 or 70 cm of organic rich deposits dependent on country and scientific discipline. British peat soils have been mapped where deposits are greater than 40 cm in England and Wales (Avery 1990), 50 cm in Scotland (Cannell *et al.* 1993) and 55 cm in Northern Ireland (Cruickshank and Tomlinson 1990).

The Ramsar Convention on Wetlands of International Importance (1971) defined peat as “ecosystems with a peat deposit that may currently support a vegetation that is peat-forming, may not, or may lack vegetation entirely.” By this definition peatlands include areas with vegetation typical of peatlands over deposits too thin to be defined as peatland by soil mapping as well as areas underlain by a peat deposit which no longer support peat-forming vegetation. Therefore, peatlands can include areas of actively forming peat as well as

“inactive” peatlands which contain historical peat deposits. Appropriate management of these “inactive” peatlands has been shown to restart peat formation (Komulainen *et al.* 1999, Samaritani *et al.* 2011) and these should therefore be considered as peatlands even though existing peat deposits may be marginal.

2.1.2 Peatlands

Peatlands form in areas with high precipitation where impermeable substrates and/or topographic convergence maintains saturation (Holden *et al.* 2004). They represent 50 to 70 % of wetlands globally (Joosten and Clarke 2002) and are distinguished from other wetlands by the presence of accumulated organic rich deposits. Although peatlands cover only 3 % of the global land surface they are found across a range of biomes, encompassing a wide latitudinal and altitudinal distribution (Figure 2.1).

Despite the wide geographical spread of peatlands they can be classified into two types based on their source of water and nutrients. Ombrotrophic mires (e.g. raised bog, blanket bog and bog forest) have their surface elevated above the influence of groundwater and are therefore dependent on precipitation for both water and nutrients (Moore 1987). Consequently they are relatively nutrient poor and usually acidic. Conversely minerotrophic mires (e.g. fens, carr, swamp and swamp forest) are groundwater fed (Moore 1987) resulting in alkaline conditions with greater nutrient availability. The vegetation characteristic of particular mire types varies globally and regionally for example, *Sphagnum papillosum* considered an ombrotrophic bog species in Britain is considered characteristic of minerotrophic fens in Finland (Lindsay 1985) due to different climatic regimes.

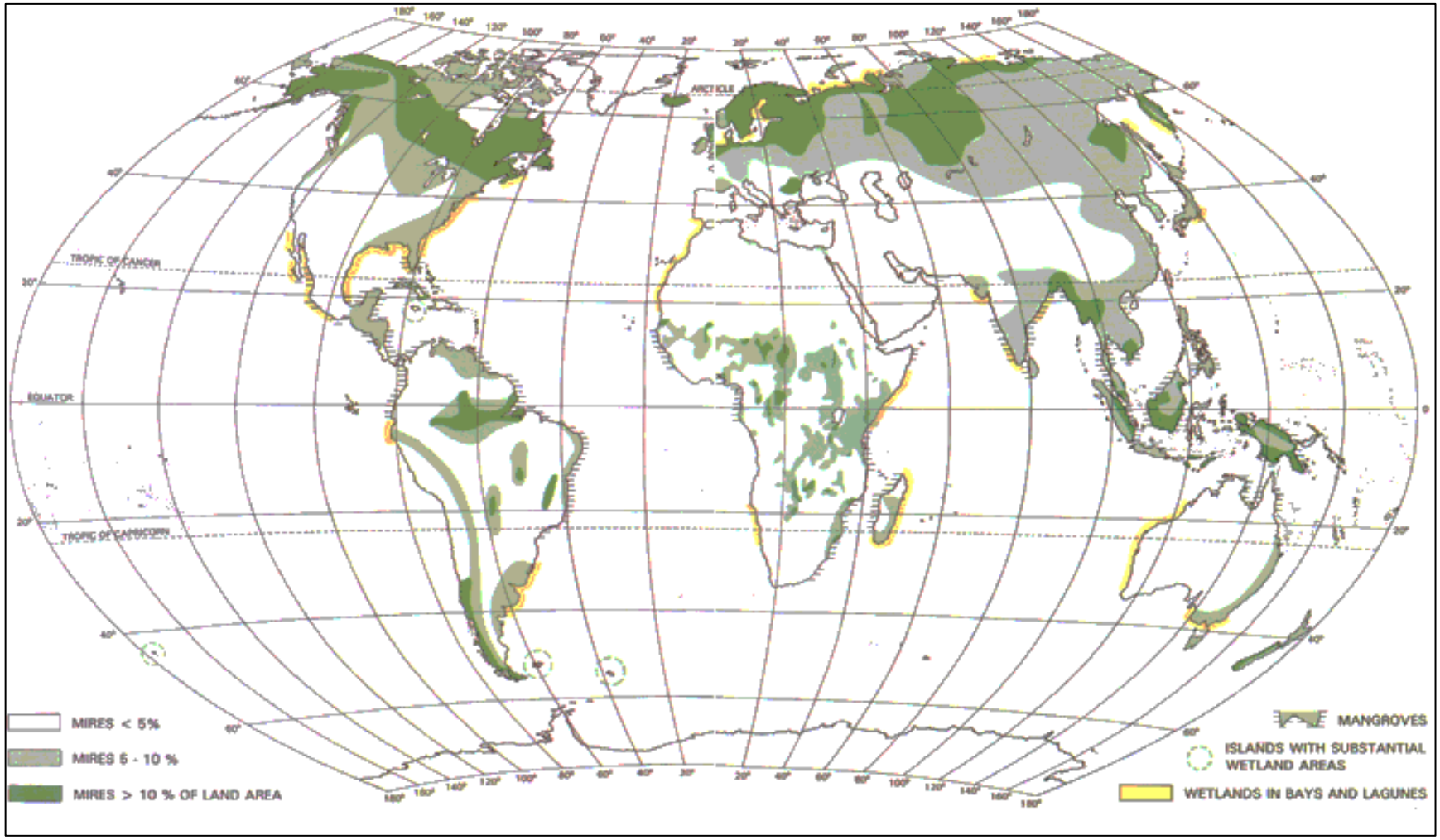

Figure 2.1 Global distribution of mires, mangroves and wetlands in bays and lagoons (Lappalainen 1996).

2.1.3 Ombrotrophic Blanket Bogs

This study is focused on ombrotrophic blanket bogs and so further discussions are concentrated on this particular type of mire. Blanket bogs are complex systems consisting of multiple peat-forming conditions including raised bogs, watershed mires, flushes etc. which have spread laterally and joined together smothering the underlying topography. For a blanket mire to develop a minimum of 1000 mm rainfall and at least 160 wet days (>1 mm rainfall) a year are required, as well as the mean summer temperature remaining below 15 °C with minor seasonal fluctuations (Lindsay *et al.* 1988). These climatic conditions are such that blanket mires are confined to temperate hyperoceanic areas such as New Zealand, Tasmania, northeast Asia, Tierra del Fuego, the east coast of Canada, southern Alaska, the Pacific Northwest and parts of Europe (Charman 2002). The UK has 10-15 % of the world's blanket peat resource (Tallis 1997) primarily located in upland areas (Figure 2.2), consequently they are globally important.

As blanket peat formation is primarily governed by climate (Lindsay *et al.* 1988), areas with the appropriate maximum annual temperature and water balance (precipitation minus potential evapotranspiration) can be mapped to delineate bioclimatic space. The peatlands of southwest England lie at the southern limit of the blanket bog forming bioclimatic space (Clark *et al.* 2010) as such they are particularly vulnerable to climate change. It is predicted that over the 21st century British climate will change towards warmer, wetter winters and warmer, drier summers (Jenkins *et al.* 2009). Under the UKCIP2 low emission scenarios only two bioclimatic models predicted at least 50 % of the current bioclimatic space of Dartmoor, Exmoor and Bodmin Moor would remain by 2080 (Clark *et al.* 2010). As these models have been calibrated against the current distribution of blanket peat it is unknown if these bioclimatic envelopes represent the conditions required to sustain existing blanket bogs or initiate peat growth. It may be that once a blanket bog has formed if it is in good condition it can sustain its own water balance despite an unsuitable climate. However, if the blanket bog is degraded, bioclimatic conditions suitable for peat initiation would

be required to enable the re-establishment of peat formation. This highlights the need to re-establish peat forming conditions on these moors whilst they lie within the bioclimatic space in order to increase their resilience to climate change.

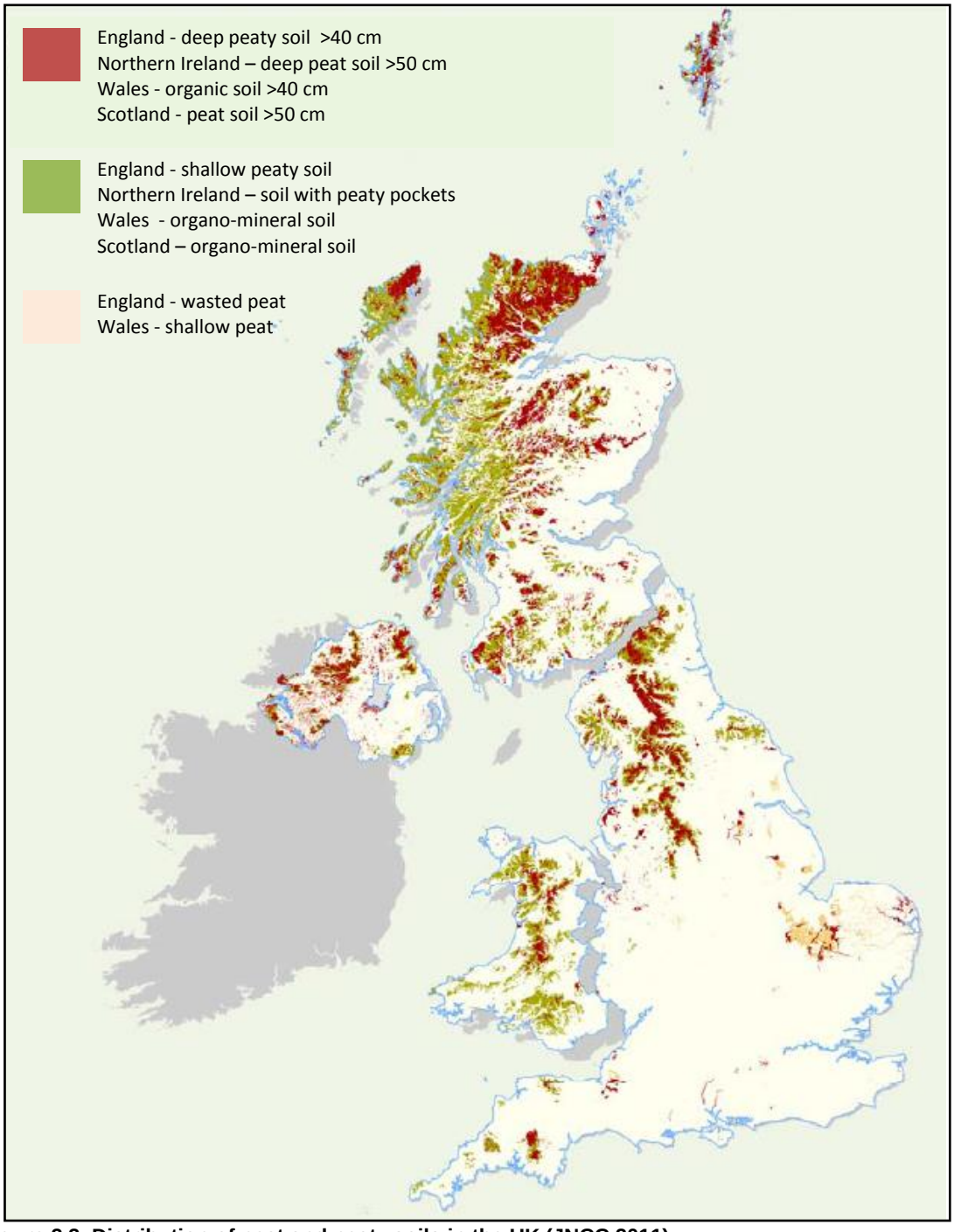

Figure 2.2. Distribution of peat and peaty soils in the UK (JNCC 2011).

2.1.4 *Sphagnum* Peat: Structure and Function of a Layered System

Peat forming ombrotrophic bogs of the UK are usually dominated by *Sphagnum* species which form a loose carpet over the bog surface (Clymo 1983). Unlike shrubs and herbaceous plants, *Sphagnum* species die from the base as they grow upwards to form four structural layers (Figure 2.3) (Charman 2002). The uppermost green layer, approximately 2 cm thick, is where new biomass is added as the *Sphagnum* grows upwards. Below the depth of light penetration, the *Sphagnum* becomes pale and starts to die forming a litter layer. The stems and branches of the *Sphagnum* break down over the next few centimetres (the collapse layer) until the overlying mass causes the litter to collapse; below this lies amorphous peat.

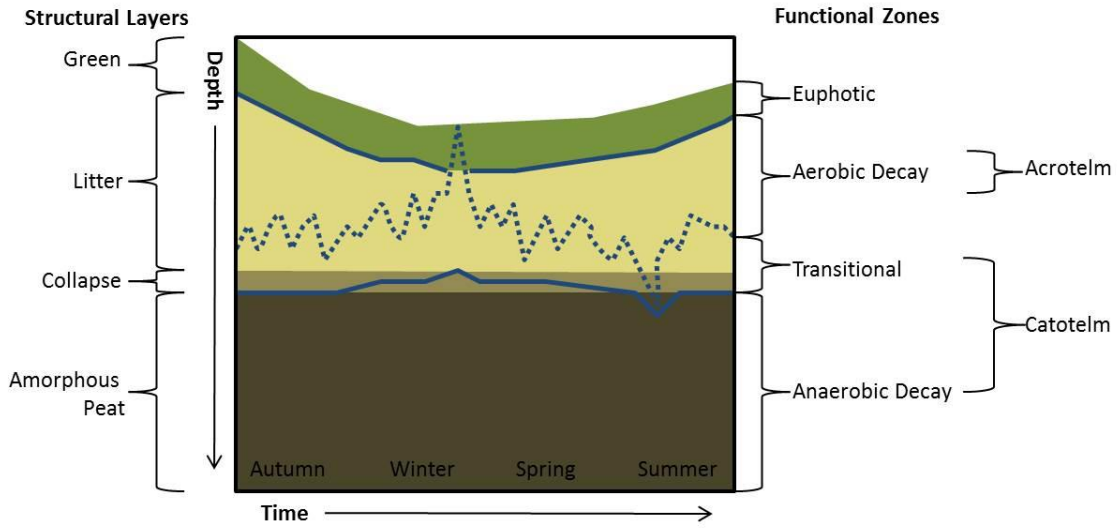

Figure 2.3. The structure and function model for peatlands. Water table represented by the dashed line. Adapted from (Clymo 1992).

There are also four functional zones beneath the soil surface, primarily determined by the position of the water table. The uppermost euphotic zone, coincident with the green structural layer (Figure 2.3), is the location of the majority of primary production. Below this is the zone of aerobic decay (Figure 2.3), also referred to as the acrotelm. The location of this zone fluctuates with the water table, reaching as low as the amorphous peat in very dry weather and

disappearing altogether when the water table is at the surface (Charman 2002). In this zone microbial activity is high as oxygen is readily available enabling rapid decomposition of the biomass.

Immediately below the water table is a transition zone where oxygen declines with depth as it is consumed by aerobic decay. Beneath this lies the anaerobic decay zone usually coincident with the amorphous peat layer. The transitional and anaerobic decay zones are collectively referred to as the catotelm. A lack of oxygen in the catotelm prevents more efficient aerobic decay occurring; thereby reducing microbial activity (Clymo 1983). Furthermore, the most labile fractions of the organic matter are decomposed in the acrotelm so the underlying peat has a greater proportion of recalcitrant organic matter.

As *Sphagnum* grows at the surface, the water table rises by capillary forces and reduced hydraulic conductivity so the structural and functional zones advance upwards. If the rate of anaerobic decomposition in the catotelm cannot keep pace with the organic matter supply from the overlying acrotelm, organic matter will accumulate to form peat deposits (Lindsay 2010). If the rate of anaerobic decomposition is greater than the rate of organic matter supply from the acrotelm then organic matter stored in the catotelm will be decomposed, consequently the bog is no longer peat forming and has become a carbon source.

2.1.5 Damaged *Sphagnum* Peat: Structure and Function of a Haplotelmic Bog

A haplotelmic bog is a single layered system where the acrotelm has been lost or destroyed, usually through human influence, leaving the catotelm exposed at the surface (Ingram 1978). The aerated catotelm in a haplotelmic bog has contrasting characteristics to a functioning acrotelm. For example, vegetation where present, is dominated by tussock-forming bog species with some wet-heath and dry heath species; gases can penetrate deeper into the peat especially where cracks are present and water table fluctuations are greater due to narrower pore spaces (Lindsay 2010). Haplotelmic bogs no longer maintain a functioning *Sphagnum* dominated acrotelm, consequently the bog is

no longer actively accumulating organic matter and the catotelm is exposed to oxidative wastage reducing the long-term carbon store (Lindsay 2010).

2.1.6 *Sphagnum* Cycle and Vascular Plant Cycle

In damaged ombrotrophic bogs (haplotelmic or not) *Sphagnum* may not be the dominant species. Instead, vascular plants such as *Molinia caerulea* (purple moor grass), *Calluna vulgaris* (heather) and *Eriophorum sp.* (cotton grass) may dominate. As vascular plants grow and decay at a faster rate than *Sphagnum* it may be better to consider the cycling of carbon in blanket bogs as occurring in two separate cycles, the *Sphagnum* cycle and the vascular plant cycle (Lindsay 2010).

The vascular cycle has larger and more dynamic fluxes than the *Sphagnum* cycle but contributes little to the carbon store compared to *Sphagnum*. Three *Calluna vulgaris* covered blanket bogs were found to be carbon sources indicating none of the biomass produced was being added to the existing peat store (Dixon *et al.* 2015). Grasses such as *Molinia caerulea* have been shown to have greater carbon uptake and biomass production (Otieno *et al.* 2009) than mosses *Sphagnum fallax* and *Polytrichum commune* due to greater light use efficiency. However, vascular plant material is more labile and readily decomposed than *Sphagnum* species with *Calluna vulgaris* losing 26 % by mass respectively over 12 months and *Eriophorum vulgaris* 44 % compared to only 16 % for *Sphagnum recurvum* (Coulson and Butterfield 1978). Thormann *et al.* (1999) found 16 % of the *Sphagnum teres/Sphagnum angustifolium* material was lost in the first year of decomposition compared to 52 % of *Carex sp.* in a Canadian poor fen. Despite their greater biomass production, Wallen (1993) found that only 0.2 % of the 720 g m^{-2} of vascular biomass (*Calluna vulgaris* and *Eriophorum sp.*) produced annually was transferred to the catotelm compared to 36 % of the original 28.5 g m^{-2} of *Sphagnum* biomass. The vascular component consisted predominantly of more recalcitrant *Eriophorum sp.* roots and leaf sheaths which remained reliant on the maintenance of waterlogged conditions to minimise further decomposition.

Sphagnum sp. have much smaller fluxes of photosynthesis and respiration (McNamara *et al.* 2008, Otieno *et al.* 2009) and considerably less biomass

(Wallen 1993, Otieno *et al.* 2009). However, *Sphagnum sp.* tissue is more resistant to decay (Coulson and Butterfield 1978), may actively suppress enzymic decomposition through phenols (Freeman *et al.* 2004) and so more of it is passed down into the catotelm where it creates the bulk of the long-term peat store (Wallen 1993).

In addition, vascular plants such as *Molinia caerulea* produce significant amounts of biomass below ground, equivalent to 20 % of the above ground biomass (Murphy and Moore 2010), as they extend their roots into the peat. At the surface microbes derive energy from fresh organic matter to decompose more recalcitrant compounds. However, at depth, fresh organic material is limited which restricts decomposition. If fresh organic material is added to the subsurface e.g. via root exudates, then microbes can be stimulated to decompose older soil organic matter (Fontaine *et al.* 2007). Vascular plants are a source of labile carbon both at the surface as leaf litter and at depth through their fine roots and root exudates stimulating the decomposition of deeper peat (Gogo *et al.* 2011), reducing the volume of carbon being stored, and potentially the existing carbon store.

It is known that vegetation with aerenchyma (air channels) such as *Eriophorum sp*. transport oxygen from the surface to their roots enabling them to function in anaerobic conditions by oxygenating the area around their roots (Lindsay 2010). *Molinia caerulea* may also produce oxygenated zones around their roots (Taylor *et al.* 2001) further encouraging more efficient aerobic respiration of organic matter resulting in reduced peat formation.

2.1.7 Global Warming Potential

The global warming potential (GWP) is a relative measure of how much warming a greenhouse gas produces over a time period compared to the same volume of CO_2 over the same period. It is important to consider in peatland systems because changes in water table depths and vegetation composition, resulting from drainage or ditch blocking, often have opposing influences on carbon dioxide and methane emissions (CH_4). Over 100 years, CH_4 has 25 times the GWP of CO_2 (Lashof and Ahuja 1990). Therefore, in the short-term, restoration may reduce CO_2 emissions but even a small increase in CH_4

emissions would result in a net increase in GWP (Bain 2011). Methane emissions have been shown to increase when water tables rose in response to ditch blocking (Komulainen *et al.* 1998) especially where *Eriophorum vaginatum* dominated (Cooper *et al.* 2014), although areas of methane production are geographically limited (e.g. 9.3 % of the land surface in a gullied blanket bog) they can be "hotspots" of methane production accounting for 95.8 % of methane emitted from the entire gullied blanket bog (McNamara *et al.* 2008). This thesis has focused solely on the effects of restoration on gaseous CO_2 fluxes. A complementary study investigating the effects of restoration on CH_4 and N_20 across Exmoor has been carried out (Hornibrook *et al.* 2012) future work will bring these results together.

2.2 PEATLAND STRUCTURE

2.2.1 Spatial Hierarchy

The link between mire topography, hydrology and ecology has long been noted in *Sphagnum* dominated peatlands (Ivanov 1981). Feedback mechanisms occur at a range of spatial extents and temporal scales (Couwenberg 2005, Belyea and Baird 2006, Pellerin *et al.* 2009, Waddington *et al.* 2015). The effects of these controls are expressed through self-organising landforms of comparable extent. For example, a large scale temporal control such as glacial-interglacial cycles will have an equivalently large spatial scale response e.g. mire type (Figure 2.4).

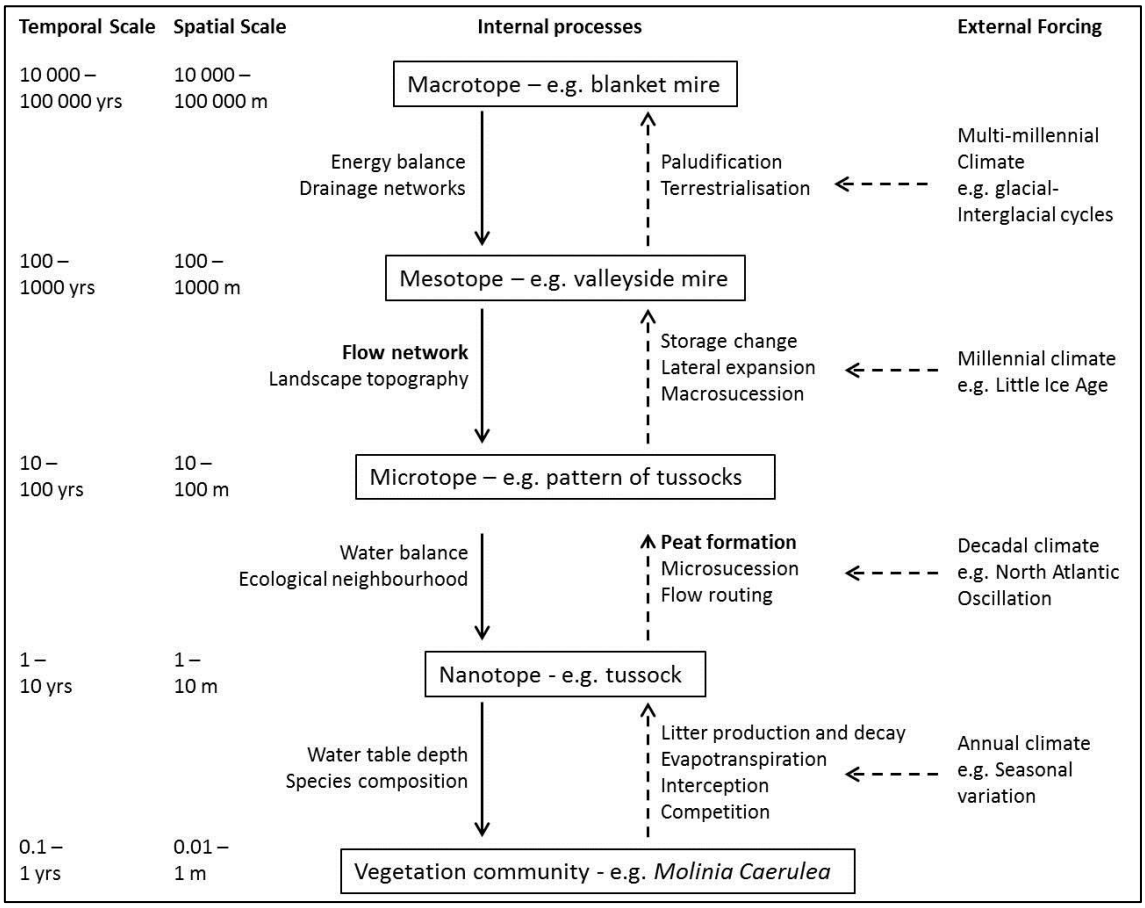

Figure 2.4. Peatlands as hierarchical complex systems. State, flux and forcing variables are arranged in order of increasing temporal scale and spatial extent. Boxes identify the spatial hierarchy of landforms. Solid arrows denote boundary conditions (constraints) and dashed arrows internal driving variables and external forcing at particular temporal scales (Belyea and Baird 2006).

Quantifying peatland landforms at a given spatial scale enables equivalent temporal scale controls on processes occurring in peatlands to be elucidated (Figure 2.4). For example, Anderson *et al.* (2010) demonstrated through a space for time substitution that the microtope pattern of a lowland ombrotrophic bog could be used to assess ecological and hydrological function in peatlands. Healthy hummock-hollow peatland at Wedholme Flow Cumbria formed an isotropic (non-directional) pattern with vegetation aggregating in nanotopes of <1 m. The degraded peatland dominated by high shrubs, including *Calluna vulgaris,* aggregated in larger nanotopes 3-4 m in size and exhibited an anisotropic (directional) pattern reflecting the underlying slope and drainage ditches (Anderson *et al.* 2010, Bennie *et al.* 2011). This change from *Sphagnum sp.* to vascular plant dominance as evident in the vegetation

composition, nanotope size and microtope pattern is significant for the magnitude of gas fluxes and the longer-term carbon storage as discussed in section 2.1.5. Measurement of vegetation structure and gas fluxes at the microtope scale may enable spatial patterning to be used as a proxy for ecological and hydrological functioning as well as carbon-sequestration. In order to study these landforms at a meaningful scale a clear and systematic description of landforms is required.

Starting with the largest landscape unit; a single continuous expanse of peatland soil bounded on all sides by mineral soil outcrops is called a macrotope. Blanket mire is an example of a macrotope which may extend for 10-15 km and contain several mesotopes. Mesotopes are discrete, hydrologically distinct peatland units, usually defined by their landscape position e.g. watershed mire, saddle mire, valley mire etc. (Lindsay 1995). Within each mesotope the fine scale surface structures (<2 m) combine in various ways to produce areas with distinctive 3-dimensional surface patterns or microtopes. The most obvious example of which is the hummock and hollow microtopography but patterns can be linear, smooth, orientated and without orientation (Lindsay 2010). Individual surface structures (tussocks, hummocks, high ridges, low ridges, hollows, pools, erosion gullies) used to be referred to as microforms but are now known as nanotopes. These nanotopes exist in vertical zones related to the water table and have distinctive plant communities associated with them, controlled by competition within each vertical zone (Ivanov 1981).

Each landform has distinct functional properties which influence and are influenced by the landforms they form part of (level above) and contain (level below) (Figure 2.4). The level below provides internal stimulus to change while the level above constrains any change. The spatial extent of a response corresponds to the temporal scale of external forcing (Belyea and Baird 2006). For example, when hydrological conditions become drier on a sub-decadal scale the water table drops and the *Sphagnum* species shift towards species more typical of hummocks. As hummock *Sphagnum* species are more effective at binding water than hollow species, the rates of evaporation decrease and

waterlogged conditions are maintained (Lindsay 2010). The expansion of hummocks over wetter areas is constrained by the longer-term water balance of the existing microtope (e.g. hummock and hollow complex) which remains unchanged over a sub-decadal scale.

2.2.2 Microtope of a Damaged Peatland

Drainage ditches change the flow network, altering the constraints on the microtope and allowing it to change (Figure 2.4). This alters the water balance resulting in a larger and more prolonged drop in the water table which results in a more significant shift in vegetation (Figure 2.5), initially towards *Sphagnum* species typical of hummocks e.g. *S. capillifolium* but later to non-*Sphagnum* mosses, dwarf shrubs (e.g. *Calluna vulgaris*) and tussock forming graminoids (e.g. *Molinia caerulea*) above a haplotelmic peat (section 2.1.5). This has a positive feedback further lowering the water table as decreased *Sphagnum* and increased *Molinia caerulea* cover would be expected to increase evapotranspiration rates (Spieksma *et al.* 1997) and promote overland flow between tussocks reducing infiltration. Changing vegetation composition also alters the balance of litter production and decay so the hollow nanotopes are lost and the hummocks become less pronounced (Figure 2.5). This decreases the rate of peat formation, flattens the peat surface and increases the number and extent of tussocks. Changes to the microtope are constrained by landscape topography and the new flow network so the mesotope remains unchanged (Figure 2.4).

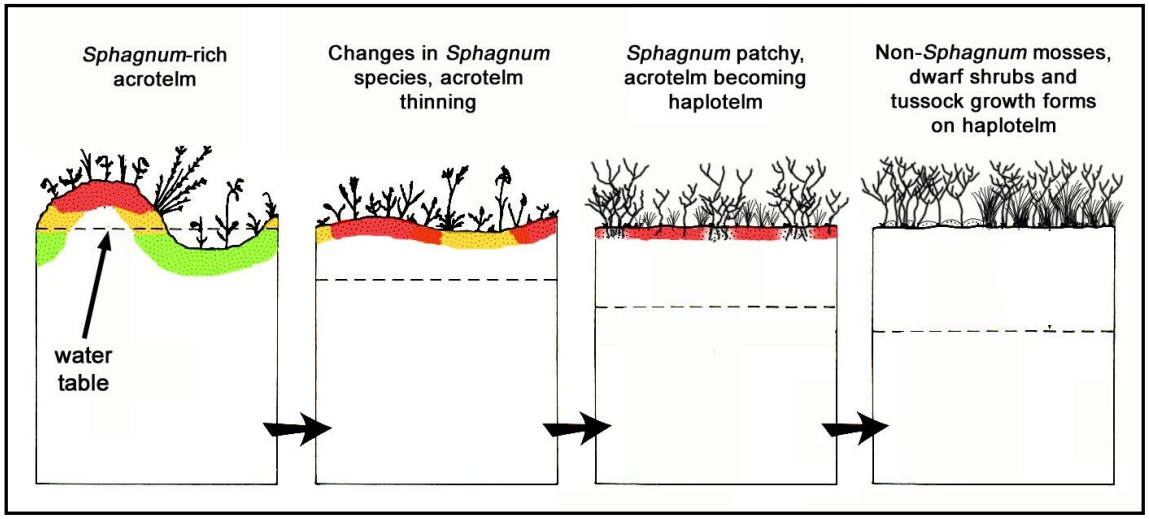

Figure 2.5 The effect of a falling water table and drying acrotelm on the microtope and vegetation composition of a blanket mire. First the microtope becomes smooth with the loss of hollows and associated species (green area). Then hummock species (red area) (e.g. *Sphagnum capillifolim)* become dominant and form a smooth carpet underlying dwarf shrubs. Finally *Sphagnum* species are completely replaced by non-*Sphagnum* mosses, dwarf shrubs and tussock forming graminoids (Lindsay 2010).

Although drained peatlands have often lost the typical hummock-hollow topography associated with functioning peatlands (Lindsay 1995), many of these peatlands, including Exmoor, have been encroached by *Molinia caerulea.* In 1984 it was estimated that *Molinia caerulea* covered 10 % of the British uplands (Bunce and Barr 1988) and this species is also widespread across Europe particularly on peaty gleys or deep peats (Taylor *et al.* 2001). *Molinia caerulea* thrives where water table depths fluctuate (Jefferies 1915) due to drainage, can tolerate denser grazing regimes and recover rapidly following burning allowing it to outcompete other bog species in poorly managed peatlands. *M. caerulea* exhibits phenotypic plasticity, with tussock morphology (nanotope) varying in response to environmental conditions (Taylor *et al.* 2001). Additionally the distribution of tussocks (microtope) varies with environment, in some areas scattered isolated tussocks form, in other areas a continuous cover forms which may be of large tussocks or shorter lawn-like sward (Taylor *et al.* 2001). Rutter (1955) demonstrated that tussock structure was related to a combination of mean water table depth and water table fluctuation. In drier conditions (Figure 2.6b), where mean water table depths were 30-35 cm below ground level, tussocks were fairly distinct from one another, steep sided and up to 25 cm high. Where the mean water table was only 15 cm below ground level

(Figure 2.6c) the tussocks reached up to 40 cm in height. In the area of wet heath, where *Calluna vulgaris* and *Erica tetralix* were present, the tussocks were shorter (~20 cm) and less distinct (Figure 2.6a).

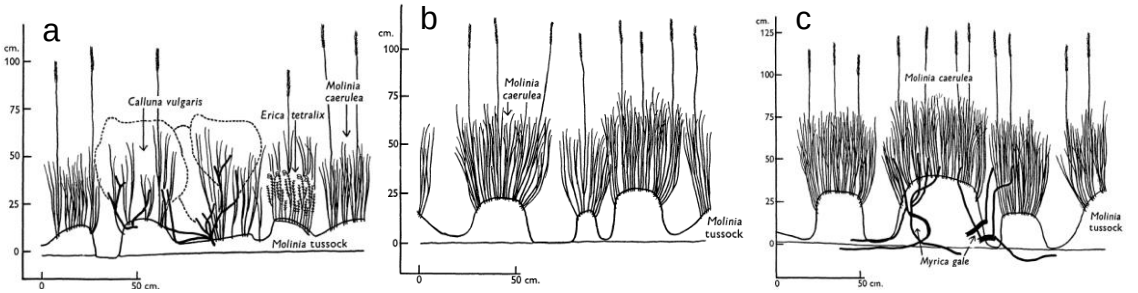

Figure 2.6 Vegetation profiles of wet-heath (a), drier Molinietum (b) and wetter Molinietum (c) (Rutter 1955).

Rutter (1955) also found variation in tussock height to have a greater impact on vegetation composition than water table depth. Within a headwater catchment of Exmoor, Luscombe *et al.* (2014a) found vegetation including *M. caerulea* to be taller within wetter areas, in particular comparatively tall *Juncus effusus* occurred in flushes. Therefore, vegetation structure could be used as an indicator of both vegetation composition and environmental conditions despite the absence of a traditional hummock-hollow topography.

2.3 PEAT: A VALUABLE BUT VULNERABLE CARBON STORE

Peatlands cover only 3% of the globe (Joosten and Clarke 2002) but it has been estimated that globally peatlands have accumulated between 530-694 GtC (Yu *et al.* 2010). In a functioning peatland organic matter accumulates due to a small imbalance between primary productivity and decay. However, it is estimated that 74 % of deep (>40 cm thick) peatland (including upland and lowland) in England is subject to damaging land management practices (Natural England 2010) such as drainage (Holden *et al.* 2004), afforestation (Martikainen *et al.* 1995), rotational burning (Yallop *et al.* 2006), overgrazing (Tucker 2003), peat cutting (Tomlinson 2010) and commercial extraction (Soini *et al.* 2010). Inappropriate management has altered the condition of British peatlands so that only 18 % of upland blanket bogs are in a natural or near natural condition

(Littlewood *et al.* 2010), potentially altering the balance between primary productivity and decay turning some peatlands from carbon sinks to carbon sources.

In their natural state peatlands provide a range of highly valuable ecosystem services, including carbon storage, river flow regulation, drinking water provision, biodiversity, food and fibre provision and cultural services (Grand-Clement *et al.* 2013b). Anthropogenic pressures e.g. burning are known to alter the ecosystem services provided by a blanket bog however, the application of this concept to economic valuation and policy decisions remains problematical. Evans *et al.* (2014) developed a series of pressure-response functions for a blanket bog in order to evaluate how multiple, often interacting, anthropogenic pressures affect a range of ecosystem services, many of which are economically intangible e.g. amenity value. Vegetation condition functioned as an intermediary; responding to anthropogenic pressures (e.g. drainage) and controlling ecosystem functions (e.g. CO_2 emissions) which support ecosystem services (e.g. climate regulation).

The biodiversity of peatlands has been recognised and protected though legislation such as the European Union Habitats Directive and UK Biodiversity Action Plan Priority Habitats (Littlewood *et al.* 2010). Initially restoration occurred primarily to protect these ecosystems; funded through agricultural subsidies (Lunt *et al.* 2010). In light of the impact of degraded peatlands on drinking water provision some UK water companies have chosen to fund peatland restoration rather invest in energy and chemical intensive treatments downstream e.g. United Utilities funded restoration of blanket bogs within the Pennines (Anderson *et al.* 2011) and South West Water funded restoration of blanket bogs in Exmoor and Dartmoor (Grand-Clement *et al.* 2012).

Since the inclusion of wetland rewetting as a specific activity under Article 3.4 of the Kyoto Protocol, governments can include emission reductions resulting from restoration since 1990 in their international greenhouse gas accounting (IPCC 2014). Peatland restoration has been identified as “amongst the most cost-effective options for mitigating climate change” Achim Steiner, Executive Director UN Environment Programme (from Bain 2011).

Interest from private investors in funding restoration is also increasing. The compliance carbon market was established via the Kyoto Protocol, primarily for climate mitigation, however, there are currently limited opportunities to apply this to land use projects within the UK (Bonn *et al.* 2014) due to low voluntary carbon prices and high verification and accreditation costs. Within the voluntary carbon market, businesses are prepared to pay a premium to restoration projects connected to their business and those which provide multiple corporate social responsibility benefits in addition to climate change mitigation (Reed *et al.* 2013). Most voluntary carbon markets use a Greenhouse gas Emission Site Type (GEST) approach, where species assemblage is used as a proxy for greenhouse gas emissions (Couwenberg *et al.* 2011). This approach should reduce the verification costs making the peatland carbon market more viable. In 2011 there were no default international emission factors for most UK peatland management practices (Birkin *et al.* 2011) including *Molinia caerulea* dominated uplands. A need to quantify emissions from a wider range of vegetation and management types was identified (Evans *et al.* 2011) to support emerging carbon markets.

2.4 Current Knowledge on the Effects of Drainage and Ditch-Blocking on Water Table Depths, Vegetation Composition and CO_2 Fluxes

2.4.1 Drainage

Historically drainage has been carried out primarily for agricultural improvement to both arable and pastoral lands or to support forestry (Sjörs 1980) consequently drained peatlands are widespread across Europe. In Britain although some peatland drainage occurred from the 19th century most of the upland drainage of blanket bogs occurred during the 1960s and 1970s in a drive to increase food production (Holden *et al.* 2004). It was hoped drainage would improve the quality of vegetation for grazing and game bird rearing as well as ensure the safety of stock (Ratcliffe and Oswald 1988). It was estimated that 21 % of English blanket bogs were drained (Natural England 2010). Despite the presence of contoured or herring-bone pattern drainage systems, there was

no evidence that grouse populations increased (Stewart and Lance 1983) or that the drained moors were capable of sustaining higher stocking densities (Holden *et al.* 2004).

Drainage ditches alter the flow pattern of a blanket bog by locally draining the catotelm (Coulson *et al.* 1990, Wilson *et al.* 2010, Holden *et al.* 2011). Water tables are generally deeper closer to the ditch although other factors such as position upslope or downslope of the drain and microtopography also influence water table depths (Wilson *et al.* 2010, Holden *et al.* 2011, Luscombe *et al.* In prep). A network of drainage ditches creates connected pathways for overland flow (Holden *et al.* 2004). This alters the run-off production from the bog and consequently reduces the water retention (Holden *et al.* 2004). The drained, shallow peatlands of Exmoor were found to exhibit a flashy run-off response and poorly maintained baseflows (often close to 0 $m^3 s^{-1}$) with total rainfall explaining 38 to 83 % of variation in total discharge across a range of ditch sizes (Luscombe *et al.* In Review).

In a pristine mire, the water table lies close to or at the surface much (>80 %) of the time (Holden *et al.* 2011). Drainage typically lowers the mean water table by only a few centimetres but the water table is then subject to larger and more frequent fluctuations (Wilson *et al.* 2010, Holden *et al.* 2011). This increases the depth to which oxygen can penetrate allowing aerobic respiration to occur. Aerobic respiration is more efficient at releasing energy from organic matter than anaerobic respiration so there is a resultant increase in decomposition (Silvola *et al.* 1996a) and CO_2 flux from the peat, and a decrease in organic matter reaching the catotelm and therefore peat formation.

Decomposition may also be enhanced in a drained mire due to an 'enzymic latch' mechanism (Freeman *et al.* 2001). Phenol oxidase, an enzyme able to fully degrade phenols, requires molecular oxygen to function and is therefore inhibited in anaerobic conditions allowing phenols to accumulate (Freeman *et al.* 2004). As phenols inhibit the activity of other enzymes, which may not themselves be oxygen limited, decomposition is further reduced. If the peat becomes aerated, through drainage for example, phenol oxidase activity is

stimulated, reducing the concentration of phenolic compounds so enzymes are no longer inhibited and decomposition increases (Fenner and Freeman 2011).

Drainage has also been shown to reduce the richness of species dependent on a water table close to the surface, particularly *Sphagnum* species (Bellamy *et al.* 2012) resulting in a plant community dominated by heathland species up to 15 m from the drain. Although historically present (Chambers *et al.* 1999) on Exmoor drainage may have contributed to the current dominance of *Molinia caerulea*. Murphy and Moore (2010) found drainage of an ombrotrophic bog also increased both above and below ground biomass particularly at depth. The potential effects of increased vascular plant cover and root biomass on CO_2 fluxes and soil carbon storage have been discussed above (section 2.1.5).

Lowering the water table from 1-5 cm above the soil surface to 0-5 cm below the soil surface was found to double ecosystem respiration from a subalpine fen (Chimner and Cooper 2003). No further increase in CO_2 emissions occurred as water tables were further lowered, suggesting the increase in CO_2 emissions was due to oxidisation of a labile carbon pool near the soil surface (Chimner and Cooper 2003). Total below-ground respiration rates were highest in the driest areas of a drained area of a Finnish raised bog compared to a pristine area however, the decomposition potential of the peat remained greater in the wetter areas (Jaatinen *et al.* 2007) indicating this labile organic pool was depleted over time by drainage. The ratio of humic to fulvic acids in dissolved organic carbon exported from the drained, shallow peats of Exmoor indicates the labile carbon pool has already been depleted and the remaining peat is more humified (Grand-Clement *et al.* 2014).

In short-term (2 year) field manipulations of water table depths, ecosystem respiration increased when the water table was lowered by 7 cm in an Alaskan wet sedge tundra but photosynthesis showed a small and variable change so that the drained plots were a net source of CO_2 (Oechel *et al.* 1998). Over an eight year experiment in a Canadian poor fen water tables were lowered by ~20 cm. This was sufficient to change the vegetation community, *Sphagnum* cover decreased on hummocks but increased in hollows whilst Sedges increased on lawns. Ecosystem respiration was significantly greater at the

drained site but whilst photosynthesis declined at the hummocks it increased in the lawns and hollows (Strack *et al.* 2006). This experiment shows how CO_2 fluxes are dependent on ecohydrology and different nanotopes may respond to drainage in different ways dependent on their initial ecology and water table depth as well as the relative magnitude of drainage.

In a Czech upland ombrotrophic bog, drainage was found to increase both photosynthesis and ecosystem respiration over the growing season (Urbanová *et al.* 2012). This was attributed to changes in vegetative green area and vegetation composition, in particular increased grass coverage. The greatest fluxes of CO_2 were reported where the bog was dominated by *Molinia caerulea*. This is the only known study reporting photosynthesis and ecosystem respiration rates for a drained *Molinia caerulea* dominated peatland indicating the scarcity of knowledge of these ecosystems.

2.4.2 Ditch Blocking

A range of restoration techniques have been developed depending on the nature of the degradation including ditch or gully blocking with wood, peat, heather bales, plastic or stones; gully re-profiling and surface stabilisation with heather brash, coir, geojute or heather bales (Parry *et al.* 2014). Generally all techniques aim to re-establish high water levels and encourage the re-colonisation of peat forming species (especially *Sphagnum*) (Holden *et al.* 2004). Re-establishing a surface cover of *Sphagnum* has been identified as particularly important where restoration aims to increase carbon sequestration (Lunt *et al.* 2010).

The most commonly reported restoration technique, possibly due to the prevalence of drainage, is ditch blocking. A series of blocks or dams are placed along a ditch to prevent the rapid flow of surface water along the drains. “Leaky” dams decrease flow velocities and trap sediment upslope of the dam reducing erosion, whilst impermeable dams form small pools upslope of the blocks locally raising the water table. These methods were mostly developed on deeper peats but have been adapted to the environmental and cultural conditions present on Exmoor (Grand-Clement *et al.* 2015).

Studies on the effects of restoration have traditionally focused on hydrology (Wilson *et al.* 2010, Holden *et al.* 2011), water quality (Wilson *et al.* 2011) and vegetation composition (Haapalehto *et al.* 2010, Bellamy *et al.* 2012) reflecting the initial aims of restoration (Parry *et al.* 2014). Within three years of blocking ditches in a Welsh blanket bog the water table had risen by an average of 2 cm but still remained up to 10 cm below the ground surface (Wilson *et al.* 2010). Additionally, water retention and storage increased compared to areas with unblocked ditches. Although ditch blocking reduced the frequency and magnitude of water table fluctuations (Wilson *et al.* 2010, Holden *et al.* 2011) a restored blanket bog had not recovered the hydrological functioning of a pristine mire even after 6 years (Holden *et al.* 2011). Fluctuating water table depths intermittently relieve the build-up of anaerobic respiration products (dissolved organic carbon, nitrite, ferrous iron, hydrogen sulphide and methane) and regenerate electron acceptors (nitrate, ferric iron and sulphate) used by microbes to respire thereby enhancing anaerobic respiration (Blodau and Moore 2003a, b, Goldhammer and Blodau 2008, Knorr *et al.* 2009). Therefore, a restored bog should not be expected to return to the CO_2 flux baseline of a pristine bog rapidly even if the mean water table depth is restored (Silvola *et al.* 1996a).

No change in hydrolase enzyme activity was observed in porewater from a blocked ditch compared to a control in a Welsh blanket bog 4 to 9 months following restoration (Peacock *et al.* 2015). It was suggested that enzyme activity, which had been stimulated by drainage, was not supressed by the presence of phenol oxidase following restoration as re-wetting had not increased soil moisture and therefore reduced oxygen availability. Fenner and Freeman (2011) suggested it would take months to years for the decomposition rate to return to pre-drainage levels once water table depths stabilise, as the microbes and soil enzymes have been stimulated by increased labile carbon and nutrients.

Although *Molinia caerulea* is a wetland species evolved to live in waterlogged conditions, vegetation often close stomata in response to raised water tables; this limits gases exchange through the leaf surface limiting the availability of

CO_2 for photosynthesis and ability to release waste products from photosynthesis (O_2). Both reduced CO_2 and increased O_2 inhibit the rate of photosynthesis (Pezeshki 2001). *Sphagnum squarrosum* and *Sphagnum angustifolium* growing in the tundra areas of Alaska reduced photosynthesis once the water content rose above optimal conditions (Murray *et al.* 1989) as the diffusion of CO_2 to photosynthetically active sites was limited. Plant stress may be expressed by early senescence (Bubier *et al.* 2003), reduced above- and below- ground primary productivity (Murphy and Moore 2010) and/or altered reflectance particularly at specific wavelengths e.g. 920 nm, 1200 nm (Harris *et al.* 2005) and 531 nm (Gamon *et al.* 1997). However, most remote sensing systems, with the exception of airborne hyperspectral systems cannot deliver sufficient spectral and spatial resolution to scale this up necessitating a structural approach. Water stress would be expected to have a direct effect on photosynthesis and autotrophic respiration and an indirect effect on heterotrophic respiration though changes in leaf litter and root exudates. Over time a stressed plant may be outcompeted and replaced by a species better adapted to the new conditions.

The recovery of vegetation is likely to be even slower than the recovery of hydrological functioning. Two sites on Exmoor that were assigned National Vegetation Classification (Rodwell 1991) type of M25 *Molinia caerulea – Potentilla erecta* mire prior to restoration were classified three years post-restoration as M6a *Carex echinata* sub-community and M6d *Juncus acutiflorus* sub-community both of which are underlain by a *Sphagnum* carpet (Barrowclough 2014). A third site remained M25, arguably due to failure of the ditch block preventing continued drainage. However, the percentage cover of species indicative of bog recovery in Forsinard Flows blanket bog UK (*S. cuspidatum, S. papillosum, S. capillifolium, Eriophorum angustifolium*, dead *Calluna vulgaris* and open water) continued to increase from 10 to 25 % between 4 and 11 years after drain blocking (Bellamy *et al.* 2012). After 10 years, the total cover of *Sphagnum* mosses in a Finnish ombrotrophic bog had increased from 20 % to 50 % but many species found in pristine bogs were still absent (Haapalehto *et al.* 2010). This indicates although a fairly rapid initial

change in vegetation may occur it will take longer (>10 years) for vegetation communities typical of pristine bogs to re-establish.

Studies on CO_2 fluxes in peatlands have generally been focused either on, a) determining carbon budgets (Worrall *et al.* 2009, Dinsmore *et al.* 2010) or net ecosystem exchange (Laine *et al.* 2006, Riutta *et al.* 2007) over annual timescales and large extents (≥300 m radius) or b) investigating the controls on gas fluxes such as temperature and water table (Bubier *et al.* 2003), vegetation (McNamara *et al.* 2008) and leaf area (Street *et al.* 2007) in finer spatial extents (≤1 m) over sub-annual timescales. Few studies have focused on the effects of restoration on gas fluxes.

Although Urbanová *et al.* (2012) included an upland Czech drained *Molinia caerulea* dominated ombrotrophic peatland in their study, the restored peatlands were dominated by *Vaccinium myrtillus, Vaccinium uglinosum, Sphagnum magellanicum and Sphagnum cuspidatum* with no significant change in plant community reported due to restoration. It is therefore not possible to separate the effects of restoration from the effects of vegetation composition.

Komulainen *et al.*(1999) measured the effects of restoration of CO_2 fluxes over three years at two sites in a Finnish ombrotrophic low-sedge bog; one site remained drained throughout, the other was restored at the end of the first year. The response of gross photosynthesis to a prolonged rise in water tables of 20-25 cm varied with vegetation composition. *Calluna vulgaris* located in a hollow became waterlogged and photosynthesis significantly decreased, an increase in typical hollow species (*Andromeda polifolia*, *Vaccinium oxycoccos* and *Vaccinium microcarpum*) was not sufficient to compensate for this. However, on hummocks the vegetation composition changed towards *Empetrum nigrum* which significantly increased gross photosynthesis (640 to 870 mg m^{-2} h^{-1}). Despite having lower rates of photosynthesis, the hollows were larger seasonal (May–September) CO_2 sinks (101 gC m^{-2}) than the hummocks (54 gC m^{-2}). The un-restored sites were much smaller CO_2 sinks (3 gC m^{-2}) primarily because the rates of soil respiration were twice as high in the drained sites than the blocked sites.

There is no similar work at present for blanket bogs in Britain where mean annual temperatures are higher than in Finland. In British blanket bogs, the response of temperature-dependent processes such as ecosystem respiration (Komulainen *et al.* 1999, Bubier *et al.* 2003, Laine *et al.* 2006, Riutta *et al.* 2007), root-derived respiration (Heinemeyer *et al.* 2011) and soil respiration (Silvola *et al.* 1996a) would be expected to be greater due to the warmer soil temperatures. Unlike Finnish bogs which are frozen for several months of the year British bogs have a prolonged growing season and continue to exchange CO_2 all year (Lindsay 2010).

Clay *et al.* (2012) and later Dixon *et al.* (2013) compared the effects of a range of restoration techniques (seeding with grass, geojute cover, *Calluna vulgaris* mulch or plastic dams) on CO_2 fluxes from erosional gullies in British blanket bogs. Photosynthesis and ecosystem respiration were greatest in the naturally re-vegetating gully and least in the bare soil gully due to the type or absence of vegetation. Vegetation also controlled the spatial distribution of CO_2 fluxes with greater fluxes from the gully floors than the gully walls and interfluves (Clay *et al.* 2012). Gullies where re-vegetation and slope stabilisation were carried out were found to be the largest CO_2 sinks and bare peat sites were the largest sources (Dixon *et al.* 2013). These erosional gullies are generally larger (up to 3 m) than drainage ditches, the underlying peat is thicker (2-3 m) and the peat surface is often bare prior to restoration consequently the techniques used for restoration differ. Therefore, even though these peatlands share a similar climate to Exmoor they do not offer a direct comparison with the shallow, *M. caerulea* dominated, drained peatlands.

2.5 MONITORING APPROACHES

2.5.1 Carbon Dioxide Fluxes in the Field

2.5.1.1 EDDY COVARIANCE METHODS

Eddy covariance methods of estimating CO_2 fluxes allow non-intrusive, direct and continuous ecosystem scale measurements at both sub-hourly and annual timescales (Baldocchi 2003). The widespread use of these methods is due, in

part, to the standardisation of protocols across international research initiatives such as FLUXNET, a network of over 650 towers across five continents focused in Europe, north America, Japan and Brazil (Baldocchi *et al.* 2001). Characterising the footprint of eddy covariance towers is challenging and varies over time with meteorological conditions, in particular wind speed and direction. It would not be possible to distinguish the effect of restoration on CO_2 fluxes unless the entire area of the footprint is homogeneous and under the same management. Conversely to scale up to a landscape scale the footprint is too small and measurements are site specific. Currently there are no standard methods for scaling site specific measurements to regional estimates using other proxies (e.g. vegetation classification/structure). Remote sensing measurements could be used to upscale but the discrepancy between pixel size and footprint size must be addressed.

To separate net ecosystem exchange into photosynthesis and ecosystem respiration flux partitioning algorithms are required. These extrapolate the measured night-time ecosystem respiration into the daytime using a temperature response function (Reichstein *et al.* 2005). Ideally eddy covariance towers would be sited on flat ground where the vegetation is homogeneous within the footprint (Baldocchi 2003), although the vegetation of Exmoor is dominated by *Molinia caerulea* the topography is not flat. In addition wet or still weather results in data gaps (Laine *et al.* 2006). On the moors where wet weather is frequent, data gaps could be numerous and potentially extensive. Additionally the logistical requirements (e.g. reliable power source) and primarily the initial cost prevent its use in this study.

2.5.1.2 CHAMBER METHODS

Chambers have frequently been used to measure CO_2 fluxes as they are easy to use, relatively inexpensive (Pumpanen *et al.* 2004) but are labour intensive. Gas flux chambers enable the measurement of fluxes over an extent at which fluxes can be attributed to processes e.g. different vegetation types, drained/blocked management etc. understanding these processes allows the prediction of responses in other areas or under different conditions. By varying light levels within the chamber, photosynthesis and ecosystem respiration can

be separated experimentally. Although systems can be automated usually the frequency of chamber measurements is such that estimation of annual fluxes requires models based on empirical relationships with other variables e.g. water table depth, leaf area index.

There are three main chamber systems (Norman *et al.* 1997); closed-dynamic, closed-static and open chamber. Air is circulated between the chamber and an external infra-red gas analyser (IRGA) in the closed-dynamic method. Gases with carbon-oxygen bonds strongly absorb infrared light at 4.26 microns. An IRGA measures the concentration of CO_2 in a gas sample by detecting the absorption of an emitted infrared light source at this wavelength. The chamber is closed for short periods of time (up to 5 minutes) during which time the IRGA continuously measures the concentration of CO_2, fluxes are determined from the change in CO_2 concentration over time (e.g. Shaver *et al.* 2007). Although the chamber alters conditions (e.g. temperature, air pressure, humidity, CO_2 accumulation/depletion) within the chamber, the short sampling time limits the effect of this on the vegetation and soil within the chamber. The short sampling time also enables more samples to be collected within a day allowing either greater spatial or temporal sampling.

Closed-static chambers are left in place for longer, typically >20 minutes, during which time gas samples (three or four) are collected using syringes and analysed by gas chromatography in the laboratory (Norman *et al.* 1997). Again fluxes are determined from the change in CO_2 concentration over time, however, due to the reduced number of measurements static chambers are more vulnerable to error than dynamic chambers (Norman *et al.* 1997). Compared to a LiCor Li-6200 closed dynamic system the closed static chambers tested underestimated CO_2 fluxes and required a correction factor of 1.3 and 1.45 for samples collected after 10 minutes, this increased for samples collected after 30 minutes (Norman *et al.* 1997). A dynamic closed chamber also underestimated CO_2 (1.10 correction factor) whilst the open chamber overestimated CO_2 fluxes (0.93 correction factor). In addition the longer closed period may alter conditions within the chamber sufficient to effect CO_2 fluxes, although the use of fans and pressure equilibration balloons aims to minimise

this. As this system does not require an IRGA it is not limited to dry weather conditions, guaranteeing a more regular sampling frequency.

A continuous stream of air is passed through an open chamber system and the CO_2 flux determined from the difference in CO_2 concentration between the inflow and outflow (e.g. Kutsch *et al.* 2001). This system enables short-term temporal responses to be monitored e.g. temperature responses however, extended use at the same location alters conditions within the chamber so that fluxes measured are not representative of the wider ecosystem (Norman *et al.* 1997).

Many gas flux chambers sit upon and make an airtight seal with a collar inserted up to 30 cm (Riutta *et al.* 2007) into the ground. However, collars inserted only a few centimetres sever fine roots near the soil surface decreasing root respiration by an average of 15% (Heinemeyer *et al.* 2011) and reduce lateral water flow resulting in waterlogging. Alternatively the gas flux chamber can be rested on permanently installed legs (as in Shaver *et al.* 2007, Street *et al.* 2007) to ensure the same area is being monitored over time and that the hydrological properties of the peat are not altered.

2.5.1.3 Partitioning Below ground Respiration

Net ecosystem exchange will not provide information on the individual responses of soil-derived and root-derived respiration to ditch blocking; these fluxes are small compared to NEE but are key in determining the amount of organic matter reaching and being stored in the catotelm (see section 2.1.3). It is likely these components will have distinct responses to ditch blocking as soil-derived CO_2 efflux is known to depend mainly on organic matter content and its recalcitrance, soil temperature, moisture content and aeration, whilst root-derived respiration is primarily driven by photosynthesis (Kuzyakov and Larionova 2005). Few studies on the effects of restoration have partitioned respiration into root-derived and soil-derived respiration despite their importance in carbon storage and potentially different and contradictory responses to restoration.

Trenching and clipping are inexpensive, simple and established methods to separate heterotrophic and autotrophic components of below ground respiration subject to well documented uncertainties (Subke *et al.* 2006). Clipping removes the above-ground vegetation ensuring only below-ground fluxes are measured. Trenching excludes live roots allowing for the measurement of the below-ground heterotrophic component.

The effect of trenching can be small and ambiguous for a period, possibly a year (Silvola *et al.* 1996b), following installation. Trenching initially overestimates heterotrophic respiration and therefore underestimates autotrophic respiration as severed residual roots decompose. Severed roots have been found to contribute as much as 12 % of heterotrophic respiration (Subke *et al.* 2006). This can be corrected for by, for example, the buried-root-bag method (Lee *et al.* 2003). The trench must be sufficiently deep to sever the deepest roots and of sufficient diameter around the collar to prevent diffusion of CO_2 into the trenched area from nearby roots (Bond-Lamberty *et al.* 2011).

Silvola *et al.* (1996b) isolated soil-derived respiration in a Finnish peatland using trenching and clipping, they used plastic lining to prevent root in-growth however, linings significantly alter the hydraulic properties of the peat. Removing roots reduces water uptake in the trenched area this can also induce water logging within the collar (Subke *et al.* 2006). Conversely clipping reduces shading to the soil surface increasing evaporation potentially drying out the collar. In one study soil moisture was found to be higher in trenched plots. but no impact on respiration rates was observed (Makiranta *et al.* 2008). In addition clipping removes litter from the surface of the peat reducing inputs of labile carbon which can cause total soil efflux to decrease by 7-25 % (Makiranta *et al.* 2008) over time.

Other methods have been used to partition respiration in different soils but these are not appropriate for peat. Physical separation of components (e.g. roots, soils, leaf litter etc. (Subke *et al.* 2006)) of peat is very difficult given it is almost entirely made up of partly decomposed vegetation. Substrate induced respiration is used to separate heterotrophic from autotrophic components by adding glucose to stimulate heterotrophic respiration. However, it is only useful

at moisture levels of between 10 and 80 % (Kuzyakov and Larionova 2005) and peat has a soil moisture of 85 to 98 % (Lindsay 2010). Any incubation experiment involves disturbance to the peat in removing a core. Controlling the environmental conditions enables a single factor to be investigated but the unnatural conditions and very fine temporal and spatial scales make upscaling problematic.

2.5.2 Vegetation Phenology, Biomass, Structure and Composition

Photosynthesis is strongly dependent on vegetation phenology (e.g. Richardson *et al.* 2007), health (e.g. Benner *et al.* 1988), structure (e.g. Dixon *et al.* 2015), biomass (e.g. Nieveen *et al.* 1998) and composition (e.g. Laine *et al.* 2007) all of which can vary both spatially and temporally. As the microtope reflects changes in peat formation and drives changes in carbon storage (see section 2.2.1) it is most appropriate to measure changes in vegetation at this scale. Measuring the vegetation characteristics over time may provide a proxy to measure temporal changes in peat formation and carbon storage. Measuring vegetation characteristics across a landscape extent offers a potential means of upscaling gaseous carbon exchange.

To upscale fluxes spatially using models and parameters derived from plot scale measurements, gaseous fluxes are usually linked to either nanotope dependent or nanotope independent variables. Where fluxes are associated with a particular nanotope (e.g. hollow, tussock etc.) the fluxes can be estimated for each nanotope type and then summed based on areal extent (Laine *et al.* 2006, Riutta *et al.* 2007). Alternatively a single set of parameters weighted by the areal extent of each nanotope can be used to estimate landscape scale fluxes. Both flux and parameter upscaling methods require a detailed knowledge of the spatial distribution of nanotopes. This traditionally has been mapped using aerial imagery from aeroplanes or satellites but the use of unmanned aerial vehicles is rapidly developing (see section 2.5.2.1).

Alternatively gaseous fluxes may be linked to nanotope independent variables (e.g. LAI (Shaver *et al.* 2007) and biomass (Lafleur *et al.* 2003)) in which case the distribution of these variables across the landscape and/or over time is required to enable upscaling. Methods to measure either the spatial distribution

of nanotopes and/or key variables such as water table depth and LAI at a fine scale (<<1 km^2, daily) over a broad extent are discussed below (see section 2.5.2.2 and 2.5.2.3).

2.5.2.1 VEGETATION COMPOSITION AND CLASSIFICATION

Vegetation composition is increasingly being used as a proxy when estimating greenhouse gas emissions, especially for carbon trading (Couwenberg *et al.* 2011) as different vegetation communities have been shown to have different NEE rates. The distribution of these communities often varies in space (and time) in response to the mean water table (Laine *et al.* 2007). However, the ability of a plant to withstand a rise in water tables is related to its ability to cope with being waterlogged but also competition from other plants better suited to wetter conditions. Therefore, vegetation community may also change in time, particularly following a perturbation such as ecohydrological restoration.

At the plot scale vegetation composition is usually monitored by visual inspection, a labour intensive and subjective method that requires considerable plant identification skill. With this method vegetation cover can be identified to the species level. Errors of up to 20 % cover occurred due to variation in species morphology, distribution and incorrect identification of species by the same observer over a ten day period in lower strata of *Pinus contorta* stand (Kennedy and Addison 1987). Multiple observers achieved only 34 % agreement in National Vegetation Classification mapping of an area of dry heath, wet heath, blanket bog and acid grassland at the community level (Hearn *et al.* 2011).

Manual interpretation of aerial photographs has been used to delineate features, such as bog islands (Glaser 1987). Increasingly pixel-based and object-based classifiers “trained” using either ground validated data (often based on manual surveys) or photo-interpretation are being used to classify vegetation communities (Morgan *et al.* 2010). Becker *et al.* (2008) demonstrated that in a heterogeneous boreal peatland aerial images with 100 cm pixels overestimated CO_2 uptake by 5 % compared to 6 cm pixels, mostly due to miss-classification of flarks (mud-bottomed pools). Increasingly unmanned aerial vehicles (UAV) are being used to collect red-green-blue aerial

photographs. The cost of these systems compared to an aircraft makes repeat flights feasible (Lelong *et al.* 2008), additionally the lower altitude flight path of UAVs, typically 50 to 100 m compared to 1000 to 2000 m for a piloted aircraft, allows a significant improvement in resolution (<5 cm if a high quality camera is used) compared to aircraft-based imaging (around 25 cm) thus enabling more of the finer scale 2-dimensional patterns and 3-dimensional structures to be captured. Digital photography from UAVs has been used to classify the vegetation (grass, tree and soil) within the footprint of eddy covariance towers in US rangelands using the red, green and blue spectral signatures of the landcover types (Vivoni *et al.* 2014). This enabled ground-based measurements of soil temperature and moisture to be aggregated by landcover to characterise the time-variable eddy covariance footprint. UAV digital photography has also been used to distinguish three land covers (water, floating vegetation and emergent vegetation) with a spatial resolution of 8.8 cm and 92 % classification agreement in a Canadian wetland (Chabot and Bird 2013). Using a colour near infra-red camera on a UAV Knoth *et al*. (2013) classified cut-over bog vegetation (bare peat, *Sphagnum, Eriophorum vaginatum* and *Betula pubescens*) with an accuracy of 91 % at a spatial resolution of 3 cm.

Where historic aerial imagery is available it provides a means of assessing vegetation change over longer timescales (Morgan *et al.* 2010). For example, aerial images with a 1 m resolution revealed changes in vegetation structure in a Swedish ombrotrophic mire between 1970 and 2000 (Malmer *et al.* 2005) explaining a loss 7-17 g m^{-2} a^{-1} of carbon over the 30 year period. Alternatively repeat UAV flights would enable future fine scale vegetation community changes to be quantified.

2.5.2.2 Vegetation Structure and Biomass

Fine scale structural characteristics of vegetation have been related to both environmental conditions and CO_2 fluxes across a range of landscapes. Examples include, in order of increasing scale, leaf area in Californian grasslands, Chaparral and woodlands (Gamon *et al.* 1995), vegetation green area in Czech peatlands (Urbanová *et al.* 2012), leaf morphology in boreal trees (Raich and Schlesinger 1992), *Calluna vulgaris* height (Dixon *et al.* 2015) in UK

blanket bogs, above-ground biomass in temperate grasslands (Flanagan and Johnson 2005), tree stand parameters (including basal area, stem diameter, height and volume) in forested bog margins (Karu *et al.* 2014), microtope type in an Irish blanket bog (Laine *et al.* 2006) and vegetation mapping in American rangelands (Vivoni *et al.* 2014). Structural changes occurring over two years following restoration are likely to be small and therefore a method that can measure small changes (<cm) repeatedly over a fine spatial extent (0.3 m^2) is required.

Airborne Light Detection and Ranging (LiDAR) typically has a vertical accuracy of <0.2 m, horizontal accuracy and support (footprint of the laser beam) are dependent on the flying height but range from 0.1-0.5 m and 0.2-1.0 m respectively. LiDAR has been shown capable of detecting vegetation structure (Lefsky *et al.* 1999, Straatsma and Middelkoop 2007, Vierling *et al.* 2008, Korpela *et al.* 2009) and microtopography (Rosso *et al.* 2003, Wang *et al.* 2009, Chassereau *et al.* 2011) at a landscape extent. For short vegetation (<1 m) a single echo may be returned (Morsdorf *et al.* 2006). Therefore, other methods are required to separate the ground and canopy surface such as inflection labelling (Straatsma and Middelkoop 2007) or statistical methods based on the vertical distribution of all first and last laser pulses (Hopkinson *et al.* 2004). A further restriction of LiDAR is that it cannot detect gaps smaller than the support (footprint of the beam) (0.2-1 m) this restricts the size of objects (e.g. tussocks, drainage ditches) which can be detected to those larger than the support. In the tussock grasses of Exmoor 0.5 x 0.5 m LIDAR returns have been found to be a mix of tussock top and ground surface (Luscombe *et al.* 2014b) demonstrating at present the horizontal and vertical resolution of LiDAR is insufficient to capture the full range of tussock structure as tussock height is underestimated.

Despite the disadvantages of LiDAR this could be useful as a benchmark to assess other, even more novel, methods. For example, off-the-shelf digital cameras mounted on UAVs are increasingly being used to derive digital surface models (DSM) over large extents at a fine resolution. A 2 cm resolution DSM of a 64 x 43 m Antarctic moss bed was derived using digital images collected from a multirotor UAV using Structure from Motion (SfM) software (Lucieer *et al.*

2014). SfM software identifies matching features, “keypoints”, in multiple overlapping photographs from different viewpoints (Snavely *et al.* 2008). The software then optimises the 3-dimensional location of these “keypoints” to form a point cloud, in an arbitrary coordinate system. Fixed wing UAVs are capable of covering a larger extent but their higher ground speeds and generally higher flight altitude, compared to multirotors, sometimes delivers data with a slightly coarser pixel resolution (Anderson and Gaston 2013).

Terrestrial laser scanning (TLS), has been shown to be capable of capturing the soil surface and vegetation structure of peatlands (Anderson *et al.* 2010, Luscombe *et al.* 2014b) at a suitable spatial resolution (<50 cm). However, a tracked vehicle was required to elevate the scanner tripod to reduce shadowing effects behind solid structures. Therefore, access issues as well as equipment cost, size and weight reduce the applicability of this method to isolated peatland areas. Again SfM software could be used, but this time at the plot scale. A 2.5 cm resolution 1 m x 1 m DSM was created from 273 photographs using SfM algorithms. The image derived DSM had a mean difference of -0.005 mm from a manually measured DSM, most of which was attributed to uncertainty in the manual DSM (Dowling *et al.* 2009).

2.5.2.3 PHENOLOGY

Molinia caerulea is the overwhelmingly dominant vegetation on the drained uplands of Exmoor. It thrives in open situations (e.g. moors, heaths, bogs, fens, mountain grasslands, cliffs and lake shores) on seasonally wet, acid sandy or peaty soils (Taylor *et al.* 2001). This perennial grass has striking seasonal behaviour; the onset of growth is delayed until mean air temperature increases to 10 °C (Taylor *et al.* 2001) so shoots do not start to develop until April to May, there is a second flush of growth in June-July (Jefferies 1915) before purple flowers occur in August, senescence starts in September and by November all the leaves are dead (Taylor *et al.* 2001) leaving a thick matt of leaf litter. Nieveen *et al.* (1998) found a *Molinia caerulea* dominated lowland raised bog swapped between a sink of CO_2 in June, July and August to a source of CO_2 from September to May with leaf area index (LAI), soil temperature and vapour pressure deficit (VPD) determining the flux of CO_2. LAI was strongly linked to

vegetation phenology rising from 0 when the first green leaves became visible to a maximum of 1.7 coincident with flowering then returning to 0 when only brown leaves remained.

The timing of the onset of shoot growth, flowering and senescence in *M. caerulea* as well as the biomass produced will vary from year to year influenced by environmental conditions. Identifying the timing of these events is important in modelling CO_2 fluxes, in particular knowing when an ecosystem swaps between net CO_2 uptake and release aids understanding of the overall carbon balance of that ecosystem.

Often abiotic variables (e.g. degree-days, temperature thresholds, day length) are used as a proxy for seasonal vegetation development in CO_2 flux models (e.g. Schneider *et al.* 2012). However, vegetation is sensitive to a range of abiotic (water stress, frost damage, nutrient availability etc.) and biotic (competition and grazing etc.) factors that are not readily captured by abiotic metrics. Traditional methods for estimating phenology require frequent and regular field visits subjectively determining the day-of-year of specific events such as first leaf appearance, first flowering and first leaf fall of a given specimen. These use discrete days to describe events such as leaf growth which occur over a period of several weeks. They describe the phenology of an individual plant or plants rather than the plant community and are site specific and therefore not transferable even over short distances.

Direct methods for estimating biomass or LAI are time consuming and often destructive (Breda 2003) preventing their use as a measure of phenology. Indirect methods such as downward-facing photography (Weiss 2010), hemispherical photography (Demarez *et al.* 2008) and canopy analysers (Garrigues *et al.* 2008) allow an area to be re-sampled to capture temporal variation but significantly underestimate LAI (Breda 2003). More crucially these proximal remote sensing methods have a small footprint so multiple repeats are required to describe heterogeneous landscapes and increasing temporal resolution greatly increases labour requirements.

Satellite data have repeated global coverage at a range of spatial and temporal scales making these a viable tool for monitoring vegetation phenology at regional scales. The commonly used Normalised Difference Vegetation Index (NDVI) derived from Moderate resolution Imaging Spectroradiometer (MODIS) data has been shown to predict melt-out, start of growth and end of growth in the Alps to within 1.5 ±12.4 days (Fontana *et al.* 2008) whilst Advanced Very High Resolution Radiometer (AVHRR) NDVI data correlated with end of season phenophases in northern China (Chen *et al.* 2001). MODIS-NDVI has also correlated with LAI (r=0.9) and fraction of photosynthetically active radiation absorbed (fPAR) (r=0.95) again in the Alps (Rossini *et al.* 2012) and explained between 39 and 71 % of the variability in photosynthesis in northern peatlands (Kross *et al.* 2013). MODIS Enhanced Vegetation Index (EVI) together with photosynthetically active radiation was found to predict up to 85 % of variation in gross primary productivity (GPP) in a Swedish peatland (Schubert *et al.* 2010).

The choice of satellite data to use when monitoring vegetation phenology requires the user to make decisions that trade-off between temporal, spatial and spectral resolution as well as cost. Worldview 2 has a 4 day revisit time and a spatial resolution of 50 cm for panchromatic data or 1.84 m for multispectral data but is prohibitively expensive. Comparing freely available multispectral data, Landsat data has the finest spatial resolution (30 m) but a 16-day repeat cycle whereas AVHRR has a daily repeat cycle but 1000 m spatial resolution. MODIS has processed products at 250, 500 and 1000 m spatial resolutions for 4, 8 and 16 days. These sensors have distinct wavelength centres and bandwidths over which they are sensitive that influence the reflectance measured by a given band. Low spatial resolution may result in “mixed pixels” where a variety of species with distinct phenophases and differing micro-environmental conditions will occur within a single pixel (Fisher and Mustard 2007), whilst the accuracy in timing of phenological change becomes more uncertain as temporal resolution reduces (Zhang *et al.* 2009). Temporal resolution is often further reduced from that stated as observations are often of poor quality due to contamination by clouds and aerosols or high sensor

geometry angles. This has greatest impact if data gaps coincide with periods of rapid change.

Comparisons between ground-based discrete measures of the phenology of individual plants to continuous measures of whole plant communities by satellite have proven to be very difficult due to the aforementioned temporal or spatial scaling problems. Digital cameras and webcams capture images over a spatial extent (10s to 100s metres) between plot and satellite scales. Both web-cams (Richardson *et al.* 2007, Mizunuma *et al.* 2013) and repeat digital images from unattended year-round digital camera positions (Ahrends *et al.* 2008, Ide and Oguma 2010, Migliavacca *et al.* 2011, Sonnentag *et al.* 2012) have been used to track vegetation phenology in a range of ecosystems. Digital cameras can be automated to provide a high temporal resolution (sub-daily) record capturing colour on a continuous scale allowing the progressive green-up or senescence to be captured. If a standard processing protocol is used the data are objective and optically meaningful in relation to satellite data and the images remain as a permanent record that can be useful for data interpretation. Vegetation indices derived from digital cameras have been found to be related to NDVI measured at both at the field scale (Richardson *et al.* 2007) and by satellite (r^2 = 0.62) (Westergaard-Nielsen *et al.* 2013).

Besides identifying the timing of phenological events (Ide and Oguma 2010) vegetation indices derived from digital images have been directly related to primary productivity in subalpine pastures (r^2=0.79) (Migliavacca *et al.* 2011), northern mountain fen (r^2=0.85) (Westergaard-Nielsen *et al.* 2013) and deciduous broadleaf forests in all weather (r^2=0.4 to 0.46) (Mizunuma *et al.* 2013) and only on sunny days (r^2=0.85 to 0.90) (Saitoh *et al.* 2012). Additionally vegetation indices have been used as a measure of physiological capacity to scale CO_2 models driven primarily by photosynthetically active radiation (Migliavacca *et al.* 2011, Zhou *et al.* 2013).

2.6 SUMMARY

The literature presented here demonstrates an increasing interest in, and understanding of, the controls and feedbacks of peatland function including

water table depths, vegetation composition and CO_2 fluxes within pristine, drained and restored peatlands. The majority of these studies have been focused on *Sphagnum* dominated peatlands, the most common peat forming vegetation. The few studies in *M. caerulea* dominated peatlands (Nieveen and Jacobs 2002, Urbanová *et al.* 2012) have demonstrated distinct functional traits (e.g. greater biomass and seasonal variation) that influence CO_2 fluxes, which at present remain poorly characterised. This study aims to increase understanding of the controls on, and magnitudes of, CO_2 fluxes from *Molinia caerulea* peatlands. These distinct functional traits, including a tolerance to high and fluctuating water tables (Jefferies 1915) and vegetation dominance, have made transferring the recorded effects of ditch blocking to these peatlands difficult. Assessing the short-term effects of restoration on water table depth, vegetation composition and CO_2 fluxes will add to a limited pool of experimental studies attempting to understand the effects of ditch blocking in a range of peatland types.

Drained peatlands are widespread across Europe and in these peatlands drainage features are often the primary control on ecohydrological process. Despite this no known studies have looked at the spatial distribution of the control of drainage ditches (rather than erosional gullies) on CO_2 fluxes. Investigating the impacts of functioning and blocked drainage ditches on water table depths, vegetation composition and CO_2 fluxes within these shallow maritime peatlands acknowledges the importance of these understudied features.

The peatlands of Exmoor are shallow (Bowes 2006) and lie at the southern limit of the peatland bioclimatic envelope (Clark *et al.* 2010) as such they may function differently to other peatlands. The following chapter provides more detail on the conditions and management across Exmoor, as well as the experimental design. This provides more site specific context for this study and enables a more informed comparison between this study and both the existing literature and future studies.

3 SITE DESCRIPTION AND OVERVIEW OF EXPERIMENTAL DESIGN

3.1 CATCHMENT SELECTION AND LOCATION

In order to understand the factors controlling CO_2 fluxes and predict the effect of restoration on other sites across the Southwest of England and in Exmoor in particular, locations were chosen to be characteristic of the widespread drained areas. Two areas of open moorland suitable for restoration were identified in consultation with Exmoor National Park Authority, The Environment Agency, Natural England and English Heritage. These small headwater catchments were chosen as they a, contained typical vegetation communities and species diversity; b, encompassed a range of environmental characteristics (e.g. slope morphology, aspect and peat thickness), c, included the expected variation in ditch width, depth and style and d, were in use as rough grazing, the most common land-use for these upland areas.

The permission and co-operation of the land owners and managers was vital in allowing the placement and installation of monitoring equipment, luckily these were both forthcoming at the chosen catchments.

The two catchments selected were Aclands (51°7’51.3N 3°48’44.4W) and Spooners (51°7’21.9N, 3°44’52.9W) (Figure 3.1). Aclands is slightly higher in altitude (425-465 metres above sea level (m asl)) than Spooners (380-445 m asl). Both catchments are underlain by the Morte Slates Formation. Long-term (1981-2010) average annual rainfall at nearby Liscombe (UK Meteorological Office 2012) (49°46’50.4N 7°31’07.6W) totals 1445 mm with mean monthly temperature ranging from a minimum of 1.1 °C in February rising to 18.6 °C in July and August. Both catchments are located within North Exmoor Site of Special Scientific Interest (SSSI). They have been classified as National Vegetation Classification class M25: *Molinia caerulea – Potentilla erecta* mires (Rodwell 1991).

Peat thickness is variable over short distances (e.g. 50 cm difference in 10 m), nonetheless of the estimated 65 km^2 (Merryfield 1977) of blanket bog present on Exmoor it is estimated 53 km^2 is less than 30 cm thick and 4 km^2 is greater

than 60 cm thick (Bowes 2006). The peat is underlain by thin (~15 cm) silty clayey palaeosols (Carey 2015) which contain significant quantities of organic carbon. For Spooners (63 ha) it has been estimated that 12,800 tC are stored in the peat and a further 9,500 tC are stored in the underlying palaeosols. This is a significant additional carbon store which could be preserved by restoration (Hornibrook 2015). In addition, these clay-rich palaeosols will limit downward seepage, due to low hydraulic conductivity, helping to maintain water tables near the surface in the overlying peat.

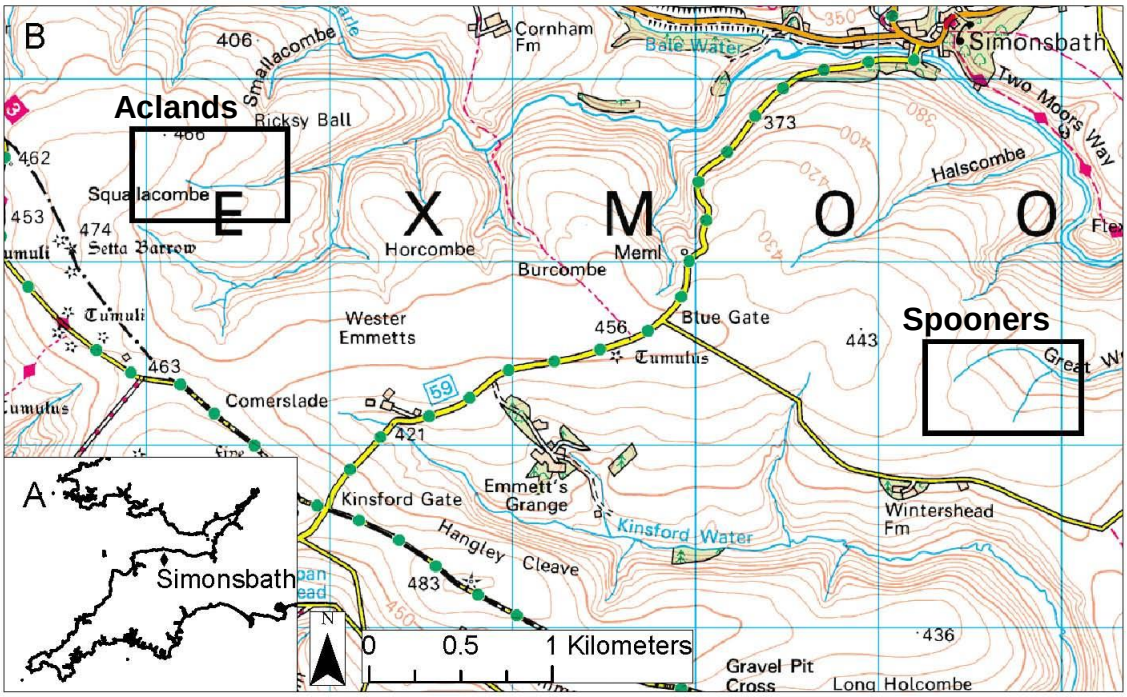

Figure 3.1 Location of study areas within Southwest England (a). Aclands lies to the west and Spooners to the east (b). (Ordnance Survey 2008a, d).

From the 1830s John Knight and later his son, Frederic Knight, constructed a series of surface drains aiming to reclaim and enclose the high moors of Exmoor for arable production (Hegarty and Toms 2009). Many miles of parallel surface drains were hand dug, they are of variable size with some measuring up to 1.5 m wide, nearly 1 m deep and at 10 to 45 m spacing. The Knight family were unsuccessful in reclaiming the high moors for arable production but the ditches remain visible and functioning. Between the 1960s and 1980s larger

ditches (>1.5 m wide) were dug by machine to drain specific areas such as springs (Mills *et al.* 2010).

Analysis of pollen in peat cores has shown that *Molinia caerulea* and *Calluna vulgaris* have alternatively dominated the moorlands of Exmoor (Chambers *et al.* 1999) indicating their presence but not their current dominance should be maintained following restoration. At Spooners cores collected for paleo-ecological analysis indicated a basal woody peat with *Sphagnum* overlain by an herbaceous peat with *Sphagnum.* Above a depth of 60 cm monocot rootlets dominated. Unfortunately preservation was insufficient to warrant further investigation (Fyfe *et al.* 2012). A core collected at Aclands from a raised-bog located in the valley bottom indicated that a sedge dominated peat surrounded by hazel woods slowly accumulated from ~8000 years before present to the first millennium AD. It is proposed that clearance of the hazel woodland (supported by the presence of charcoal and an abrupt change in all pollen taxa) increased wetness resulting in increased accumulation initially of a sedge dominated peat surrounded by alder woodland. Evidence of S*phagnum* appeared in samples dated to the 15th century. An abrupt shift in vegetation occurred at a depth of 9 cm (estimated to be mid-1940s) when *Sphagnum* disappeared from the macrofossil record, it is proposed this coincided with moorland drainage (Fyfe *et al.* 2014).

This core demonstrates the historic presence of peat forming *Sphagnum* on Exmoor from the 15th to 16th century and the abrupt shift circa 1940s (Fyfe *et al.* 2014). This indicates that although it is likely the current mire is inactive (section 2.1.1) with a haplotelmic structure (section 2.1.5) appropriate management could re-initiate peat forming conditions. Although due to anthropogenic influence over the last 1000 years there is no stable pre-drainage baseline vegetation assemblage to aim for (Fyfe *et al.* 2014).

At the start of the research project both catchments were scheduled for ecohydrological restoration in spring 2013 following a year of baseline monitoring. Restoration occurred at Spooners as planned in April 2013 but was delayed till April 2014 at Aclands due to legal negotiations. Restoration was funded by South West Water under the ‘Upstream Thinking’ programme

(Grand-Clement *et al.* 2012) and carried out by project partners, including Exmoor National Park Authority and the Environment Agency.

3.2 Within-Site Selection and Experimental Design

In order to investigate the spatial effect of ditches across the expected range of environmental conditions whilst maintaining statistical robustness a factorial design was used with site, distance from the drainage ditch and restoration as factors. Within each experimental catchment three pairs of sites (Figure 3.2) were selected so that each pair were as similar as possible in terms of vegetation, altitude, aspect, slope, peat depth, ditch dimensions and functionality, and initial wetness. One of the pair remained unrestored ('control') so that the effects of ditch blocking could be isolated from inter-annual variability whilst the other was restored following baseline monitoring. To ensure that gas fluxes measured were representative of all areas within the catchment it was necessary to measure both close to the ditch and at various distances in the inter-ditch areas. As ditches are unevenly spaced the location of plots within each site were also unevenly spaced, ⅛, ¼ and ½ of the distance to the adjacent ditch along a transect perpendicular to the ditch.

It was recognised that variation between sites (e.g. peat thickness, aspect etc.) may obscure relationships between environmental and vegetation variables and gaseous fluxes complicating mechanistic understanding. However, this study aimed to identify the processes driving gas fluxes in different environmental conditions so that fluxes can be upscaled for the whole catchment. It was therefore necessary to have three pairs covering a range of environmental conditions.

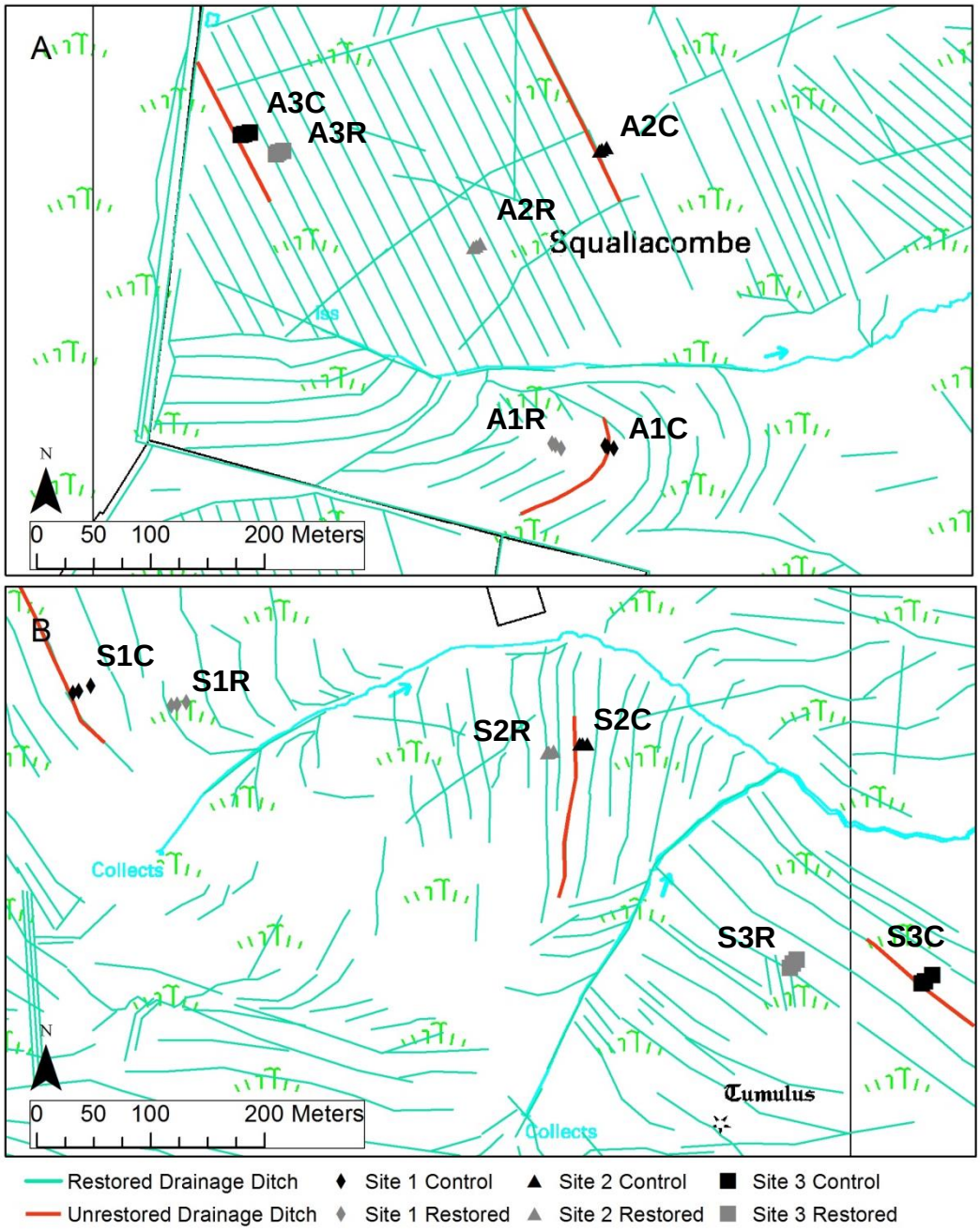

Figure 3.2 Location of control and restored paired sites within a, Aclands and b, Spooners. Plots were located ⅛, ¼ and ½ the distance between adjacent ditches. (Ordnance Survey 2008b, c)

Both catchments were dominated by *Molinia caerulea* with limited patches of *Juncus sp.* along flushes, bog species (e.g. *Sphagnum sp., Eriophorum vaginatum* and *Narthecium ossifragum*) especially in peat cuttings and wet heath species (e.g. *Calluna vulgaris and Erica tetralix*) near the watershed. In order to better understand the effect of restoration on vegetation change it was

decided to focus on areas dominated by *Molinia caerulea* prior to restoration in order that the effect of water table depths and vegetation composition could be separated until vegetation composition alters.

As the catchments are dominated by a deciduous grass they differ in colour and living biomass in summer (Figure 3.3) and winter (Figure 3.4). Although hand-dug drainage ditches cut deep (up to 50 cm) into the shallow peat (often <30 cm), they are not obvious from the ground particularly in the summer (Figure 3.3, Figure 3.5) but are striking when viewed and measured from a synoptic viewpoint from an overflying aircraft (Figure 3.6 and Figure 3.7).

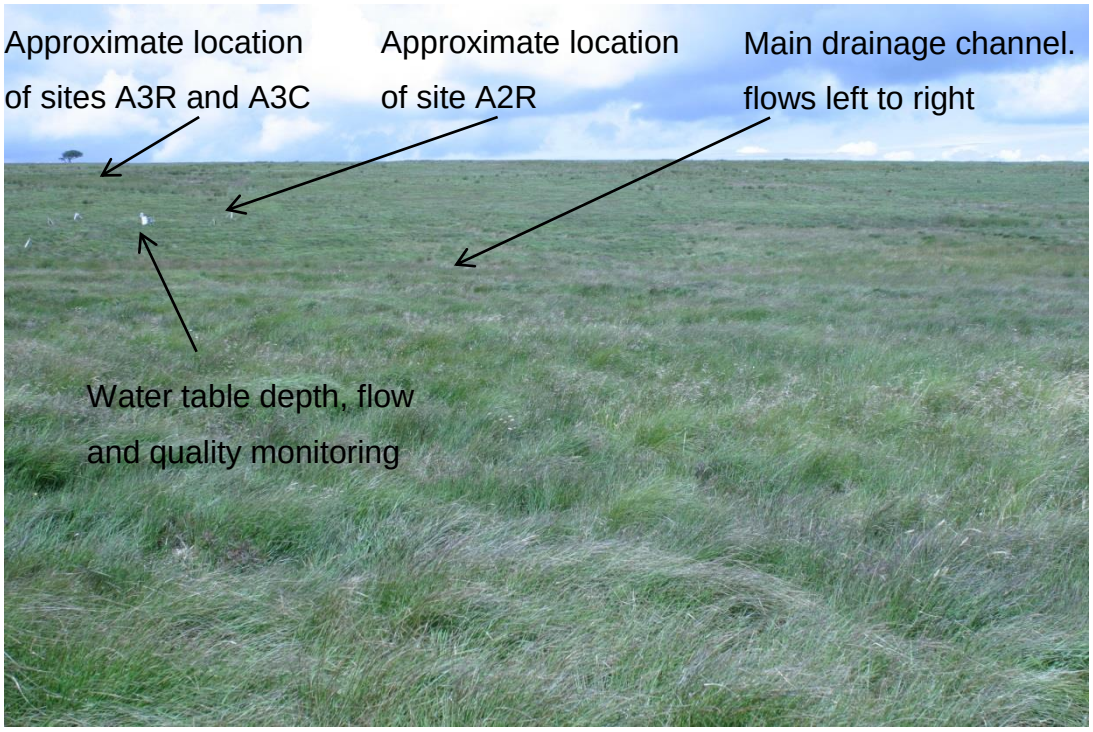

Figure 3.3 Aclands catchment in July 2012, pre-restoration. Looking north from site A1R across the main drainage channel towards sites A2R, A3R and A3C. The water table depth, flow and quality monitoring equipment can also be seen. Of note is the dominance of *Molinia caerulea* across the catchment.

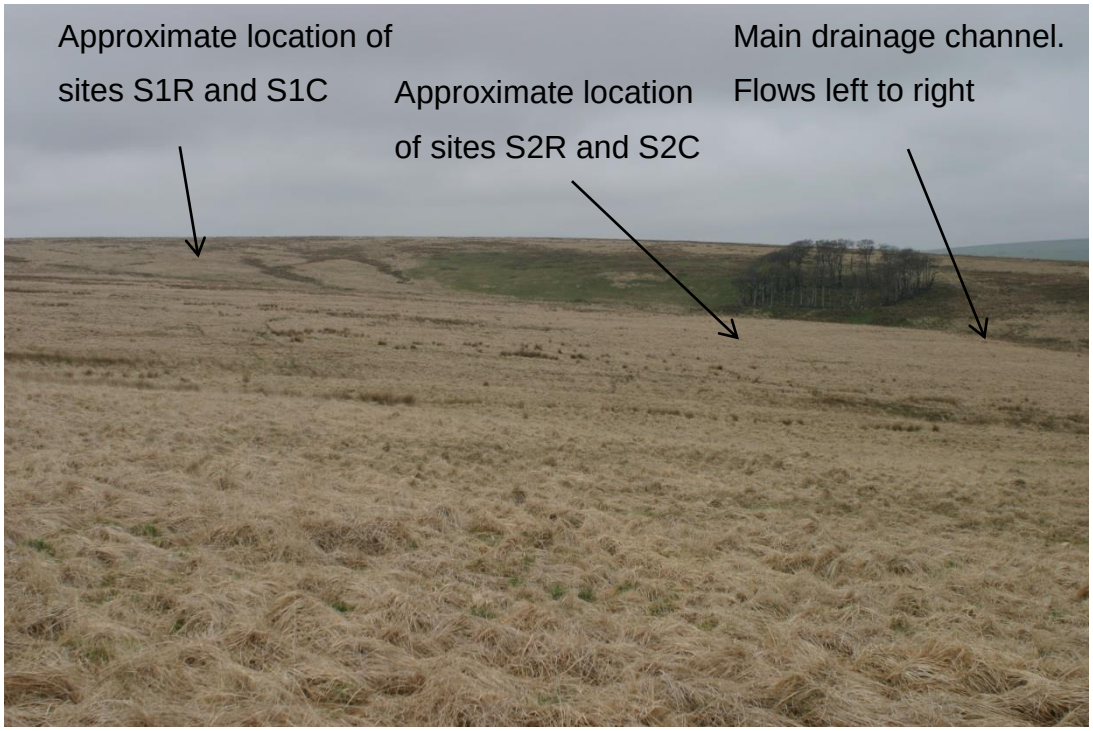

Figure 3.4 Spooners catchment in May 2012, pre-restoration. Looking northeast from site S3R towards sites S2 and S1. Again note the dominance of *Molinia caerulea* across the catchment and the volume of leaf litter and dormant vegetation.

Figure 3.5 Looking up-gradient along a straight, down-slope hand-dug ditch at site A2C prior to equipment installation (March 2012). The ditch is 38 cm wide and 24 cm deep but not easily visible within the landscape apart from in late winter when the vegetation is dormant and flattened by winter rain and wind.

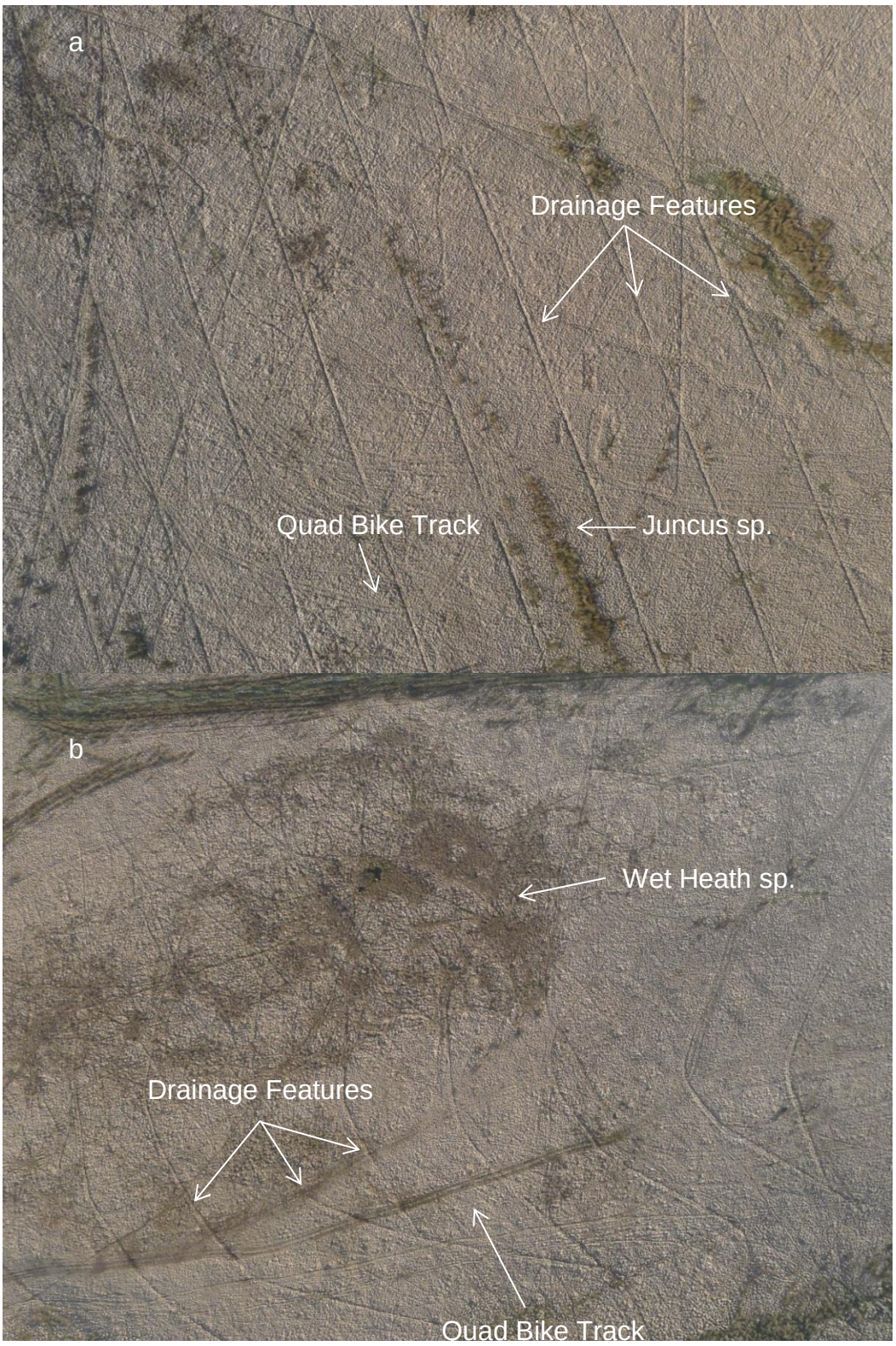

Figure 3.6 Visible aerial photograph collected from a QuestUAV fixed wing aircraft at approximately 100 m altitude over Aclands catchment in March 2012. a, Straight hand-dug up-slope ditches (typically <50 cm) running from top left to bottom right. Patches of green *Juncus sp*. typical of more nutrient rich flushes can be seen. b, Shallower (15-20 cm) Herringbone hand-dug ditches and a mauve patch of wet heath species on the watershed dominated by *Calluna vulgaris* and *Erica tetralix* with some *Sphagnum sp. and Eriophorum vaginatum.*

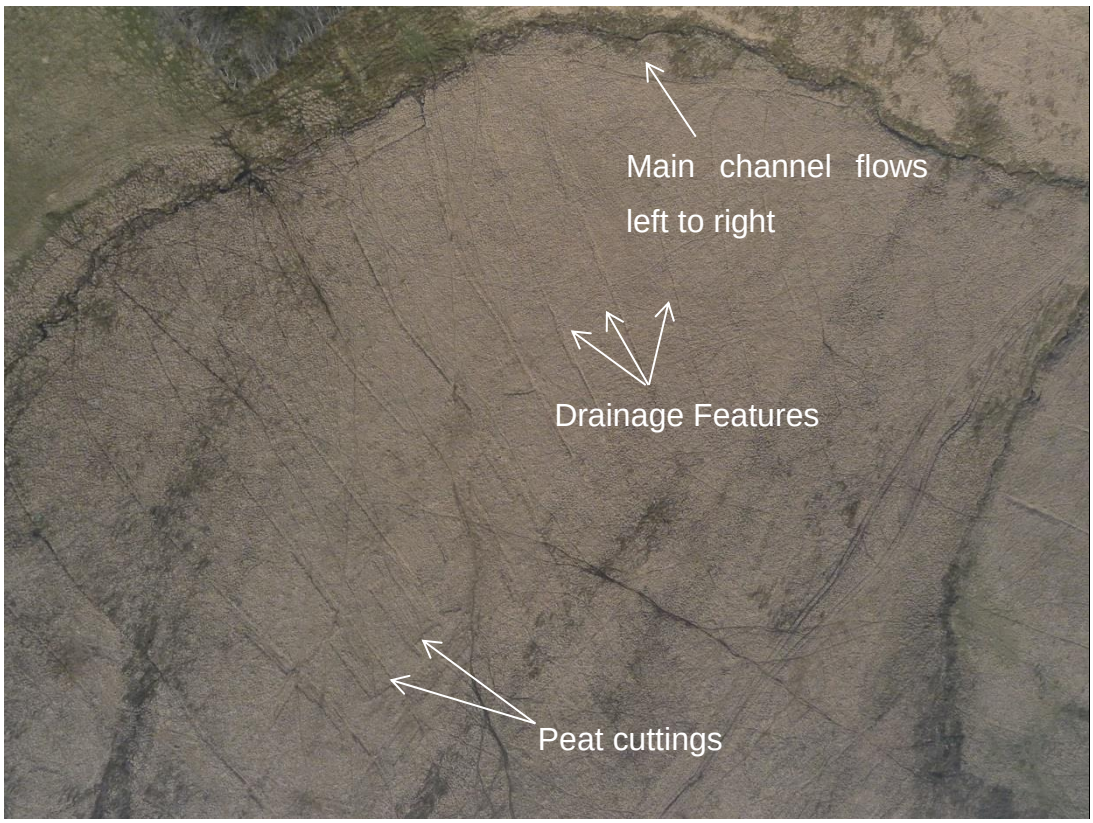

Figure 3.7 Visible aerial photograph collected from a QuestUAV fixed wing aircraft at approximately 100 m altitude over Spooners catchment in March 2012. Straight hand-dug up-slope ditches (typically <50 cm) and rectangular peat cuttings can be seen.

Equipment was installed in March 2012 at ⅛, ¼ and ½ the distance between adjacent ditches (Figure 3.8). At each plot equipment was installed to monitor net ecosystem exchange (Figure 3.9, Figure 3.10) and partitioned below-ground respiration (Figure 3.9, Figure 3.11).

The microtope (pattern of tussocks or hummocks and hollows) reflects changes in peat formation which in turn affects changes in carbon storage (Figure 2.4). Therefore, measuring gas fluxes at the microtope scale should provide information on the changes in peat formation due to restoration. The distance over which measurement occurs should be large enough to be representative of a microtope but remain practical. A plot 0.55 m x 0.55 m positioned to include tussock and inter-tussock areas was selected to be practical but sufficiently large to capture the microtope as *Molinia caerulea* tussocks range from 0.2 m^2 to more than 1 m^2 (Nieveen *et al.* 1998).

Over the growing season of 2012 vegetation phenology was measured at every plot (n=36) approximately fortnightly by a series of downward facing images collected as shown in Figure 3.12. Due to equipment failure it was not possible to continue this in 2013 and 2014. Instead it was decided to increase the temporal resolution to daily timesteps at the expense of spatial resolution (n=1) using a time-lapse camera (Figure 3.13) located at Spooners.

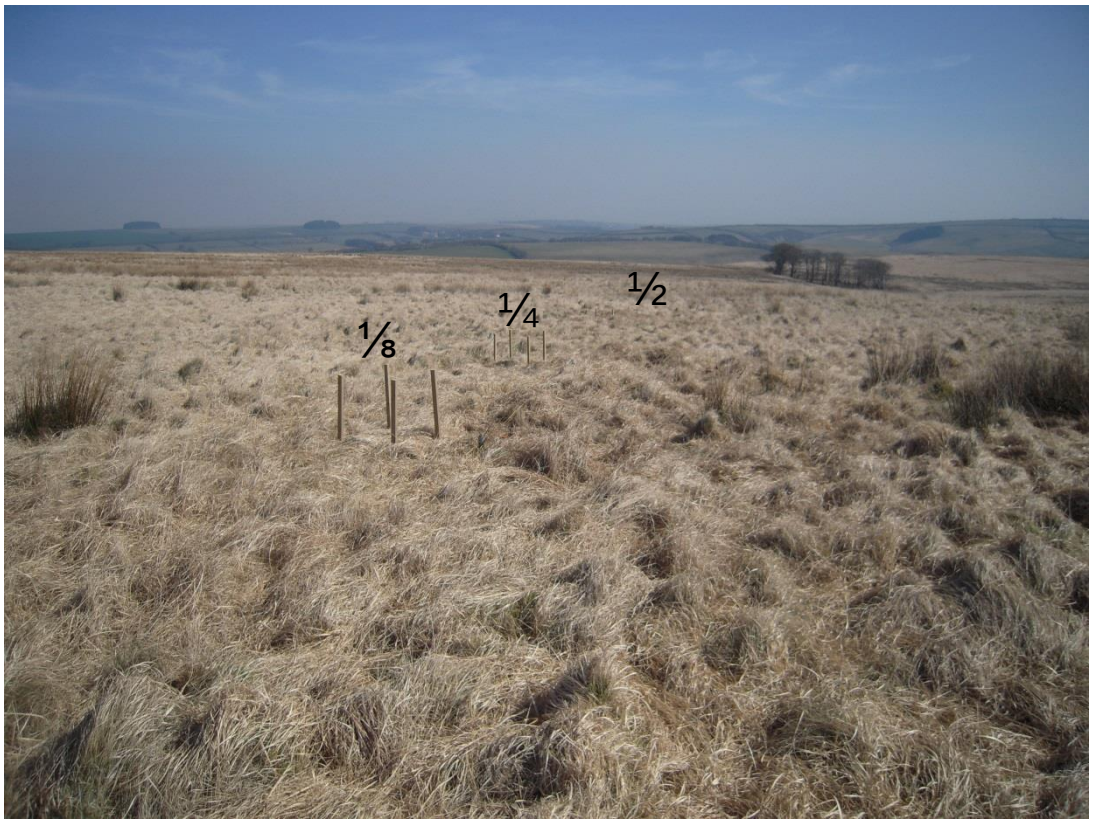

Figure 3.8 Arrangement of plots at ⅛, ¼ and ½ the distance between adjacent ditches perpendicular to the ditch at site A1C following installation in March 2012 looking away from the ditch.

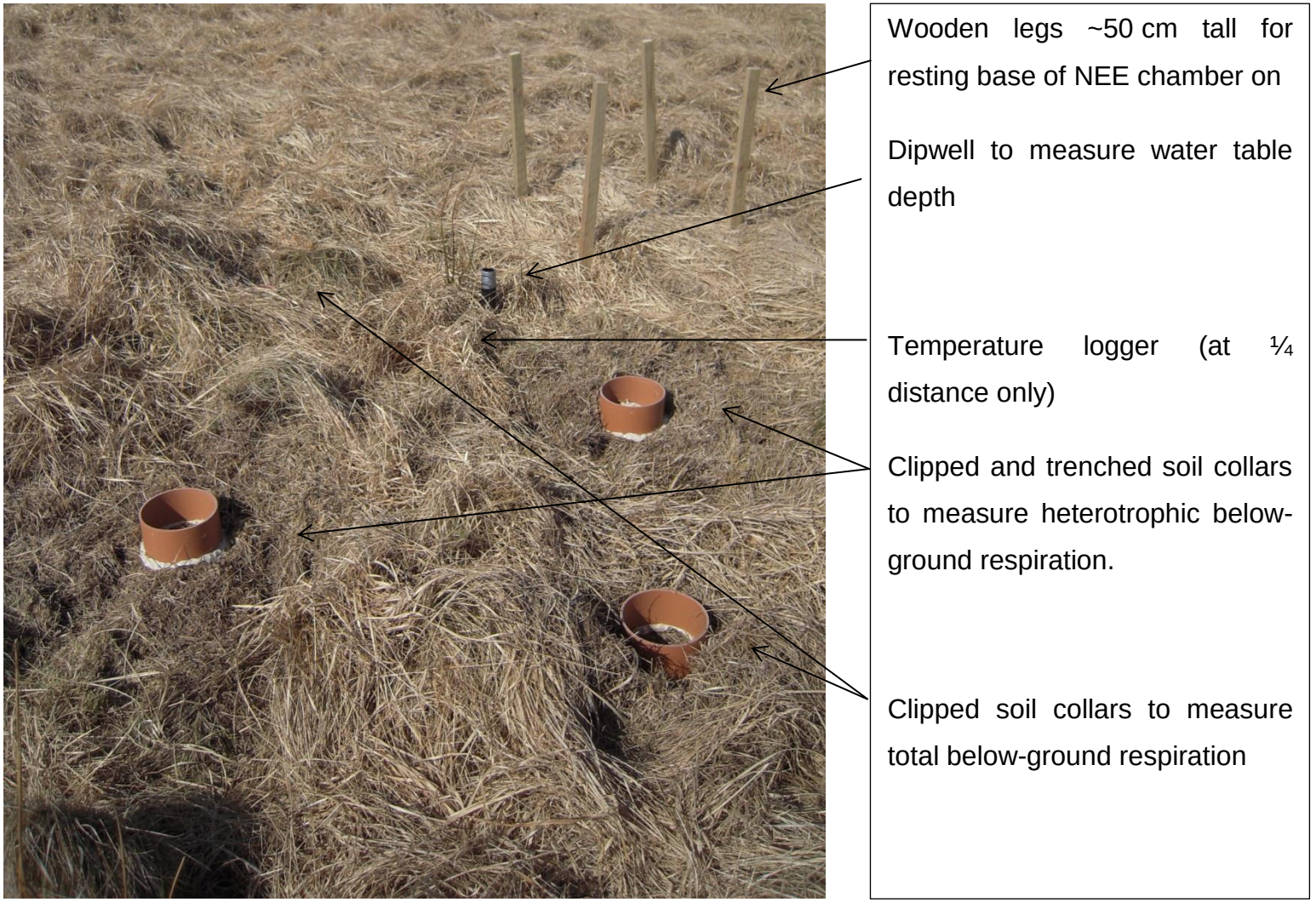

Figure 3.9 Equipment permanently installed at each location in March 2012.

Figure 3.10 Full-light net ecosystem exchange measurement in progress (shade cloths not shown) September 2014.

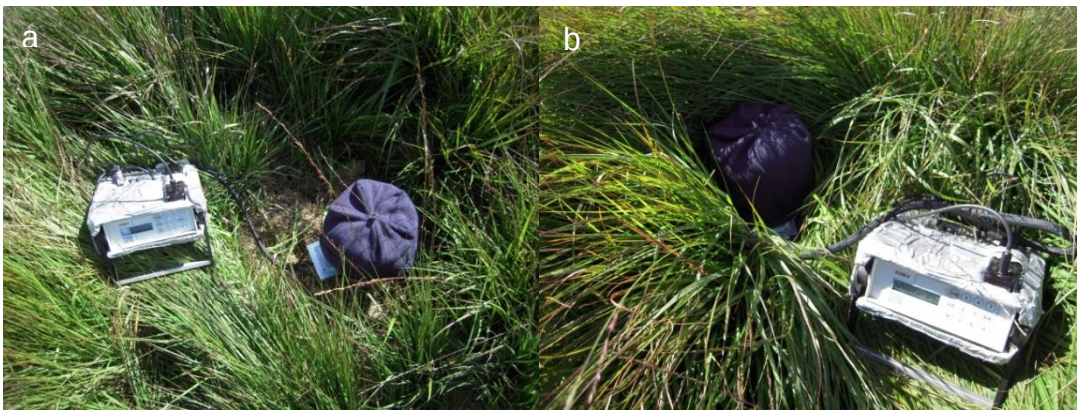

Figure 3.11 Measurement of below-ground heterotrophic respiration from a trenched and clipped soil collar (a) and below-ground total respiration from a clipped soil collar (b), September 2014.

Figure 3.12 Tripod set up for downward facing images used to derive greenness excess index between 20/06/2012 and 25/10/2012.

Figure 3.13 Photograph of Brinno TLC time-lapse camera *in situ* at Spooners, installed in April 2013.

Figure 3.14 One week following restoration at Spooners site S2R. The peat dams can be seen with small pools of water up-gradient.

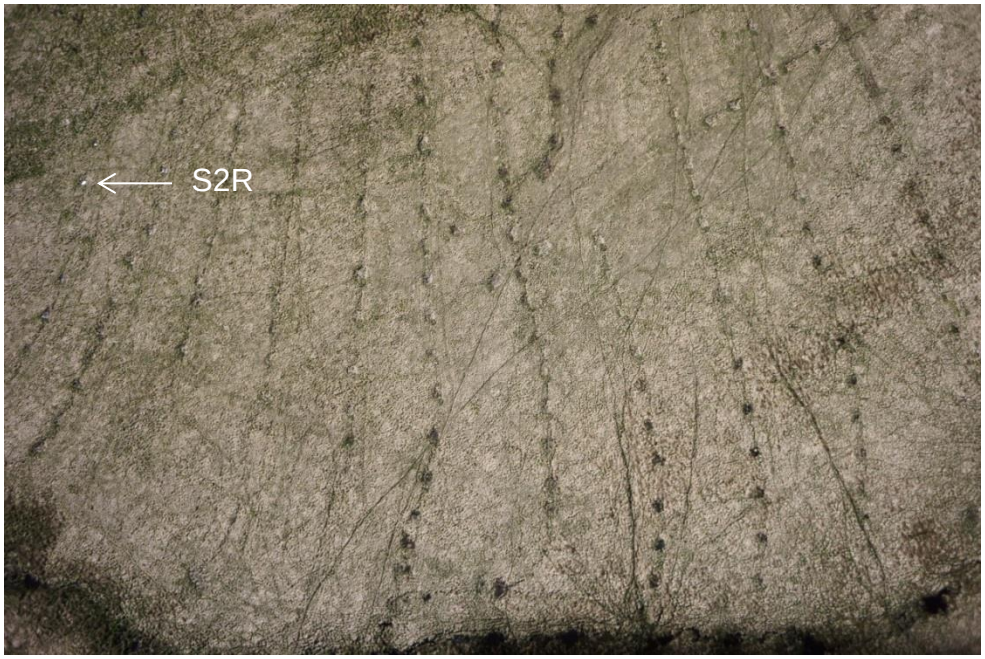

Figure 3.15 Visible aerial photograph collected from a QuestUAV fixed wing aircraft at approximately 100 m altitude over Spooners catchment in November 2014. The pattern of regular ditch blocks using peat dams can be seen. The approximate location of site S2R is marked

Restoration occurred in April 2013 at Spooners and April 2014 at Aclands (Table 3.1). Drainage features were blocked using regular spaced peat dams made from peat taken from borrow pits adjacent to the ditch (Figure 3.14, Figure 3.15), a common ecological restoration technique on blanket bogs (Armstrong *et al.* 2010) adapted for shallow peatlands (Grand-Clement *et al.* 2015).

Table 3.1 Timeline of key milestones related to this project.

Milestone	**Aclands**	**Spooners**
Exmoor Mire Restoration Project	Apr-2006 to Mar-2010	
LiDAR datasets acquired by Geomatics Group for ENPA	May-2009	
Start of Exmoor Mires Project	01/04/2011	
Start of PhD	01/09/2011	
Final site selection	16/02/2012	
Pre-restoration UAV Flight	14/03/2012	13/03/2012
Start of installation of soil collars, dipwells and NEE stakes	26/03/2012	
End of installation of soil collars, dipwells and NEE stakes	09/04/2012	
First gas flux measurements	27/04/2012	16/04/2012
Start of collection of ground based photograph of NEE plots for SfM	.	04/05/2012
End of collection of ground based photograph of NEE plots for SfM	.	25/05/2012
First downward facing photographs of the NEE plots	19/07/2012	20/06/2012
Vegetation composition monitoring	14/08/2012	
Last downward facing photographs of the NEE plots (camera failure)	09/01/2013	07/06/2013
Installation of timelapse camera	.	23/04/2013
Start of Restoration	17/03/2014	15/03/2013
End of Restoration	10/04/2014	12/04/2013
Post-restoration UAV Flight	23/05/2014	21/05/2014
Last gas flux measurements for this thesis	23/09/2014	22/09/2014
End of this phase of the Exmoor Mires Project	31/03/2015	

3.3 SUMMARY

More detail on the ecology, topography, meteorology, land management etc. of Exmoor in general and the two study catchments in particular has been provided to demonstrate how representative these locations are of this region. It provides a paleoecological context within which the success of restoration can be assessed. It also allows for more informed comparisons to be made with peatlands studied elsewhere with different climate, vegetation composition and land management.

This chapter allowed for a full description of the within-site selection process not possible within the subsequent chapters. Photographs have been included here to enable the locations, equipment and techniques described in the following chapters to be envisioned. Many of these methods occur in multiple chapters, further details specific to the hypothesis being addressed are provided within the appropriate chapter. The following chapters contain the primary research carried out in the catchments described above, starting with the development of a proxy for vegetation phenology.

4 MODIS VEGETATION PRODUCTS; USEFUL MEASURES OF VEGETATION PHENOLOGY AND PEATLAND CO_2 EXCHANGE

Naomi Gatis, Karen Anderson, Emilie Grand-Clement, David J. Luscombe, Iain P. Hartley, David Smith & Richard E. Brazier.

4.1 ABSTRACT

Plant phenology varies from year to year and is influenced by environmental conditions. The timing and amplitude of plant growth and senescence is known to affect carbon cycling and alters the annual balance between net ecosystem carbon dioxide (CO_2) uptake and release. In a *Molinia caerulea* dominated peatland CO_2 uptake increases with leaf growth from April increasing to a maximum in August, by November all the leaves have died and CO_2 release dominates. Accurate measurement of green leaf phenology over the whole landscape is therefore vital to improving understanding of ecosystem carbon dynamics. This study builds on previous work by assessing a greater range of Moderate resolution Imaging Spectroradiometer (MODIS) products as measures of vegetation phenology and CO_2 exchange within a maritime peatland of upland Britain.

Daily true colour digital images were taken with an inexpensive, off-the-shelf, time-lapse camera (Brinno TLC100) at an upland peatland field site on Exmoor, UK between 23/4/2013 and 29/10/2013. The Green Red Vegetation Index (GRVI) derived from these images was used to validate multiple MODIS derived vegetation products (Normalised Difference Vegetation Index (NDVI), Leaf Area Index (LAI8), fraction of absorbed Photosynthetically Active Radiation (fPAR8), Enhanced Vegetation Index (EVI16) and Gross Primary Productivity (GPP8)) at a spatial resolution of 250, 500 or 1000 m and temporal resolution of 8 or 16 days.

Comparison of the phenological metrics; start, peak and end of growth and season length determined from camera derived GRVI and MODIS vegetation

products (VPs) using the half-maximum method showed EVI16, fPAR8 and LAI8 to be the best predictors of start, peak and end of growth respectively. Over the three metrics NDVI in an 8 day period (NDVI8) was the most accurate being an average of 8 days out from the three metrics (start, peak and end of growth). VPs with finer spatial resolution (250 and 500 m) more accurately captured spring green-up whilst VPs with finer temporal resolution (8-days) better captured whole season dynamics in this ecosystem. Pearson's correlation of daily VPs indicated NDVI8 and fPAR8 to have the strongest correlation with camera derived GRVI (r=0.89). In addition fPAR8 was significantly correlated with net ecosystem exchange at 600 µmol Photons m^{-2} s^{-1} (r=0.93) measured using static chambers.

Freely available MODIS satellite images enable vegetation phenology to be monitored at the landscape scale. Using the *in situ* digital camera images as a validation of conditions on the ground this work demonstrates that MODIS data captures up to 90 % of the daily variation in phenology of this peatland. For use in CO_2 flux models MODIS-fPAR8 and NDVI8 exhibited the most potential as measures of physiological activity at a landscape scale.

4.2 HIGHLIGHTS

- Comparison of phenology from digital camera images to MODIS derived products
- Start of growth, end of growth and season length best predicted by EVI16, fPAR16 and LAI8
- NDVI8 and fPAR8 showed best day-to-day correlation with *in situ* measurements
- In a *Molinia caerulea* peatland fPAR8 and NDVI8 show most promise for CO_2 modelling at landscape scales

4.3 KEY WORDS

MODIS NDVI/fPAR; time-lapse camera; *Molinia caerulea*; peatland; CO_2.

4.4 INTRODUCTION

Peatlands are known to be large carbon stores (Gorham 1991), many of which are damaged by poor land management (Littlewood *et al.* 2010), reducing their ability to provide a range of ecosystem services (Grand-Clement *et al.* 2013b). With recent alterations to the Kyoto Protocol, carbon trading provides a possible means of funding peatland restoration projects (Birkin *et al.* 2011, Dunn and Freeman 2011, Bonn *et al.* 2014). Water level, vegetation composition and subsidence have been proposed as potential proxies for greenhouse gas emissions (Couwenberg *et al.* 2011). However, carbon dioxide (CO_2) fluxes are affected by water level in some peatlands (Laine *et al.* 2006, Riutta *et al.* 2007, Maanavilja *et al.* 2011) but not all (Urbanová *et al.* 2013) and vary considerably from year to year influenced by environmental conditions (Lafleur *et al.* 2003). For example Helfter *et al.* (2015) found mean winter temperature of a Scottish temperate lowland bog to strongly correlate with carbon uptake in the subsequent growing season. The timing and amplitude of plant growth and senescence is known to influence gas exchange within a range of habitats (Richardson *et al.* 2013) including deciduous forests (Muraoka and Koizumi 2005, Keenan *et al.* 2013, Mizunuma *et al.* 2013), mixed forests (Davis *et al.* 2003, Saitoh *et al.* 2012, Keenan *et al.* 2013), subalpine pastures (Migliavacca *et al.* 2011, Rossini *et al.* 2012), shrub land, grass land and bamboo (Piao *et al.* 2009) and northern peatlands (Schubert *et al.* 2010, Westergaard-Nielsen *et al.* 2013, Helfter *et al.* 2015). Earlier and longer growing seasons have been connected to higher net ecosystem uptake (Goulden *et al.* 1996, Richardson *et al.* 2013, Helfter *et al.* 2015). Measurement of green leaf phenology over the whole landscape is therefore vital in understanding the carbon dynamics of an ecosystem.

Attempts have been made to model regional canopy development using meteorological controls (Jolly *et al.* 2005). However, these models are not sensitive to biotic controls such as grazing and disease and abiotic controls such as frost and drought damage. Repeat digital images from unattended *in situ* digital cameras or webcams (Richardson *et al.* 2007, Ahrends *et al.* 2008, Ide and Oguma 2010, Migliavacca *et al.* 2011, Sonnentag *et al.* 2012, Mizunuma *et al.* 2013) have been used to track vegetation phenology in a range of ecosystems at a fine temporal resolution (daily to sub-daily) averaged over a greater spatial extent (10s to 100s of metres) than traditional, manual, methods. Vegetation products, based on the relative reflectance of green to red and/or blue in these digital images, are at a temporal and spatial scale where they can be directly related to measured CO_2 fluxes (Migliavacca *et al.* 2011, Saitoh *et al.* 2012, Mizunuma *et al.* 2013, Westergaard-Nielsen *et al.* 2013, Zhou *et al.* 2013). However, this method is site specific without standard protocols (Ide and Oguma 2010, Migliavacca et al. 2011) and is not straightforward in isolated upland areas such as peatlands where multiple cameras would be required to characterise an entire landscape.

Satellite data have repeated global coverage at a range of spatial and temporal scales making these a viable tool for monitoring vegetation phenology at regional scales in remote, unmonitored areas. In addition, the accessible Moderate resolution Imaging Spectroradiometer (MODIS) database (2000 - present) allows existing CO_2 measurements to be retrospectively related to MODIS vegetation products. Studies have shown the potential for using the 16 day Normalised Difference Vegetation Index (NDVI) MODIS data combined with meteorological data in light use efficiency models (Schubert *et al.* 2010, Kross *et al.* 2013) and 8 day MODIS Gross Primary Productivity (GPP) (Moore *et al.* 2006) as measures of CO_2 exchange in northern peatlands. This study builds on such work by assessing a greater range of MODIS products within a maritime peatland of upland Britain. It is hypothesised that (a) MODIS derived vegetation products (Normalised Difference Vegetation Index (NDVI), Leaf Area Index (LAI8), fraction of absorbed Photosynthetically Active Radiation (fPAR8), Enhanced Vegetation Index (EVI16) and Gross Primary Productivity (GPP8))

can be used to model vegetation phenology as measured by an on-site time-lapse camera and (b) both time-lapse camera and MODIS derived vegetation products correlate with temporal variations in CO_2; making them useful measures of vegetation phenology for peatland CO_2 budgets.

4.5 Materials and Methods

4.5.1 Site Description

The study site is located in the uplands of Exmoor National Park in the southwest of England (51°7'21.9N, 3°44'52.9W). These peatlands have been drained for agricultural improvement since the 1830s (Hegarty and Toms 2009). The site was selected to be characteristic of the widespread drained peatland areas which are currently being restored by ditch blocking. This site is being intensively monitored to understand the effects of ecological-restoration on a range of ecosystem services including carbon and water storage, biodiversity and food and fibre provision. The landscape is dominated by the grass *Molinia caerulea* and classified as an M25: *Molinia caerulea – Potentilla erecta* mire (Rodwell 1991). The site lies between 380 and 445 metres above sea level. Long-term (1981-2010) average annual rainfall totals 1445 mm with daily mean air temperature ranging from a minimum of 3.7 °C in January rising to 14.5 °C in July and August (UK Meteorological Office 2012).

4.5.2 Digital Camera

A battery powered Brinno TLC100 (Brinno Design, California, USA) time-lapse camera was installed facing due north (magnetic) at an angle of 5° from the horizontal to maximise reflected back-scatter. The camera was at a height of 0.95 m above the ground and the field of view was approximately 49.5°. A daily true-colour image was taken at solar noon (13:00 h British Summer Time) to minimise the angular effect of the canopy's bidirectional reflectance function (Ahrends *et al.* 2008). A total of 190 images were collected between 23 Apr 2013 and 29 Oct 2013.

Images were processed with MATLAB (R2011b The Mathworks Inc., Natick, Massachusetts). A region of interest (ROI) was selected (Figure 4.2) and the red and green digital numbers extracted and averaged across the ROI. The ROI was selected to maximise spatial sampling of the foreground canopy without giving undue weighting to the closest vegetation. Background vegetation was excluded as it was more likely to have different light conditions, contain a mix of species and be increasingly affected by atmospheric moisture content.

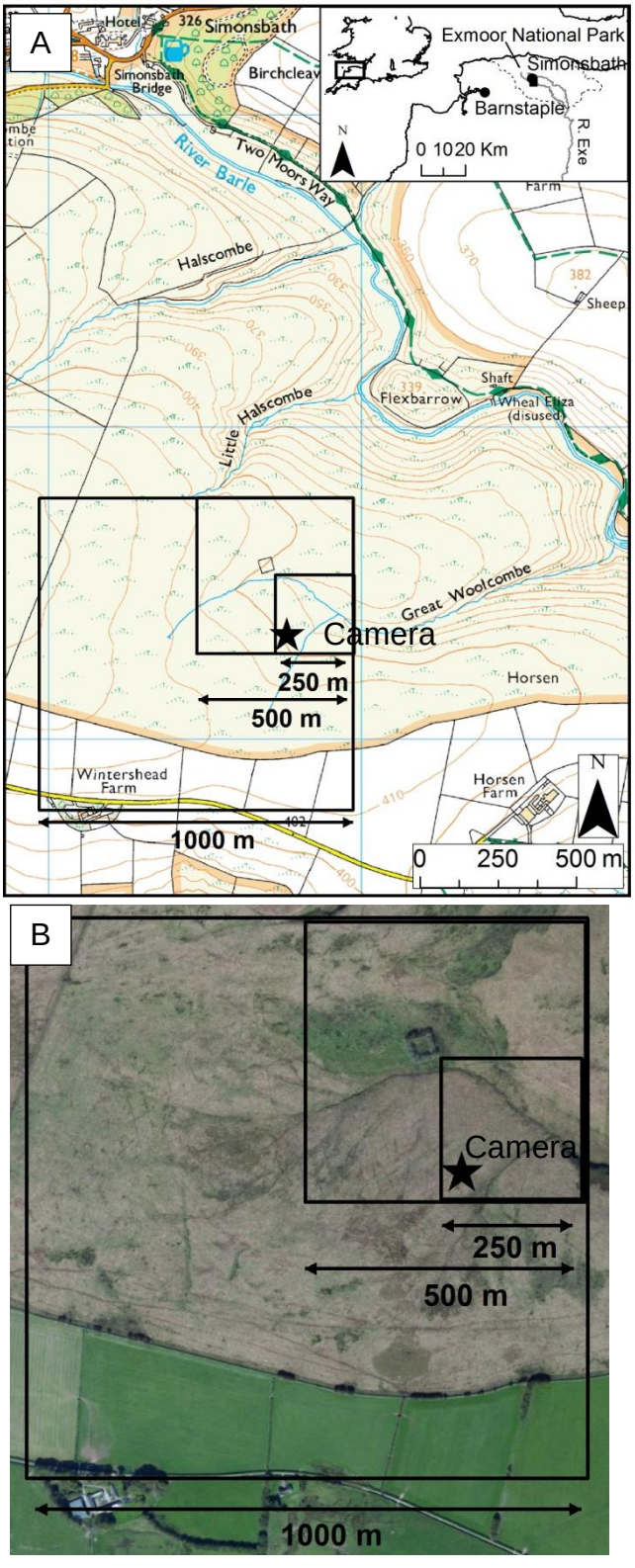

Figure 4.1 a, Location of study site within the UK and Exmoor National Park (inset). Location of time-lapse camera and extent of the 250 m, 500 m and 1000 m MODIS pixels. b, Aerial photo of the pixel extent. 1:25000 Ordnance Survey Map (Ordnance Survey 2008d)

The camera has an 8-bit charge-coupled device with which it records 256 possible brightness values (0-255) for three broad bands (red, green and blue). From this green-red vegetation index (GRVI) (Tucker 1979) was calculated (Equation 4.1) GRVI = $(G_{DN}-R_{DN}) / (G_{DN}+R_{DN}) \times 100$ where G_{DN} and R_{DN} are the green and red brightness values respectively. The GRVI was selected as it is not sensitive to blue, as blue has been found to show greater day-to-day variation dependent on the quality of incident radiation (spectral distribution) (Richardson *et al.* 2007). Chromatic coordinates and green excess index (GEI) were not used as they showed a greater sensitivity to illumination conditions in initial trials (Supplementary Material Figure 10.1).

Rain, moisture on the lens and uneven illumination adversely affected image quality. To remove noise within the data a 3rd order Fourier adjustment was fitted to the data, points outside the 95 % confidence interval were excluded (Figure 4.3a). A 3rd order Fourier adjustment was chosen above Gaussian (Jonsson and Eklundh 2002) or logistic (Zhang *et al.* 2003) growth models as GRVI showed distinct secondary maxima in early September. Data gaps created by excluding data were filled by linear interpolation. After removing outliers the data were still "noisy" so a daily timeseries was calculated from an 8-day moving average to reduce the noise but minimise smoothing of natural variability (Figure 4.3b). An 8-day average was chosen to match the frequency of MODIS data.

The effect of seasonal variation in solar altitude has not been accounted for here despite having a known effect on digital image derived vegetation products (Ahrends *et al.* 2008) as it is assumed that the effect is negligible compared to the effect of seasonal leaf growth and is therefore difficult to decouple.

4.5.3 Terra MODIS

Terra Earth Orbiting System's Moderate resolution Imaging Spectroradiometer (MODIS) data were selected as they are freely available and are a good compromise between spatial and temporal resolution compared to Landsat's Enhanced Thematic Mapper (ETM) data which has 30 m spatial resolution but a

minimum 16 day revisit time or the Polar-orbiting Operational Environmental Satellites AVHRR data with daily revisits at 1000 m spatial resolution. The other main advantage of MODIS data compared to ETM data is that MODIS samples the same area on every pass whereas the orbital characteristics of Landsat mean that the area sampled varies for each pass increasing the data manipulation requirements.

MODIS tile h17 v3 (49 to 60°N, 0E to 20°WE) of the MOD09A1 land surface reflectance, MOD13Q1 vegetation indices, MOD15A2 LAI/fPAR and MOD17A2 gross primary productivity (GPP8) products were downloaded from USGS Earth Explorer (http://earthexplorer.usgs.gov) for the period 1st Jan 2013 to 24th Oct 2013. Details of the spatial and temporal resolution of the datasets within each tile are given in Table 4.1.

Table 4.1 Spatial and temporal resolution of the MODIS products downloaded and the number of time-steps available between 1st Jan 2012 and 24th Oct 2013.

MODIS Product Code	MODIS Product Name	Spatial Resolution (m)	Temporal Resolution (days)	Data Selection Method	Number of Time-steps	Pixel Sample	Pixel Line
MOD9A1	Land Surface Reflectance	500	8	8 day best quality	84	1836	2131
MOD13Q1	Vegetation Indices	250	16	16 day maximum	82	3671	4262
MOD15A2	LAI/fPAR	1000	8	8 day average	84	918	1066
MOD17A2	Gross Primary Productivity	1000	8	8 day cumulative	84	918	1066

The products used in this study were either reflectance values estimated at the Earth's surface or derived from these values. Algorithms have been applied to radiometrically calibrated data to remove the effects of scattering and absorption by atmospheric gases and aerosols, contamination by thin cirrus clouds and bidirectional reflectance distribution function (Vermote and Vermeulen 1999). The data produced are within 5 % of field data for more than 86 % of observations (2012), and have been shown to be suitable for monitoring vegetation dynamics at regional and global scales (Zhang *et al.* 2003).

NASA's data quality assessment is based on cloud cover and observation geometry (solar and satellite zenith angles). MOD9A1 is the best quality observation (no cloud cover and low solar and satellite zenith angles) within the 8-day period. MOD13Q1 is the maximum value of the Normalised Difference Vegetation Index (referred to as NDVI16) and the Enhanced Vegetation Index (EVI16) from available "good quality" data within a 16-day period. The acquisition date (for MOD9A1 and MOD13Q1), first day of the interval (for MOD15A2 and MOD17A2), data quality and cloud cover data were extracted for the pixel of interest. Data from MOD9A1 was used to calculate the NDVI8 (Equation 4.2). To enable a direct comparison between GRVI derived from digital images with that derived from MODIS data, GRVI8 (Equation 4.1) was also calculated from MOD9A1 data.

Equation 4.2 Normalised Difference Vegetation Index

$$NDVI8 = \frac{Band\ 1\ (Near\ Infrared) - Band\ 2\ (Red)}{Band\ 1\ (Near\ Infrared) + Band\ 2\ (Red)}$$

NDVI has been used widely to track spring green-up (e.g. Zhang *et al.* 2003) as it is known to relate to Leaf Area Index (LAI) and total biomass. EVI was developed to overcome some of the problems associated with NDVI such as saturation at high LAI, sensitivity to atmospheric conditions and background signals. Both vegetation products (VPs) have been included as NDVI was better than EVI at predicting the timing of onset of greenness and maturity in deciduous forest (Ahl *et al.* 2006) but worse than EVI at predicting GPP8 in a northern peatland (Schubert *et al.* 2010).

LAI8 and fraction of absorbed Photosynthetically Active Radiation (fPAR8) (MOD15A2) are reverse modelled from top of atmosphere reflectance values using a biome classification. All good quality data (no cloud cover or mixed cover, low or average aerosol and where the main radiographic testing method was used) collected are averaged over an 8-day period. The MOD17A2 value of GPP8 was extracted, it is an 8-day cumulative composite of values calculated using a radiation-efficiency use model based on fPAR, LAI, minimum air

temperature, and vapour pressure deficit. The landcover assigned to the pixel of interest was annual grassland, which although not appropriate for most peatlands was suitable for this *Molinia caerulea* dominated peatland. Data quality and cloud cover data were extracted for the pixel of interest. LAI8 and fPAR8 were chosen for analysis as they are known to vary seasonally in *M. caerulea* dominated ecosystems (Nieveen and Jacobs 2002) and are important variables in estimating net ecosystem exchange (NEE) (e.g. Street *et al.* 2007). GPP8 was also included as it has shown potential for monitoring carbon dioxide (CO_2) fluxes in northern peatlands (Schubert *et al.* 2010, Kross *et al.* 2013).

As blanket peatlands typically only form where precipitation is greater than 1000 mm per year (Lindsay *et al.* 1988) the probability of cloud cover is high so a MODIS data processing method where questionable data are not immediately omitted or automatically used, but rather excluded based on an objective assessment against data of good quality is required to minimise data loss. To obtain a continuous timeseries the 8 and 16 day MODIS products were processed as follows. Data prior to Day of Year (DOY) 70 were removed to focus on the growing season, average temperature on DOY 70 (11 Mar 2013) was -3 °C, indicating this date was still prior to the commencement of spring green-up. Data were screened and poor quality data (cloudy, high aerosol concentrations or poor geometry) given a weighting of zero and all other data a weighting of one. To minimise variation due to atmospheric conditions, illumination and observation geometry a smoothing filter was applied. Logistic functions (Zhang *et al.* 2003, Fisher *et al.* 2006, Richardson *et al.* 2007), high order polynomials (Cook *et al.* 2009), asymmetrical Gaussian functions (Jonsson and Eklundh 2002) and second and third order Fourier (Fontana *et al.* 2008) functions were tested on the MODIS data.

A Fourier series describes a series by summation of sinusoidal components each with their own distinct phase and amplitude. Third order Fourier series were found to be the best fit for the data as they allowed for the multiple senescence periods observed but did not assume that all data were exact and

temporally accurate. Points outside the 99 % confidence interval were excluded. All remaining points were then weighted equally and a Fourier third order series fitted to form a continuous timeseries for each VI. Figure 4.4 provides an example of the data processing used to derive the fPAR8 timeseries.

4.5.4 Ancillary measurements

The rate of CO_2 accumulation in a closed chamber over 2 minutes was measured using an EGM-4 infra-red gas analyser (PP Systems, Hitchin, UK) at full light (x2), full dark (x2) and ~60% ~40%, ~10% light levels using shade cloths from 18 locations (55 x 55 cm) monthly from May to September following Shaver *et al.* (2007). Photosynthetic active radiation inside the chamber was measured (PAR Quantum, Skye Instruments, Llandrindod Wells, UK). Net ecosystem exchange (NEE) measurements from all locations were used to derive parameters (P_{max}, K and R_{Eco}) for a hyperbolic light response curve (Equation 4.3) for each month (n=5). Using these parameters NEE at a PAR of 600 µmol Photons m^{-2} s^{-1} was then estimated for each month.

Equation 4.3 hyperbolic light response curve

$$\mathrm{NEE} = R_{\mathrm{Eco}} - \frac{P_{max}.\mathrm{PAR}}{k + \mathrm{PAR}}$$

where NEE is the net ecosystem exchange (µg C m^{-2} s^{-1}), P_{max} is the rate of light saturated photosynthesis (µg C m^{-2} s^{-1}), k is the half-saturation constant of photosynthesis (µmol Photons $m^{-2}s^{-1}$), PAR the incident PAR (µmol Photons $m^{-2}s^{-1}$) and R_{Eco} the ecosystem respiration (µg C m^{-2} s^{-1}).

4.5.5 Analysis

Four phenological metrics were identified to compare the timing and amplitude of seasonal vegetation change, the start, peak and end of growth and length of season. Several methods have been proposed to identify the timing of start and end of growth; the slope method identifies the steepest part of the curve (e.g. Ahrends *et al.* 2008), the half-maximum identifies the point half-way between the

minimum and maximum measured values (e.g. Coops *et al.* 2011), other threshold methods use site specific percentages on a cumulative frequency curve (e.g. Fontana *et al.* 2008), with noisy or complex data even visual inspection has been used (Ide and Oguma 2010). The slope method is considered more ecologically meaningful as it does not use arbitrary thresholds and is not dependent on the amplitude of maximum and minimum values. However, in a direct comparison the half-maximum method was found to be more accurate at capturing observed phenological events than the slope method (Studer *et al.* 2007).

Start of growth and end of growth were identified as the day of year (DOY) when the value first reached half the maximum value, each limb calculated separately. Peak was the DOY when maximum value occurred. Length of season is the number of days between start and end of growth. The average number of days difference between the three phenological metrics (start, peak and end of growth) estimated by GRVI and the MODIS-VI were calculated (Days Out).

GRVI goes from negative winter values to positive summer values, the point at which GRVI crosses between negative and positive offers another possible metric of phenology (Motohka *et al.* 2010) which is independent of the maximum and minimum values, this enables dates estimated by these two different methods to be compared.

To test for correlations between digital camera derived GRVI and MODIS derived VPs two-tailed Pearson's tests for data from DOY 116 to DOY 302 were carried out. Two-tailed Pearson's tests were also carried out to test for correlations between vegetation products and net ecosystem exchange.

4.6 RESULTS

4.6.1 Phenology of 2013

Digital images clearly captured phenological variation in the vegetation community (Figure 4.2); from early spring, through the first appearance of green shoots (Start of Growth) to mid-summer (Peak Growth), flowering and autumn senescence (End of Growth). Some condensation can be seen affecting image quality For example, on DOY 243, 218 and 283 (Figure 4.2). A dramatic change in green vegetation cover occurred between DOY 156 and 164 before start of growth. Less obvious changes in vegetation occurred around peak and end of growth. Green and red digital numbers ranged between 47-204 and 50-213 during the study period respectively, indicating that neither underexposure nor saturation occurred.

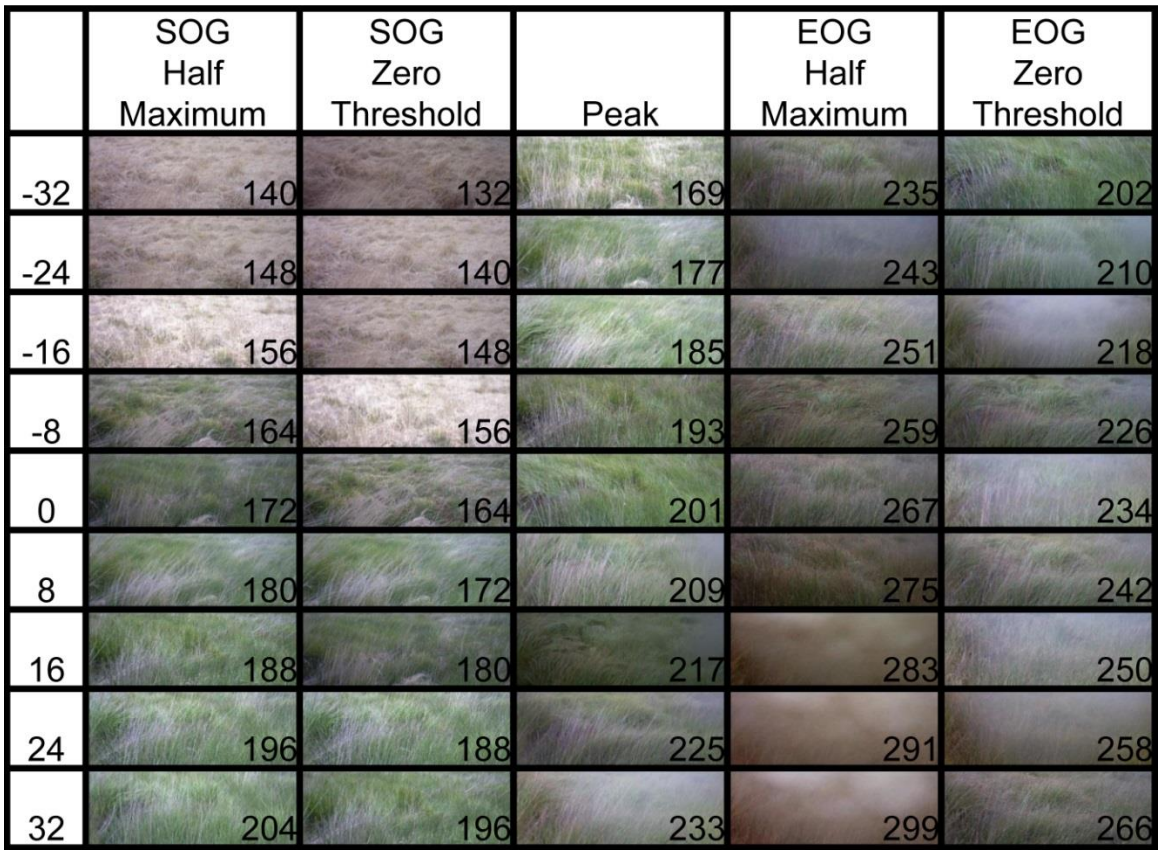

Figure 4.2 Series of images of the Region of Interest used to calculate average red and green digital numbers taken with a digital camera. Images are from 32, 24, 16, 8 and 0 days before and after the start, peak and end of growth estimated using the half-maximum and zero-threshold methods. Day of Year indicated on each image.

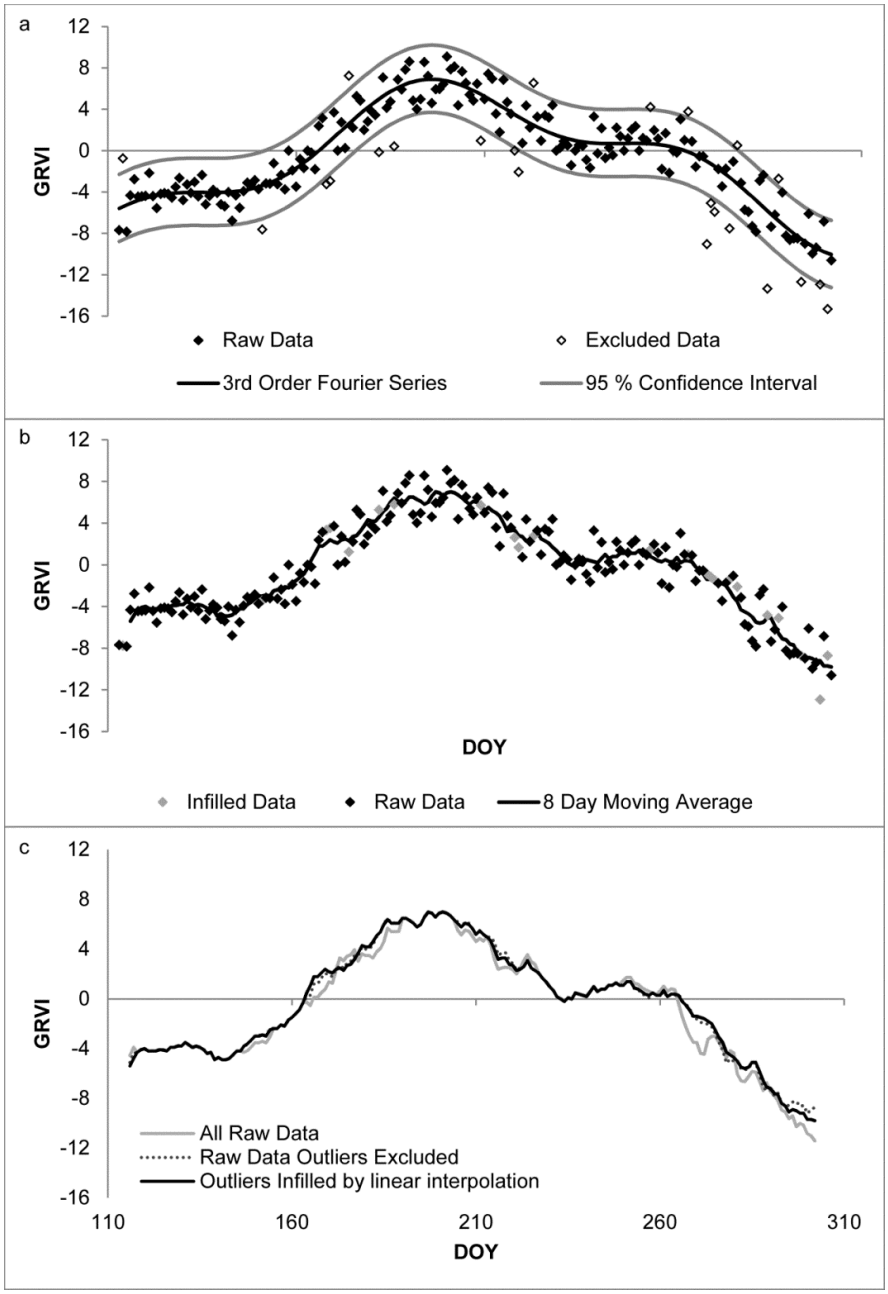

Figure 4.3 GRVI Data Processing. Third order Fourier Series fitted to raw Green Red Vegetation Index (GRVI) data, points outside the 95% confidence interval were excluded (a). Data gaps were filled by linear interpolation and an 8-day moving average calculated (b). Comparison of 8-day moving average calculated from raw GRVI data, raw data with points outside the 95 % confidence interval excluded and data with gaps filled by linear interpolation (c).

Table 4.2 Effect of data processing of Green Red Vegetation Index thresholds derived from the time-lapse camera.

	Start Of Growth		Peak Growth	End Of Growth	
	Half Maximum	Zero Threshold		Half Maximum	Zero Threshold
Raw Data	170	166	201	267	234
Outliers Excluded	166	164	201	269	234
Outliers Infilled	172	164	201	267	234

It can be seen that removing outliers due to variation in moisture and illumination conditions then infilling data gaps by linear interpolation (Table 4.2, Figure 4.3) had no effect on the estimated DOY of peak growth. There was a maximum of 4 and 2 days difference in start and end of growth between the 8-day averaged raw data, data with outliers excluded and GRVI timeseries used to represent vegetation phenology (Outliers Infilled). The zero threshold method showed least variation (2 days). No stage of the data processing resulted in consistently earlier or later dates than the GRVI timeseries used. This limited range in estimated threshold dates is indicative of the confidence in these dates and the robustness of the method. Figure 4.4 demonstrates how using this method maximises the MODIS data used to model the timeseries by only removing the poor quality data which outlies the 99 % confidence interval.

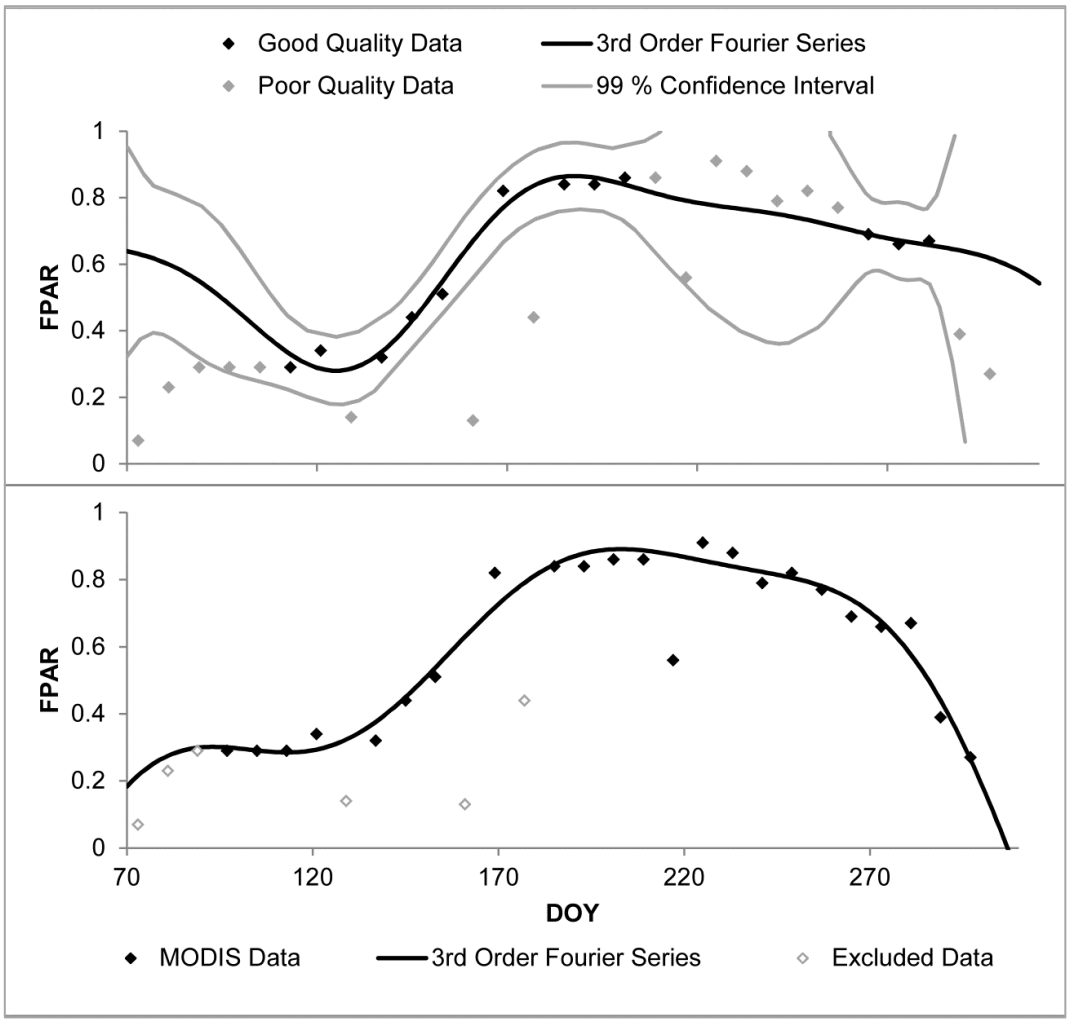

Figure 4.4 MODIS Data Processing. Third order Fourier series with 99 % confidence interval fitted to weighted MODIS fPAR data, good quality data weighted 1 and poor quality data weighted 0 (a). Data outside the 99 % confidence interval was excluded from further analysis. Third order Fourier series fitted to non-weighted MODIS fPAR8 data (b).

Green Red Vegetation Index (GRVI) increased from a spring minimum of -4.9 on 22/05/2013 (Day of Year (DOY) 142) to a maximum of 6.8 20/07/2013 (DOY 201) before reaching a seasonal minimum of -9.8 on DOY 302 (29/10/2013) (Figure 4.3). There were notable peaks on DOY 177, 224 and 252 and notable troughs on DOY 180, 221 and 234.

GRVI and temperature showed little correlation in the spring and autumn. The summer increase in air temperature started on day 174 preceding the increase in GRVI (DOY 181) and reached a maximum four days earlier than GRVI on

16/07/2013. There was a warm period around day 236 around the same time as the start of the secondary peak.

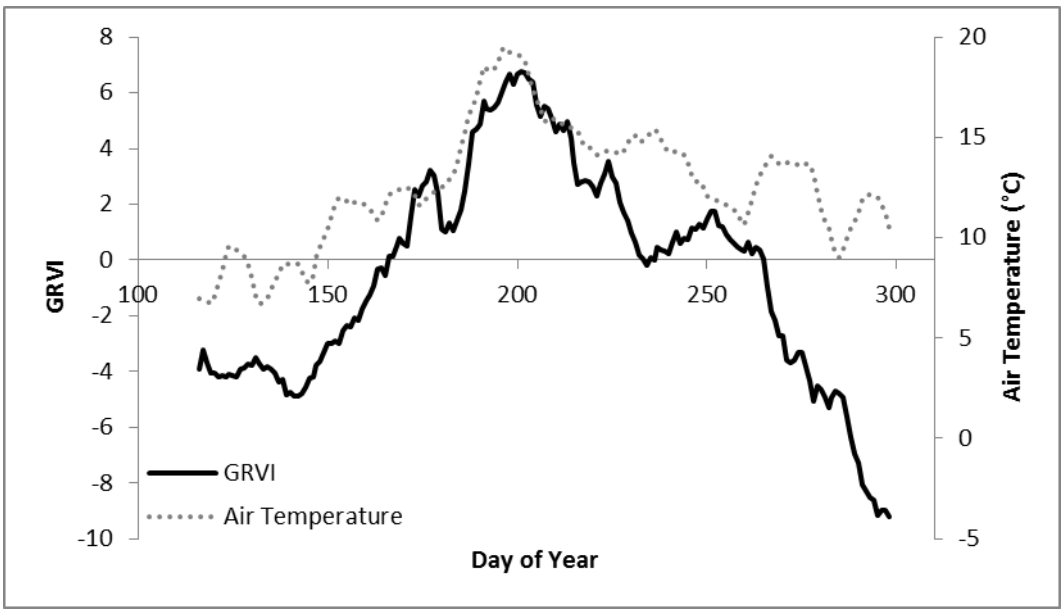

Figure 4.5 Temporal variation in eight day average Green Red Vegetation Index (GRVI) and air temperature over the 2013 growing season. A total of 190 north facing images taken at solar noon were collected between 23 Apr 2013 and 29 Oct 2013, 23 of these images were excluded as outliers and replaced by linear interpolation prior to averaging.

The timing of digital camera derived GRVI was used as a baseline to assess the timing of MODIS derived vegetation products (VPs). Visual inspection of the VPs compared to GRVI (Figure 4.4a) showed Gross Primary Productivity (GPP8) peaked 15 days earlier than GRVI and reached half maximum 16 days earlier than GRVI. The magnitude of decrease following peak growth was consistent with that observed in GRVI but the autumn maximum visible in GRVI was expressed as a reduction in gradient in GPP8. The higher spring values compared to autumn values were captured by GPP8 as well as fraction of absorbed Photosynthetically Active Radiation (fPAR8) and NDV16 (Figure 4.4a, c & d).

fPAR8 peaked only 1 day later than GRVI (Table 4.3), it then started to decrease but not as rapidly as GRVI Figure 4.4c). The gradient increased markedly around DOY 255, reflecting rapid structural decay of leaves, declining to a seasonal minimum consistent with GRVI. Enhanced Vegetation Index (EVI16) and Normalised Difference Vegetation Index over a 16 (NDVI16) and 8 day period (NDVI8) all show this rapid decrease from around DOY 255 (Figure 4.4d, e & f). EVI16 and NDVI16 show a similar bimodal pattern with maxima occurring near peak growth and the autumn maximum. The relative amplitude of these two peaks is more even in NDVI16 compared to GRVI.

NDVI8 and fPAR8 exhibit a smoother seasonal increase (Figure 4.4d) and decrease that visually appears to capture the seasonal dynamics of GRVI poorly. Despite this finding, they had a day to day correlation coefficient (Table 4.3) of r=0.899, indicating these VPs captured the seasonal dynamics of the vegetation but small scale temporal variation was smoothed out.

MODIS-GRVI8 had a single summer peak 10 days later than that estimated by GRVI (Table 4.3). The secondary maximum is not captured, autumn values are greater than spring values which were not seen in GRVI and here was a late autumn increase, again not present in GRVI (Figure 4.4g).

Start of growth and end of growth dates were estimated for camera derived-GRVI using the half-maximum method and the zero threshold method. Start of growth values (Table 4.3) estimated using MODIS VPs were earlier than that estimated using the half-maximum method except EVI16 which predicted start of growth on the same day as camera derived GRVI and NDVI8 which predicted start of growth 3 days later. Start of growth estimated by zero-threshold method was 8 days earlier than that estimated using half-maximum and was closest to Leaf Area Index (LAI8) (DOY 163). All VPs predicted start of growth within an 18 day period from DOY 157 to DOY 175.

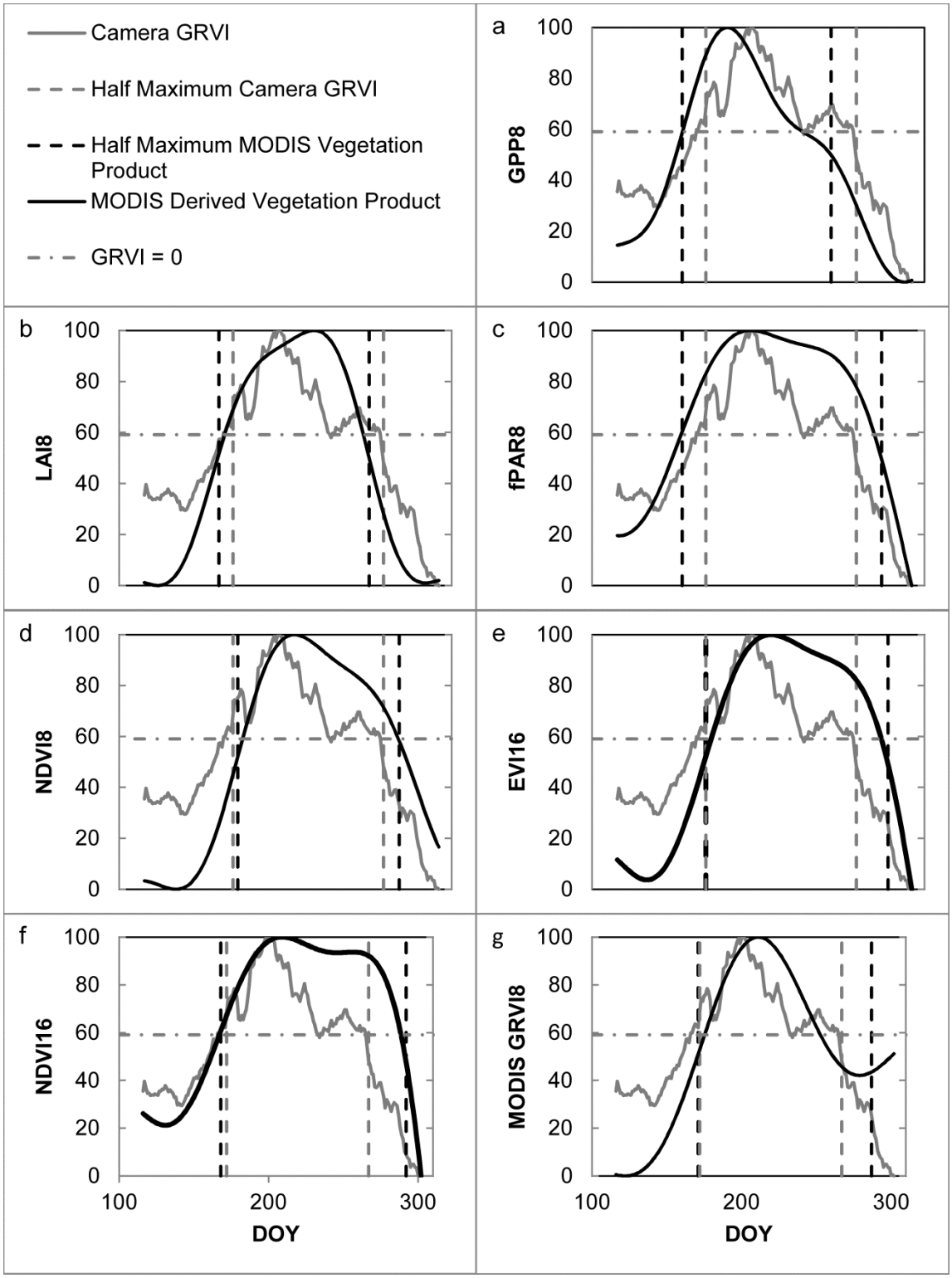

Figure 4.6 Time series of digital camera measured Green Red Vegetation Index and MODIS derived Vegetation Products scaled to percentage of maximum value to allow for direct comparison.

Table 4.3. Summary of phenological measures, day of year for start, peak and end of growth and length of season. Number in brackets indicate the number of days difference between phenological measures, measured with Green-Red Vegetation Index derived from the digital camera estimated using the half-maximum method (first number) and the zero threshold method (second number) and those estimated using MODIS vegetation products. Days Out is the average number of days difference for start, peak and end of growth. Pearson's correlation coefficient between GRVI and the other vegetation products is shown (p<0.001) n=187.

Data Source	Vegetation Product	Spatial Resolution (m)	Start of Growth (DOY)	Peak (DOY)	End of Growth (DOY)	Days Out Half-Maximum Method	Days Out Zero Threshold Method	Length of Season (Days)	Pearson Correlation Coefficient
Digital Camera GRVI	Half-Maximum		172	201	267	3	0	95	1
	Zero Threshold		164	201	234	0	3	70	1
MODIS	GPP8	1000	157 (15/7)	186 (15/15)	251 (16/17)	15	13	94 (1/24)	0.756**
	LAI8	1000	163 (9/1)	223 (22/22)	258 (9/24)	13	16	95 (0/25)	0.887**
	fPAR8	1000	157 (15/7)	200 (1/1)	283 (16/49)	11	19	126 (31/56)	0.899**
	NDVI8	500	175 (3/11)	211 (10/10)	277 (10/43)	8	21	102 (7/32)	0.899**
	NDVI16	250	168 (4/4)	209 (8/8)	292 (25/58)	12	23	124 (29/54)	0.755**
	EVI16	250	172 (0/8)	213 (12/12)	287 (20/53)	11	24	115 (20/45)	0.752**
	MODIS-GRVI8	500	171 (1/7)	211 (10/10)	244 (23/10)	11	9	73 (22/3)	0.741**
Met	Temp	N/A	182 (10/18)	197 (4/4)	282 (15/48)	10	23	100 (5/30)	0.763**

The timing of the peak growth varied from DOY 186 (GPP8) to 213 (EVI16) a 37 day period. The peak was most accurately estimated by fPAR8 being 1 day early. Only GPP8, fPAR8 and air temperature predicted the peak before GRVI.

The timing of end of growth from MODIS derived data ranged from DOY 244 (MODIS-GRVI8) to DOY 292 (NDVI16) a spread of 48 days. End of growth estimated by the zero-threshold was earlier (DOY 234) than all of the MODIS derived VPs and 33 days earlier than that estimated by the half-maximum. MODIS-GRVI8 was the closest MODIS derived VP, 10 days late. MODIS VPs were closer to end of growth estimated by the half-maximum ranging from 9 (LAI8) to 25 (NDVI16) days out.

The length of season estimated by LAI8 was the same as that estimated by the half-maximum, (95 days), the growing season estimated by GPP8 was 1 day shorter. MODIS-GRVI8 estimated the length of season to be 73 days whilst the

other VPs estimated longer seasons (94-136 days) as the end of growth dates were later. The average days out across the three metrics (DO) indicated that NDVI8 and MODIS-GRVI8 were the best predictors of phenological timings across the whole season based on half-maximum and zero-threshold respectively.

GRVI greened-up between start of growth (half-maximum) and peak growth (Figure 4.4) more rapidly than all the other VPs except GPP8 taking 29 days and air temperature taking 15 days. Green-up between the start of growth (zero-threshold) and peak was longer than that calculated by the half-maximum method, GPP8, NDVI8 and air temperature but more rapid than NDVI8, LAI8, fPAR8, EVI16 NDVI16 and MODIS-GRVI8. Zero-threshold GRVI and MODIS-GRVI8 were approximately symmetrical about the peak taking a similar number of days (within 7 days) to return to half-maximum and rise from half-maximum to peak (Figure 4.4g). The other VPs were notably asymmetrical with GPP8, fPAR8, NDVI8, NDVI16, EVI16 and air temperature showing a much shallower decrease in autumn than spring increase, taking up to 85 days (air temperature) to return to the half-maximum value. LAI8 was the only VP quicker to decrease from the peak than increase in the spring.

Comparing each day individually all VPs showed a statistically significant correlation ($p<0.001$) with GRVI (Table 4.3). fPAR8 and NDVI8 had the strongest correlations ($r=0.899$), fPAR8 was also the best predictor for the timing of peak growth.

4.6.2 Comparing Vegetation Products to Carbon Dioxide Fluxes

Net Ecosystem Exchange (NEE) became more strongly negative as all vegetation products (VPs) increased indicating greater CO_2 draw-down. MODIS and camera GRVI as well as fPAR8 were significantly related to NEE (Figure 4.5a, d & h). Camera GRVI was the only VP to be significantly related to ecosystem respiration ($r=0.94$, $p=0.019$) whilst MODIS ($r=0.89$, $p=0.041$) and camera ($r=0.97$, $p=0.005$) GRVI were the only VPs to be significantly related to photosynthesis at 600 Photons m^{-2} s^{-1}.

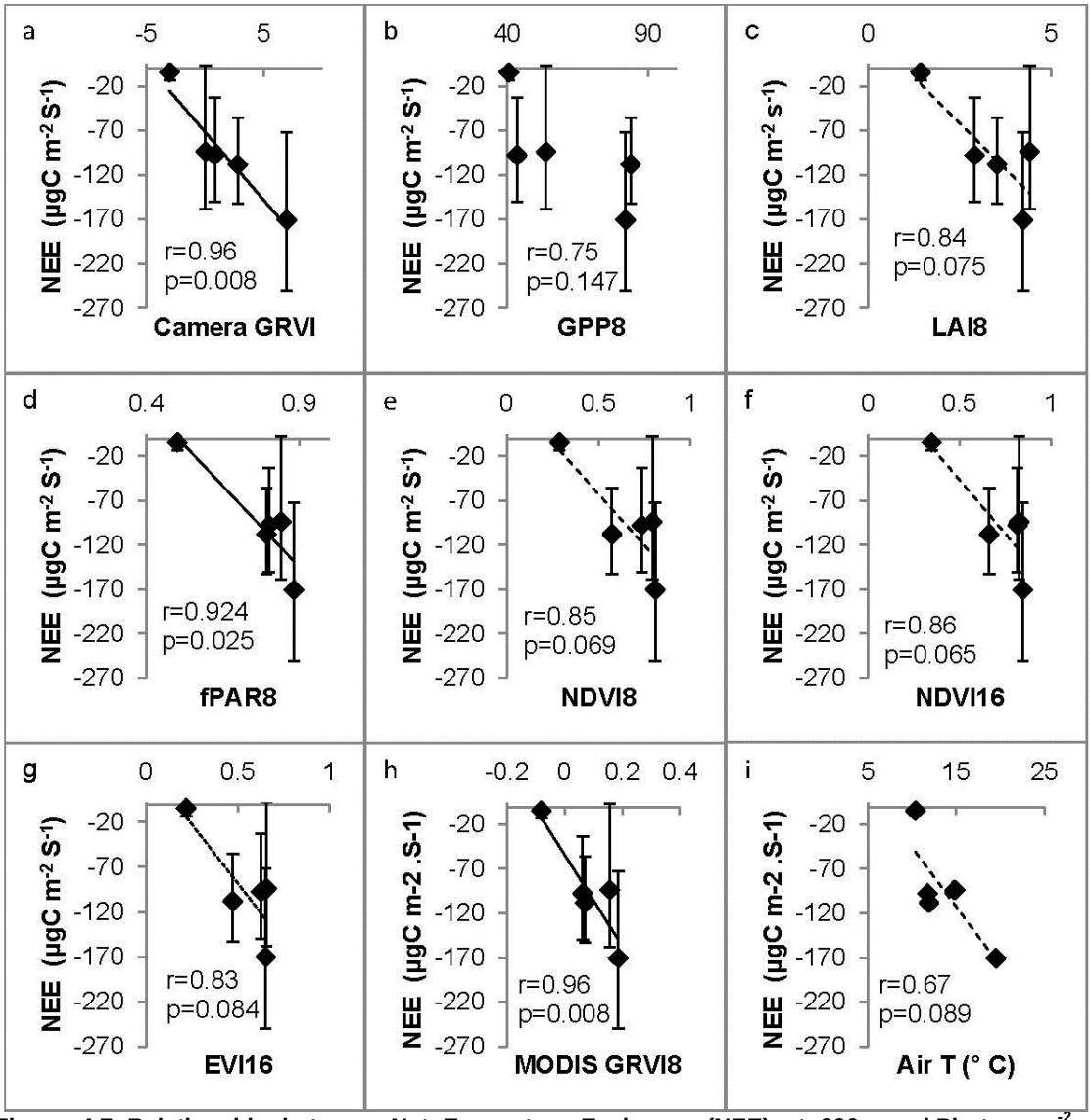

Figure 4.7 Relationship between Net Ecosystem Exchange (NEE) at 600 µmol Photons m^{-2} s^{-1} (µgC m^{-2} s^{-1}) and digital camera Green Red Vegetation Index, MODIS derived Vegetation Products and air temperature (° C). Linear correlations shown are with solid lines where p<0.050 and dashed lines where p<0.099. Error bars show 95 % confidence intervals.

4.7 DISCUSSION

4.7.1 MODIS Vegetation Products as Measures of Phenology

Studies using digital images to track phenology have typically used relative brightness of green (Richardson *et al.* 2007, Ahrends *et al.* 2008, Parihar *et al.* 2013, Alberton *et al.* 2014), greenness excess index (Ide and Oguma 2010, Coops *et al.* 2011, Hufkens *et al.* 2012, Saitoh *et al.* 2012) or both (Migliavacca *et al.* 2011, Mizunuma *et al.* 2013). These products are strongly affected by illumination conditions (Sonnentag *et al.* 2012), with the blue band showing

most variability. Other products such as hue have been proposed to overcome variation in illumination (Saitoh *et al.* 2012) but the green-red vegetation index (Tucker 1979) was selected for this study. It does not use the more variable blue band and is therefore less sensitive to variation in illumination conditions, this is in keeping with Zhou *et al.* (2013) who found the ratio of green to red to be better suited to monitor winter wheat phenology than relative brightness of green.

Comparing Start of Growth and End of Growth estimated using the zero-threshold method to the half-maximum method there was an 8-day difference between the zero-threshold method and the half-maximum method in the spring and a 33 day difference in the autumn (Table 4.3). Green Red Vegetation Index (GRVI) then increased and remained above zero until Day Of Year (DOY) 266 only 1 day earlier than end of growth estimated using the half-maximum method. This illustrates the problem of using a threshold method on bimodal data, that there are two potential end of growth dates (Figure 4.4). Excluding the first crossing of the threshold both methods show remarkable agreement for both start of growth and end of growth (8 and 1 day(s)) indicating the robustness of the zero-threshold (Motohka *et al.* 2010) and half-maximum (Fisher and Mustard 2007, Coops *et al.* 2011, Henneken *et al.* 2013).

MODIS has often predicted start of growth earlier than ground measurements, this has been attributable to both understory development (Ahl *et al.* 2006) in forests and spatial integration across a topographic gradient (Fisher and Mustard 2007). In this ecosystem there is limited understory vegetation and the range in elevation in this study is around 30 m, insufficient to affect start of growth as observed across an 800 m gradient by Fisher and Mustard (2007). However, the height of the object to which the camera was fixed limited the elevation of the camera restricting it to a low viewing angle. Therefore, early green shoots were not observed within the dead biomass of the previous year. Vegetation products may have started to green up only once the shoots protruded above the dead biomass, resulting in a later start of growth date than if a downwards facing camera had been used (Mizunuma *et al.* 2013). This

may also explain why many of the MODIS VPs (Table 4.3) predicted start of growth earlier than digital camera derived GRVI, as MODIS has a near nadir view, green shoots may have been visible earlier leading to earlier estimates of start of growth.

The range in the timing of onset of greenness for each site using Enhanced Vegetation Index (EVI) (1-24 days) and Normalised Difference Vegetation Index over an 8 day period (NDVI8) (2-26 days) (Hufkens *et al.* 2012) were similar to the number of days out between start of growth estimated by GRVI and either the half-maximum (0-15 days) or zero threshold (1-22 days) methods despite the different phenological metrics used. The difference between peak greenness, a more comparable measure, was within the range observed by Hufkens *et al.* (2012) for individual cameras for individual years (EVI 8-day composite 0-25 days out and NDVI8 0-26 days out).

NDVI8 has been found to be a better predictor of the onset of greenness and maturity compared to NDVI16, EVI16, Leaf Area Index (LAI8) and fraction of absorbed Photosynthetically Active Radiation (fPAR8) in a broadleaf forest (Ahl *et al.* 2006) as it has a better temporal resolution and does not rely on biome classification like fPAR8 and LAI8. However, when using the half-maximum method to predict start of growth it would appear that spatial resolution is more important in this ecosystem than temporal resolution. In this study EVI16 (0 days) and MODIS-GRVI8 (1 day) were the best predictors of start of growth whilst NDVI8 and NDVI16 were 3 and 4 days out (Table 4.3), all these VPs have a spatial resolution of 500 m or less. Gross Primary Productivity (GPP8), LAI8 and fPAR8 with a 1000 m spatial resolution were nine or more days out.

This study used a combination of MODIS VPs with an acquisition date (NDVI8, GRVI8, NDVI16 and EVI16) and composite VPs averaged over an 8-day interval arbitrarily assigned to the first day of the interval (LAI8, fPAR8 and GPP8). It has been shown that using first date of the interval rather than acquisition dates for 16-day NDVI affects the resultant timeseries; significant bias especially in the spring and autumn, reduced the accuracy of start of

growth estimation (Testa *et al.* 2014). From this it would be expected that composite VPs would be less accurate at predicting start and end, therefore acquisition dates were used where available. GPP8, LAI8 and fPAR8 estimated start of growth earlier than GRVI (Table 4.3) indicating a bias in spring, possibly due to using the first date in the interval. However, these VPs both over and underestimated peak growth and end of growth indicating no systematic bias over the period studied.

For ecosystems where green-up occurs rapidly, such as temperate woodlands where bud-burst to canopy maturity occurs in the region of 10-12 days (Ahl *et al.* 2006), a higher temporal resolution VP is vital so that at least one data point lies within the greening-up period. If for example, due to cloud cover, there is no data within the period of rapid change, the accuracy of start of growth estimated is dramatically decreased (Zhang *et al.* 2009). The ecosystem measured in this study took around 75 days to go from small shoots to maximum green leaf extent (Figure 4.4), comparable to the 40-60 days to maximum leaf height observed for alpine grasslands (Migliavacca *et al.* 2011). However, a dramatic change in green vegetation cover occurred over an 8-day period between DOY 156 and 164 (Figure 4.2) a time interval equivalent to the temporal resolution of NDVI8 etc. This indicates the precision of start of growth estimated is likely to be better using a finer temporal resolution VP but, neither 8-day nor 16-day MODIS data are likely to “miss” green-up in these ecosystems where the green-up and senescence periods are longer.

In an evergreen *(Chamaedaphne calyculata, Ledum groenlandicum and Kalmia angustifolia) a*nd deciduous *(Vaccinium myrtilloides*) shrub covered northern peatland the temporal resolution of NDVI16 was also found to be insufficient to capture start of growth (Moore *et al.* 2006). This may be because the vegetation was dominantly evergreen so differences in the spectral characteristics of the vegetation were small and obscured by large changes in VPs due to snow melt. In the uplands of the UK snow coverage is generally intermittent and unlikely to last until the start of growth, when mean daily temperatures are 7.8 °C in April (UK Meteorological Office 2012). Additionally

the deciduous nature of the vegetation present makes its phenological behaviour more striking.

MODIS GPP8, LAI8 and fPAR8 products have lower spatial resolution (1000 m^2) resulting in pixels containing both deciduous *Molinia caerulea* dominated moorland and improved acidic grassland (Figure 4.1). These products will therefore reflect the phenology of both land-cover types. Many of the species typical of upland acid grasslands such as Common Bent grass (*Agrostis capillaris*), Sheep's Fescue (*Festuca ovina*), Sweet Vernal Grass (*Anthoxanthum odoratum*) and Wavy Hair Grass (*Deschampsia flexuosa*) are present within the *Molinia caerulea* dominated moorland. VPs of 1000 m spatial extent (LAI8, GPP8, and fPAR8) were the poorest predictors of start of growth (9-15 days) but best predictors of peak (fPAR8) and end of growth (LAI8 and GPP8). Start of growth may be earlier in the VPs containing acidic grassland as the previous year's vegetation was removed by grazing so the new shoots were visible sooner. The improved and natural grassland vegetation were responding to the same environmental conditions therefore peak growth and end of growth were similar for both land covers.

VPs with 8-day temporal resolution (LAI8, GPP8, fPAR8 and NDVI8) had the strongest day-to-day correlations with camera derived GRVI (Table 4.3). This indicates that to capture the full season phenology rather than start of growth, a finer temporal resolution becomes more important than spatial resolution.

MODIS-GRVI8 might be expected to have the strongest correlation with camera derived GRVI as it uses the same wavelengths of light and has an 8 day temporal resolution. However, MODIS-GRVI8 had the weakest day-to-day correlation. This may be because GRVI8 uses the visible wavelengths where the noise to signal ratio is greater than in other bands such as near infra-red used by NDVI8.

Once the vegetation had started growing air temperature showed a good agreement to GRVI (Figure 4.5). However, the poor correlations in the spring

and autumn mean that air temperature cannot be used to define the start and end of growth.

Start of growth and end of growth predicted using the half-maximum method on a fusion of 30 m resolution Landsat and daily resolution MODIS data were 4.5 and 3.3 days out across seven sites (Coops *et al.* 2011). The best predictors of start and end of growth, EVI16 and LAI8, were 0 and 9 days out indicating the potential improvement in phenological accuracy, particularly in the autumn, that is possible with better spatial and temporal resolution. Improvements could also be obtained by enhancing estimates of the half-maximum value. The gradual green-up and senescence in this ecosystem makes the timing of start and end of growth estimated using the half-maximum method more sensitive to changes in the value of the half-maximum. It also explains why there was greater uncertainty in the estimates of end of growth, with a shallower gradient, compared to start of growth within this study (Table 4.3).

One of the issues with using digital camera imagery to validate MODIS data is the uncertainty in what is actually being measured by the digital camera (Keenan *et al.* 2014). For example, LAI8 showed rapid spring growth to around DOY 180 (Figure 4.4b) then continued to increase to a late peak on DOY 238 before rapid senescence, this is consistent with the expected pattern of leaf growth (Nieveen *et al.* 1998) for *Molinia caerulea* but in contrast to the phenology measured by GRVI (Figure 4.4b). MODIS-LAI continued to increase beyond maximum GRVI (Figure 4.4b) probably as leaf area continued to increase but the canopy had closed in the direction of the camera. Without ground validation it is not possible to assess if MODIS-LAI8 accurately measured the dynamics of LAI. However, as both leaf structure and pigment influence photosynthetic activity it is the combined affect that is of interest.

4.7.2 Vegetation Products as Proxies for Net Ecosystem Exchange

It is known that seasonal variation in physiological pigments as well as shrub and tree leaf area, both measurable by digital camera VPs, result in variation in

photosynthetic capacity (Muraoka and Koizumi 2005). This study investigated if MODIS vegetation products could also identify this seasonal variation.

Direct comparisons between GPP and MODIS-GPP8 or NDVI have found MODIS VPs to underestimate GPP in both northern peatlands (Moore *et al.* 2006, Kross *et al.* 2013) and African savannahs (Sjöström *et al.* 2011). In this study, GPP was also significantly underestimated by MODIS-GPP8, -41 to -84 μgC m^{-2} s^{-1} compared to -11 to -304 μgC m^{-2} s^{-1} measured. Additionally MODIS-GPP8 was not significantly correlated to measured NEE (Figure 4.5). As the radiation efficiency use model used to derive MODIS-GPP8 includes air temperature it has been found to correlate more strongly with ecosystem respiration (Schubert *et al.* 2010).

In northern peatlands NDVI16 saturated (Schubert *et al.* 2010) so EVI16 was considered a better proxy for GPP. In this study the canopy closed during the summer but NDVI did not saturate so EVI16 and NDVI behaved similarly (Figure 4.4e & f). NDVI8 and NDVI16 were non-significantly correlated to NEE ($r>0.85$, $p<0.069$) (Figure 4.5e & f). The correlation coefficient was greater than in other studies, NDVI16 explained 25-53 % of the temporal variation in 8 day averaged NEE (Kross *et al.* 2013) across four northern peatland sites and MODIS-GPP8 44-45 %. The explanatory power was greater in alpine grasslands where NDVI16 and EVI16 explained 71 % and 44 % of the variation in gross primary productivity (GPP) (Rossini *et al.* 2012). This reflects both the limited number of samples (n=5) and aggregated short-term variation (due to variation in illumination and environmental conditions) in this study. Additionally in this research best quality (e.g. fPAR8) or greatest value (e.g. NDVI8) data has been compared to NEE at 600 μmol Photons m^{-2} s^{-1}, equivalent to a clear, sunny day. This would be expected to have a better correlation than comparing average NEE, including cloudy periods, to MODIS data from cloud free days.

The small sample size (n=5) means this study cannot state which of the VPs is best as a direct proxy for NEE. However, fPAR8, NDVI8 and LAI8 show good day to day agreement with camera derived GRVI (Table 4.3) highlighting their

potential to be used as phenological proxies in CO_2 models. Where meteorological data such as PAR and/or temperature have been used in conjunction with MODIS data the explanatory power has increased markedly (Rossini *et al.* 2012).

In northern peatlands the relationship between MODIS-NDVI and NEE has been found to be both site specific (Schubert *et al.* 2010) and valid across multiple sites (Kross *et al.* 2013). Further work is required to determine if a CO_2 model derived for a *M. caerulea* dominated site, based on meteorological data and a MODIS VI, is transferable to other sites thereby providing a means of upscaling CO_2 fluxes to a landscape scale.

4.8 CONCLUSION

Start, peak and end of growth and season length were estimated using the Green Red Vegetation Index (GRVI) derived from time-lapse camera images. The Moderate resolution Imaging Spectroradiometer (MODIS) derived vegetation products (VPs) with the closest start, peak and end of growth dates were EVI16 (0 days), fPAR8 (-1 day) and LAI8 (-9 days) respectively. Over the three metrics NDVI8 (NDVI in an 8 day period) was the most accurate being 8 days out on average. In general VPs with finer spatial resolution (250 and 500 m) more accurately captured spring green-up whilst VPs with finer temporal resolution (8-days) better captured whole season dynamics in this ecosystem. Pearson's correlation between daily MODIS VPs and camera derived GRVI indicated NDVI8 and fPAR8 to have the strongest correlations (r=0.89). These data were capable of characterising the phenology of this *Molinia caerulea* dominated peatland.

Manual measurements of phenology are laborious, site specific and subjective. This study outlines a robust and objective method for measuring the phenology of a remote, deciduous ecosystem with a daily time-step at a spatial scale (500 - 1000 m) appropriate for carbon budgeting. MODIS fPAR8 and NDVI8

demonstrate great potential as proxies of vegetation phenology at a landscape scale for use in net ecosystem exchange models.

4.9 ACKNOWLEDGEMENTS

The authors would like to thank the Exmoor Mires Project for their help with site access. This research received financial support from South West Water and The University of Exeter (SK05284). The authors thank the editor and two anonymous reviewers for their comments on an earlier version of the manuscript.

5 TEMPORAL VARIABILITY IN GROWING SEASON CO_2 FLUXES IN A DRAINED *MOLINIA CAERULEA* DOMINATED PEATLAND.

5.1 ABSTRACT

Peatlands are a declining ecological resource damaged by inappropriate management such as drainage. Carbon markets may provide funding for peatland restoration however, there are currently no quantified or appropriate emission factors for *Molinia caerulea* dominated peatlands. There is clearly a need to quantify CO_2 fluxes in these landscapes to support these schemes.

Over the growing seasons of 2012 to 2014 photosynthesis at 600 µmol Photons m^{-2} s^{-1} (P_{G600}) and ecosystem respiration (R_{Eco}) were measured approximately monthly from vegetated plots and partitioned below-ground respiration was measured fortnightly from clipped and trenched or clipped plots using closed chamber techniques. Plots were located in six sites across two catchments (Aclands and Spooners) (n = 18) in Exmoor National Park, southwest England.

All CO_2 fluxes measured showed strong seasonal variability with greatest fluxes in mid-summer. Soil temperature explained up to 82 and 87 % of the variation in P_{G600} and R_{Eco} observed. MODIS Normalised difference Vegetation Index (NDVI) explained up to 77 % of the variation in P_{G600}. At Spooners, P_{G600} and below-ground autotrophic respiration increased during drier (and warmer) periods but not at Aclands. Ecosystem respiration and below-ground heterotrophic respiration both showed no response to variation in water table depth. An empirically derived net ecosystem exchange model parameterised using closed chamber measurements taken in both catchments at a range of light levels (n = 1190) estimated the drained peatland to have been a larger CO_2 source from 01/05/2012 to 30/04/2013 (88 ±129 gC m^{-2}) than 01/05/2013 to 30/04/2014 (16 ±155 gC m^{-2}). This suggests that ecohydrological restoration of these ecosystems is vital to prevent further losses from this long-term peat store.

5.2 INTRODUCTION

Peatlands are known to be significant stores of carbon (Gorham 1991, Yu *et al.* 2010). In a functioning peatland, over time a small imbalance between primary productivity and decay leads to the gradual accumulation of carbon. Damaging land management practices including drainage (Holden *et al.* 2004), afforestation (Martikainen *et al.* 1995), burning (Yallop *et al.* 2006), grazing (Tucker 2003) and commercial extraction (Soini *et al.* 2010) have altered the functioning of these ecosystems. This has turned some peatlands from carbon sinks to carbon sources (Littlewood *et al.* 2010). Although carbon markets have been identified as possible sources of funding for peatland restoration schemes, currently most UK peatland management practices (Birkin *et al.* 2011) have no default international emission factors. This highlights the need to quantify emissions from a greater range of management and vegetation types (Evans *et al.* 2011).

As direct measurements of CO_2 fluxes are challenging and expensive, quantifying emissions in a way that links them directly to more readily measured proxies (e.g. water table depth, vegetation composition and soil temperature) so that CO_2 fluxes can be estimated for other sites is increasingly important. In addition, partitioning below-ground heterotrophic respiration from ecosystem respiration separates the decomposition of the peat store from the larger more dynamic ecosystem respiration, dominated by the vegetation component. Using a combination of gas flux chambers and soil collars enables both the above and below ground processes to be examined at a scale that is directly attributable to processes (Tuittila *et al.* 1999). This will give a better understanding of the biotic and abiotic variables driving temporal variation in CO_2 fluxes and their effect on primary productivity and decay.

Most studies investigating the effect of drainage have compared “pristine” to drained areas of high-latitude peatlands (boreal, arctic and subarctic) (Silvola *et al.* 1996a, Alm *et al.* 1999a, Makiranta *et al.* 2008, Straková *et al.*). Maritime peatlands are rarely prone to winter frosts, as in boreal peatlands (Aurela *et al.*

2004, Lund *et al.* 2007) and therefore the start of the growing season is dependent on winter soil temperature and the occurrence of dry days (Sottocornola and Kiely 2010) rather than snow melt and spring soil temperatures (Moore *et al.* 2006) resulting in a more gradual start and end to the growing season compared to more continental peatlands (Lund *et al.* 2015). Where studies have focused on the temperate maritime peatlands typical of Britain, the study sites have been dominated by *Calluna vulgaris* rather than *Molinia caerulea (Rowson et al. 2010)*. Grasses such as *Molinia caerulea* have been shown to have a greater annual carbon uptake and biomass production (Berendse 1998, Otieno *et al.* 2009, Ward *et al.* 2009) but also be more labile and readily decomposed (Coulson and Butterfield 1978, Berendse 1998) than dwarf shrubs (e.g. *Erica tetralix* and *Calluna vulgaris*) and *Sphagnum* species. *Molinia caerulea* is widespread across northern Europe (Taylor *et al.* 2001) and dominates approximately 10 % of British uplands (Bunce and Barr 1988). At present there are no appropriate estimates of CO_2 emissions for drained *Molinia caerulea* dominated peatlands and only a limited understanding of the processes that drive CO_2 fluxes in these ecosystems.

It is hypothesised that in a *Molinia caerulea* dominated, drained, shallow peatland, temporal variation in CO_2 fluxes (ecosystem respiration; gross photosynthesis; total below-ground respiration; heterotrophic respiration of soil organic matter and below-ground autotrophic respiration including root respiration and microbial respiration of root exudates) will primarily be driven by vegetation phenology and temperature due to the deciduous nature of the vegetation. It is also hypothesised that water table depth will have no effect on CO_2 fluxes as *Molinia caerulea* has evolved to live in environments with fluctuating water table depths (Taylor *et al.* 2001).

5.3 METHOD

5.3.1 Study Sites

The study sites were located in Exmoor National Park in the southwest of England in two *Molinia caerulea* dominated headwater catchments subject to

drainage (Aclands 51°7’51.3N 3°48’44.4W) and Spooners (51°7’21.9N, 3°44’52.9W) catchments, Figure 5.1). Exmoor has 65 km^2 (Merryfield 1977) of blanket bog, of this 53 km^2 is less than 30 cm thick. In both catchments, drainage ditches of variable size, up to 0.5 m wide and 0.5 m deep, were hand dug from the 1830s (Hegarty and Toms 2009). Between the 1960s and 1980s larger ditches (>1.5 m wide) were dug by machine to drain specific areas such as springs (Mills *et al.* 2010). Aclands is slightly higher in altitude (425-465 metres above sea level (m asl)) than Spooners (380-445 m asl). Both catchments are classified as National Vegetation Classification class M25: *Molinia caerulea – Potentilla erecta* mires (Rodwell 1991).

Long-term (1981-2010) average annual rainfall at nearby Liscombe (UK Meteorological Office 2012) (49°46’50.4N 7°31’07.6W) totals 1445 mm with mean monthly temperature ranging from a minimum of 1.1 °C in February rising to 18.6 °C in July and August.

Six sites across the two catchments were chosen to encompass the expected variation in altitude, aspect, slope, peat depth and ditch dimensions (Table 5.1), three replicates were collected at each site, their locations are shown in Figure 5.1c & d. Ditches surrounding these sites were blocked in April 2013 at Spooners and April 2014 at Aclands, these sites were left unblocked. It is assumed they were unaffected by the surrounding disturbance. A separate study (chapter 8) investigated the effect of restoration on CO_2 fluxes with data from this study defining the baseline.

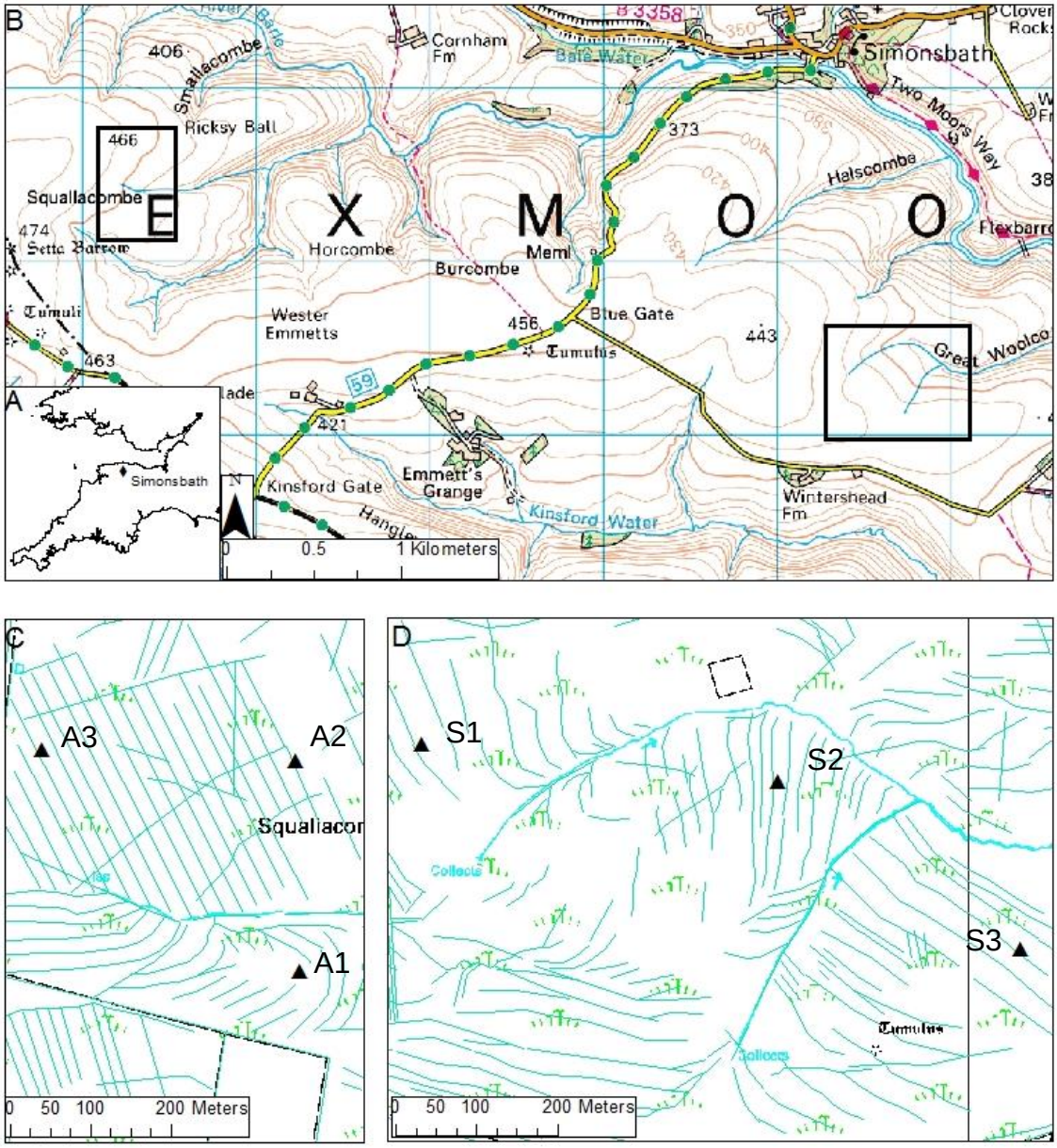

Figure 5.1 Location of Aclands and Spooners catchments (b) within the southwest of England (a). Location of study sites within Aclands (c) and Spooners (d) study catchments. Man-made drainage ditches and "natural" streams are shown in light blue. Coastline shapefile (Ordnance Survey 2008a), 1:50 000 Ordnance Survey Map (Ordnance Survey 2008e) 1:10000 Ordnance Survey map (Ordnance Survey 2008b, c).

Table 5.1 Site properties of experimental sites at Aclands and Spooners.

Site	Mean Peat Depth[1] (cm)	Mean Ditch Width (cm)	Mean Ditch Depth[2] (cm)	Distance from ditch to down-gradient ditch[3] (m)	Altitude[4] (m)	Slope[4] (°)	Aspect	Direction of Ditch[4] (°)	Ditch Direction w.r.t slope
S1C	23	67	18	43.9	418	4	ESE	150	Cross-Slope
S2C	56	80	45	15.4	395	5	NE	0	Down-Slope
S2C	29	42	24	32.8	407	5	N	300	Down-Slope
A1C	38	32	20	20.3	443	2	NE	10	Down-Slope
A2C	43	43	21	19.1	448	5	SE	150	Down-Slope
A3C	36	42	18	18.7	461	3	SE	151	Down-Slope

1. Measured during dipwell installation from base of peat (n=3), 2. Measured from base of ditch to tussock shoulder, 3. Measured using tape measure, 4. From LiDAR.

5.3.2 Gas Flux Measurements

5.3.2.1 Net Ecosystem Exchange

A 55 cm x 55 cm x 25 cm Perspex gas flux chamber, with two fans to mix the air inside the chamber, was rested on permanently installed 50 cm tall legs with a plastic skirt weighted down to the soil surface with a heavy chain to form an airtight seal (following Shaver *et al.* 2007, Street *et al.* 2007). An EGM-4 infra-red gas analyser (PP Systems, Hitchin, UK) measured accumulated CO_2 every 10 seconds for 2 minutes concurrently with chamber temperature and photosynthetic active radiation (PAR) (PAR Quantum, Skye Instruments, Llandrindod Wells, UK). The soil temperature at 5 cm and the depth of the water table below the peat surface were also measured using a meter rule. The chamber was removed between measurements to restore ambient conditions. CO_2 flux measurements were taken at full light, full dark and ~60% ~40%, ~10% light levels using a combination of shade cloths. The net CO_2 exchange at each light level was calculated from the linear change in CO_2 concentration in the chamber. The volume inside the chamber was estimated by measuring the height from the ground to the base in a grid of nine points and this volume was added to that of the chamber.

Samples were collected approximately monthly at both catchments during the 2012 and 2014 growing seasons. The measurements are very time consuming, therefore in 2013, it was decided to put all efforts into quantifying the effects of restoration on the CO_2 fluxes from Spooners (Supplementary Material Table 11.1 control locations only). To assess temporal variation, light response curves were determined for each sample round (14 in total) for each site (three replicates) separately using a non-linear regression to a hyperbolic light response curve (Equation 4.3);

Equation 5.1 hyperbolic light response curve

$$\mathrm{NEE} = R_{\mathrm{Eco}} - \frac{P_{max}.\mathrm{I}}{k + \mathrm{I}}$$

where NEE is the net ecosystem exchange (μgC m^{-2} s^{-1}), P_{max} is the rate of light saturated photosynthesis (μgC m^{-2} s^{-1}), k is the half-saturation constant of photosynthesis (μmol Photons m^{-2} s^{-1}), I the incident PAR (μmol Photons m^{-2} s^{-1}) and R_{Eco} the ecosystem respiration (μgC m^{-2} s^{-1}). As there is no theoretical limit to the PAR at which P_{max} (Equation 4.3) occurs, unrealistically high values may be determined, therefore photosynthesis at 600 μmol Photons m^{-2} s^{-1} was calculated for each sample round.

5.3.2.2 Soil CO_2 Efflux

At each plot, four PVC collars (16 cm diameter, 8 cm height) were sealed to the peat using Plumbers Mait (Eco-Stick). Collars were installed in March 2012. All collars had above-ground vegetation removed by regular clipping so they measured below-ground fluxes only. In addition circular 20 cm deep trenches with a diameter of 56 cm were dug around half the collars. Thus live roots were excluded allowing for the measurement of the below-ground heterotrophic component. The collars with only above-ground vegetation removed were used to measure total below-ground respiration (including autotrophic and heterotrophic components). In each plot, the two replicates of each treatment were averaged to produce a single value for total and heterotrophic respiration for each plot to reduce spatial variability.

CO_2 measurements were taken in a semi-randomised pattern approximately every three weeks over the growing season (Supplementary Material Table 11.2 control locations only). CO_2 flux was measured over 2 minutes using an EGM-4 infra-red gas analyser and a CPY-4 canopy assimilation chamber (PP Systems, Hitchin, UK). Autotrophic respiration was calculated from the difference between average total (n≤2) and average heterotrophic respiration (n≤2) measured at each location for each sample round. At the same time as CO_2 flux measurements were made, the depth of the water table below the peat surface and soil temperature at 5 cm were measured. The soil temperature measurement depth was selected based on the highest r^2 values obtained.

below-ground respiration has been shown to be strongly controlled by soil temperature (Lloyd and Taylor 1994), adjusting soil respiration to a fixed temperature enables the effects of other variables to become apparent. Regression between the mean soil temperature at 5 cm (T) and the mean respiration rate (R_T) for each sample day at each site enabled the calculation Q_{10} (the increase in respiration rate for a 10 °C increase in temperature) (Equation 5.2). Using the Q_{10} values calculated by Equation 5.2 for total, heterotrophic and autotrophic respiration (Table 5.4) for each site, all respiration rates were normalised to 10 °C (r_{10}) (Equation 5.3).

Equation 5.2

$$LnR_T = LnR_{10} + \frac{LnQ_{10}}{10}(T - 10)$$

Equation 5.3

$$r_{10} = R_t . Q_{10}^{\,10-t/10}$$

5.3.3 Vegetation Phenology Proxy

A number of studies have found photosynthesis to be strongly related to vegetation phenology measured by leaf area (Nieveen *et al.* 1998, Street *et al.* 2007, Otieno *et al.* 2009), vegetative green area (Riutta *et al.* 2007, Urbanová *et*

al. 2012) and leaf biomass (Bubier *et al.* 2003). These metrics are arguably more accurate measures of vegetation phenology at the plot scale. However, they are hugely labour intensive and site specific. In order to relate CO_2 fluxes to readily measured variables, so they are transferable, it was decided to use Moderate resolution Imaging Spectroradiometer (MODIS) data as a proxy for vegetation phenology. MODIS tile h17 v3 (49 to 60°N, 0E to 20°WE) of the MOD15A2 fraction of incoming photosynthetic active radiation (fPAR) product (1000 x 1000 m resolution) and the MODIS9A1 surface reflectance product (500 x 500 m resolution) were downloaded from USGS Earth Explorer (http://earthexplorer.usgs.gov). The normalised difference vegetation index (NDVI) was derived from bands 1 and 2 of the surface reflectance (Equation 5.4).

Equation 5.4 Normalised Difference Vegetation Index

$$NDVI8 = \frac{Band\ 2\ (NIR) - Band\ 1\ (Red)}{Band\ 2\ (NIR) + Band\ 1\ (Red)}$$

MODIS data quality labels and cloud cover data were extracted for the pixels of interest (2 for each catchment). Data were screened and poor quality data (cloudy, high aerosol concentrations or poor geometry) given a weighting of 0 and all other data a weighting of 1. To minimise variation due to atmospheric conditions, illumination and observation geometry a third order Fourier smoothing filter was applied. Points outside the 99 % confidence interval were excluded. All remaining points were then weighted equally and a Fourier third order series fitted to form a continuous timeseries for each pixel (chapter 4). These were then averaged to form a composite fPAR and NDVI timeseries for each catchment separately and for both catchments together. Winter values were set to the spring or autumn minimum values as appropriate.

5.3.4 Statistical Analysis

The temporal relationship between average abiotic (water table depth and soil temperature) and biotic (fPAR and NDVI) variables and average R_{Eco}, P_{G600}, total, heterotrophic and autotrophic respiration at 10 °C for each sample round

(time step) were tested using linear regression analysis for each catchment. In addition exponential, Arrhenius (Arrhenius 1898) and Lloyd-Taylor (Lloyd and Taylor 1994) soil temperature relationships were tested by non-linear regression with P_{G600} and R_{Eco}. As vegetation phenology strongly varies with temperature, exponential fPAR and NDVI relationships were also tested by non-linear regression with P_{G600} and R_{Eco}.

As temperature co-varied with fPAR and NDVI two multiple stepwise linear regressions were carried out for P_{G600} and R_{Eco}, the first with water table depth, NDVI and soil temperature at 5 cm, the second with fPAR instead of NDVI. NDVI, fPAR and soil temperature at 5 cm were natural logarithm transformed as they demonstrated an exponential relationship with P_{G600} and R_{Eco}.

5.3.5 Net Ecosystem Exchange Modelling

An empirically derived non-linear regression model (Equation 5.5) was parameterised across both catchments using SPSS 19.0 Statistical package (SPSS Inc., Chicago, Illinois, USA). All measurements collected (full dark, shaded and full light) (n=1190) were used to determine coefficients which maximised the determinant of coefficient (r^2) and minimised parameter standard errors. The model consisted of two components the first represented ecosystem respiration, based on a Lloyd-Taylor response to soil temperature. The Lloyd-Taylor function was selected as it allows for variation in temperature sensitivity with temperature. It produced lower parameter errors and greater r^2 values than exponential or Arrhenius functions. The second was a photosynthesis component based a hyperbolic light response curve regulated by vegetation phenology (NDVI) and soil temperature. .

Equation 5.5 NEE Model

$$NEE = a.\exp\left[E_0.\left(\frac{1}{T_{Ref} - T_0} - \frac{1}{T_5 - T_0}\right)\right] + \frac{P_1.\mathrm{NDVI}.T_5.\mathrm{I}}{k_1 + \mathrm{I}}$$

where T_5 is the soil temperature at a depth of 5 cm (K), T_{Ref} the reference temperature set at 283.15 K or 10 °C, T_0 the temperature at which respiration

reaches zero (227.13 K or -46 °C) (Lloyd and Taylor 1994), I the incident PAR (μmol Photons m^{-2} s^{-1}), NDVI the eight day average NDVI and a, E_0, P_1 and k_1 are empirically derived coefficients.

Instantaneous soil temperature measurement at a depth of 5 cm, measured concurrently with NEE measurements, was found to have the highest r^2 values (compared to 10, 15, 20, 25 and 30 cm) with photosynthesis and ecosystem respiration. Soil temperature was continuously measured at a depth of 15 cm every 15 minutes (Gemini Data Loggers, Chichester, UK) at Spooners site 2. A timeseries of soil temperature at 5 cm was derived by linear regression of soil temperature measured concurrently with the flux measurements against logged soil temperature (r^2=0.70). Soil temperature at 15 cm would be expected to show a dampened temperature response compared to soil temperature at 5 cm so a timeseries derived by linear regression will underestimate highs and lows. The 15 minute timeseries was then averaged to create an hourly timeseries.

An hourly timeseries of PAR was created by regressing (r^2=0.87) full light PAR measurements taken concurrently with the flux measurements (n=583) to global irradiation measured hourly at Liscombe Met Station (UK Meterological UK Meteorological Office 2012). Monthly and annual estimates of NEE were calculated as the sum of the hourly NEE values either monthly or annually from the 1st May for 2012-2013 and 2013-2014.

5.4 RESULTS

5.4.1 Environmental Variables

Conditions were generally cooler (Figure 5.2a, Table 5.2), duller (Figure 5.2b) and wetter (Figure 5.2d) in the summer of 2012 than 2013 and 2014. Following a year of above average temperatures (Figure 5.2a, Table 5.2), the warmest month was July 2014 (14.9 °C). The coolest month was March 2013 (2.8 °C) during a particularly cool spring (Table 5.2). Summer sunshine hours were lower in 2012 than 2013, 2014 and the 30 year average (Table 5.2). Photosynthetically active radiation was also lower in 2012-2013 than 2013-2014

with the brightest month in July 2013 (438 µmol Photons m^{-2} s^{-1}) and the dullest December 2012 (41 µmol Photons m^{-2} s^{-1}) (Figure 5.2b). This was also the wettest month (437 mm) largely due to a single storm event, although 2012 was unusually wet from June onwards (Figure 5.2d, Table 5.2). In contrast, 2013 was usually dry over the summer months (182 mm compared to a long term average of 243 mm), but the driest month was June 2014. Water tables were higher in 2012 reflecting the wetter conditions and decreased through the 2013 growing season as the period of warm and dry weather continued (Figure 5.2c). Water tables reached their deepest in 2014 (30 cm below ground level) coinciding with the warmest and driest months. Standard error in mean water table depth was greater when the water table was higher (wetter) indicating not all sites responded similarly to rainfall events.

Table 5.2 Comparison between seasonal and annual mean temperature (°C), total rainfall (mm) and sunshine (hours) for 2012, 2013, 2014 and the 30 year regional (Southwest England) mean (1982-2011) (UK Meteorological Office 2015).

		Winter	Spring	Summer	Autumn	Annual
Mean Temperature (°C)	**30 Yr Av**	4.9	8.7	15.2	10.6	9.9
	2012	5.8	9.1	14.8	9.9	9.8
	2013	4.7	6.7	15.9	11.1	9.7
	2014	6.2	9.6	15.6	12.0	10.8
Rainfall (mm)	**30 Yr Av**	374	240	243	371	1228
	2012	322	264	476	433	1566
	2013	449	230	182	390	1225
	2014	694	270	239	331	1419
Sunshine (hrs)	**30 Yr Av**	188	496	623	337	1645
	2012	214	520	509	343	1589
	2013	172	425	694	304	1588
	2014	214	529	710	310	1784

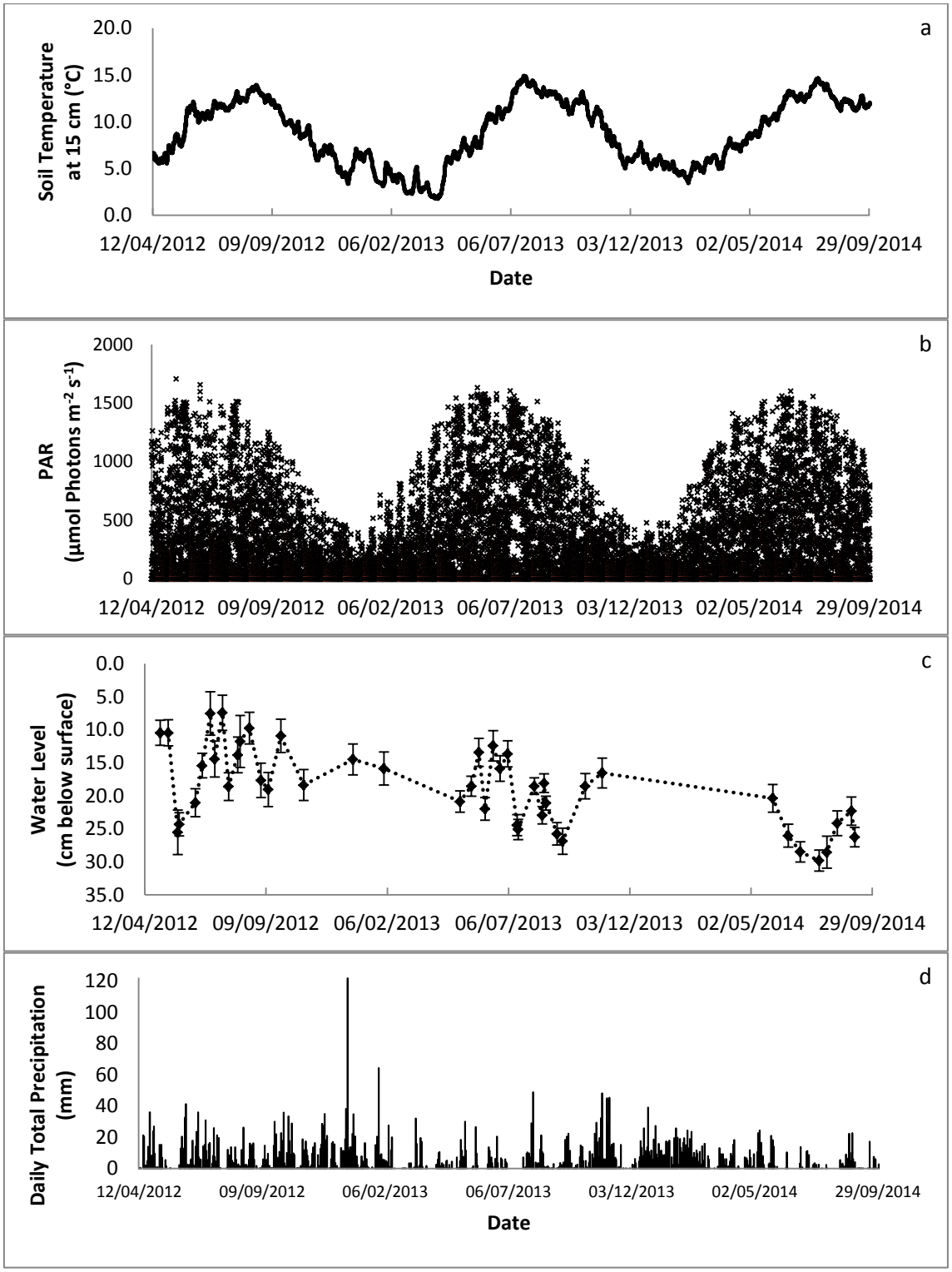

Figure 5.2 Temporal variation in a, soil temperature at 15 cm (°C) at S2R2, b, photosynthetically active radiation (µmol Photons m^{-2} s^{-1}), c, total daily precipitation at Spooners (mm) and d, water table depth (cm below surface). Error bars are one standard error.

5.4.2 Seasonality

Both Aclands and Spooners showed seasonal variation in ecosystem respiration (R_{Eco}) and photosynthesis at 600 µmol Photons m^{-2} s^{-1} (P_{G600}) and full light ($PG_{Full\ Light}$), and NEE at ambient temperature (Figure 5.3) with greater fluxes during the growing season. Similar values of P_{G600} and $P_{G\ Full\ Light}$ were measured at both Aclands and Spooners during 2012. $P_{G\ Full\ Light}$ was also similar in both catchments in 2014, normalised to a PAR of 600 µmol Photons m^{-2} s^{-1}, P_{G600} was greater in July at Aclands and September at Spooners. Maximum P_{G600} was similar in both catchments; 277 ±33 µgC m^{-2} s^{-1} at Aclands and 275 ±22 µgC m^{-2} s^{-1} at Spooners although one was measured in 2013 and the other in 2014. Winter values were low but not zero even though *M. caerulea* is deciduous. Net ecosystem exchange was negative for all measurements taken indicting CO_2 was drawn from the atmosphere during these measurements.

Apart from July 2012 when R_{Eco} was greater at Spooners, the values measured for Aclands and Spooners were similar (Figure 5.3b). Maximum R_{Eco} measured at Aclands was 88 ±36 µgC m^{-2} s^{-1} in September 2014. This was lower than the maximum recorded at Spooners in July 2013 (131 ±10 µgC m^{-2} s^{-1}). However, no comparable data were collected for Aclands during 2013. Winter values were noticeably lower than summer values at both Aclands and Spooners (0.7 ±0.3 and 5 ±4 µgC m^{-2} s^{-1} respectively).

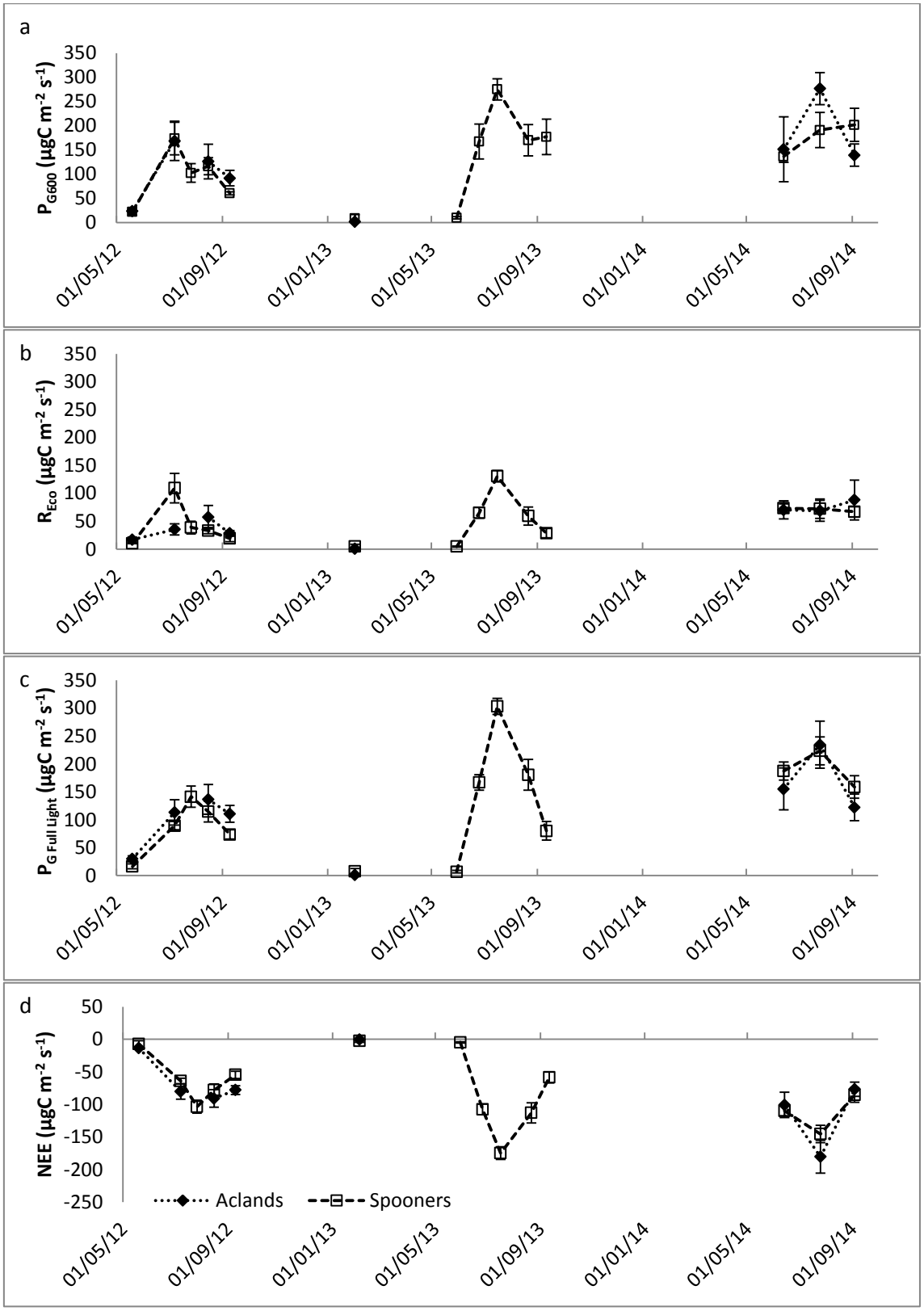

Figure 5.3 Temporal variation in a, photosynthesis at 600 µmol Photons m^{-2} s^{-1} (P_{G600}) (µgC m^{-2} s^{-1}) b, ecosystem respiration (R_{Eco}) (µgC m^{-2} s^{-1}) (not temperature corrected), c, photosynthesis at full light (µgC m^{-2} s^{-1}) and d, net ecosystem exchange at full light (µgC m^{-2} s^{-1}) at Aclands (black diamonds) and Spooners (white boxes) (n=9). Error bars are one standard error.

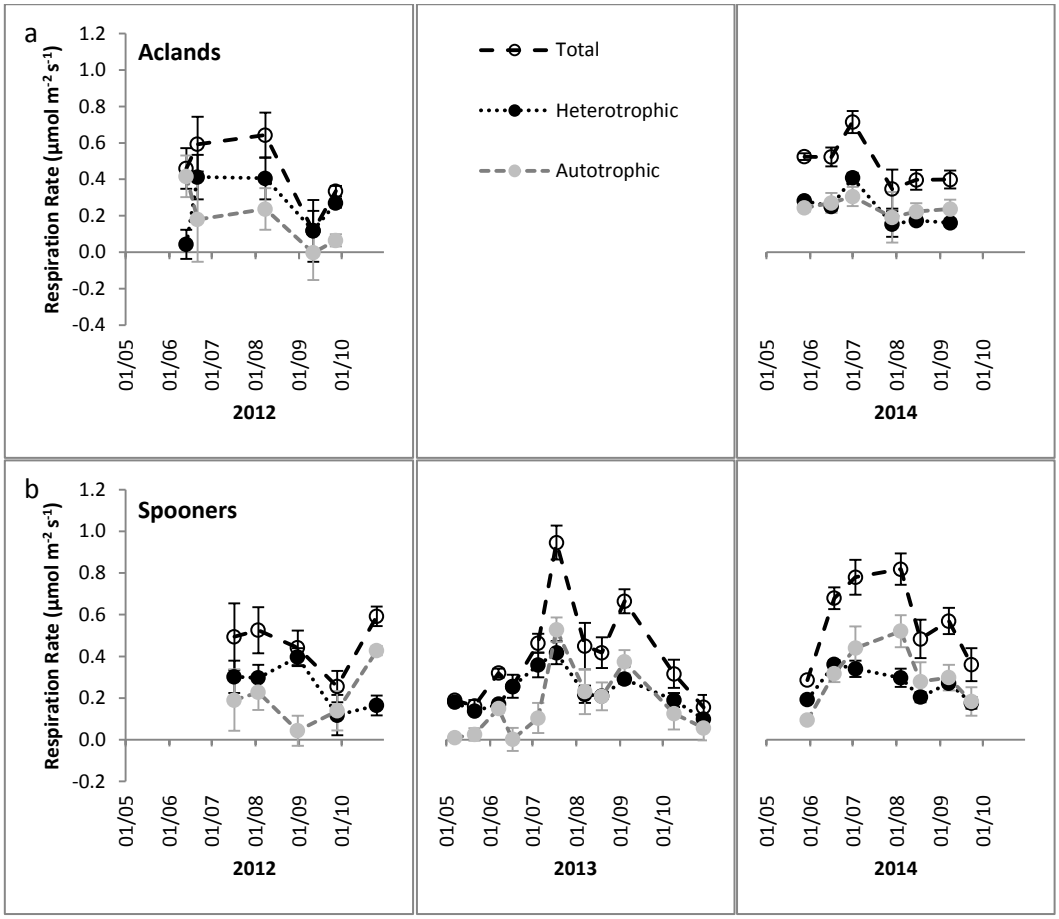

Figure 5.4 Seasonal variation in below-ground respiration rates as measured. Total (white), heterotrophic (black) and autotrophic (grey) mean respiration rates measured at a, Aclands and b, Spooners Error bars are one standard error.

Below-ground respiration also showed clear seasonal variation at both Aclands and Spooners (Figure 5.4) particularly in 2013 and 2014, with greater fluxes during mid-summer. Total and autotrophic respiration were generally greater at an equivalent time of the year in 2014 and 2013 than in 2012, a cooler, wetter summer (Figure 5.2).

Maximum values of total and autotrophic respiration were greater at Aclands than Spooners in 2012 but the reverse in 2014. In 2014, maximum total and autotrophic respiration occurred in August (total, 0.82 ±0.090µmol m^{-2} s^{-1}) and June (autotrophic, 0.36 ±0.04 µmol m^{-2} s^{-1}) at Spooners and July (0.71 ±0.11 and 0.31 ±0.14 µmol m^{-2} s^{-1}) at Aclands. Greater values occurred in July 2013

at Spooners suggesting the greatest respiration rates may have also been observed at this time in Aclands had they been measured. Maximum heterotrophic respiration was the same in both catchments 0.4 μmol m^{-2} s^{-1} and showed less variation between years than autotrophic respiration.

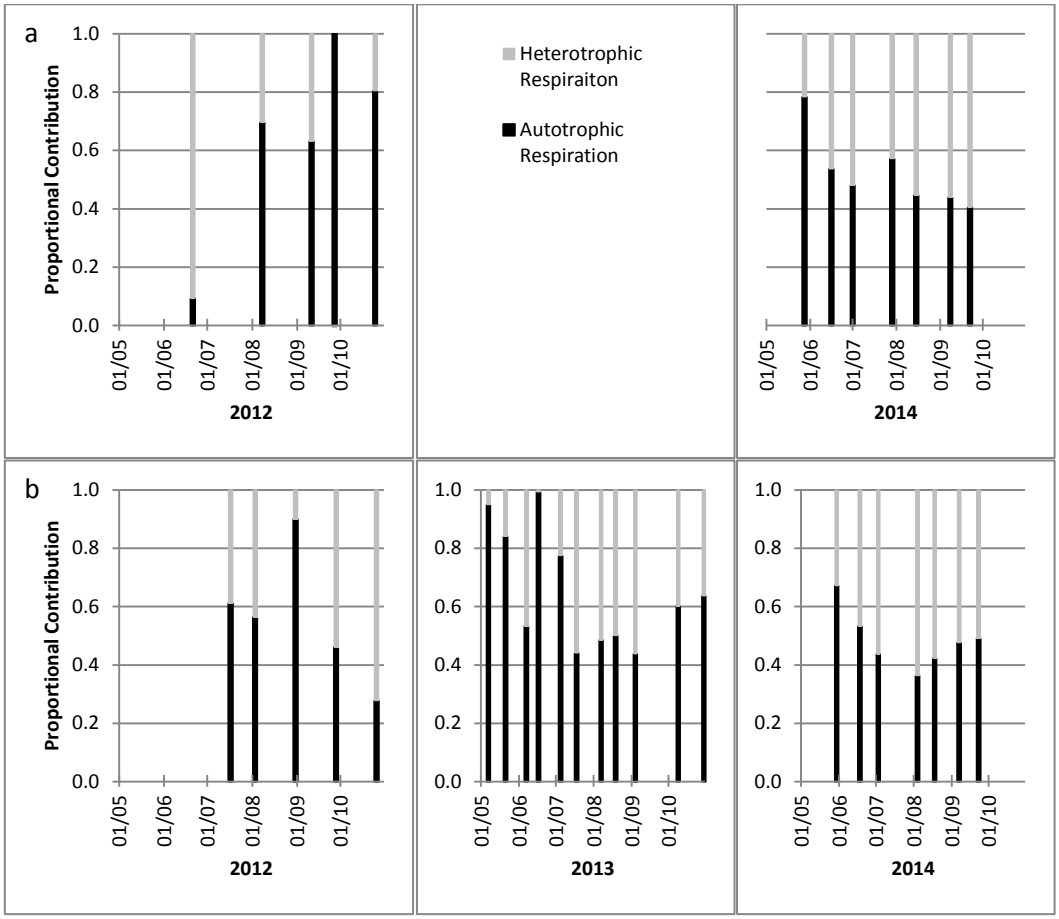

Figure 5.5 Seasonal variation in the proportional contribution of heterotrophic (black) and autotrophic (grey) respiration to total below-ground respiration at a, Aclands and b, Spooners.

Heterotrophic and autotrophic respiration both showed a seasonal increase over the summer (Figure 5.4) however, their relative contributions to total respiration varied (Figure 5.5) indicating they respond differently to biotic and abiotic controls. At Spooners in 2013 and 2014 the proportion of autotrophic respiration (Figure 5.5b) was lower in May and October (<40 %) with seasonal

maxima of 56 and 64 % in July 2013 and August 2014 respectively, coinciding with seasonal peaks in P_{G600} (Figure 5.3a). In 2012 the pattern was different, with a general increase in autotrophic respiration over the season to 72 % by late-October. Again at Aclands the seasonal pattern was less distinct. In 2012, autotrophic respiration generally contributed less than 37 % whilst in 2014 it increased from 22 to 60 % by late September. Overall the average contribution of autotrophic respiration to total respiration was 42 % in both catchments meaning the remaining 58 % was derived from heterotrophic respiration.

5.4.3 Drivers of Temporal Variation

Photosynthesis showed significant relationships with soil temperature, fPAR and NDVI in both catchments separately and together (Figure 5.6). Photosynthesis was greater when the soil was warmer and fPAR and NDVI greater. At Spooners the strongest relationship was with NDVI (Figure 5.6k) and then fPAR (Figure 5.6h). Conversely at Aclands, fPAR showed the strongest relationship with P_{G600} (Figure 5.6g), then soil temperature (Figure 5.6d) and then NDVI (Figure 5.6j). There was a weak but significant linear relationship between water table depth and P_{G600} at Spooners (Figure 5.6b); P_{G600} increased when the water table fell i.e. during dry conditions. There was no significant relationship between P_{G600} and water table depth at Aclands (Figure 5.6a) so both catchments together showed a weaker relationship that at Spooners alone (Figure 5.6c). It can be seen that variability in water table depths between sites within a sample round was significant (Figure 5.6a & b). Greater variability in water table depth was measured at Aclands which may explain the lack of relationship between P_{G600} and water table depth.

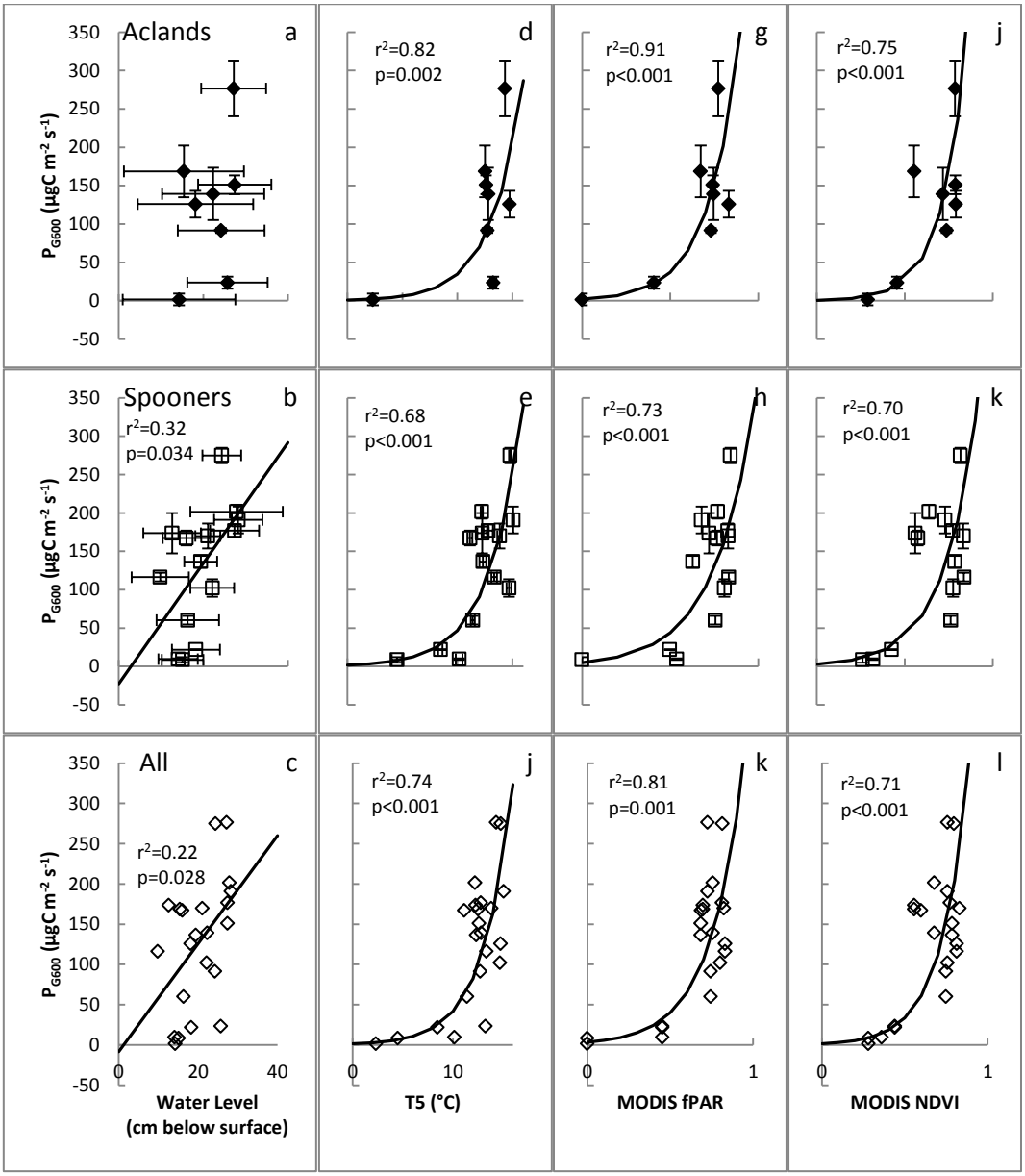

Figure 5.6 Relationship between photosynthesis at 600 µmol Photons m^{-2} s^{-1} (P_{G600}) (µg C m^{-2} s^{-1}) and water table depth (cm below ground surface) (a, b & c), soil temperature at a depth of 5 cm (°C) (d, e & f), fraction of photosynthetically active radiation absorbed (fPAR) (g, h & i) and normalised difference vegetation index (NDVI) (j, k & l)) at Aclands (a, d, g & j), Spooners (b, e, h & k) and both catchments together (c, f, i & l). Error bars are one standard error.

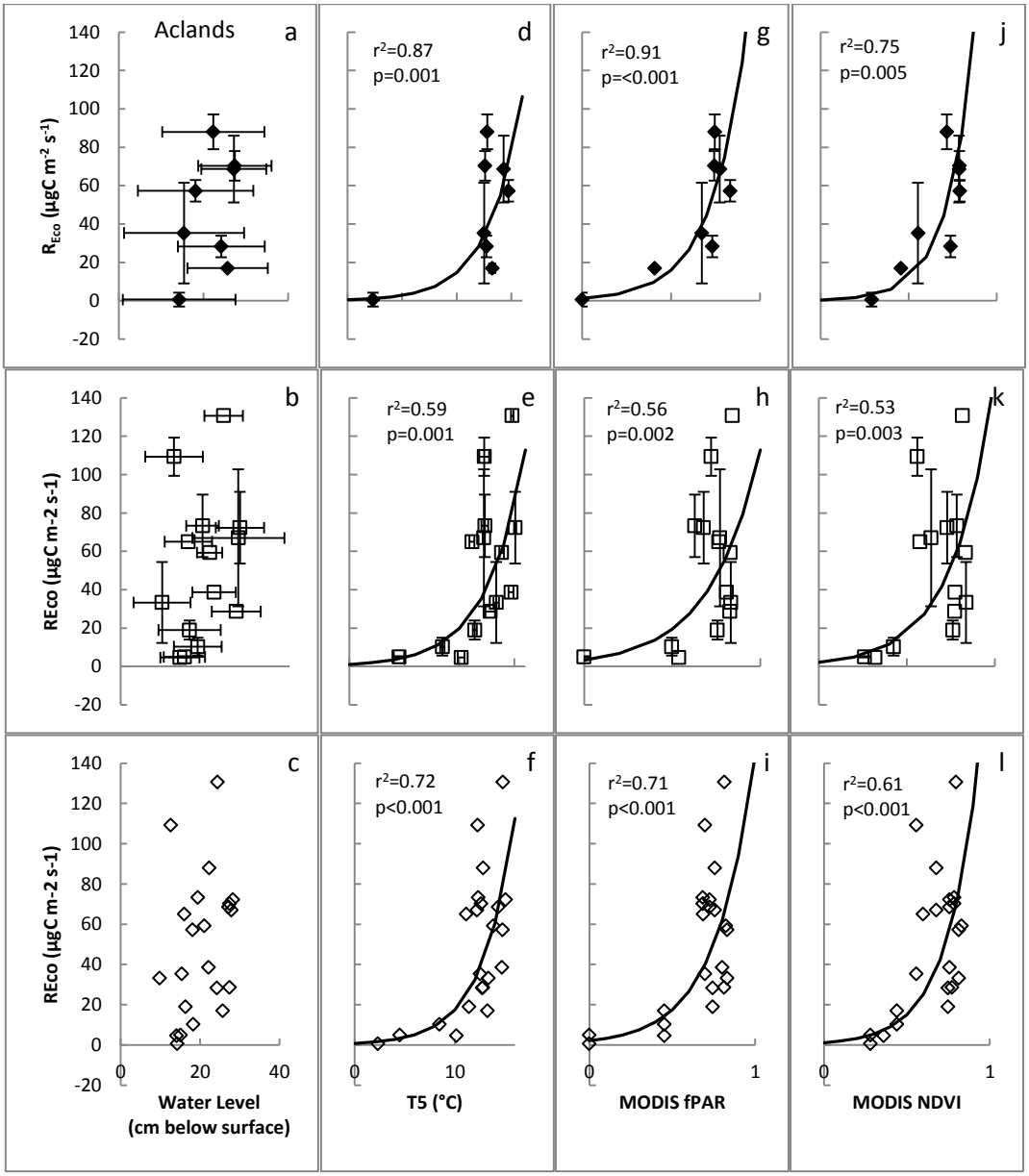

Figure 5.7 Relationship between ecosystem respiration (µgC m^{-2} s^{-1}) and water table depth (cm below ground surface) (a, b & c), soil temperature at a depth of 5 cm (°C) (d, e & f), fraction of photosynthetically active radiation absorbed (fPAR) (g, h & i) and normalised difference vegetation index (NDVI) (j, k & l) at Aclands (a, d, g & j), and Spooners (b, e, h & k) and both catchments together (c, f, i & l). Error bars are one standard error.

Ecosystem respiration also showed significant relationships with soil temperature, fPAR and NDVI (Figure 5.7). R_{Eco} increased in warm conditions when fPAR and NDVI were greater. For both catchments an exponential relationship was strongest with T5 even compared to Arrhenius and Lloyd-

Taylor relationships. Similar to P_{G600}, ecosystem respiration showed the strongest relationship with fPAR in Aclands (Figure 5.7g) and soil temperature in Spooners (Figure 5.7e). For both catchments together the strongest relationship was with soil temperature (Figure 5.7f). At both Aclands and Spooners, no significant relationship was observed between ecosystem respiration and water table depth (Figure 5.7a & b).

Stepwise multiple linear regression (Table 5.3) selected NDVI as the variable with the strongest relationship with both P_{G600} and R_{Eco} at Aclands (r^2>0.54, p<0.060). At Spooners R_{Eco} (r^2=0.31, p=0.038) showed the strongest relationship with soil temperature but P_{G600} (r^2=0.50, p=0.005) showed the strongest relationship with NDVI.. Across both catchments both PG600 and REco showed the strongest relationship with NDVI. No significant two-variable models occurred. fPAR was not selected for any models. Without NDVI no variables were selected for P_{G600} or R_{Eco} at Aclands.

Table 5.3 Input variables and results for a stepwise multiple linear regression with photosynthesis at 600 µmol Photons m^{-2} s^{-1} (P_{G600}) and ecosystem respiration (µgC m^{-2} s^{-1}) at Aclands and Spooners catchments. Variable is the one selected for the model. No significant two-variable models occurred. The proportion of variance (r^2) and the significance of the relationships (p) are shown. All relationships were positive.

Input Variables	CO_2 Flux	Catchment	Variable	r^2	p
LnT5 LnNDVI WL	P_{G600}	Aclands	LnNDVI	0.47	0.060
		Spooners	LnNDVI	0.50	0.005
		Both	LnNDVI	0.70	<0.001
	R_{Eco}	Aclands	LnNDVI	0.54	0.037
		Spooners	LnT5	0.31	0.038
		Both	LnNDVI	0.58	0.005
LnT5 LnfPAR WL	P_{G600}	Aclands			
		Spooners	LnT5	0.49	0.008
		Both	LnfPAR	0.65	0.002
	R_{Eco}	Aclands			
		Spooners	LnT5	0.30	0.053
		Both	LnfPAR	0.49	0.030

Table 5.4 Seasonal Q_{10} and mean respiration at 10 °C (µmol m^{-2} s^{-1}) (R_{10}) values for total, heterotrophic and autotrophic respiration at each site. Regression coefficient (r^2) and significance (p) of exponential relationships between soil temperature at 5 cm (°C) and total, heterotrophic and autotrophic respiration at each site. n is the number of sample days.

Respiration Source	Catchment	Site	Q_{10}	R_{10}	n	r^2	p
Total	Aclands	1	2.7	0.34	13	0.67	0.001
		2	1.4	0.22	14	0.40	0.009
		3	1.5	0.26	13	0.35	0.031
	Spooners	1	2.5	0.40	23	0.86	0.000
		2	1.6	0.17	23	0.53	0.000
		3	2.1	0.23	22	0.67	0.000
Heterotrophic	Aclands	1	1.9	0.17	12	0.45	0.017
		2	1.7	0.07	12	0.61	0.003
		3	1.3	0.18	11	0.42	0.027
	Spooners	1	1.4	0.23	23	0.33	0.003
		2	1.4	0.13	23	0.58	0.000
		3	1.3	0.15	23	0.43	0.001
Autotrophic	Aclands	1	2.6	0.13	12	0.52	0.009
		2	1.4	0.03	12	0.42	0.020
		3	1.4	0.05	12	0.58	0.004
	Spooners	1	2.2	0.18	23	0.71	0.000
		2	1.3	0.00	21	0.35	0.005
		3	1.7	0.09	22	0.35	0.003

Soil temperature at 5 cm was found to exert the strongest control on total, heterotrophic and autotrophic respiration compared to other depths. An exponential function was found to better explain the relationship between temperature and below-ground respiration compared to a Lloyd-Taylor or Arrhenius relationship (not shown).

All sites show a significant exponential relationship with soil temperature at 5 cm (Table 5.4). Total respiration showed the strongest relationships (r^2 from 0.35 to 0.86) and heterotrophic respiration the weakest relationships (r^2= 0.33 to 0.61). The temperature sensitivity (Q_{10}) of below-ground respiration was between 1.3 and 2.7. Sites with a greater coefficient of regression generally had greater temperature sensitivity. On average total respiration was the most

temperature sensitive (1.9) then autotrophic (1.7) and heterotrophic respiration the least temperature sensitive (1.5).

Table 5.5 Relationships between total, heterotrophic and autotrophic respiration as measured and corrected to 10 °C and environmental variables (soil temperature at 5 cm (°C) (T5), water table depth (cm below surface) (WTD), fraction of photosynthetically active radiation absorbed (fPAR) and normalised difference vegetation index (NDVI)). Regression coefficient (r^2) and significance (p) of quadratic, (Quad), exponential (Exp) or linear (Lin) relationships. Only relationships with p<0.050 are shown. + indicates a positive relationship, – a negative relationship.

Respiration Source	Variable	Aclands				Spooners				Both			
			r^2	p			r^2	p		r^2	p		
Total	T5	E	0.64	0.002	+	E	0.57	0.000	+	E	0.58	0.000	+
	WTD	.	.	.	.	L	0.23	0.022	+	L	0.15	0.230	+
	fPAR	L	0.37	0.037	+	E	0.45	0.000	+	E	0.39	0.000	+
	NDVI	.	.	.	.	E	0.50	0.000	+	E	0.34	0.000	+
Heterotrophic	T5	.	.	.	.	E	0.64	0.000	+	E	0.31	0.000	+
	WTD	.	.	.	.	.	.	.	.	.	.	.	.
	fPAR	.	.	.	.	E	0.45	0.000	+	E	0.31	0.001	+
	NDVI	E	0.39	0.029	+	E	0.49	0.000	+	E	0.35	0.000	+
Autotrophic	T5	E	0.53	0.008	+	L	0.28	0.009	+	E	0.34	0.000	+
	WTD	.	.	.	.	L	0.33	0.005	+	L	0.18	0.012	+
	fPAR	.	.	.	.	.	.	.	.	E	0.15	0.023	+
	NDVI	.	.	.	.	E	0.28	0.009	+	E	0.14	0.024	+
Total at 10 °C	WTD	.	.	.	.	.	.	.	.	.	.	.	.
	fPAR	.	.	.	.	.	.	.	.	.	.	.	.
	NDVI	.	.	.	.	.	.	.	.	.	.	.	.
Heterotrophic at 10 °C	WTD	.	.	.	.	.	.	.	.	.	.	.	.
	fPAR	.	.	.	.	.	.	.	.	.	.	.	.
	NDVI	.	.	.	.	.	.	.	.	.	.	.	.
Autotrophic at 10 °C	WTD	.	.	.	.	.	.	.	.	.	.	.	.
	fPAR	.	.	.	.	.	.	.	.	.	.	.	.
	NDVI	.	.	.	.	.	.	.	.	.	.	.	.

Of the variables tested, soil temperature at 5 cm explained the most temporal variance in total respiration explaining 64, 57 and 58% at Aclands, Spooners and both catchments combined (Table 5.5) respectively. At Spooners soil temperature explained the most variance in heterotrophic respiration (64 %) however, at Aclands and for both catchments combined NDVI explained the most variance in heterotrophic respiration (39 and 35 %). Heterotrophic

respiration showed a non-significant linear relationship with soil temperature at Aclands (r^2=0.23, p=0.077).

Soil temperature explained 53 % of the temporal variance in autotrophic respiration at Aclands and 34 % for both catchments together but only 28 % at Spooners where water table depth explained 33 % of the variance, with autotrophic respiration increasing as water tables dropped (Figure 5.8c). Once adjusted to 10 °C the relationship between autotrophic respiration and water table depth at Aclands and across both catchments became non-significant (Figure 5.8f).

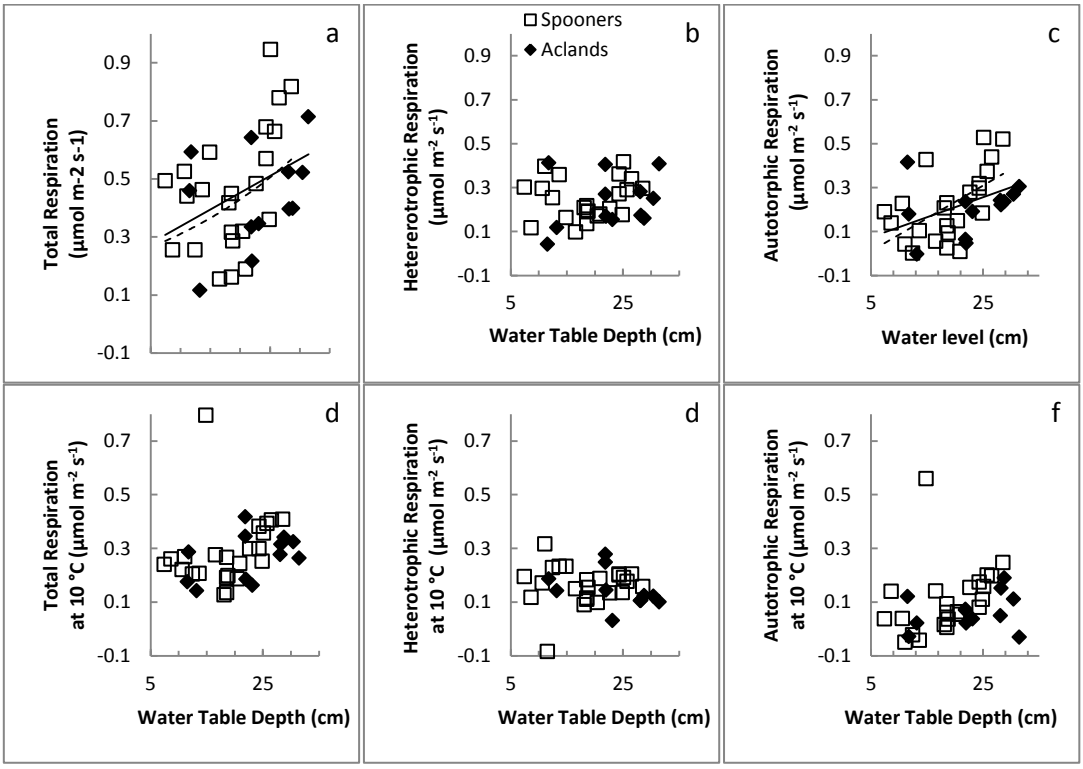

Figure 5.8 Relationship between below-ground respiration (µmol m^{-2} s^{-1}) as measured (a, b & c) and corrected to 10 °C (d, e & f) and water table depth (cm below ground surface) with total (a & d), heterotrophic (b & e) and autotrophic (c & f) at Aclands (black diamonds) and Spooners (white squares, dashed lines) and across both catchments (solid lines). Regressions drawn where p<0.050 for significant see Table 5.5.

Water table depth also explained 23 % of the variance in total respiration observed at Spooners (Table 5.5, Figure 5.8a) and 15 % across both catchments with respiration increasing when the water table fell. Again this

relationship became insignificant when respiration was adjusted to 10 °C (Figure 5.8d). There were no significant relationships between below-ground respiration, either as measured or at 10 °C, with water table depth at Aclands where variability in water table depth was greater (e.g. Figure 5.6a & b).

Total respiration increased exponentially with NDVI and fPAR at Spooners and across both catchments and linearly with fPAR at Aclands (Table 5.5). This variation was not driven by autotrophic respiration, as similar relationships did not occur; the only significant relationship was between NDVI and autotrophic respiration at Spooners. Additionally once corrected to 10 °C all relationships became non-significant. As NDVI and fPAR strongly co-varied with temperature, correcting to 10 °C may have removed any apparent relationships. Heterotrophic respiration, as measured, also showed significant exponential relationships with NDVI in both catchments and each catchment separately (Table 5.5) and fPAR at Spooners and across both catchments which also became insignificant when adjusted to 10 °C.

5.4.4 Modelled Net Ecosystem Exchange

Even though average ecosystem respiration showed a stronger exponential relationship (Figure 5.7c & d) with average soil temperature, when all measurements were used to parameterise an empirical model, it was found that a Lloyd-Taylor response resulted in greater coefficient of determination and smaller parameter errors. Adding a water table depth term to the photosynthesis component increased the coefficient of determination but it dramatically increased parameter errors. Therefore, although P_{G600} showed a significant relationship with water table depth at Spooners (Figure 5.6b), a water table depth term was not included. NDVI was found to be a better predictor of NEE than fPAR possibly due to the greater number of measurements collected at Spooners, where NDVI was a better predictor of both R_{Eco} and P_{G600} (Figure 5.7j & k, Figure 5.6j & k). NDVI and soil temperature combined were found to be better than either alone, because when considered alone, they both markedly overestimated winter photosynthesis.

Table 5.6 Coefficient estimates and standard errors of coefficients used in annual net ecosystem exchange model (Equation 5.5)

Parameter	Coefficient Estimate	Standard Error
a	31.7	2.2
E_0	437.1	39.0
P_1	-18.2	0.5
K_1	164.7	17.5

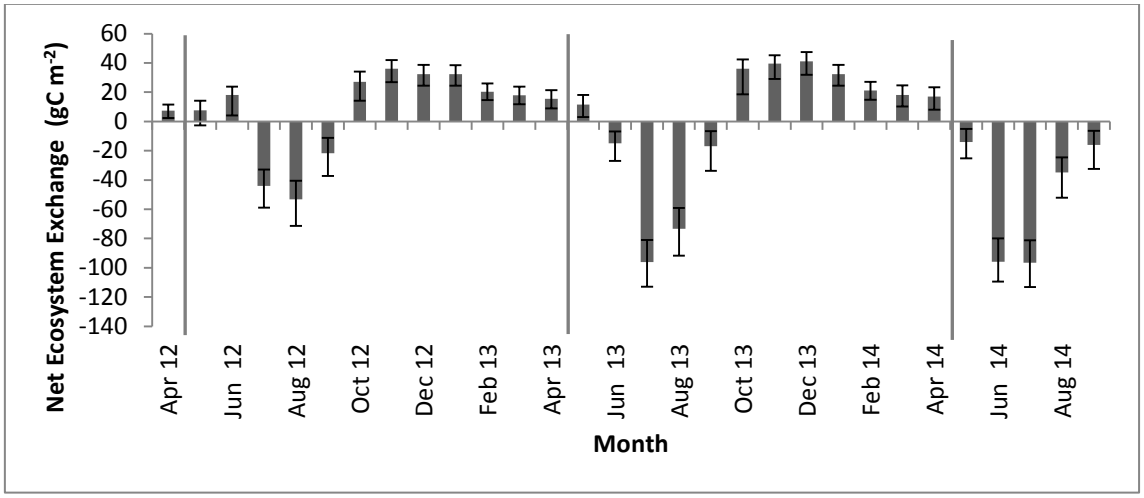

Figure 5.9 Modelled average monthly net ecosystem exchange (NEE) (gC m^{-2}). Positive values indicate a release of CO_2 to the atmosphere. Vertical lines indicate start and end of annual flux calculation periods. Error bars indicate 95 % confidence intervals for modelled NEE fluxes.

The NEE model explains 62 % of the variability observed. Significant uncertainty remains particularly during the summer months (May to September) when both photosynthesis and ecosystem respiration fluxes were larger and diurnal variation was greater. During the winter months (October to April) (October to April) the peatland was a source of CO_2 with fluxes modelled up to 41 gC m^{-2} during December 2013.

Modelled NEE in July 2012 was less negative (smaller sink) than in 2013 and 2014 reflecting the cooler and wetter growing conditions (Figure 5.2). Modelled NEE was notably more negative in June 2014 reflecting the warmer conditions and the earlier greening-up of the vegetation in response to a mild spring.

Conversely, June 2012 was most likely a source of CO_2 reflecting the cooler and wetter conditions. Annual fluxes were calculated from 1st May, it is most likely that the moorland was a source of CO_2 in both years (Table 5.7) with 2012-2013 a larger source (88 gC m^{-2}) than 2013-2014 (16 gC m^{-2}). Modelled winter NEE was similar in both years (Table 5.7) but summer maximum monthly NEE varied between years (Table 5.7-) resulting in 2012-2013, a cooler and wetter year, being a larger source of CO_2 than 2013 and 2014, a warmer and drier year.

Table 5.7 Modelled annual net ecosystem exchange and maximum monthly CO_2 uptake and release, the month is indicated. Values in brackets are the 95 % confidence intervals.

	Annual Flux (gC m^{-2})	Monthly Maximum Uptake (gC m^{-2})	Winter Maximum Release (gC m^{-2})
01/05/2012 to 30/04/2013	88 (-2 to 217	-53 (-66 to -35) Aug	36 (30 to 45) Nov
01/05/2013 to 30/04/2014	16 (-67 to 171)	-96 (-111 to -79) Jul	41 (35 to 50) Dec

5.5 DISCUSSION

5.5.1 Seasonal Variation

Growing season photosynthesis at 600 µmol Photons m^{-2} s^{-1} (Figure 5.3) was higher (Supplementary material Table 11.3) than growing season average photosynthesis on a Czech *M. caerulea* dominated upland ombrotrophic bog (Urbanová *et al.* 2012). It is probable that values found by their study were lower as it is unlikely PAR averaged for their study period was as high as 600 µmol Photons m^{-2} s^{-1} as they included both overcast days and night-time. The author is unaware of any further reported photosynthesis rates (maximum or at a set PAR) for a *Molinia caerulea* dominated landscape and so this paper provides the first such study. This enables photosynthesis rates to be compared between vegetation communities under standard conditions which will inform ecosystem management designed to increase CO_2 sequestration.

Compared to other maritime bogs (Supplementary material Table 10.3), the P_{G600} values from this study were higher than those reported for *Sphagnum* hummocks and lawns containing *Calluna vulgaris* and *Molinia caerulea* in an Atlantic raised bog in Ireland (Laine *et al.* 2006) and a *Calluna vulgaris* dominated British blanket bog (Lloyd 2010). However, a direct comparison is confounded by the different species measured in each study. Greater P_{G600} for Exmoor may reflect the dominance of *M. caerulea* which has been shown to have greater rates of CO_2 uptake and release than *Calluna vulgaris* (Aerts 1990, Otieno *et al.* 2009).

Growing season ecosystem respiration measured in this study was similar to values reported for a Czech *M. caerulea* dominated upland ombrotrophic bog (Urbanová *et al.* 2012). Maximum R_{Eco} values were higher than night-time eddy covariance fluxes from a Dutch *M. caerulea* dominated raised bog (Nieveen *et al.* 1998) perhaps reflecting warmer daytime temperatures in this study. Compared to other, mostly *Calluna vulgaris* dominated, upland blanket bogs summer ecosystem respiration was greater from Exmoor. Again this most likely reflects the difference in vegetation present with greater rates of CO_2 uptake and release from *M. caerulea* compared to *Calluna vulgaris* (Aerts 1990, Otieno *et al.* 2009).

The range in winter P_{G600} observed for Exmoor encompassed reported values from a *Calluna vulgaris* upland blanket bog (Lloyd 2010) and a Russian *S.angustifolium* pine bog (Schneider *et al.* 2012) (Figure 5.10a). Winter ecosystem respiration values were similar to a Dutch *M. caerulea* dominated raised bog (Nieveen *et al.* 1998), lower than *Sphagnum* dominated Finnish (Alm *et al.* 1999a) and Russian (Schneider *et al.* 2012) ombrotrophic bogs but greater than a *Calluna vulgaris* dominated blanket bog (Chapman and Thurlow 1996) (Figure 5.10b). Both P_{G600} and R_{Eco} would be expected to be lower on Exmoor where the vegetation was predominantly deciduous compared to peatlands covered in evergreen *Sphagnum* sp. and *Calluna vulgaris.*

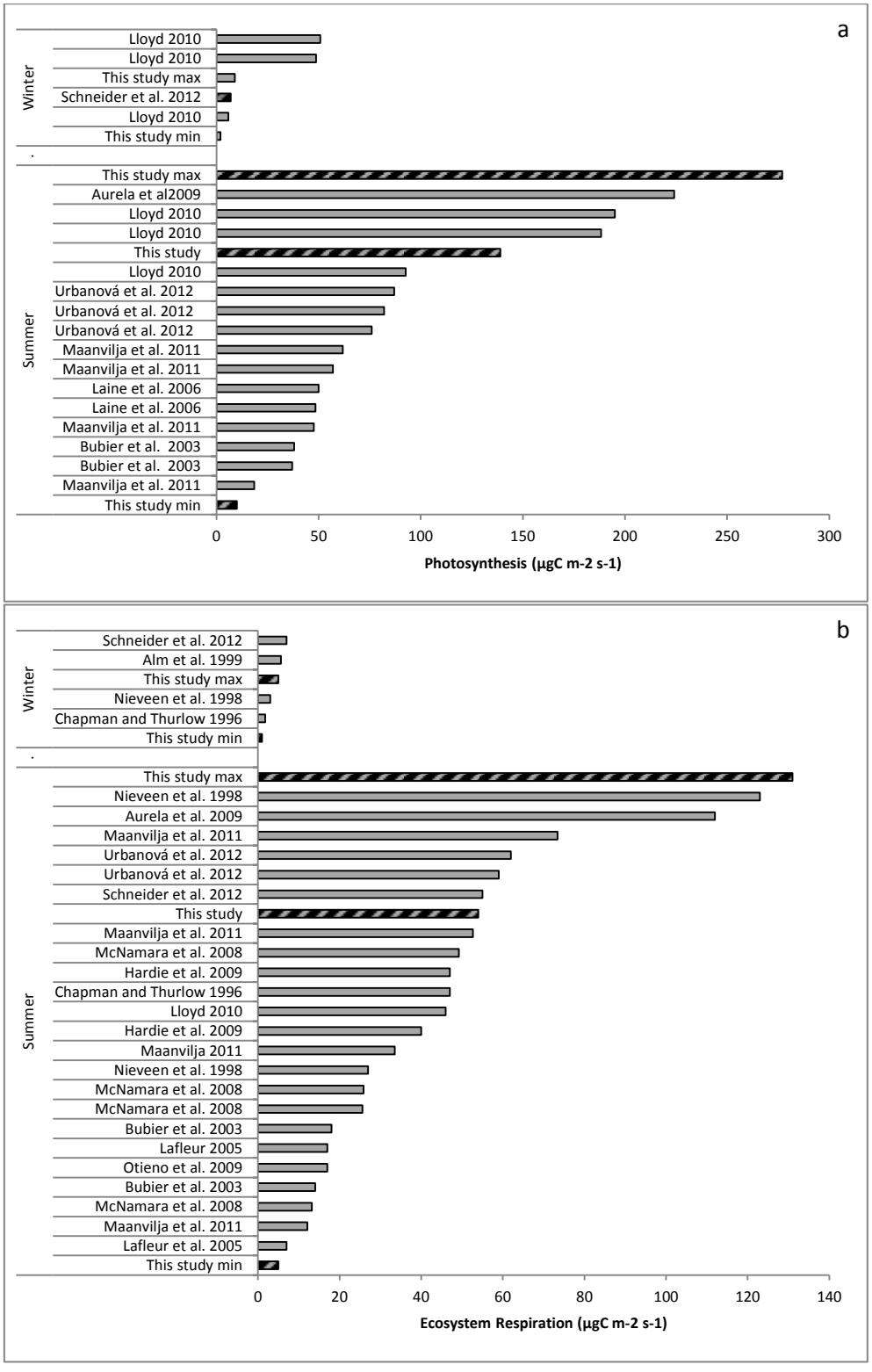

Figure 5.10 Comparison of photosynthesis and ecosystem respiration rates (µgC m^{-1} s^{-1}) measured in this study to those reported in other studies. More details in Supplementary Material Table 10.3

Maximum heterotrophic respiration (Supplementary material Table 10.4) was less than that observed in October from a collar inserted 20 cm in a *Calluna*

dominated British blanket bog (Heinemeyer *et al.* 2011) and substantially lower than summer values observed for drained Finnish ombrotrophic bogs (Silvola *et al.* 1996a, Silvola *et al.* 1996b). Lower heterotrophic respiration rates are unlikely to be directly due to temperature differences, as Exmoor was equivalent or slightly warmer than these other studies (Silvola *et al.* 1996a, Silvola *et al.* 1996b, Heinemeyer *et al.* 2011).

Exmoor's peatlands are shallow, 0.37±0.04 m in this study and 0.33 m across Exmoor as a whole (Bowes 2006). In comparison stated peat depths were 1-2 m (Heinemeyer *et al.* 2011) and 1.8-3.9 m (Silvola *et al.* 1996a). Some argue that total peat thickness has little effect on heterotrophic respiration. They assert that most respiration occurs near the surface of the peat (Blodau *et al.* 2007), within the upper 0.35 m (Maanavilja *et al.* 2011) or within 0.01-0.03 m of the water table (Blodau and Moore 2003b) due to a lack of oxygen below the water table. However, if a significant proportion of heterotrophic respiration were occurring in the saturated peat, as suggested by Hardie *et al.* (2009) then thin peat thickness could explain the low heterotrophic respiration values observed.

Additionally as the drainage ditches are over 150 years old, much of the labile organic matter may have already degraded leaving a humified peat (Bridgham and Richardson 1992) which, although potentially vulnerable to priming (Freeman *et al.* 2004, Fontaine *et al.* 2007), will decompose more slowly than more labile organic matter, resulting in lower heterotrophic respiration rates.

As photosynthesis observed on Exmoor was greater than in *Calluna vulgaris* dominated bogs, and *M. caerulea* allocates more carbon to its root system than dwarf shrubs (e.g. *Erica tetralix*) (Aerts and Berendse 1988) it would be expected that autotrophic respiration would be greater in a *M. caerulea* peatland. However, no values for autotrophic respiration could be found for comparison, reflecting the large uncertainty that occurs when measuring autotrophic respiration (Subke *et al.* 2006).

Comparison with other upland blanket bogs (Supplementary material Table 10.4) showed that maximum total below-ground respiration observed in this study was lower than reported for other studies from a *Calluna Vulgaris* dominated blanket bog (Hardie *et al.* 2009, Heinemeyer *et al.* 2011). Total respiration observed on Exmoor was considerably lower than reported for a Finnish minerotrophic fen (Komulainen *et al.* 1999) and Swedish and Finnish ombrotrophic bogs (Svensson 1980, Silvola *et al.* 1996b, Komulainen *et al.* 1999). Total respiration consists of a heterotrophic and autotrophic component, although heterotrophic respiration was smaller on Exmoor, the autotrophic respiration would be expected to be greater from a *M. caerulea* dominated ecosystem as discussed above. However, the comparatively small total respiration rates indicate enhanced autotrophic respiration did not compensate for diminished heterotrophic respiration.

Autotrophic respiration produced on average 42 % of the total below-ground respiration measured (Figure 5.5) similar to the 38 % (root and mycorrhizal respiration) reported for lowland grassland (Heinemeyer *et al.* 2012) and just greater than the range (30-40 %) reported for a dwarf-shrub bog (Silvola *et al.* 1996b). Autotrophic respiration showed a mid-summer maximum at Spooners but a less clear pattern at Aclands. The proportional contribution of autotrophic respiration has been found to follow the phenology of the vegetation when measured monthly (Silvola *et al.* 1996b), but to also show significant hourly variation responding to both the previous days PAR and hourly PAR 6 hours previous (Heinemeyer *et al.* 2012). This short-term variation in autotrophic respiration may explain the less clear pattern at Aclands and the mid-season lows e.g. June 2013 at Spooners. A notable low in autotrophic respiration occurred (17/06/2013) the day after a total PAR of 3908 μmol Photons m^{-2} compared to 13267 μmol Photons m^{-2} the day before the previous measurement. It may be that a temporal lag in below-ground carbon allocation means autotrophic respiration is responding to previous rather than current environmental conditions.

5.5.2 Drivers of Temporal Variation in CO_2 Fluxes

5.5.2.1 Photosynthesis and Below-Ground Autotrophic Respiration

Photosynthesis at 600 µmol Photons m^{-2} s^{-1} showed significant relationships (r^2>0.68) with fPAR, NDVI and soil temperature (Figure 5.6). Multiple regression analysis (Table 5.3) was carried out to determine if this relationship was direct i.e. temperature controlled photosynthesis (Bernacchi *et al.* 2001) or indirect i.e. temperature controlled vegetation phenology (Jolly *et al.* 2005) which controlled photosynthesis. At Aclands, Spooners and in both catchments together P_{G600} was most strongly related to NDVI indicating photosynthetic activity responded to vegetation phenology which happened to coincide with seasonal temperature variation.

Laine *et al.* (2009) found using temperature as well as PAR in photosynthesis models produced better results in some, but not all, of their hummock and lawn sites. Otieno *et al*. (2009) believed temperature sets an upper limit on the maximum CO_2 uptake observed; photosynthesis increases with temperature as metabolic processes are enhanced at higher temperatures up to a point after which damage occurs to the vegetation and photosynthesis decreases (Atkin and Tjoelker 2003). Photosynthesis from a Dutch lowland, *M. caerulea* dominated raised bog was found to decrease when temperature increased beyond 30-35 °C (Nieveen *et al.* 1998). It is unlikely a similar supra-optimum temperature reduction in photosynthesis occurred on Exmoor where the warmest average air temperature observed for a sample round was 29 °C at Spooners in July 2013, an unusually warm period. For this reason, over the range of temperatures observed in this study, photosynthesis increased with temperature.

At Spooners both P_{G600} and autotrophic respiration increased as the water table fell (Figure 5.6b & Figure 5.8c & f). At Aclands there were no relationships between water table depths and any of the fluxes measured. This may be because spatial variability in water table depths was greater at Aclands resulting

in larger standard errors for sample round averages (8 to 14 cm) compared to Spooners (3 to 11 cm).

Molinia caerulea has adapted to grow in areas of fluctuating water table depths (Taylor *et al.* 2001) so it is surprising that water table depth affected photosynthesis even in one catchment (Figure 5.6b). Urbanová *et al.* (2013) found photosynthesis to increase during a drought year, with this result being attributed to the competitive advantage of shrubs over sedges. Given the plots in this study have no sedges present and few non-*Molinia* species present (9 ±3 %) it is unlikely a competitive advantage between species caused the increase observed during drier periods. Despite their adaptations to wet environments (Taylor *et al.* 2001) it may be that conditions are closer to optimum during drier conditions promoting increased root growth (Gore and Urquhart 1966) and photosynthesis.

Most studies where the water table depth was found to impact photosynthesis have been on *Sphagnum* peatlands (Alm *et al.* 1999a, Riutta *et al.* 2007, Maanavilja *et al.* 2011), and because mosses do not have roots, they are more susceptible to drying out when the water table drops. These studies have found photosynthesis to decrease during drier conditions due to water stress. Where vegetation has deeper roots, such as ericaceous shrubs, photosynthesis has not varied significantly with water table depths (Bubier *et al.* 2003). It may be that because photosynthesis is dependent on temperature (Figure 5.6d) which co-varies with water table depth ($r=0.45$, $p=0.029$), with warmer and drier conditions frequently coinciding, an indirect relationship has occurred.

MODIS NDVI has been found to explain up to 71 % of the variation in gross primary productivity in northern peatlands (Kross *et al.* 2013) and alpine grasslands (Rossini *et al.* 2012). In this study NDVI explained 77 and 68 % of variation in photosynthesis (Table 5.6). It has been suggested that NDVI is best used as a measure of potential photosynthetic activity (Gamon *et al.* 1995) with actual photosynthetic activity lower due to local variations in water availability, temperature, leaf shading etc. In this study NDVI was used as a measure of

potential photosynthetic activity moderated by hourly variation in PAR and soil temperature in the NEE model (Equation 5.5). It limited maximum NEE during spring green-up and autumn senesce, when PAR and temperature could both be high (Figure 5.2) but photosynthetic biomass was diminished either because leaf growth was not complete or because the leaves had stated to discolour and die off from the tips (Jefferies 1915).

Below-ground autotrophic respiration also showed a dependence on soil temperature (Table 5.5 & Table 5.6) and water table depth at Spooners (Figure 5.8c & d). During periods of high photosynthetic activity the concentration of carbon compounds in root tissue has been found to increase resulting in increased passive loss of CO_2 and autotrophic respiration (Subke *et al.* 2006). As photosynthetic activity is correlated with temperature (Figure 5.6 c & d) and autotrophic respiration is dependent on photosynthesis an apparent temperature dependence may have occurred (Heinemeyer *et al.* 2011). A similar indirect effect may have occurred between below-ground autotrophic respiration and water table depths as sunny and therefore more photosynthetically active conditions and dry conditions tend to coincide.

5.5.2.2 Ecosystem Respiration and Heterotrophic Respiration

Variation in ecosystem respiration has been explained by both air temperature (Schneider *et al.* 2012) and soil temperature at a range of depths; 5 cm (Bubier *et al.* 2003, Lund *et al.* 2007), 10 cm (Blodau *et al.* 2007, Otieno *et al.* 2009, Lloyd 2010) and 15 cm (Updegraff *et al.* 2001). The soil temperature measurement depth was selected based on the highest r^2 values obtained. Soil temperature at 5 cm was found to exert the strongest control on total respiration. This is in accord with studies which showed shallower temperature measurements to be better predictors of soil respiration, with temperature measured at the peat surface the best (Lafleur *et al.* 2005, Lloyd 2010). It is thought that air temperature and shallow soil temperatures have a stronger impact on ecosystem respiration where the proportion of autotrophic respiration and leaf litter respiration are greater. Air temperature was not as good a

predictor of above or below-ground respiration because air temperature fluctuated too widely over a diurnal cycle.

Soil temperature explained 87 and 58 % of the temporal variability in ecosystem respiration at Aclands and Spooners respectively in this study (Figure 5.7 c & d). Otieno *et al*. (2009) found soil temperature at 10 cm to explain 83 % of the temporal variability in daily maximum ecosystem respiration in grass plots, which is similar to the value calculated for Aclands. Studies using eddy covariance towers have found soil temperature at 5 cm to explain around 62 % of the variability in ecosystem respiration (Lafleur *et al.* 2005, Lund *et al.* 2007) and soil temperature at 8 cm to explain 50 % (Lloyd 2010). In all these studies, as in this study, ecosystem respiration increased during warmer conditions.

Soil temperature also explained the most variance in total and heterotrophic below-ground respiration (Table 5.5 & Table 5.6). However, the coefficient of regression ranged from 0.33 to 0.86, sites with a greater coefficient of regression were generally more temperature sensitive (higher Q_{10}). Water levels have been shown to increase the temperature sensitivity of respiration as moisture content increases (Svensson 1980). For example, Silvola *et al.* (1996a) found that dry (water table >20 cm below the ground surface) areas of a Finnish ombrotrophic bog were less temperature sensitive than wet areas. It is likely that variation in water levels between sites explains the variation in both Q_{10} values and the strength of the regression relationships observed.

The Q_{10} values of total respiration (1.3 to 2.8) on Exmoor were similar to those observed for a British upland blanket bog against air temperature (1.9) (Lloyd 2010), an incubated mesocosm from a Canadian raised bog (1.6 to 2.2) (Bubier *et al.* 2003) and Finnish ombrotrophic bogs against soil temperature at 2 cm (1.1 to 3.9) (Silvola *et al.* 1996a). However, the values were lower than that found for soil respiration from a *M. caerulea* dominated lowland raised bog when soil temperature was measured at 2.5 cm (4.8) (Nieveen *et al.* 1998).

On average autotrophic respiration showed a stronger temperature sensitivity (1.3 to 2.6) than heterotrophic respiration (1.3 to 1.9) (Table 5.4). Heterotrophic

respiration might be expected to be the most temperature sensitive as respiration is entirely dependent on the rate of microbial decomposition. Whilst autotrophic respiration (as defined by this study) will also have a proportion directly dependent on temperature due to microbial decomposition of root exudates it will also have a proportion dependent on photosynthetic activity. Autotrophic respiration may show greater temperature sensitivity due to autocorrelation between temperature and photosynthetically active radiation (Heinemeyer *et al.* 2011). In addition over the period studied, May to October, seasonal variation in vegetation phenology may increase the apparent temperature sensitivity of autotrophic respiration (Curiel Yuste *et al.* 2004).

There were no significant relationships between ecosystem respiration and water table depth (Figure 5.7a & b). Lowered water table have been shown to both increase respiration (Silvola *et al.* 1996a, Blodau and Moore 2003b, Riutta *et al.* 2007, Otieno *et al.* 2009, Schneider *et al.* 2012) or have no effect (Updegraff *et al.* 2001, Laine *et al.* 2006, Blodau *et al.* 2007, Riutta *et al.* 2007, Lloyd 2010). Where water table depths have had no impact on R_{Eco}, it has been argued this is because changes in water table depth do not necessarily result in comparable changes to soil moisture at the surface due to the very low hydraulic conductivity of peat (Lafleur *et al.* 2005). Therefore changes in water table depth may not always affect oxygen levels and consequently respiration. At Spooners where soil moisture content was trialled as an alternative to water table depth measurements for this study, saturation occurred for a wide range of water table depths (8 to 45 cm).

It has also been argued that as peat becomes older and more recalcitrant with depth (Updegraff *et al.* 1995), lowered water tables expose material with lower decomposition potential and therefore only a small increase in respiration occur. Given the humified nature of the peat observed on Exmoor and the length of time since drainage (~150 years) it is likely that the recalcitrant nature of the peat limited any effect of water table depth on both R_{Eco} (Figure 5.7a & b) and heterotrophic respiration (Figure 5.8c & d). Makiranta *et al.* (2008) also found heterotrophic respiration to be independent of water table depth due to the

vertical distribution of substrate quality. Conversely Silvola *et al*. (1996a) found water table depth to be the strongest control over total below-ground respiration due to an increase in the depth to which oxygen could diffuse, enabling more rapid aerobic respiration to occur. However, their sites had been drained for only 30 years so there may have been more labile organic matter remaining at depth in their study.

Ecosystem respiration showed a significant exponential relationship with both NDVI and fPAR (Figure 5.7e, f, g & h) in this study. Stepwise multiple linear regression showed that a greater proportion of ecosystem respiration was explained by NDVI at Aclands whilst temperature was more important at Spooners (Table 5.3). This indicates that at Aclands R_{Eco} was limited by photosynthesis which varies with NDVI (Figure 5.6g). It can be assumed by the inclusion of parameters such as vegetative green area (Laine *et al.* 2009, Maanavilja *et al.* 2011, Urbanová *et al.* 2012) and leaf area index (Shaver *et al.* 2007) in ecosystem respiration models containing temperature parameters, that these studies also found R_{Eco} to be dependent on vegetation phenology, at least at some sites. However, there are also studies where vegetative green area (Laine *et al.* 2009, Soini *et al.* 2010, Maanavilja *et al.* 2011) and green area index (Schneider *et al.* 2012) have been measured but not included in the ecosystem respiration model. In these studies temperature has been considered the main driver of R_{Eco} with no dependence on vegetation.

NDVI was not included in the respiration component of the NEE model in this study as it estimated April and May to be sinks of CO_2 (not shown). Given that shoots do not start to develop until April to May with the main period of leaf growth in June-July (Jefferies 1915), it is unlikely photosynthesis would be greater than R_{Eco} during April. Adding NDVI to the respiration component limited heterotrophic respiration that may have occurred during warm periods outside of the growing season. Adding two respiration components, one dependent on temperature only and one dependent on temperature and NDVI reduced the coefficient of determination and increased parameter uncertainty (not shown). Therefore either ecosystem respiration did not contain a

component solely dependent on temperature (nominally heterotrophic respiration) or this component was too small to distinguish from random error.

5.5.2.3 Modelling Net Ecosystem Exchange

The model used had two components: a photosynthesis component and an ecosystem respiration component. The photosynthesis component was non-linearly dependent on NDVI, PAR and soil temperature. NDVI was selected above fPAR as it had a greater regression coefficient and lower standard errors. In this model, NDVI functioned as a measure of potential photosynthetic activity (Gamon *et al.* 1995). Although P_{G600} varied with water table depth at Spooners (Figure 5.6b), including a water table depth term reduced the coefficient of determination and increased parameter uncertainty (not shown), further indicating the effect of water table depth was due to co-variance with temperature.

An exponential function was found to best explain the relationship between temperature and ecosystem respiration (Figure 5.7c & d). The Lloyd-Taylor function (Lloyd and Taylor 1994) which allows for variation in temperature sensitivity with temperature is arguably more biologically meaningful but produced smaller r^2 values with R_{Eco}. This could be due to the small range (12.8 °C) of average soil temperatures encountered in this study, over which variation in temperature sensitivity is minimal. When using the whole data set to model NEE, the range in temperature increased to 22.4 °C and the Lloyd-Taylor function was found to produce lower parameter errors and greater r^2 values than an exponential function.

There is considerable uncertainty (38 % of variability unaccounted for) in the model. It is derived from 18 locations which show independent spatial and temporal variation in response to environmental factors. For example, photosynthesis was found to vary spatially with water table depth (Table 6.5). It is usual to include a spatially and temporally distributed plot scale measure of vegetation, such as leaf area index or vegetation green index (Wilson *et al.* 2007) within a NEE model (e.g. Laine *et al.* 2009). Although MODIS NDVI is a

readily available proxy for vegetation phenology, it has a spatial resolution of 500 m. An inability to monitor fine scale variation in vegetation phenology may explain some of the uncertainty in the model. Despite the great uncertainty in the NEE model, these results add to the very limited pool of CO_2 flux data for *M. caerulea* dominated peatlands.

The estimates of NEE suggest that these moorlands were most likely sources of CO_2 (88 and 16 gm^{-2}). However, uncertainty was substantial so NEE estimates ranged from a sink of -207 gC m^{-2} to a source of 386 gC m^{-2} in 2012-2013 and from -319 to 388 gC m^{-2} 2013-2014. This in in contrast with annual NEE values reported for most *Sphagnum* dominated peatlands (Supplementary material Table 11.5) which act as CO_2 sinks. Similarly, a lowland degraded *M. caerulea* dominated peatland was also found to be a source of CO_2 (Nieveen *et al.* 1998) over a whole year. A Czech *M. caerulea* dominated upland bog (Urbanová *et al.* 2013) was found to be a small source even when modelled only for the growing season (May to October).

As modelled winter NEE remained similar between years (36 and 41 gC m^{-2}) but summer maximum monthly NEE varied with meteorological conditions (Figure 5.9) between years (-53 and -96 gC m^{-2}) it appears that carbon balance in these *Molinia caerulea* dominated ecosystems is controlled more by growing season uptake than winter CO_2 release.

5.6 CONCLUSION

All CO_2 fluxes measured showed temporal variability with maximum fluxes occurring in July or August of each year. An exponential relationship with NDVI explained (up to 77 and 79 %) of the temporal variation in photosynthesis at 600 µmol Photons m^{-2} s^{-1} (P_{G600}). Soil temperature at 5 cm explained the most variability (50 to 87 %) in ecosystem respiration (R_{Eco}) and all below-ground CO_2 fluxes, except autotrophic respiration at Spooners, where water table depth explained 52 % of the temporal variability observed. R_{Eco} and heterotrophic respiration both showed no response to variation in water table depth

suggesting short-term rises in water tables, resulting from ditch-blocking, may not reduce heterotrophic respiration of the peat store. At Spooners, P_{G600} and below-ground autotrophic respiration increased during drier periods suggesting *M. caerulea* may be more productive in dry conditions. However, this pattern was not observed at Aclands, where spatial variation in water table depths was greater.

An empirically derived NEE model was parameterised using closed chamber measurements taken in both catchments at a range of light levels (n = 1190). Modelled winter NEE was similar in both years (36 and 41 gC m^{-2}) but summer maximum monthly NEE varied between years (-53 and -96 gC m^{-2}) suggesting productivity controls annual ecosystem exchange rates. Annual fluxes were modelled between 1st May and 30th April for 2012-13. It is most likely that the moorland was a source of CO_2 in both years with 2012-2013 a larger source (88±129 gC m^{-2}) than 2013-2014 (16±155 gC m^{-2}). though *Molinia caerulea* produces large volumes of leaf litter each year (Taylor *et al.* 2001), it appears that this organic material is being decomposed rather than adding to the existing peat store and furthermore the existing peat store is gradually being lost to the atmosphere. It is likely that other grass-dominated peatlands are similarly losing CO_2 despite their large annual biomass production. Ecohydrological restoration aimed at altering the vegetation composition of these ecosystems is therefore vital to prevent further losses from this long-term peat store. Carbon markets may provide funding for such restoration with the data presented here providing the first appropriate emission rates for these drained *Molinia caerulea* dominated peatlands.

5.7 ACKNOWLEDGMENTS

The authors would like to thank the Exmoor Mires Project for their help with site access, Exmoor National Park and the May family for permission to work on the sites. This research received financial support from South West Water and The University of Exeter (SK05284).

6 THE EFFECT OF DRAINAGE DITCHES ON VEGETATION DIVERSITY AND CO_2 FLUXES IN A *MOLINIA CAERULEA* DOMINATED PEATLAND.

6.1 ABSTRACT

Peatlands are recognised as important carbon stores, despite this, many have been drained for agricultural improvement. Drainage has been shown to lower water tables and alter vegetation composition, modifying primary productivity and decomposition, potentially initiating peat loss. To quantify CO_2 fluxes across whole landscapes it is vital to understand how vegetation composition and CO_2 fluxes vary spatially in response to the pattern of drainage features. However, *Molinia caerulea* dominated peatlands are poorly understood despite their widespread extent.

Photosynthesis (P_{G600}) and ecosystem respiration (R_{Eco}) were modelled (12 °C, 600 µmol Photons m^{-2} s^{-1}, Greenness Excess Index of 60) using empirically derived parameters based on closed-chamber measurements collected over a growing season. Partitioned below-ground fluxes were also collected. Plots were arranged ⅛, ¼ and ½ the distance between adjacent ditches in two catchments located in Exmoor National Park, southwest England.

Water tables were deepest closest to the ditch and non-significantly ($p=0.197$) shallower further away. Non-*Molinia* species coverage and the Simpson Diversity Index significantly decreased with water table depth ($p<0.024$) and increased non-significantly ($p<0.083$) away from the ditch. No CO_2 fluxes showed significant spatial distribution in response to drainage ditches, arguably due to insignificant spatial distribution of water tables and vegetation composition. Whilst R_{Eco} showed no significant spatial variation, P_{G600} varied significantly between sites ($p=0.012$), thereby controlling the spatial distribution of net ecosystem exchange between sites. As P_{G600} significantly co-varied with water table depths ($p=0.034$), determining the spatial distribution of water table depths may enable CO_2 fluxes to be estimated across *Molinia caerulea* dominated landscapes.

6.2 KEYWORDS

Peatland, Drainage, CO_2, *Molinia caerulea,* Water table, vegetation composition,

6.3 INTRODUCTION

A small imbalance between primary productivity and decay within peatlands has led to the accumulation of large carbon stores (Yu *et al.* 2010). However, many peatlands are subject to damaging land management practices, principally drainage for agriculture and forestry (Joosten and Clarke 2002), which alters the balance between primary productivity and decomposition shifting peatlands toward CO_2 release (Gorham 1991). Due to the recent addition of peatland restoration into the Kyoto Protocol, carbon markets may provide funding for peatland restoration (Bonn *et al.* 2014), however, there are currently no appropriate default international emission factors for drained *Molinia caerulea* dominated peatlands (Alm *et al.* 1999b). Therefore, quantification of emissions from a wider range of vegetation and management types is required (Evans *et al.* 2011).

Drainage ditches are frequently the main spatial feature within managed blanket bogs. They have been shown to lower the mean water table (Coulson *et al.* 1990, Wilson *et al.* 2010, Holden *et al.* 2011) which in turn reduces species richness (Bellamy *et al.* 2012), particularly affecting species dependent on high water levels including *Sphagnum*. *Molinia caerulea* thrives where water table depths fluctuate (Jefferies 1915) and has encroached on many drained upland areas (Bunce and Barr 1988) particularly those subject to burning and/or over-grazing. Although grasses have been shown to produce more biomass and uptake more carbon annually (Berendse 1998, Otieno *et al.* 2009, Ward *et al.* 2009) than dwarf shrubs (e.g. *Erica tetralix* and *Calluna vulgaris*) and *Sphagnum,* the biomass produced is more labile and readily decomposed (Coulson and Butterfield 1978, Berendse 1998). Understanding how vegetation composition and CO_2 fluxes vary spatially in response to these features is

therefore vital in upscaling CO_2 fluxes across the whole landscape through models. Using a combination of gas flux chambers and soil collars enables the measurement of both ecosystem and partitioned below-ground fluxes at discrete distances from drainage features. Such monitoring facilitates understanding of the variables driving spatial variation in CO_2 fluxes assisting upscaling (Laine *et al.* 2006).

Most studies investigating the effect of drainage have compared pristine to drained areas of northern peatlands (Silvola *et al.* 1996a, Alm *et al.* 1999a, Straková *et al.*) as they sought to understand the broad effect of drainage in these ecosystems. Methane emissions (Minkkinen *et al.* 1997) and nitrogen mineralisation (Tarvainen *et al.* 2013) have been shown to be greater near or in a drainage ditch compared to half-way between ditches. Studies on CO_2 exchange have compared microforms within drained peatlands (Komulainen *et al.* 1999) or microforms along natural hydrological gradients (Laine *et al.* 2007) rather than investigate the explicit role of the drainage features.

It is hypothesised that increased proximity to drainage ditches will lower the water table which will alter vegetation composition, increase primary productivity and consequently increase CO_2 fluxes (ecosystem respiration; photosynthesis and total, heterotrophic and autotrophic below-ground respiration) in a drained *Molinia caerulea* dominated peatland. The following paper tests this hypothesis in two drained, temperate, maritime blanket bogs in the United Kingdom.

6.4 STUDY SITES

The study sites were located in Exmoor National Park, southwest England, in two *Molinia caerulea* dominated headwater catchments subject to extensive drainage; Aclands (51°7’51.3N 3°48’44.4W) and Spooners (51°7’21.9N, 3°44’52.9W) (Figure 6.1). Drainage ditches of variable size, up to 0.5 m wide and 0.5 m deep, were hand dug since the 1830s (Hegarty and Toms 2009). Between the 1960s and 1980s larger machine-dug ditches (>1.5 m wide) targeted specific areas for example, spring lines (Mills *et al.* 2010). Both

catchments have been classed as UK National Vegetation Classification M25: *Molinia caerulea – Potentilla erecta* mires (Rodwell 1991). Long-term (1981-2010) average annual rainfall at nearby Liscombe (UK Meteorological Office 2012) (49°46'50.4N 7°31'07.6W) totals 1445 mm with mean monthly temperature ranging from 1.1 °C in February rising to 18.6 °C in July and August.

Within each catchment six pairs of sites were chosen to encompass the expected variation in altitude, aspect, slope, peat depth and ditch dimensions (Table 6.4). As the ditches are unevenly spaced, plots were located on transects perpendicular to the ditch at ⅛, ¼, and ½ of the distance between the ditch being monitored and the adjacent ditch. Mean distances were 3.0, 6.0 and 12.0 m for ⅛, ¼, and ½ distances respectively whilst the range of distances in each class was 1.6 to 5.5 m, 3.1 to 11.0 m and 6.3to 22.0 m. Proportional distances from the ditch were chosen to test whether CO_2 fluxes could be upscaled for the whole peatland rather than discrete bands either side of a drainage ditch despite the known variations between sites. Locations are shown in Figure 6.1c & d (n=36).

Table 6.1 Site properties of experimental sites at Aclands and Spooners.

Site	Replicate	Mean Peat Depth[1] (cm)	Mean Ditch Width (cm)	Mean Ditch Depth[2] (cm)	Distance from ditch to down-gradient ditch[3] (m)	Altitude[4] (m)	Slope (°)[4]	Aspect	Direction of Ditch[4] (°)	Ditch Direction w.r.t slope
S1	R	22	58	24	37.8	425	4	ESE	144	Cross-slope
	C	23	67	18	43.9	418	5		150	
S2	R	71	84	42	12.5	397	5	NE	2	Down Slope
	C	56	80	45	15.4	395	6		0	
S2	R	29	38	24	29.3	405	5	N	302	Down-slope
	C	29	42	24	32.8	407	5		300	
A1	R	33	25	14	22.4	442	2	N	20	Down Slope
	C	38	32	20	20.3	443	2	NE	10	
A2	R	40	40	26	19.1	446	4	SE	154	Down Slope
	C	43	43	21	19.1	448	4		150	
A3	R	30	50	18	18.3	463	3	SE	144	Down Slope
	C	36	42	18	18.7	461	3		151	

1. Measured during dipwell installation from base of peat (n=3), 2. Measured from base of ditch to tussock shoulder, 3. Measured using tape measure, 4. From LiDAR.

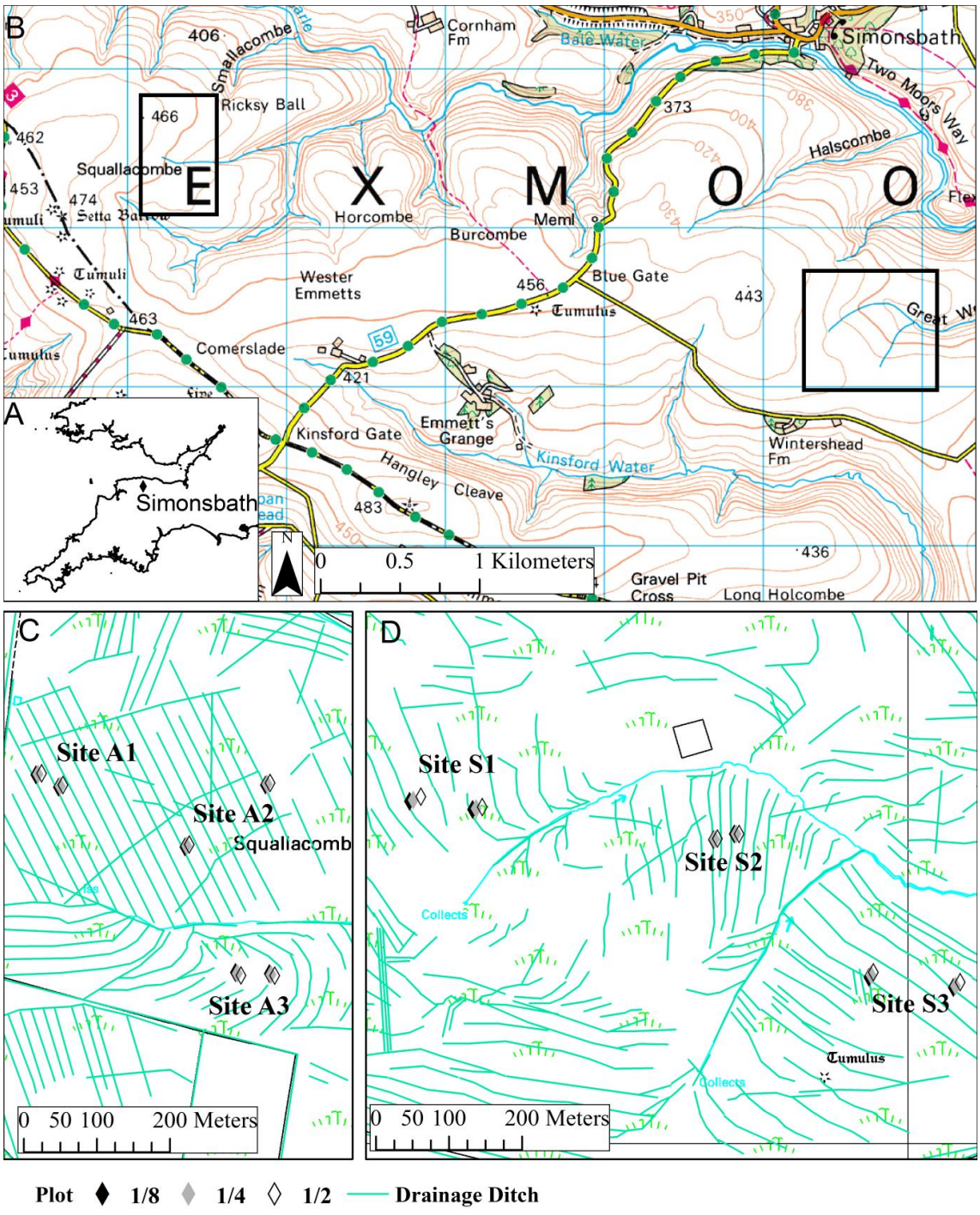

Figure 6.1 Location of Aclands and Spooners study catchments (b) within the southwest of England (a). Location of study sites within Aclands (c) and Spooners (d) study catchments. Coastline shapefile (Ordnance Survey 2008a), 1:50 000 Ordnance Survey Map (Ordnance Survey 2008e) 1:10 000 Ordnance Survey Map (Ordnance Survey 2008b, c).

6.5 METHOD

6.5.1 Net Ecosystem Exchange Measurements

Net Ecosystem Exchange (NEE) was measured from three pairs of plots located ⅛, ¼, and ½ distance from the ditch at each site (n=6) a total of 36 plots. A 55 cm x 55 cm x 25 cm Perspex gas flux chamber was rested on permanently installed 50 cm tall legs with a plastic skirt weighted down by a heavy chain to form an airtight seal with the soil surface (following Shaver *et al.* 2007, Street *et al.* 2007). An EGM-4 infra-red gas analyser (PP Systems, Hitchin, UK) measured CO_2 concentration every 10 seconds for 2 minutes concurrently with chamber temperature and photosynthetic active radiation (PAR) (Skye Instruments, Llandrindod Wells, UK). CO_2 flux measurements were taken at full light, full dark and ~60% ~40%, ~10% light levels using a combination of shade cloths. Chamber air temperature was not directly controlled. Measurements were alternated between brighter and darker light levels to minimise any heating/shading effects. Neither condensation in the chamber, which reduces transparency, nor high humidity, which alters gas diffusion from the leaves, was noted over the sample period due to the abnormally cool weather conditions. The chamber was removed between measurements to restore ambient conditions. The net CO_2 exchange at each light level was calculated from the linear change in CO_2 concentration in the chamber (Pumpanen *et al.* 2004). The headspace volume was estimated by measuring the height from the ground to the base in a grid of nine points added to the chamber volume. The water table depth below the peat surface and soil temperature at 5 cm were also measured at every plot (n=36).

6.5.2 Vegetation Greenness

Vegetation colour, in particular the ratio of green to red and/or blue, has been shown to vary seasonally and be useful as a proxy for vegetation phenology (Richardson *et al.* 2007, Migliavacca *et al.* 2011) and health (Mizunuma *et al.* 2013). Downward facing true colour photographs of the vegetated NEE plots (n=36) were collected on 10 occasions between 20/06/2012 and 25/10/2012

(n=282). Due to equipment bulk, images were not collected on the same day as CO_2 flux measurements. Between 22 and 36 plots were photographed on each occasion, except 10/8/2012 when only eight images were collected. Images were taken 116 cm above the ground using a Canon EOS-10D with a 28 mm fixed lens set to auto-focus and fully-automatic aperture and shutter speed. The mean red ($DN_{Red)}$ and green (DN_{Green}) colour values for the images collected were determined using MATLAB R2011b (Mathworks Inc, Natick, MA, US). The greenness excess index (GEI) has been shown to be useful as an indicator of spring green up (Richardson *et al.* 2007, Migliavacca *et al.* 2011). It was calculated for each image where $GEI=(DN_{Green}-DN_{Red}) / (DN_{Green}+DN_{Red})$. A daily GEI timeseries was modelled for each catchment using a third order Fourier series.

Originally it was planned to use down-ward facing images to estimate leaf area index (Weiss 2010). However, a weak relationship (r^2=0.15) was found between LAI estimated using downward facing photographs (Macfarlane and Ogden 2011) and destructive samples collected for calibration. This method was not investigated further.

6.5.3 CO_2 Exchange Measurements and Modelling

NEE measurements were collected approximately monthly over the growing season from 16/05/2012 to 19/09/2012 (n=163 sets). A complete set of measurements (n=36, a "sampling round") took between 5 and 14 days dependent on weather conditions, to remove this temporal variability photosynthesis and ecosystem respiration were modelled (Equation 6.1 and Equation 6.2) using all data collected for each plot (n=36). R_{Eco} was assumed to be equivalent to NEE under dark conditions, and photosynthesis (P_G) was calculated as the difference between average R_{Eco} (2 measurements taken in dark conditions) and NEE measured at different light levels.

Equation 6.1 Photosynthesis Model

$$P_G = \frac{P_1.\mathrm{GEI.I}}{k_1 + \mathrm{I}} + a.exp^{-b/T_5}$$

Where P_1 is the maximum rate of photosynthesis (μgC m^{-2} s^{-1}), GEI the modelled greenness excess index, I the incident PAR (μmol Photons $m^{-2}s^{-1}$), k_1 is the half-saturation coefficient (μmol Photons $m^{-2}s^{-1}$), T_5 the soil temperature at a depth of 5 cm (°C) and a (dimensionless) and b ($°C^{-1}$) are empirically derived coefficients describing an Arrhenius (Arrhenius 1898) response to temperature.

Equation 6.2 Ecosystem Respiration Model

$$R_{Eco} = c.exp^{-d/T_5} + e.exp\left(-0.5.\left(\frac{T_5 - T_{Opt}}{T_{Tol}}\right)^2\right)$$

Where T_5, T_{Opt} and T_{Tol} are the measured, optimum and maximum tolerable soil temperature at a depth of 5 cm (°C) and c (dimensionless), d ($°C^{-1}$) and e (dimensionless) are empirically derived coefficients describing an Arrhenius (Arrhenius 1898) response to temperature and e an empirically derived coefficient describing a Gaussian temperature response.

R_{Eco} and P_{G600} were then calculated for a soil temperature of 12 °C, GEI of 60 and PAR of 600 μmol Photons $m^{-2}s^{-1}$ (typical of a summers day) using the empirically derived parameters (Supplementary Material Table 10.6). A PAR of 600 μmol Photons $m^{-2}s^{-1}$ was selected as it lay within the range of PAR observed and most plots were light saturated at this PAR enabling photosynthetic efficiency to be compared between locations.

6.5.4 Soil CO_2 Efflux Measurements

At each plot, four polyvinyl chloride (PVC) collars (16 cm diameter, 8 cm high) were placed on and sealed to the surface of the peat using non-setting putty (Evo-Stik 'Plumbers Mait'). Collars installed in March 2012 were located between 0.5 and 2 m down gradient of the NEE exchange plots. Above-ground vegetation was removed by regular clipping from all PVC collars enabling the measurement of below-ground fluxes only. In addition circular 20 cm deep trenches (56 cm diameter) were cut around half the collars to sever live roots, allowing the below-ground heterotrophic component to be measured. The collars with only above-ground vegetation removed were used to measure total

below-ground respiration. Trenches 20 cm deep were considered sufficient as although cord roots are 15-45 cm long (Jefferies 1915) most of the root biomass is concentrated nearer the surface (Taylor *et al.* 2001). For each plot, the two replicates of each treatment were averaged to produce a single value. Autotrophic respiration (including root respiration and microbial respiration of root exudates) was calculated from the difference between average total (n≤2) and average heterotrophic below-ground respiration (n≤2) measured at each location for each sampling round (complete set of measurements from 144 collars).

CO_2 measurements (n=222) were taken in a semi-randomised pattern approximately every three weeks from 16/04/2012 to 26/10/2012 data collected between 16/04/2012 and 25/05/2012 were excluded due to obvious treatment effects. CO_2 flux was measured over 2 minutes using an EGM-4 infra-red gas analyser and a CPY-4 canopy assimilation chamber (PP Systems, Hitchin, UK). At the same time as CO_2 flux measurements were made, the depth of the water table below the peat surface and soil temperature 5 cm were measured at each plot (n=36).

As below-ground respiration has been shown to be strongly controlled by soil temperature (Lloyd and Taylor 1994) which varies diurnally and seasonally, adjusting soil respiration to a fixed temperature removes the direct effect of temperature to enable effects such as seasonal changes in vegetation productivity or water table depth to be observed.. The mean soil temperature at 5 cm (T) (°C) and the mean respiration rate (R_T) for each sample day at each site (n=6) (μmol m^{-2} s^{-1}) were regressed (Equation 6.3) and the Q_{10} (the increase in respiration rate for a 10 °C increase in temperature) calculated.

Equation 6.3

$$LnR_T = LnR_{10} + \frac{LnQ_{10}}{10}(T - 10)$$

Using the Q_{10} values calculated by Equation 6.3 for total, heterotrophic and autotrophic below-ground respiration for each site (Supplementary Material Table 11.7), all respiration rates were normalised to 10 °C (r_{10}) (Equation 6.4).

Equation 6.4

$$r_{10} = R_t . Q_{10}^{\,10-t/10}$$

Where r_{10} is the temperature adjusted respiration at 10 °C for a measured respiration rate (μmol m^{-2} s^{-1}) (R_t) at a given location (n=1) at temperature t °C and Q_{10} as above.

6.5.5 Vegetation Composition and Primary Productivity

Annual net primary productivity (ANPP) was measured in late August by destructive harvest of a 55 x 55 cm plot (n=36) approximately 2 m down-gradient of the NEE plot. Vegetation composition of vascular plants and bryophytes (% cover) of the NEE plot was estimated by visual inspection in August. As 14/18 of the species present were observed in <6 locations the total percentage cover of non-*Molinia* species was calculated. The number of species present at each location was counted to derive the species richness. The Inverse Simpson Diversity Index (Equation 6.5) was also calculated. This determines the probability that two individuals randomly selected from a sample will be of the same species. D increases from one to n as diversity increases.

Equation 6.5 Inverse Simpson Diversity Index

$$D = 1 \Big/ \frac{\sum n(n-1)}{N(N-1)}$$

Published Ellenberg's Moisture Indicator Values (Hill *et al.* 1999) were assigned to all species identified where these species have been classified. These ranged from 6 (Moist to Damp e.g. *Vaccinium myrtillus* and *Gallium saxatile*) to 9 (wet e.g. *Narthecium ossifragum and Sphagnum fallax*), *Molinia caerulea* has a value of 8 (damp to wet). The Ellenberg's Moisture Indicator Values for the

classified species present at each location were averaged to give the Ellenberg's Moisture Indicator Value.

Principal component analysis was used to identify which vegetation types provided the maximum discrimination between locations by assessing their weightings along the first and second principal axes. Minimal vegetation diversity resulted in uncommon species having stronger factor weightings (Supplementary Material Figure 10.2) and both axes explained only 34 % of the variability so this was not pursued further.

6.5.6 Statistical Analysis

To test for spatial variation, a two-way ANOVA was carried out on seasonal mean water table depths, measured vegetation indices, P_{G600} and R_{Eco} with site, proportional distance from the ditch and proportional distance from the ditch nested within site as between subject effects. A repeated measures ANOVA was carried out on below-ground respiration rates, with site or proportional distance from the ditch (plot) as between subject factors, and sampling round (time) as a within subject factor. *Post-hoc* Least Squares Difference tests were carried out to identify statistically different groups. Linear and quadratic regressions were carried out to test for a relationship between distance from the ditch and water table depth, measured vegetation indices, P_{G600}, R_{Eco} and below-ground respiration. The most significant relationships are reported.

It was expected that spatial variation in CO_2 fluxes would be driven primarily by variation in water table depth and/or vegetation composition. Water table depth and vegetation indices (percentage cover of *Molinia caerulea*, leaf-litter and non-*Molinia* species, ANPP, species richness, Inverse Simpson Diversity Index and Ellenberg's Moisture Indicator Values) were regressed against CO_2 fluxes (modelled ecosystem respiration, modelled photosynthesis, seasonal mean total, heterotrophic and autotrophic below-ground respiration at 10 °C for each location). In addition, spatial variables such as altitude, aspect, peat depth etc. were regressed individually and as part of a multiple-stepwise regression. All

statistical analyses were performed with SPSS 19 (SPSS Inc., Chicago, Illinois, USA).

6.6 RESULTS

6.6.1 Spatial Variation with Distance from a Drainage Ditch

Water table depth was deepest closest to the ditch (⅛-distance) and became shallower at ½-distance (Figure 6.2a) but the difference was not significant (p=0.197, Table 6.3). Although vegetation properties showed variation (Table 6.5, Supplementary Material Table 10.8), analysis of variance indicated none varied significantly with proportional distance from the ditch (Table 6.3). Both percentage coverage of non-*Molinia* species and the Simpson Diversity Index were lower at ⅛-distance than ½-distance (Figure 6.2d & e). However, the difference between proportional distances from the ditch (Table 6.3) was not significant (p=0.083 and p=0.076 for non-*Molinia* and the Simpson Diversity Index respectively). Species richness (Figure 6.2f) also showed a non-significant increase at greater proportional distance from the ditch but no significant relationship with absolute distance from the ditch (p=0.135). ANPP, percentage cover of leaf litter and *M. caerulea* were lowest at ¼-distance (Figure 6.2g, h & i), but showed no significant differences between proportional distances from the ditch (Table 6.3) or from the absolute distances from the ditch (Table 6.5).

Table 6.2 Mean and standard error (in brackets) distance from the ditch (m)water table depth (cm below surface), percentage coverage of *Molinia caerulea*, leaf litter and non-*Molinia* species, annual net primary productivity (ANPP), species richness and Inverse Simpson diversity index for different sites and proportional distances from the ditch.

		Distance from the Ditch (m)	Water Table Depth (cm)	*Molinia* (%)	Leaf Litter (%)	Non- *Molinia* (%)	ANPP (gm^{-2})	Species Richness	Simpson Diversity
Proportional Distance from the Ditch	**1/8**	3.01 (0.34)	21 (2)	90 (4)	87 (4)	4 (1)	309 (18)	2.8 (.4)	1.1 (0.0)
	1/4	6.04 (0.70)	20 (3)	81 (6)	82 (6)	7 (3)	292 (20)	3.2 (0.7)	1.2 (0.1)
	1/2	12.07 (1.39)	16 (3)	87 (4)	87 (3)	15 (6)	322 (22)	3.3 (0.6)	1.4 (0.1)
Site	**A1**	6.23 (1.49)	15 (1)	88 (5)	87 (2)	5 (2)	295 (22)	3.8 (0.9)	1.1 (0.0)
	A2	5.57 (1.33)	31 (3)	83 (7)	89 (3)	3 (2)	281 (19)	2.3 (0.7)	1.1 (0.0)
	A3	5.40 (1.29)	14 (3)	83 (6)	85 (3)	6 (2)	299 (32)	4.0 (0.8)	1.1 (0.0)
	S1	11.92 (2.88)	11 (1)	88 (6)	80 (7)	21 (9)	294 (34)	4.0 (1.0)	1.5 (0.2)
	S2	4.08 (1.0)	21 (5)	78 (9)	100 (0)	6 (5)	373 (27)	1.7 (0.3)	1.1 (.01)
	S3	9.07 (2.18)	20 (2)	97 (3)	71 (9)	12 (8)	303 (26)	2.7 (0.8)	1.3 (.2)
Total	**Mean**	7.04 (0.82)	19 (2)	86 (3)	85 (2)	9 (2)	307 (11)	3.1 (0.3)	1.2 (0.1)
	Min	1.56	2	40	35	0	199	1.0	1.0
	Max	21.95	40	100	100	53	488	8.0	2.3

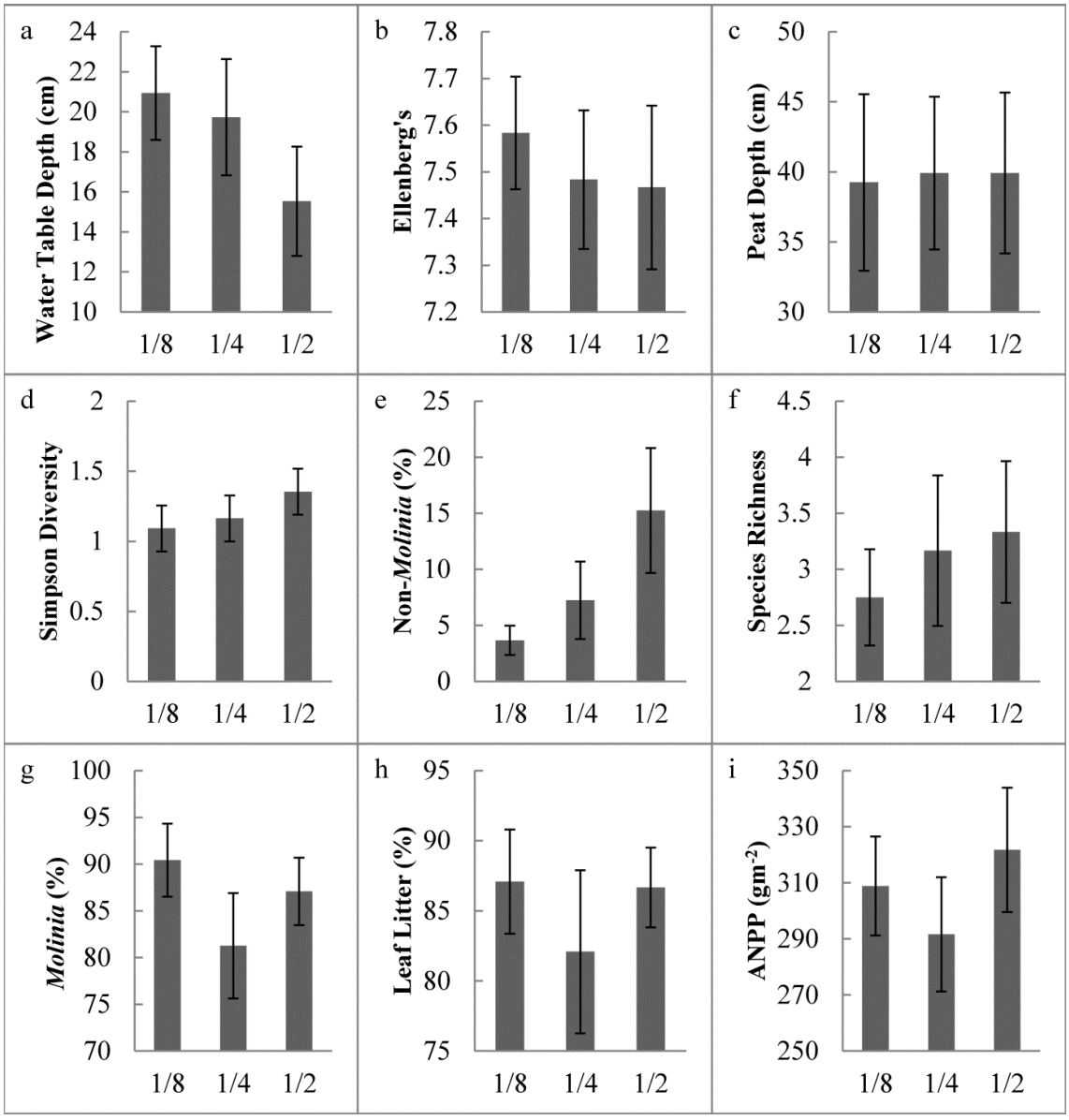

Figure 6.2 Variation with proportional distance from the ditch in a, water table depth (cm below ground surface), b, Ellenberg's Moisture Indicator Values, c, peat thickness (cm), d, Inverse Simpson Diversity Index, e, percentage coverage of Non-*Molinia* species, f, species richness, g, percentage coverage of *Molinia caerulea*, h, percentage coverage of leaf litter and i, annual net primary productivity (ANPP) (g m^{-2}). n=12. Error bars are one standard error.

Table 6.3 Two-way ANOVA for mean water table depth, vegetation indices, peat depth and modelled ecosystem respiration (R_{Eco}) and photosynthesis at 600 µmol Photons $m^{-2}s^{-1}$ (P_{G600}) (µgC m^{-2} s^{-1}) at all locations (n=36) with site, proportional distance from the ditch (Plot) and proportional distance from the ditch nested within site as between subject variables. SS is sum of squares, df degrees of freedom, MS mean sum of squares, F the F-ratio and p the significance. Shaded dark grey where p<0.050.

	Source	SS	df	MS	F	p
Water Table Depth	Site	1479	5	296	5.4	0.003
	Plot	194	2	97	1.8	0.197
	Plot(Site)	367	10	37	0.7	0.734
% *Molinia*	Site	1265	5	253	1.2	0.334
	Plot	517	2	258	1.3	0.307
	Plot(Site)	3000	10	300	1.5	0.231
% Leaf Litter	Site	2822	5	564	3.0	0.040
	Plot	185	2	92	0.5	0.623
	Plot(Site)	1115	10	112	0.6	0.805
% Non-*Molinia*	Site	1365	5	273	1.9	0.154
	Plot	844	2	422	2.9	0.083
	Plot(Site)	1894	10	189	1.3	0.309
ANPP	Site	32970	5	6594	1.4	0.284
	Plot	5498	2	2749	0.6	0.586
	Plot(Site)	41057	10	4106	0.8	0.591
Species Richness	Site	30	5	6.0	1.8	0.162
	Plot	2	2	1.1	0.3	0.725
	Plot(Site)	47	10	4.7	1.4	0.246
Inverse Simpson Diversity Index	Site	0.7	5	0.1	1.9	0.146
	Plot	0.4	2	0.2	3.0	0.076
	Plot(Site)	1.1	10	0.1	1.4	0.246
Ellenberg's Moisture Indicator Value	Site	2.2	5	0.4	2.0	0.135
	Plot	0.1	2	0.0	0.2	0.814
	Plot(Site)	2.5	10	0.2	1.1	0.421
Peat Depth	Site	11547	5	2309	24	0.000
	Plot	3.5	2	1.8	0.02	0.982
	Plot(Site)	235	10	23.5	0.2	0.986
R_{Eco}	Plot	215	2	108	0.4	0.678
	Site	477	5	95	0.4	0.874
	Plot(Site)	2807	10	281	1.0	0.453
P_{G600}	Plot	877	2	438	0.3	0.760
	Site	31947	5	6389	4.1	0.012
	Plot(Site)	21522	10	2152	1.4	0.269

Table 6.4 Repeated measures ANOVA results for total, heterotrophic and autotrophic respiration adjusted to 10 °C. Proportional distance from the ditch (Plot) and site were between subject effects and sample round (Time) was a within subject effect. SS is sum of squares, df degrees of freedom, MS mean sum of squares, F the F-ratio and p the significance. Shaded dark grey where p<0.050.

Respiration Source	Effect	SS	df	MS	F	p
Total at 10 °C	Time	3.60	2.05	1.75	10.60	0.000
	Site	1.42	5.00	0.28	1.32	0.283
	Plot	0.18	2.00	0.09	0.38	0.689
	Time x Site	2.53	10.25	0.25	1.49	0.163
	Time x Plot	0.72	4.54	0.16	1.00	0.421
Heterotrophic at 10 °C	Time	3.24	3.56	0.91	17.36	0.000
	Site	1.05	5.00	0.21	3.28	0.018
	Plot	0.01	2.00	0.01	0.07	0.937
	Time x Site	1.92	18.22	0.11	2.67	0.001
	Time x Plot	0.06	7.13	0.01	0.15	0.994
Autotrophic at 10 °C	Time	0.43	2.80	0.15	1.13	0.342
	Site	0.71	5.00	0.14	0.70	0.626
	Plot	0.10	2.00	0.05	0.25	0.781
	Time x Site	2.26	13.98	0.16	1.19	0.298
	Time x Plot	0.93	5.76	0.16	1.21	0.309

Ellenberg's Moisture Indicator Values were greater at ⅛-distance than ½-distance (Figure 6.2b) indicating a drier plant community further away from the ditch, which contrasts with the measured water table depths (Figure 6.2a). The Ellenberg's Moisture Indicator Values ranged from 6.6 to 8.5 with a mean of 7.5 (constantly moist or damp but not wet) and showed a non-significant positive relationship (r^2=0.08, p=0.105) to water table depth, indicating drier conditions (lower Ellenberg's Moisture Indicator Values) occurring where the water table was closer to the soil surface. Ellenberg's Moisture Indicator Values could not be used as indicators of moisture conditions and were therefore excluded from further investigation.

Neither modelled P_{G600} nor R_{Eco} varied significantly with proportional distance from the ditch (Figure 6.2, Table 6.3) or absolute distance from the ditch (Supplementary Material Figure 10.3)). P_{G600} was greatest furthest from the ditch and least at ¼-distance (Figure 6.3a) whilst R_{Eco} increased non-significantly between closest to the ditch and ¼-distance (Figure 6.3a). The

interaction term between site and proportional distance from the ditch was not significant for either P_{G600} or R_{Eco} (Figure 6.3, Table 6.3) indicating that the effect of proportional distance from the ditch did not depend on which site was being analysed. No below-ground respiration source varied significantly with proportional distance from the ditch (Table 6.4) or absolute distance from the ditch (Supplementary Material Figure 10.3). However, they were all greatest at ¼-distance with ½-distance smallest (Figure 6.4a).

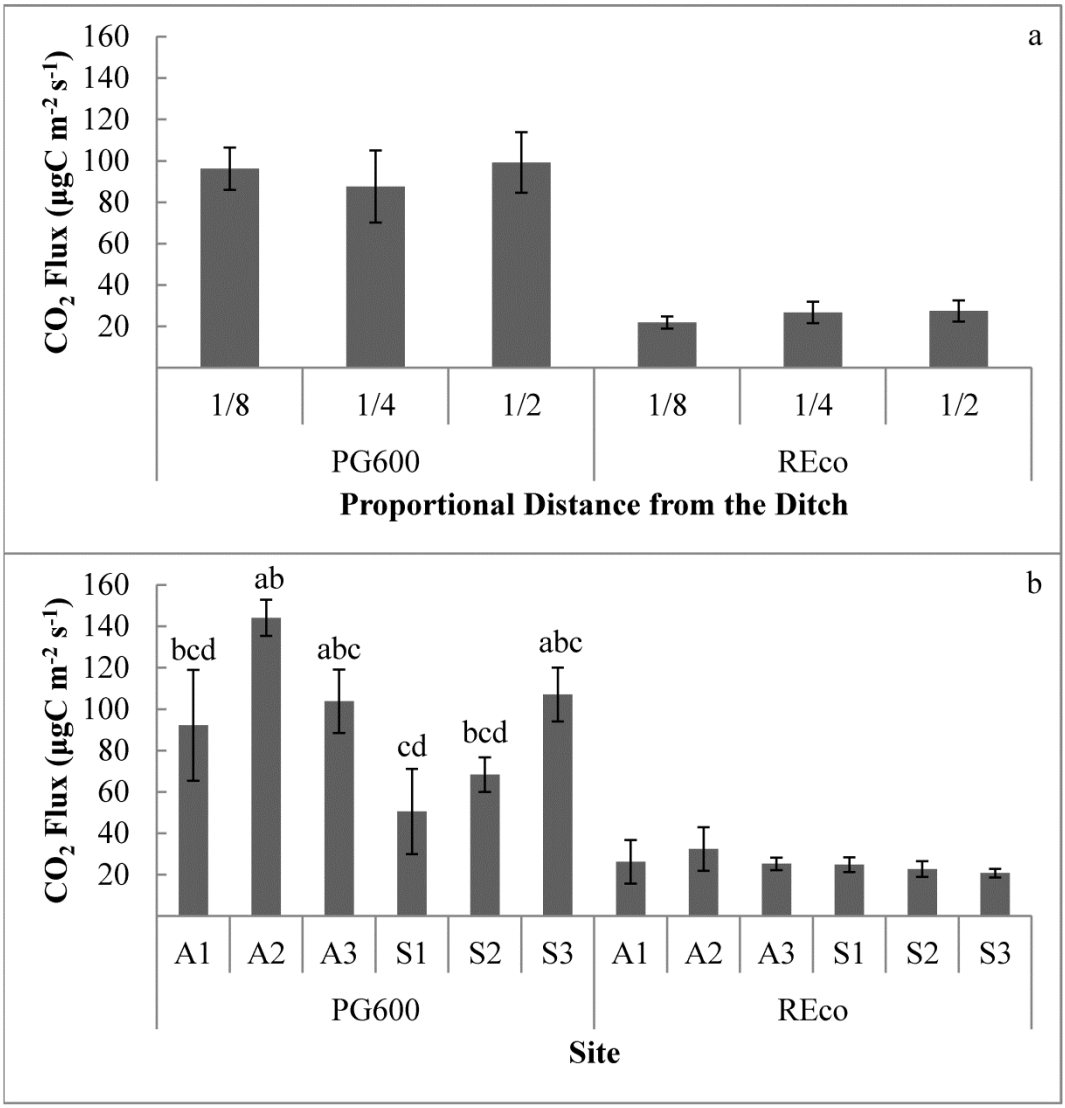

Figure 6.3 Variation in modelled photosynthesis (P_{G600}) (µgC m^{-2} s^{-1}) and ecosystem respiration (R_{Eco}) (µgC m^{-2} s^{-1}) with a, proportional distance from the ditch and b, site. Error bars are one standard error. Letters denote statistically significant groups p=0.012.

6.6.2 Spatial Variation between Sites

Water table depth, percentage coverage of leaf litter and peat depth all varied significantly between sites (Table 6.3). Site A2 was drier and site S1 wetter than all other sites (Table 6.2). Peat depth was also significantly greater at site S2 than all other sites (Table 6.1). The sites could be divided into two groups based on the percentage coverage of leaf litter, those with ≥85 % coverage (A1, A2, A3, and S2) and those with ≤85 % coverage (A3, S1 and S3) (Table 6.2). The interaction term between site and proportional distance from the ditch was not significant for any of the spatial variables tested (Table 6.3). Indicating that, for example, the effect of proportional distance from the ditch on water table depth did not depend on which site was being analysed.

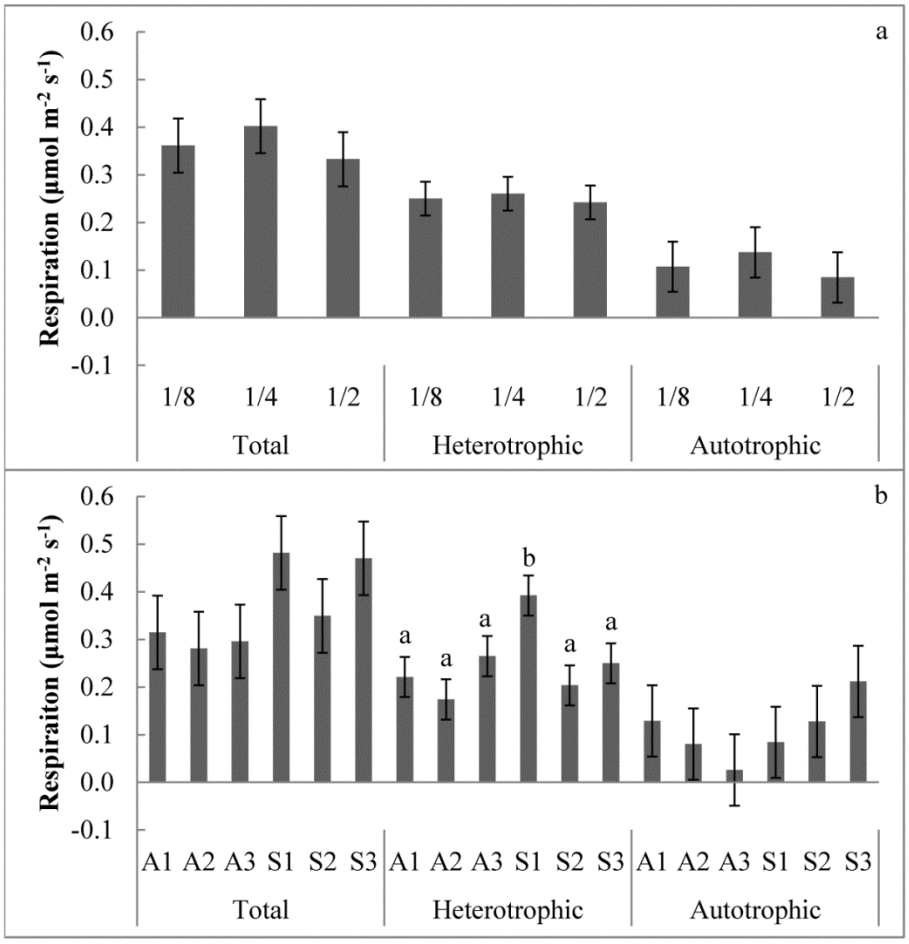

Figure 6.4 Variation in total, heterotrophic and autotrophic respiration at 10 °C (µmol m^{-2} s^{-1}) with a, proportional distance from the ditch and b, site. Error bars are one standard error. Letters denote statistically significant groups p=0.018.

P_{G600} varied significantly between sites (Figure 6.3b), with photosynthesis at site A2 greater than sites S1 and S2 with the other sites intermediate. Sites A2 and S1 were also the driest and wettest sites respectively (Table 6.2). Ecosystem respiration was also greatest at site A2 but did not vary significantly between sites (Table 6.3). Total and heterotrophic below-ground respiration showed similar spatial variation between sites with total and heterotrophic respiration greatest at S1 and least at A2 whereas autotrophic respiration was greatest at S3 and least at A3. Only heterotrophic respiration varied significantly between sites (Table 6.4) with site S1 having significantly greater respiration than at all other sites (Figure 6.4b). The significant interaction term between site and sampling round (time) for heterotrophic respiration (Table 6.4) indicates that heterotrophic respiration varied differently over time dependent on which site was being analysed.

6.6.3 Drivers of Spatial Variability

Percentage cover of non-*Molinia* species and the Inverse Simpson Diversity Index both showed a significant negative covariance with water table depth (Table 6.5). Greater diversity and more non-*Molinia* species occurred where the water table depth was closer to the surface.

Water table depth showed a significant positive covariance (Table 6.5) with $P_{G600,}$ greater photosynthesis occurred where the water table was deeper. No other CO_2 fluxes co-varied with water table depth. P_{G600} showed no significant relationships with ANPP or vegetation composition indices (*M. caerulea*, non-*Molinia*, leaf litter, species richness or Inverse Simpson Diversity Index) (Table 6.5). R_{Eco} and autotrophic respiration showed no significant relationships with any of the variables tested (Table 6.5). However, autotrophic respiration showed some level of co-variation (r^2=0.09) with percentage cover of *M. caerulea*, autotrophic respiration was greater where there was more *Molinia caerulea* coverage. Heterotrophic respiration significantly co-varied (r^2=0.11, p=0.046) with peat thickness with greater respiration where the peat was thinner (Table 6.5) whilst total soil respiration was significantly greater (r^2=0.15, p=0.021) where there was less coverage of leaf litter.

No other significant relationships were found between CO_2 fluxes and spatially distributed variables (e.g. altitude, aspect etc.). Stepwise regression indicated additional variables did not increase the proportion of variability explained.

Table 6.5 Regression coefficients (r^2) and significance (in brackets) of linear regression between water table depth (cm below-ground surface) and annual net primary productivity (ANPP), peat thickness and vegetation indices. Regression coefficients (r^2) and significance (in brackets) of linear regression between modelled photosynthesis at 600 µmol Photons m^{-2} s^{-1} (P_{G600}), modelled ecosystem respiration (R_{Eco}), total (R_{Tot}), heterotrophic (R_{Het}) and autotrophic (R_{Aut}) below-ground respiration at 10 °C and water table depth, annual net primary productivity (ANPP), peat thickness and vegetation indices (n=36). Shaded dark grey where p<0.050. + positive covariance – negative covariance.

	Water table depth (cm)	ANPP (gm-2)	*Molinia* (%)	Non-*Molinia* species (%)	Leaf Litter (%)	Species Richness	Inverse Simpson Diversity	Peat Thickness (cm)
Water Table depth (cm)	.	0.01 (0.662) +	0.06 (0.169) -	0.15 (0.021) -	0.03 (0.322) +	0.16 (0.087) -	0.14 (0.024) -	.08 (0.106) +
P_{G600}	0.13 (0.034) +	0.00 (0.896) +	0.03 (0.322) +	0.01 (0.479) +	0.00 (0.913) -	0.00 (0.850) -	0.02 (0.459) -	0.00 (0.884) -
R_{Eco}	0.01 (0.511) +	0.01 (0.595) +	0.07 (0.132) -	0.04 (0.256) -	0.01 (0.534) +	0.10 (0.062) -	0.04 (0.268) -	0.01 (0.641) -
R_{Tot}	0.01 (0.613) -	0.01 (0.646) -	0.04 (0.224) +	0.00 (0.923) +	0.15 (0.021) -	0.00 (0.746) +	0.00 (0.881) +	0.00 (0.856) -
R_{Het}	0.05 (0.172) -	0.08 (0.096) -	0.01 (0.582) -	0.02 (0.440) +	0.07 (0.109) -	0.03 (0.332) +	0.02 (0.396) +	0.11 (0.046) -
R_{Aut}	0.00 (0.934) +	0.09 (0.587) +	0.09 (0.077) +	0.04 (0.709) -	0.05 (0.181) -	0.00 (0.940) -	0.00 (0.719) -	0.03 (0.327) +

6.7 DISCUSSION

6.7.1 Drainage Ditches, Water Table Depths and Vegetation

The drainage features on Exmoor although small (typically <0.5 m wide and <0.5 m deep) penetrate deep into the shallow peat (Exmoor average 0.33 m (Bowes 2006)) and are regularly spaced (approximately 20 m) (Figure 6.1) making them important spatial features governing ecohydrological processes in these uplands (Grand-Clement *et al.* 2013b). The mean water table was deeper closer to the ditch than at ½–distance (Figure 6.2a) but the significant variability between sites (Table 6.3) was such that the difference between proportional distances from the ditch was not significant. Differences between sites may have been due to a combination of different site conditions (e.g. peat thickness, ditch direction etc.) as well as the distance between adjacent ditches and hence absolute distance of ⅛, ¼ and ½ plots from the ditch. On different ditches within the same catchments Luscombe *et al.* (2014) found water table depths to be deeper nearer the ditch but that distance from the ditch explained only 13.6 % of the observed spatial variance. Fine scale topography and position up- or down-slope of the ditch altered the effect of proximity to a ditch. On deeper *Eriophorum vaginatum, Deschampia myrtillus* and *Molinia caerulea* dominated peats, Holden *et al.* (2011) also found water table depth to be deeper closest to the ditch with the effect localised within a few metres due to the low hydraulic conductivity of peat. However, when comparing 1.5 m to 6 m from the ditch in a *Calluna vulgaris–Eriophorum vaginatum* upland blanket bog, Coulson *et al.* (1990) found no significant difference in water table depths, possibly due to high rainfall conditions.

This non-significant variation in water table depth may explain why there was no significant (Table 6.3) variation in percentage coverage of non-*Molinia* species and the Inverse Simpson Diversity Index. Coulson *et al.* (1990) found coverage of *Calluna vulgaris* to increase away from the ditch with a concurrent decrease in grass species in two low-altitude British blanket bogs where they observed difference in water table depths but in two higher altitude, higher rainfall bogs

where no variation in water table depth was observed, there was no significant change in vegetation composition.

6.7.2 Site, Water Table Depths and Vegetation

Given the range of average water table depths for each site in this study (11 to 34 cm) (Table 6.22), and previous work, a greater range of vegetation communities across the sites studied would be expected. For example, a 22 to -2 cm range in mean water table depth affected a change in vegetation from *Eriophorum vaginatum* to *Scheuchzeria palustris* in an undisturbed Finnish fen (Riutta *et al.* 2007). In this study *Molinia caerulea* (86 ± 3 %) dominated with minimal non-*Molinia* species present (9 ± 2 %). This vegetation composition reflects deeper water table depths under wet conditions, the competitive nature of *M. caerulea,* its ability to flourish where water table depths fluctuate (Jefferies 1915) and tendency to exclude other plants (Taylor *et al.* 2001). Minimal variability in vegetation composition would be expected to limit the magnitude of variation possible in CO_2 both between sites and with distance from the ditch.

Across all locations more non-*Molinia* species (r^2=0.15, p=0.021), greater species richness (r^2=0.16, p=0.087) and higher diversity (r^2=0.14, p=0.024) occurred where the water table depth was closer to the surface (Table 6.5). Indicating *M. caerulea* may be less dominant where water tables are shallower enabling other species to grow. This finding is similar to Laine *et al.* (2007) who found species richness to decrease as water table depths dropped below approximately 10 cm in an undisturbed Irish blanket bog.

Other studies in pristine peatlands (Laine *et al.* 2007, Maanavilja *et al.* 2011) found vascular green area to increase as water tables fell and vegetation composition changed. In this study ANPP was not affected by water table depth (Table 6.5). Again this most likely reflects the greater vegetation diversity and wetter conditions within these studies compared to that observed on Exmoor. Rutter (1955) found mean water table depth to determine the shape of the *M. caerulea* tussock and the vegetation composition present in a wet-heath. It is known that vegetation structure varies with wetness in these catchments

(Luscombe *et al.* 2014a). However, in this study mean water table depth did not relate to percentage coverage of *M. caerulea* (Table 6.5). It may be that the vegetation survey failed to capture structural variation as the long spreading leaves covered most of the plot resulting in limited variation in *M. caerulea* cover between locations (86 ±3 %).

Bellamy *et al.* (2012) found a wet vegetation index (based on vegetation with an Ellenberg's Moisture indicator value of 8-10) to be lowest 0.5 m from the ditch in a blanket bog and increase with distance from the ditch. Conversely an index of drier vegetation (Ellenberg's Moisture Indicator Values of 4-7) was highest close to the ditch and decreased with distance. In the current study, Ellenberg's Moisture Indicator Values decreased (non-significantly) with increased distance from the ditch indicating wetter conditions nearer the ditch (Figure 6.2b). They also increased where water table depths were closer to the surface, contrary to expectations given Ellenberg's Moisture Indicator Values range from 1 (extreme dryness) to 12 (submerged plants) (Hill *et al.* 1999). This demonstrates that Ellenberg's Moisture Indicator Values are not appropriate as a proxy for wetness in this relatively dry and low diversity environment where only *Narthecium ossifragum* (9) and *Sphagnum fallax* (9) had higher Indicator Values than *Molinia caerulea* (8).

6.7.3 Spatial Variability of CO_2 Fluxes

CO_2 fluxes from the *M. caerulea*-covered peatland did not vary significantly with proportional distance from the ditch (Table 6.6 & 6.4), arguably due to limited variation in either water table depth (Figure 6.2a) and/or vegetation composition (Figure 6.2d, e, f & g). In other studies where spatial features such as ditches have been explicitly monitored, clear differences in functional responses have been measured – e.g. ephemeral erosional gullies in an British blanket bog have been shown to have significantly higher ecosystem respiration (McNamara *et al.* 2008, Clay *et al.* 2012) and photosynthesis (Clay *et al.* 2012) than the surrounding blanket bog. These gullies were deeper (up to 3 m) and wider (5-9 m) and had a greater effect on both water table depth and vegetation community than the smaller drainage ditches of Exmoor. It is likely that CO_2

fluxes varied across ephemeral erosional gullies due to the spatial variation in vegetation and vegetation cover with the greatest rates of photosynthesis and ecosystem respiration from *Eriophorum* communities and lowest fluxes from bare peat.

Photosynthesis weakly (r^2=0.13, p=0.034) co-varied with water table depth, greater photosynthesis occurred where the water table was deeper. This may have occurred as drier conditions encourage greater above-ground biomass (Murphy and Moore 2010) or promote increased coverage by graminoids which have been shown to have higher net ecosystem exchange rates than mosses (Otieno *et al.* 2009) and *Calluna vulgaris* (Aerts 1990). Although the cover of non-*Molinia* species was less where the water table was deeper(Table 6.5) there was no significant relationship between P_{G600} and non-*Molinia* directly. In addition P_{G600} showed no significant relationships with either ANPP or percentage coverage of *M. caerulea* (Table 6.5). It is possible that despite adaptations to live in conditions of fluctuating water table depths (Taylor *et al.* 2001) the conditions for *Molinia caerulea* were sub-optimum at the wetter locations (e.g. site S1) thus reducing photosynthesis.

Where water table depth has been found to control spatial variation in photosynthesis, fluxes have also been greater in drier microforms (Laine *et al.* 2006, Maanavilja *et al.* 2011, Schneider *et al.* 2012). In such studies there was clear differentiation in water table depths and vegetation community between microforms so it is less clear if variation in photosynthesis was due to water table depth, vegetation community or both. Conversely Bubier *et al.* (2003) found different microforms to have similar rates of photosynthesis, despite variation in vegetation composition and water table depth, due to similar leaf biomass.

Where variation in photosynthetic rates have been assessed within microforms in a pristine Finnish Fen; hummocks, *Eriophorum vaginatum* lawns and hollows were found to respond to water table depths but not *Carex* lawns (Riutta *et al.* 2007). However, in a pristine Russian boreal peatland, *Carex* lawns showed

the greatest within microform variability in photosynthesis driven by variation in vegetation composition and water table depth (Schneider *et al.* 2012), indicating the uncertainty in assessing controls on photosynthesis within a microform.

Where ecosystem respiration has been found to vary between microforms in pristine peatlands (Bubier *et al.* 2003, Laine *et al.* 2006, Maanavilja *et al.* 2011, Juszczak *et al.* 2013) wetter areas had distinct vegetation communities and lower respiration rates. Again the minimal variation in vegetation composition observed in this study may explain why there was no statistically significant spatial variation in ecosystem respiration (Table 6.3). This finding suggests that photosynthesis is the main control on the spatial distribution of net ecosystem exchange. Riutta *et al.* (2007) also found photosynthesis to vary more between communities than ecosystem respiration in a Finnish Fen.

Peatland restoration programmes (Grand-Clement *et al.* 2015) typically aim to raise water tables and re-establish the ecohydrological structure and functionality of peatlands. Re-colonisation by peat-forming *Sphagnum*-rich vegetation communities has been identified as particularly important to promote carbon sequestration (Lunt *et al.* 2010). Raising mean water table depths may have no effect on heterotrophic respiration of the peat store but decrease photosynthesis (Table 6.5) shifting the ecosystem towards a greater CO_2 source unless change in water table depth is sufficient to alter the vegetation composition (and leaf litter quantity and quality) beyond that observed in this study.

As below-ground autotrophic respiration is strongly dependent on photosynthesis (Metcalfe *et al.* 2011) it would be expected that autotrophic (root) respiration would mirror photosynthesis and be dependent on water table depth. Instead, photosynthesis (Figure 6.3) and autotrophic respiration (Figure 6.4) showed dissimilar spatial patterns and varied with different spatial variables (Table 6.5), suggesting that autotrophic respiration was controlled by factors additional to photosynthetic activity, such as morphological differences in root biomass (Heinemeyer *et al.* 2012), variation in the allocation of carbon between

growth and maintenance (Bond-Lamberty *et al.* 2004) and moisture and nutrient availability (Chapman and Thurlow 1998). Autotrophic respiration insignificantly ($p=0.077$) co-varied ($r^2=0.09$) with percentage cover of *M. caerulea*, with greater autotrophic respiration where there was more *M. caerulea* coverage. As above- and below-ground biomass have been shown to be linked (Murphy and Moore 2010) it may be that where there is greater *M. caerulea* coverage there is greater root biomass, resulting in increased root respiration and microbial respiration of root exudates.

Neither total nor heterotrophic below-ground respiration varied with water table depth (Table 6.5). Jaatinen *et al.* (2008) found long-term (45 years) water table draw-down of a fen to increase total soil respiration rates in the driest areas, however, the decomposition potential of the substrate remained greater in the wetter areas. As the drainage ditches on Exmoor are over 150 years old much of the labile organic matter will have already degraded (Bridgham and Richardson 1992). This will have left a humified peat which, although potentially vulnerable to priming (Freeman *et al.* 2004, Fontaine *et al.* 2007), is less responsive to variation in water table depth than recently drained peat. Grand-Clement *et al.* (2014) found consistently low humic to fulvic acid ratios for dissolved organic carbon from these catchments; indicative of more humified peats.

It was expected that heterotrophic respiration would vary with changes in leaf litter quality and quantity (Straková *et al.* 2011a). Heterotrophic respiration showed no significant co-variation with percentage coverage of non-*Molinia* or Inverse Simpson Diversity Index (Table 6.5), variables influencing litter quality or ANPP a measure of litter quantity. This may be due to the limited variation in vegetation composition and ANPP observed (Table 6.2). Instead, heterotrophic respiration significantly co-varied with peat thickness (Table 6.5) with greater respiration occurring where peat was thinner. This finding is contrary to other studies where thinner peats were found to have lower heterotrophic respiration rates in a *Calluna vulgaris* blanket bog (Hardie *et al.* 2009) and also where peat thickness was found to have little effect on heterotrophic respiration as most

respiration occurred near the surface of the peat (Blodau *et al.* 2007) primarily due to a lack of oxygen below the water table. There is no obvious explanation for this relationship.

Where microforms or spatial features were found to have distinct CO_2 fluxes they have been mapped and used to upscale CO_2 fluxes across a landscape (Laine *et al.* 2006, Riutta *et al.* 2007, McNamara *et al.* 2008). In these *M. caerulea* dominated peatlands there was significant spatial variation (Table 6.3) in $P_{G600.}$ However, this was not directly associated with proportional distance from drainage ditches (Table 6.3) so mapping these features cannot be used directly to upscale CO_2 fluxes in this landscape. Given the sparse vegetation in the ditches it is unlikely these would have large CO_2 fluxes however, as these were not measured it is currently unknown if these are important when estimating landscape scale fluxes.

6.8 CONCLUSION

Modelled CO_2 fluxes (photosynthesis and ecosystem respiration, total, heterotrophic and autotrophic below-ground respiration) showed no significant spatial distribution in response to drainage ditches, arguably due to a lack of significant spatial distribution in water table depths and minimal variation in vegetation composition (percentage cover of non-*Molinia* species and Inverse Simpson Diversity Index).

Across all locations (n=36) where the average water table depth was closer to the surface, greater non-*Molinia* species coverage increased vegetation diversity and reduced P_{G600}, indicating wetter conditions may be sub-optimum for *Molinia caerulea.* Our data emphasises that substantial reduction in heterotrophic respiration may not always occur following restoration unless water tables rise to be consistently very close to the soil surface. As a consequence, raising mean water table depths through eco-hydrological restoration in grass dominated peatlands may shift the ecosystem towards

greater CO_2 release, unless the vegetation composition alters beyond that observed in this study.

Modelled P_{G600} showed significant spatial variation between sites and significantly co-varied with water table depth this offers a potential means to estimate CO_2 fluxes at a landscape scale. Although water table depth showed variation between proportional distances from the ditch the uncertainty is such that it should not be assumed that water table depth is distributed according to proportional distance from a drainage ditch. Therefore, other methods of determining the spatial distribution of water table depth, which may be only partially explained by ditch density, such as vegetation structure (Rutter 1955) should be explored.

6.9 ACKNOWLEDGEMENTS

The authors would like to thank the anonymous reviewers for the thorough reviews, their suggestions improved this paper. The authors would also like to thank the Exmoor Mires Project for their help with site access, Exmoor National Park and the May family for permission to work on the sites. This research received financial support from South West Water and The University of Exeter (SK05284).

7 A NEW COST- AND TIME-EFFECTIVE METHOD FOR MEASURING FINE SCALE VEGETATION STRUCTURE IN COMPLEX LANDSCAPES USING GROUND AND UAV BASED DIGITAL IMAGES

7.1 ABSTRACT

Fine scale vegetation structures are intrinsically linked to underlying environmental conditions, vegetation composition and gaseous carbon fluxes. The ability to quantify these structures in a cost-effective, robust and repeatable fashion is imperative when attempting to understand change within an ecosystem. Structure from Motion (SfM) computer vision techniques allow multiple overlapping images collected by consumer grade cameras to be used to generate detailed point clouds at both the plot and landscape extent. There is great scope for these techniques to be used to derive structural characteristics of vegetation canopies but this has not yet been explored in ecological contexts. We tested the ability of this method to derive structural characteristics of a *Molinia caerulea* tussock grass at both a plot and landscape extent and examined relationships between tussock structure and environmental conditions, vegetation community and carbon fluxes.

Digital images were collected from fifteen 0.55 x 0.55 m vegetated plots using a Canon EOS-10D. In addition, 532 digital images were collected over a 1100 x 600 m area using an un-gimballed Sony Nex-7 mounted on a fixed wing QuestUAV. Both sets of images were processed using open source software (VisualSfM) to create georeferenced digital surface models (DSMs).

The number of images and image content (e.g. scale of texture, shadow and overlap with other images) affected the point cloud density. Processing time increased quadratically with the number of images but the range and variance in point cloud elevation for a 0.55 x 0.55 m vegetated plot stabilised above 120 images. A 0.05 m resolution landscape extent DSM derived from UAV images demonstrated radial distortion (doming) compared to 0.5 m resolution LiDAR DSM even with overlapping oblique flight paths. Despite this, both DSMs

significantly ($p<0.001$) correlated with elevation in an area of interest ($r=0.64$ and $r=0.75$ respectively). Finer resolution UAV-image derived DSMs were better able to distinguish tussock tops from inter-tussock areas. The 0.05 m resolution UAV-image derived DSM poorly predicted individual tussock heights (RMSE 0.061 m) but accurately predicted average tussock height (0.11 ± 0.06 m) within an area of interest (0.11 ± 0.04 m measured), thus revealing the possibility of using this method to investigate microtope properties. Despite the difficulties of using SfM on vegetation, this study highlights the potential for deriving fine scale vegetation structural characteristics at a plot and landscape extent using SfM methods on ground and UAV based digital images.

7.2 KEYWORDS

Molinia caerulea, tussock, SfM, computer vision, point cloud, DSM,

7.3 INTRODUCTION

7.3.1 Vegetation Structure at a Plot and Landscape Scale

Fine scale vegetation structures are intrinsically linked to vegetation function (Turner 1989) with self-organised patterns occurring in a range of ecosystems from savannahs to intertidal mudflats (Rietkerk and van de Koppel 2008). Ecosystems dominated by tussock forming species occur globally from semi-arid conditions (Ramírez *et al.* 2006) to arctic wetlands (Bliss and Matveyeva 1992). A method that measures vegetation structure in a spatially explicit, cost-effective, robust and repeatable fashion would enable change in vegetation structure and function within an ecosystem to be quantified.

To derive a three-dimensional surface at a plot scale, point-analysis methods are commonly used (e.g. Chassereau *et al.* 2011), these require little data processing but are relatively labour intensive (Jester and Klik 2005). A terrestrial laser scanner (TLS) has been shown to be capable of capturing the fine scale structure of *Sphagnum* microforms (Anderson *et al.* 2010) and *Molinia caerulea* tussocks (Luscombe *et al.* 2014b). However, the equipment cost, size

and weight currently preclude its more widespread use, particularly within remote environments. Airborne Light Detection and Ranging (LiDAR) has been used to capture 3D vegetation structure (Lefsky *et al.* 1999, Straatsma and Middelkoop 2007, Vierling *et al.* 2008, Korpela *et al.* 2009) and microtopography (Rosso *et al.* 2003, Wang *et al.* 2009, Chassereau *et al.* 2011) at a landscape extent. As LiDAR cannot detect objects smaller than the support of the laser beam (0.2-1 m) or too short to produce multiple echoes (<1 m) (Morsdorf *et al.* 2006) fine scale structures are averaged (Luscombe *et al.* 2014b) or mis-classified as ground. In addition the cost of LiDAR capture is often prohibitive, especially when a timeseries of vegetation structure is required.

Structure from Motion (SfM) techniques based on multiple images from consumer grade cameras are currently being explored as a tool to measure fine scale structure at a plot extent within the fields of geomorphology (Castillo *et al.* 2012, James and Robson 2012), archaeology (Ducke *et al.* 2011) and palaeontology (Lerma and Muir 2014) due to its rapid field data collection and minimal equipment requirements, although a computer with at least 1 GB graphics processing unit is required for processing. Despite the importance of fine scale structures in vegetation science, the use of SfM software to capture 3-dimensional data on vegetation has not been widely explored, particularly at the plot scale.

Increasingly digital cameras mounted on Unpiloted Aerial Vehicles (UAVs) are being used to examine vegetated areas (Salamí *et al.* 2014). Mostly these images have been used to map vegetation (Laliberte and Rango 2009, Knoth *et al.* 2013) but the potential to derive digital surface models (DSMs) of Antarctic moss beds (Turner *et al.* 2012, Lucieer *et al.* 2014), measure vineyard leaf area (Mathews and Jensen 2013) and derive canopy surface models (Dandois and Ellis 2010, 2013, Bendig *et al.* 2014) are being investigated. Images collected using cameras mounted on Unmanned Aerial Vehicles (UAVs) have been used with SfM software to produce digital surface models (DSMs) of Antarctic moss beds (Turner *et al.* 2012, Lucieer *et al.* 2014) and forests (Dandois and Ellis 2010, Wang *et al.* 2011), to monitor sub-decimetre coastal erosion (Harwin and

Lucieer 2012) and measure vineyard leaf area (Mathews and Jensen 2013). At an elevation of 50 m an accuracy of 0.0025-0.0040 m has been achieved (Harwin and Lucieer 2012) providing a potential means of measuring structural features at a scale between field-based observation and airborne or satellite observations. Additionally the relatively low-cost of a UAV flight makes repeat flights to monitor change a realistic possibility (Lelong *et al.* 2008).

In this study, ground and UAV-based digital images were collected to derive both plot and landscape scale DSMs as well as independent structural data with which the content and accuracy of these DSMs could be validated. It was hypothesised that plot scale digital photographs and SfM software can be used to derive quantitative structural measures of *Molinia caerulea* tussocks and that the same structural characteristics can be derived across large spatial extent using similar SfM techniques on images collected from a camera mounted on a fixed-wing UAV.

7.3.2 Vegetation Structure and Its Environment

Molinia caerulea, a tussock grass which frequently encroaches onto drained peatlands (Bunce and Barr 1988), exhibits phenotypic plasticity, with tussock morphology and distribution varying in response to environmental conditions (Rutter 1955, Taylor *et al.* 2001). Tussock structure may also provide information on vegetation community as all the species present would be expected to vary with environmental conditions. Additionally variation in tussock structure may affect the competitiveness of *M. Caerulea* altering the extent to which it dominates the ecosystem. Therefore, structural characteristics of the *M. caerulea* tussocks could potentially be used as an indicator of environmental conditions (e.g. mean water table depth), vegetation composition and photosynthesis, given the relationship with water table depths (Table 6.5). The microtope structure of a peatland is driven by changes in hydrological regime and vegetation community and drives changes in peat formation and carbon storage (Belyea and Baird 2006). As such, the ability to quantify these structures in a robust and repeatable fashion is imperative when attempting to

understand changes to water levels, vegetation composition and ultimately carbon cycling resulting from ecohydrological restoration (Lindsay 2010).

Upscaling processes such as net ecosystem exchange (NEE) across heterogeneous landscapes has typically been done by patch-based or continuous variation approaches (Shaver *et al.* 2007). The first of these determines the NEE value for a given patch then upscaled by the areal extent of the patch. The second determines a driving variable (e.g. water table depth) across the landscape from which spatially distributed values of NEE are modelled. Both these methods require spatially distributed information across the landscape which could be provided by fine scale structural measurements.

It was hypothesised that quantitative structural measures of *Molinia caerulea* tussocks (derived from plot scale digital photographs and SfM software) are related to water table depth, vegetation composition and CO_2 fluxes. It is proposed that the same structural characteristics, derived from UAV based images, can be used to estimate the spatial distribution of water table depth, vegetation composition and/or CO_2 fluxes across catchment extents and used to monitor change in vegetation structures post-restoration.

7.4 Materials and Methods

7.4.1 Study Site

A *Molinia caerulea* dominated headwater catchment (Spooners), located in Exmoor National Park in the southwest of England (51°7’21.9N, 3°44’52.9W) (Figure 7.1a & b) was selected as typical of drained upland shallow peatlands. The catchment lies between 380 and 445 metres above sea level. For a more detailed description of the study site see (chapter 0 and section 6.4).

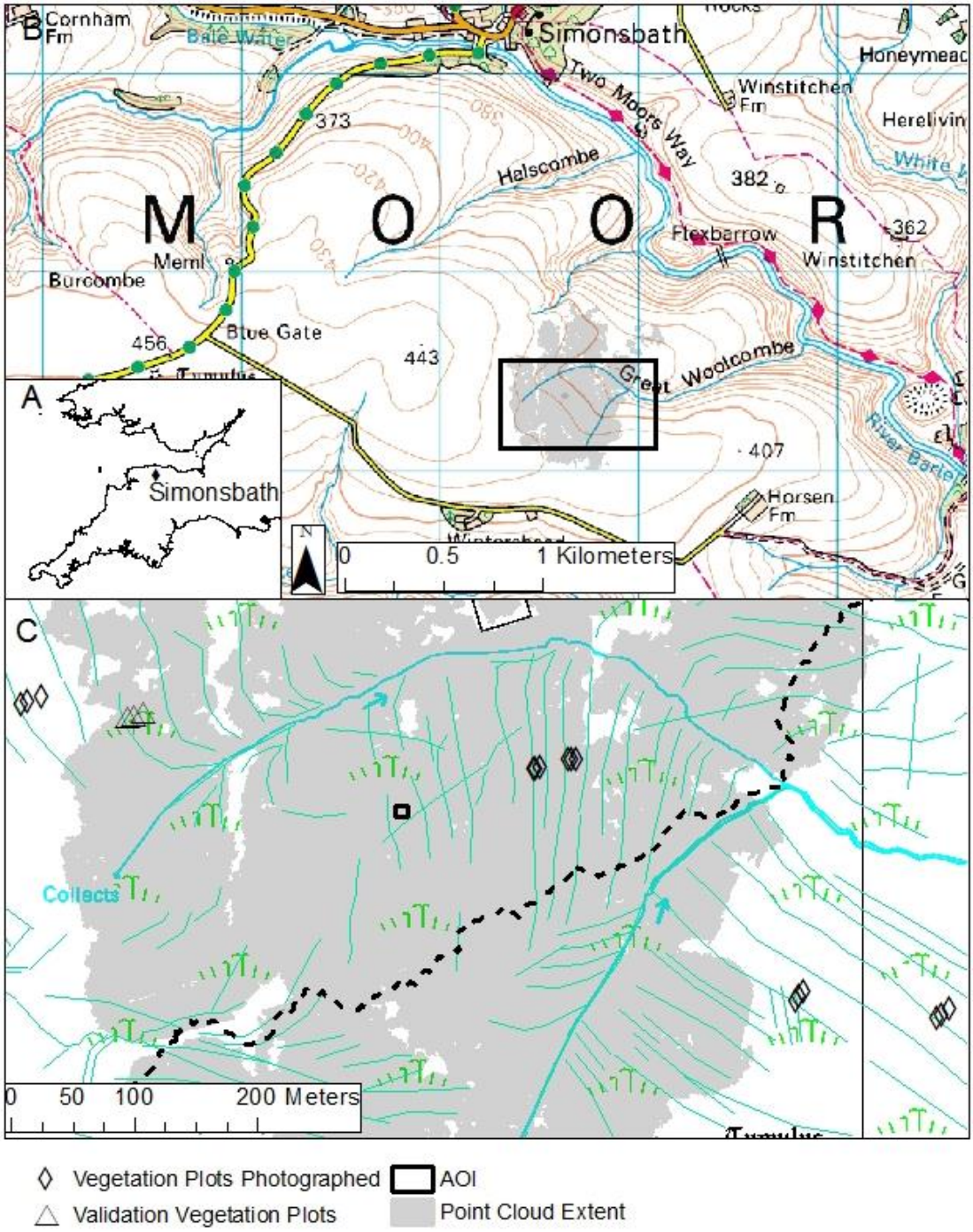

Figure 7.1 Location of Spooners study catchment (b) within the southwest of England (a). Location of vegetated plots where plots scale images were collected (diamonds), validation vegetated plots (triangles), area of interest used to compare digital surface models (DSMs) (square) and extent of point cloud (shading). (Ordnance Survey 2008a, b, e).

7.4.2 Plot Scale Image Collection

Images were taken of 15 vegetated plots (0.55 x 0.55 m) between 04/05/2012 and 25/05/2012 using a 5 megapixel Canon EOS-10D 3072 x 2048 with a 28 mm fixed lens (Figure 7.1c). Plots were named e.g. S1R2 starting with an S for Spooners, then a number based on their site (see Figure 6.1d), then either R or C depending whether the plot was restored or remained as a control during ecohydrological restoration in March 2013, the final number indicates if the plot was ⅛-distance (1), ¼-distance (2) or ½-distance (3) between adjacent ditches. Sampling days were chosen when the weather was forecast to be overcast, to minimise contrast within and between images (James and Robson 2012), with low winds speeds to minimise vegetation movement between images. Images were collected in May when the vegetation was still dormant and the leaf litter had been flattened by wind, rain and snow over the winter. This enabled the ground surface and bare tussocks, rather than the vegetation canopy, to be modelled.

SfM software identifies features or keypoints invariant to scaling and rotation present in at least three overlapping photographs from different viewpoints. It uses these keypoints to form a sparse point cloud, in an arbitrary coordinate system. To maximise keypoint identification overlap is required between images (Ducke *et al.* 2011), photographs were collected at multiple heights (e.g. standing, bent and crouching) and distances circling the plot as in Figure 7.2. Solid objects with district colours e.g. camera case were placed along each edge of the vegetated plot to increase the probability of keypoints being identified in multiple images (Figure 7.3). It was intended to collect 200 images of each plot however, technical issues with the camera meant that between 76 and 207 images were collected per plot. Data transfer between the camera and a Compact Flash card >2 GB was slow and unreliable so image collection took around 20 minutes per plot, with a newer camera this would have been quicker.

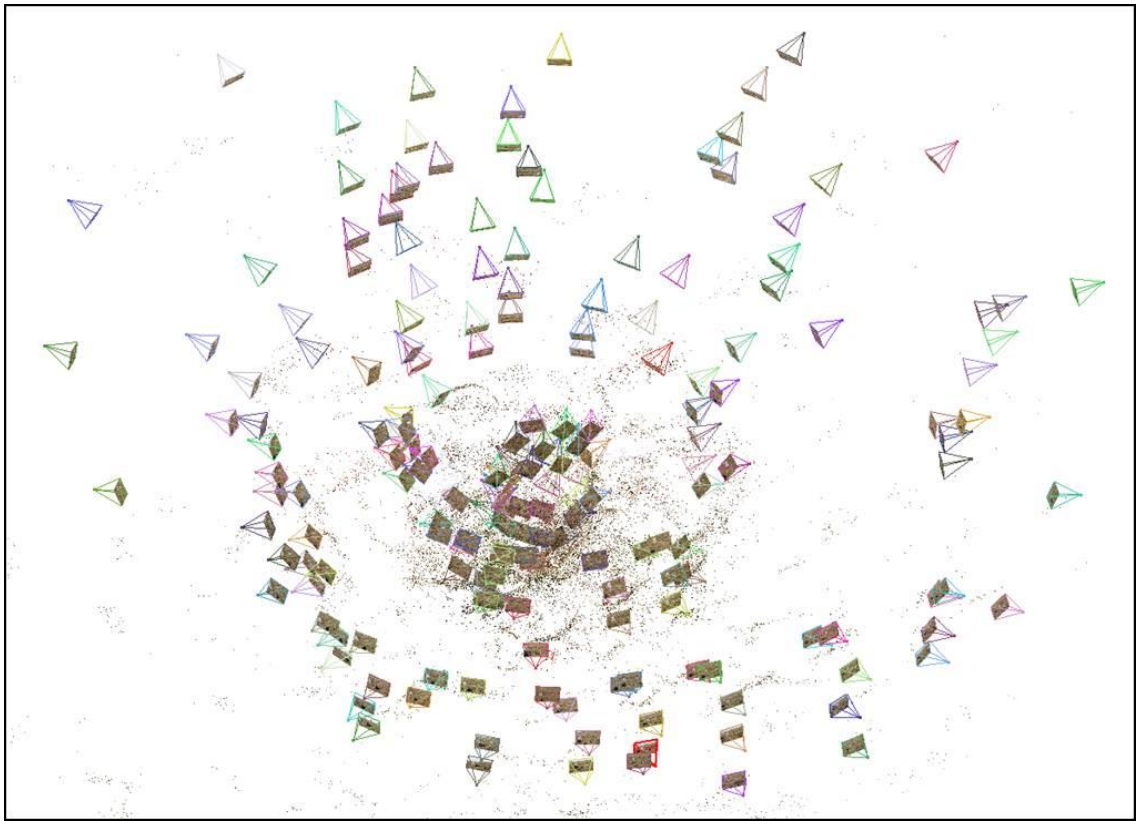

Figure 7.2 Distribution of images used by VisualSfM at S3R1 to create model (194 images used of 204 collected) demonstrating the multiple heights and distances at which photographs were taken.

Figure 7.3 Typical placement of solid static objects with distinct colours around the vegetated plot to increase the probability of keypoint identification.

Four wooden stakes surrounded each vegetated plot, the position (X, Y, Z) of the outer corner of each stake was measured using a differential GPS (Leica Viva GS08, Leica Geosystems, Heerbrugg, Switzerland). Accuracy was 0.005 m in the x and y axis and 0.02 m in the z axis.

7.4.3 Plot Scale Image Processing

Images were processed on a Dell Precision T3500 with 12 GB RAM, a 2.4 GHz Intel(R) Xenon(R) processor and a NVIDIA GTX550Ti graphics card. Georeferenced point clouds were created using the default settings in VisualSfM (Wu 2007, 2011, Wu *et al.* 2011), a freely available software (http://ccwu.me/vsfm/index.html). VisualSfM models constructed using more than 10 images were georeferenced and merged in a Geographical Information System (GIS; ArcGIS version 10.0, ESRI, California, USA). Mean elevation was determined for each point cloud clipped to the area of interest within the wooden stakes. Points greater than 3 standard deviations above or below the mean were assumed to be erroneous and excluded from the original point cloud.

Hengl (2006) proposed a range of methods to select digital surface model (DSM) grid size based on the data collected. These methods rely on even data coverage which was not the case with SfM derived point clouds. The grid size was chosen as a balance between spatial resolution and point cloud coverage. For some vegetated plots grids as fine as 0.0125 x 0.0125 m were possible, these DSMs delineated individual leaves in the leaf matter obscuring the underlying trend, additionally at this fine resolution data gaps were more prevalent. Therefore a 0.02 x 0.02 m grid resolution was chosen for the DSM which was derived from the minimum value in a 0.06 m radius circular moving window.

Where data gaps in the 0.02 x 0.02 m grid occurred within the plot (S1C2 and S2C2) the minimum value was converted to points. A surface was then interpolated between these points using ordinary spherical kriging on a 0.02 x

0.02 m grid. Data gaps in the minimum value grid were then in-filled using values from the kriged surface.

In addition to deriving a DSM for each plot, at location S3R1 DSMs were derived using a subset of 5, 10, 20, 40, 60, 80, 100, 120, 140, 160 and 180 images described in Table 7.1. The same method was used except all models which contained more than three ground control points were included irrespective of the number of images used to make the model.

As the soil surface was unknown, can be covered by the base of *M. caerulea* tussocks (Rutter 1955) and has microtopographical features often in continuity with the tussocks, the use of an *a priori* soil surface was not possible. Slope was found to vary over short distances limiting its use to delineate tussocks. Smoothing to remove this variation also removed smaller scale structural features which was undesirable.

The distribution of the elevation data within the plot was used to select a threshold between soil and tussock. The mean elevation and the elevation at which a natural break into two classes occurred (data divided into 100 discrete bins) were tested as potential thresholds. Anything at or above the elevation of the threshold was classified as tussock and anything below as soil. The area of tussock and soil were calculated for each vegetated plot. The maximum tussock height was determined as the difference between the maximum height and the threshold. The volume of tussock was calculated as the cumulative height above the threshold multiplied by the pixel size (0.02 x 0.02 m).

7.4.4 Landscape Scale Image Collection and Processing

A fixed wing QuestUAV with an un-gimballed Sony Nex-7 with 24 mm fixed lens, set to 16 mm focal length, f/3.5, auto white balance and ISO-100 was flown at approximately 100 m altitude. A total of 532 images were collected on 21/05/2014 during two flights (Figure 7.4). Each flight roughly followed a grid aiming for 60 % along track overlap and 30 % across track overlap. The two grids were at an oblique angle to each other to further increase overlap but still

enable the UAV to fly into the wind when it is more stable. Due to strong winds of >20 mph the UAV deviated from the planned flight path.

Figure 7.4 Flight paths for Unmanned Aerial Vehicle. Approximately 100 m altitude, 60 % along track overlap and 30 % across track overlap. The second flight path was at an oblique angle to the first, but still flying up-wind, to increase overlap.

All images (532) and a subset of 203 images centred on the catchment were processed following the workflow outlined above. Points more than three standard deviations away from the mean within a 3 m radius were excluded to remove outliers, assumed to be errors arising from processing. Digital surface models (DSM) were created of the soil and tussock surface using the minimum value in a 0.06, 0.15, 0.30 and 0.825 m radius to create 0.02 x 0.02, 0.05 x 0.05, 0.10 x 0.10 and 0.275 x 0.275 m grids. Data gaps were infilled by ordinary spherical kriging.

To separate fine scale microtopography from the underlying slope a 3 x 3 cell low-pass filter was applied to the DSM to create a smooth surface. This was then subtracted from the original DSM to create a detrended DSM which was able to show fine scale land surface/vegetation structure more clearly.

Semi-variogram analysis was applied to a 14 x 14 m area of the DSMs, centred on the ground validation tussocks, to enable the scale of vegetation patterning to be compared between the image and LiDAR derived DSMs. Ordinary

spherical kriging with a first order trend removal and a lag of 0.5 m, the LiDAR grid size, was selected. From this the nugget, sill and range were derived. The nugget describes error and variability in the z-direction below the sampling interval, in this case 0.5 m. The sill describes the total variability in height within the data and the range indicates the distance at which values cease to demonstrate auto-correlation, indicative of the length scale of surface structures.

Tussock heights were extracted from the UAV-image derived DSMs by finding the difference between the mean and maximum elevation for a moving 0.55 x 0.55 m window, chosen to match the plot size.

7.4.5 Ground Validation

7.4.5.1 Digital Surface Models

To assess the accuracy of the DSMs derived from UAV-based images using VisualSfM they were compared to both a DSM based on LiDAR data and ground validation data. A 0.5 x 0.5 m DSM was created from Airborne LiDAR data collected in May 2009 at a 0.5 m pixel resolution by the Environment Agency Geomatics Group (www.geomatics-group.co.uk). Data had an average systematic and random bias in elevation of 0.0004 m and 0.047 m respectively resulting in a combined root-mean-square error of 0.029 m (Luscombe *et al.* 2014b). Five cross-sections were drawn comparing the 0.05 m resolution UAV-image derived DSM and the LiDAR DSM. A raster surface was created, to visualise the difference between the two DSMs by subtracting the UAV-image derived DSM from the LiDAR DSM.

The elevation of tussock tops and inter-tussock areas were collected for an area of interest (Figure 7.1b) using a differential GPS. The elevations of these points were compared to elevations modelled by the VisualSfM and LiDAR DSMs. Correlation between the ground validated elevations and the DSMs, both VisualSfM and LiDAR, were tested using a two-tailed Pearson's correlation test for all data and the tussock tops and inter-tussock areas separately.

7.4.5.2 Quantifying Structural Characteristics

Structural characteristics (tussock height, area and volume) derived from the fourteen plot scale DSMs were compared to those measured within the area of interest using a differential GPS. Five points delineating tussock extent, roughly north, east, south, west and centre were measured for 71 tussocks. These data were used to derive average tussock height above the soil, proportional coverage of tussock and average tussock volume (assuming the tussock to be conical).

To assess if the method used to estimate tussock height at the plot scale could be extended to the landscape scale, tussock heights estimated from the landscape scale DSMs (including LiDAR) were compared (two-tailed Pearson's correlation test) to those measured using the DGPS for the 71 ground validation tussocks.

7.4.6 Linking Structural Characteristics to Environmental Conditions and CO_2 Fluxes

As tussock height has been found to vary with mean water table depth and fluctuation in water table depth (Rutter 1955) the correlation between structural characteristics of the tussocks derived at the plot scale using SfM techniques and both water table depth and the standard deviation in water table depth were tested using a two-tailed Pearson's correlation test. A two-tailed Pearson's correlation test was also carried out between structural characteristics of the tussock and vegetation composition metrics derived for the areas of interest (percentage coverage of *M. caerulea*, non-*Molinia* species and leaf litter, Shannon Diversity Index, species richness, Inverse Simpson Diversity Index and Ellenberg's Moisture Indicator Values) as the percentage coverage of *M. caerulea* was found to increase where tussocks were taller (Rutter 1955). Vegetation metrics were derived from a visual inspection of vegetation composition within the area of interest in August 2012 for more details see section 6.5.5. A two-tailed Pearson's correlation test was also carried out on photosynthesis and ecosystem respiration modelled for a PAR of

600 µmol Photons m^{-2} s^{-1}, temperature of 12 °C and greenness excess index of 60 based on empirically derived models (section 6.5.3).

To assess if relationships between structural characteristics and environmental conditions/CO_2 fluxes could be used to map environmental conditions/CO_2 fluxes, ecosystem respiration was estimated for three plots (S1R1, S1R2 and S1R3) using the relationship found between tussock height and ecosystem respiration. The estimation of ecosystem respiration derived from the landscape scale DSM was compared to that modelled for these plots based on empirically derived coefficients (section 6.5.3).

7.5 RESULTS

7.5.1 The Effect of the Number of Photographs on the Data Content of Plot Scale Point Clouds derived using SfM

SfM is increasingly being used to generate point clouds describing landscape structure at a range of scales (e.g. Westoby *et al.* 2012). It has been recognised that there is a substantial processing time requirement for SfM (Harwin and Lucieer 2012) which generally increases with the number of images input (James and Robson 2012) and the resolution of images used (Harwin and Lucieer 2012). It has been widely assumed that a greater number of images will take longer to process but ultimately produce a denser point cloud. However, very little published work has focused on the impact of using different number of photographs for deriving point clouds. It has been suggested that the process can be further refined by judicious photograph selection (to optimise overlap in more complex regions) (James and Robson 2014). Of course the number of photographs and amount of overlap required will vary from one application to another depending on the accuracy required and the complexity of the system being measured. The first part of this work shows the impact of using different numbers of photographs to drive a SfM model of a tussock. It asks, for a dormant *M. caerulea* tussock is there an optimum number of images which maximises the data content of the resultant point cloud but minimises the processing time required?

Using VisualSfM and images collected with a digital SLR it was possible to create point clouds of *M. caerulea* tussocks (Figure 7.5). It can be seen that generally the density of the point cloud increased as the number of images input increased. Some areas were better captured than others. The central hollow area shows denser points than the tussock sides. The solid wooden stakes, with their more simple texture, have denser points than the vegetation.

A digital image was used to create a point cloud model if three keypoints were identified within it. The number of images used showed a linear increase (r^2=1, $p<0.001$) with the number of images input (Table 7.1). However, the processing time required showed a quadratic increase (Figure 7.6a) with the number of images input; taking 3.1 hours to process 207 images. This indicated that optimisation may be desirable to maximise point density but minimise processing time.

The RMSE of georectification was 0.02 or 0.03 (m) regardless of the number of images input, this is likely to be because a model was included if it used at least two images with three ground control points. Therefore, all models used the same georectification method and ground control points.

The average point density showed limited increase between 100 and 160 images input (Figure 7.6b) then an increase between 160 and 180 images input perhaps indicating more images give better results. However, there was a large initial increase in both point cloud variance (Figure 7.6c) and point cloud elevation range (Figure 7.6d) between 10 and 40 images followed by a decline before levelling off beyond 120 images indicating a limited increase in information provided by those additional points for the additional number of images and processing time beyond 120 images.

Table 7.1 Description of images and number of images input in each VisualSfM run for plot S3R1 and resultant outcomes

Run Number	Images Input	Comment	Images Used	Processing time (s)	RMSE (m)	Average Point Density (points m^{-2})	Point Cloud Variance (m)	Point Cloud Elevation Range (m)	Number of cells in DSM	DSM Elevation Range (m)
1	5	N,S,E,W, Top, All standing, ~1 m	0	7	N/A	0	N/A	N/A	N/A	N/A
2	10	Run 1+ NE,SE,NW,SW, All standing, ~1 m	6	92	0.02	3355	0.0000	0.04	40	0.014
3	20	Run 2 + crouched ~1 m	16	184	0.02	605	0.0000	0.026	4	0
4	40	Run 3 + further 20 from ~1 m	36	926	0.02	212451	0.0018	0.184	626	0.144
5	40	Run 3 + N, NE, E etc. at ~2 m	27	575	0.03	10092	0.0007	0.136	345	0.131
6	60	Run 4 further 20 from ~1 m	51	1355	0.02	215398	0.0016	0.202	573	0.16
7	80	Run 7 + every 7th left	69	2141	0.02	836793	0.0015	0.215	637	0.15
8	100	Run 8 + every 6th left	85	3107	0.02	1341632	0.0016	0.225	639	0.154
9	120	Run 9 + every 5th left	105	5578	0.02	1515287	0.0013	0.204	639	0.134
10	140	Run 10 + every 4th left	131	6308	0.02	1436464	0.0014	0.206	639	0.134
11	160	Run 11 + every 3rd left	151	8195	0.02	1413388	0.0014	0.202	639	0.144
12	180	Run 12 + every other left	170	10047	0.02	2019150	0.0013	0.201	638	0.136
13	207	All images collected	194	11246	0.02	2308330	0.0014	0.205496	639	0.125

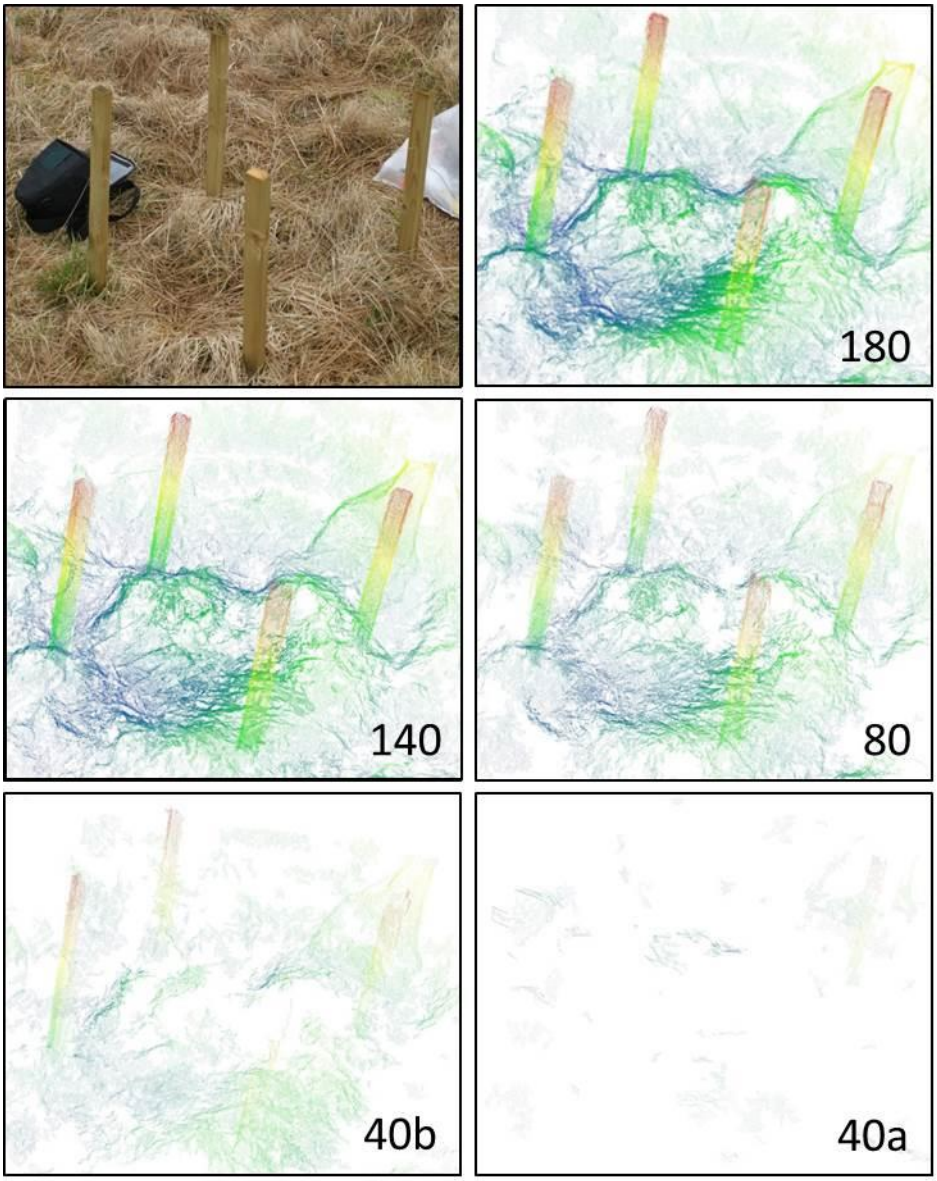

Figure 7.5 Point clouds resulting from 180, 140, 80 and 40 images input. 40a and b included the same 20 images plus a further 20 from either 1 m (40b) or 2 m distance (40a). An image taken from approximately the same view is also shown. Colours represent relative elevation. Stakes are approximately 50 cm tall.

It should also be noted that two runs (run 4 and run 5, Table 7.1) both had 40 images input but that the point cloud density and variance was different for each. Run 4 where images were all collected at a 1 m distance resulted in a denser point cloud (Figure 7.5 40b) than run 5 where 20 of the images were collected at a 2 m distance (Figure 7.5 40a). This demonstrates how the content of the images can be more important than the number of images input.

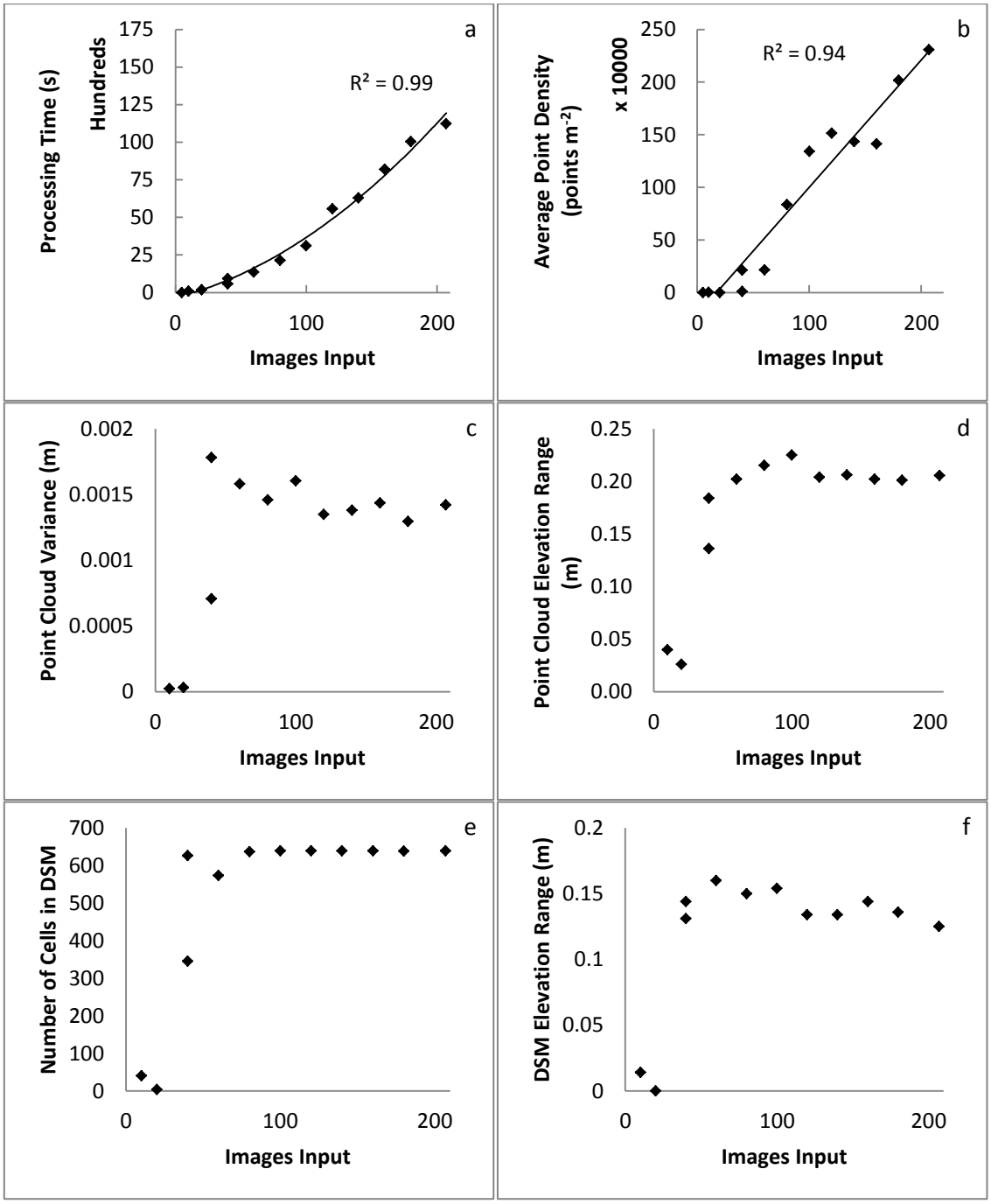

Figure 7.6 Variation in processing time (hundreds of seconds) (a), average point cloud density (thousands of points m^{-2}) (b), point cloud variance (m) (c), point cloud elevation range (m) (d), number of cells in 0.02 m resolution digital surface model (DSM) (e) and DSM elevation range (m) with number of images input to VisualSfM software for 0.55 x 0.55 m plot (S3R1).

Using these point clouds to create 0.02 m resolution DSMs indicated 80 images were required for there to be at least one point in every cell within the DSM (Figure 7.6e). The DSM elevation range showed a small decrease beyond 60 images from 0.16 m to 0.13 m for 207 images indicating a small increase in

information with every 20 extra images (Figure 7.6f). This indicates 207 images may not have been sufficient to fully capture the range in elevation within the plot however, the range in elevation observed within the point cloud stabilised beyond 120 images (Figure 7.6d).

VisualSfM made models for all fifteen plots (Figure 7.1b) based on between 14 and 194 ground based images (Table 7.2). Less than 120 images were collected at three locations (S1C1, S1C2 and S1C3) which would, from Figure 7.6c & d, be expected to overestimate point cloud elevation and variance. VisualSfM failed to produce a model that could be georeferenced at S1C3 as the images selected did not contain at least three ground control points (stakes) in two images, this location was excluded from further analysis.

Table 7.2 Images collected for each vegetated plot, number of images used to make point clouds by VisualSfM, root mean square error (RMSE) of georectified point cloud and average density of points within the area of interest. Locations shaded gravy where less than 120 images input.

Location	Images Collected	Date of Image Collection	Images Used	RMSE (m)	Average Point Density (points m^{-2})
S1C1	76	16/04/2012	31	0.04	310000
S1C2	101	16/04/2012	51	0.02	370000
S1C3	102	16/04/2012	14	N/A	0
S2C1	131	24/05/2012	43	0.01	300000
S2C2	126	24/05/2012	24	0.01	50000
S2C3	137	24/05/2012	49	0.01	530000
S2R1	137	24/05/2012	85	0.01	640000
S2R2	163	24/05/2012	115	0.02	380000
S2R3	146	24/05/2012	100	0.02	490000
S3C1	194	04/05/2012	156	0.01	1140000
S3C2	193	04/05/2012	179	0.01	1400000
S3C3	170	04/05/2012	151	0.01	2120000
S3R1	207	04/05/2012	194	0.02	2310000
S3R2	174	04/05/2012	160	0.02	3000000
S3R3	189	04/05/2012	179	0.04	1930000
Mean	148	.	102	0.02	1000000

Point clouds could be divided into two groups based on the density of points, those with >1140000 points m^{-2} and those with <640000 points m^{-2} (Table 7.2). The group of six locations with denser point clouds were all photographed on 04/05/2012 when the weather was overcast. At least 170 images were collected for each site of which at least 150 images were used to create the point cloud. At the other locations, digital images were collected when there were intermittent periods of bright sunshine, a maximum of 163 images were collected of which at most 115 images were used to derive the point cloud.

7.5.2 Plot Scale Digital Surface Models of Tussock Structure

It was hypothesised that plot scale digital photographs and SfM software can be used to derive quantitative structural measures of *Molinia caerulea.* To do this efficiently the point cloud derived for each plot (n=14) were rasterised to form digital surface models (DSMs). These DSMs were used to estimate tussock height, area and volume which were compared to ground validation data.

Plot scale digital surface models (Figure 7.7) showed both elevated tussock areas (red) and depressions (blue) in the soil surface. Two data derived thresholds for the soil surface were tested, the mean (Figure 7.7a) and natural break (Figure 7.7b). Both of these thresholds required no *a priori* knowledge of the soil surface and are based solely on the DSM.

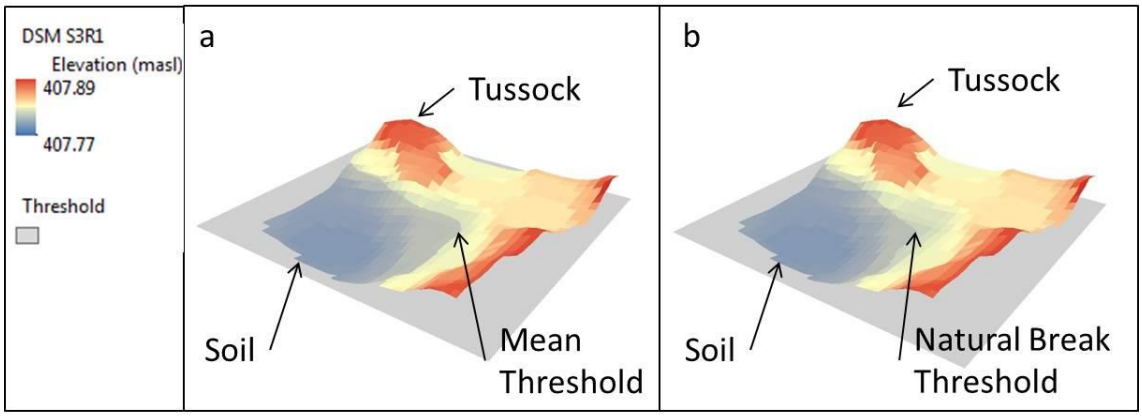

Figure 7.7 Digital Surface Models (DSM) of S3R1 created using VisualSfM showing mean (a) and natural break (b) thresholds (grey surfaces) between area classed as tussock and area classed as soil . Areal extent of plot is 0.53 x 0.59 m. DSM aligned with image in Figure 7.5.

VisualSfM derived DSMs underestimated tussock height compared to those measured (Figure 7.8a) especially when using the natural breaks threshold, although the range of tussock heights measured during ground validation was greater. Conversely the percentage area of tussock was overestimated by SfM methods (Figure 7.8b) indicating both the mean and natural break thresholds were located above the true soil surface. This resulted in an overestimation of tussock volume (Figure 7.8c) by the mean and natural breaks methods, again the range was greater in the measured (GV) tussocks.

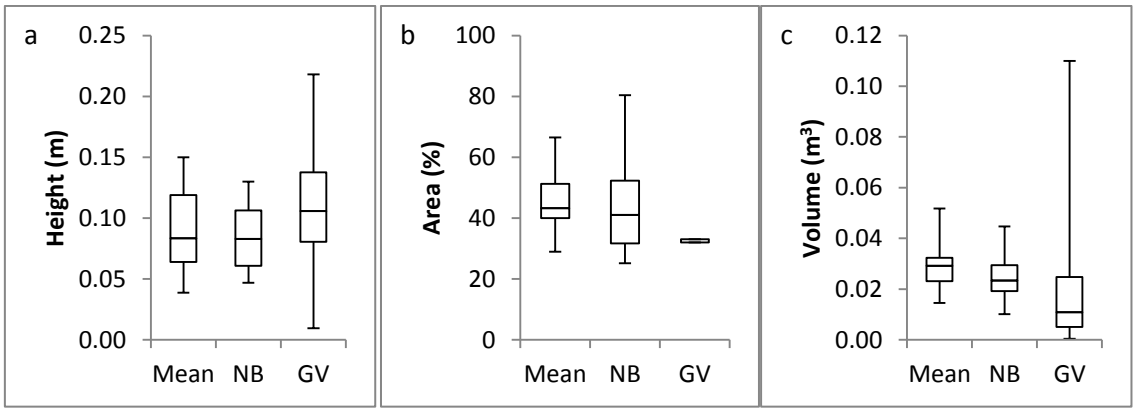

Figure 7.8 Comparison of tussock height (m), tussock area (%) and tussock volume (m^3) estimated for 14 plots using VisualSfM and the mean threshold (mean), natural breaks threshold (NB) and ground validation data (GV) measured using a DGPS (n=71). Error bars reach the maximum and minimum recorded values. The vertical box extends from the 25th to the 75th percentile with a horizontal line at the 50th percentile.

7.5.3 The Effect of Number of Photographs on the Coverage of SfM Derived Point Clouds at a Landscape Extent

UAVs are capable of capturing hundreds of images within a single flight. It seems logical that including all in focus images would maximise the area covered and the density of points. However, at a plot scale increasing the number of images dramatically increased the processing time (Figure 7.6a) but beyond a threshold little extra information was gained (Figure 7.6c & d). At a landscape scale the point cloud created from all the UAV-based images (532) (Figure 7.9a) did not have greater coverage than the point cloud created from a subset of images (Figure 7.9b). The DSM created using all the images (Figure

7.9a) focused on the areas with more defined textures, such as the field boundary and distinctive mowing pattern in the cut grass, thereby excluding the area of interest. When these images were removed to focus on the area near the centre of the catchment (Figure 7.9b) a point cloud was created for the area of interest. Linear gaps in the point cloud occurred where there was insufficient overlap in the images between flight paths.

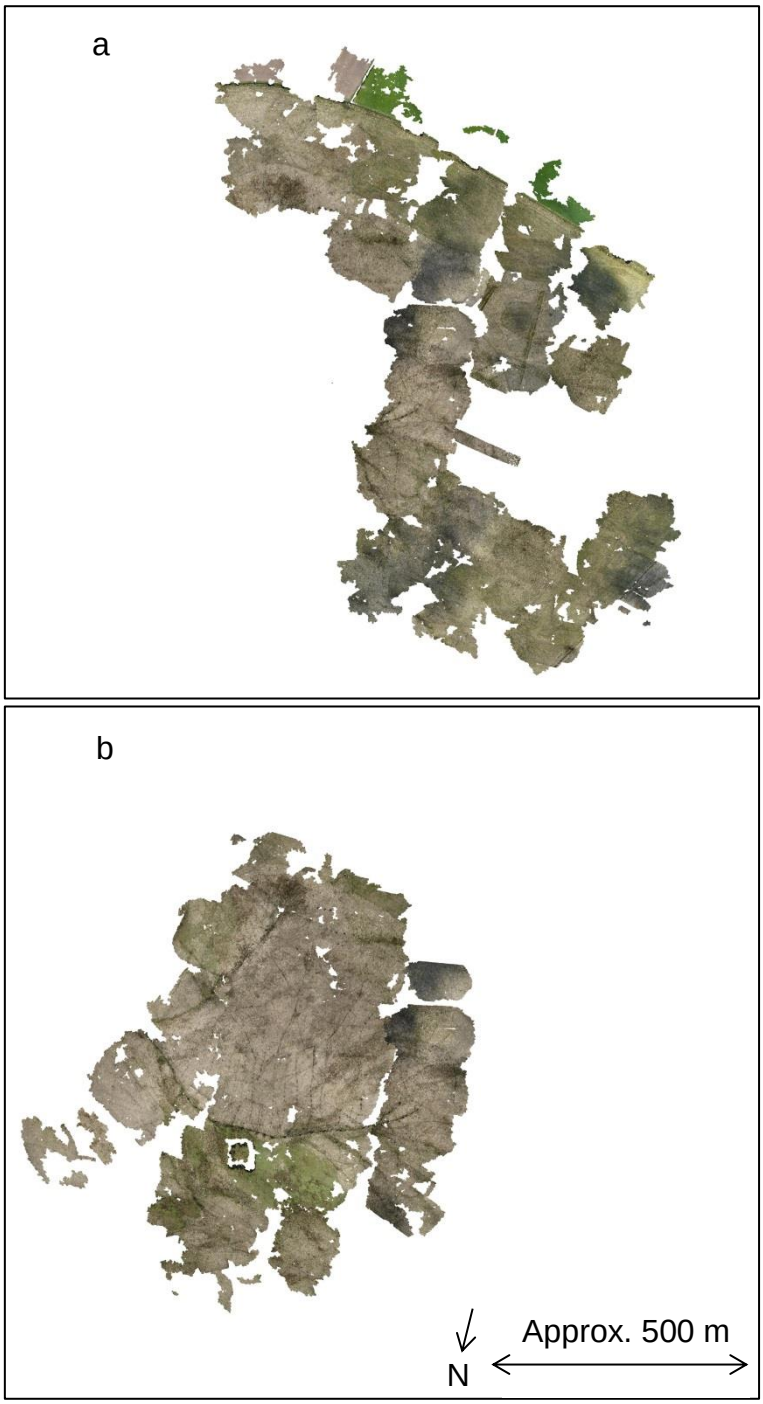

Figure 7.9 Point clouds created using VisualSfM from all images (532) (a) and a subset of 203 images focused in the centre of the catchment (b). Coloured by red, green and blue values associated with each point. Both images are in the same arbitrary scale and co-ordination prior to georectification. Approximate scale and north direction given.

7.5.4 Landscape Scale Digital Surface Models Derived from UAV Images

Data analysis using point clouds is computationally inefficient and will include unevenly spaced points from the vegetation as well as the ground, commonly raster surfaces separating ground from canopy are derived from the point cloud to facilitate further analysis. The point cloud (Figure 7.9b) derived for the central part of the catchment was rasterised using the minimum point in a circle with radius three times the resultant grid size (0.02, 0.05, 0.10 and 0.275 m). Gaps were filled by linear kriging to produce a continuous digital surface model. This demonstrates it is possible to derive digital surface models over a large extent (600 x 700 m) using digital photographs collected from a fixed wing UAV (Figure 7.10a). Using a digital surface model derived from 0.5 m resolution LiDAR the accuracy of these UAV-image derived DSMs can be assessed.

Artefacts due to kriging can be seen in the eastern side of the UAV-SfM DSM where the point cloud was sparser and more patchy. The DSM derived from these UAV-based images shows a general agreement with a DSM derived from LiDAR (Figure 7.10b) increasing in elevation away from the stream. Comparing cross-sections indicates that more surface detail is visible in the UAV-SfM DSM due to its finer resolution. Both DSMs captured similar profiles, most evident across the stream (Figure 7.11). The UAV-SfM underestimated elevation compared to LiDAR for line B, C and E (Figure 7.11b & c) and to the north of the stream for line A (Figure 7.11a) but showed good agreements with line D and to the south of the stream along line A (Figure 7.11a & d). Without the LiDAR for comparison, the UAV-SfM DSM appears to realistically capture the topography particularly over short <100 m distances. However, when the elevation differences between the LiDAR and the UAV-SfM DSM are observed over the whole catchment it can be seen that the UAV-SfM DSM domes towards the centre of the catchment (Figure 7.12) despite an oblique flight path designed to prevent this.

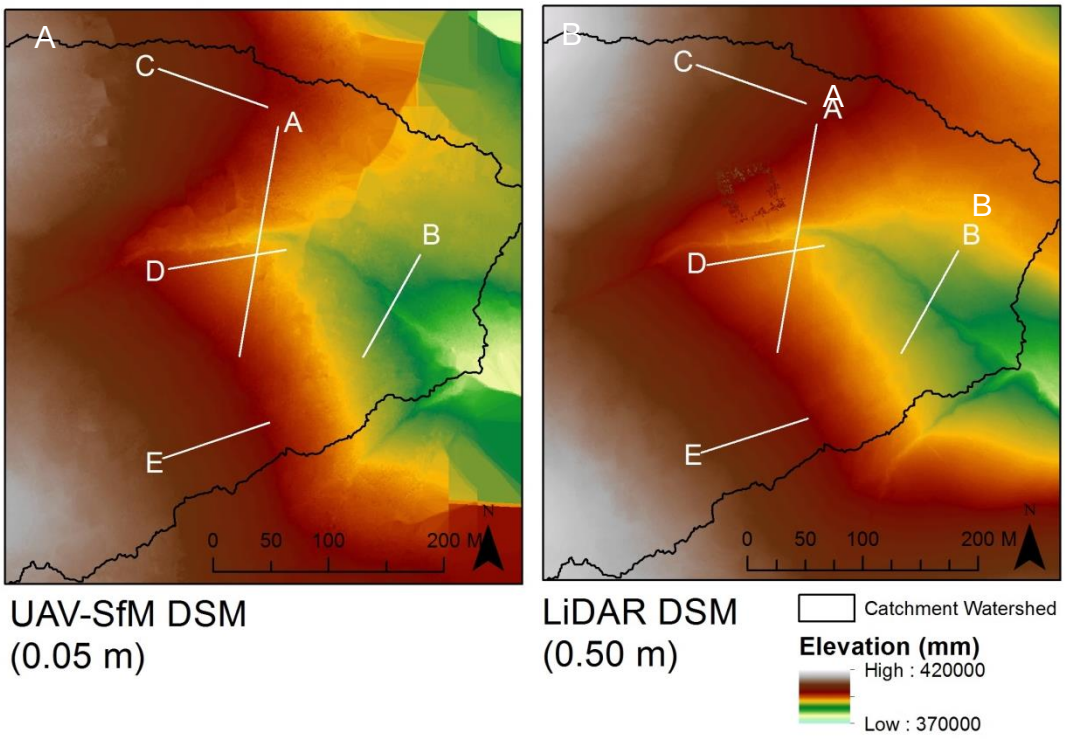

Figure 7.10 Digital Surface Models for the catchment from UAV-based images with a cell resolution of 0.05 m (a) and from a 0.5 m resolution LiDAR. Lines indicate locations of cross-sections in Figure 7.11.

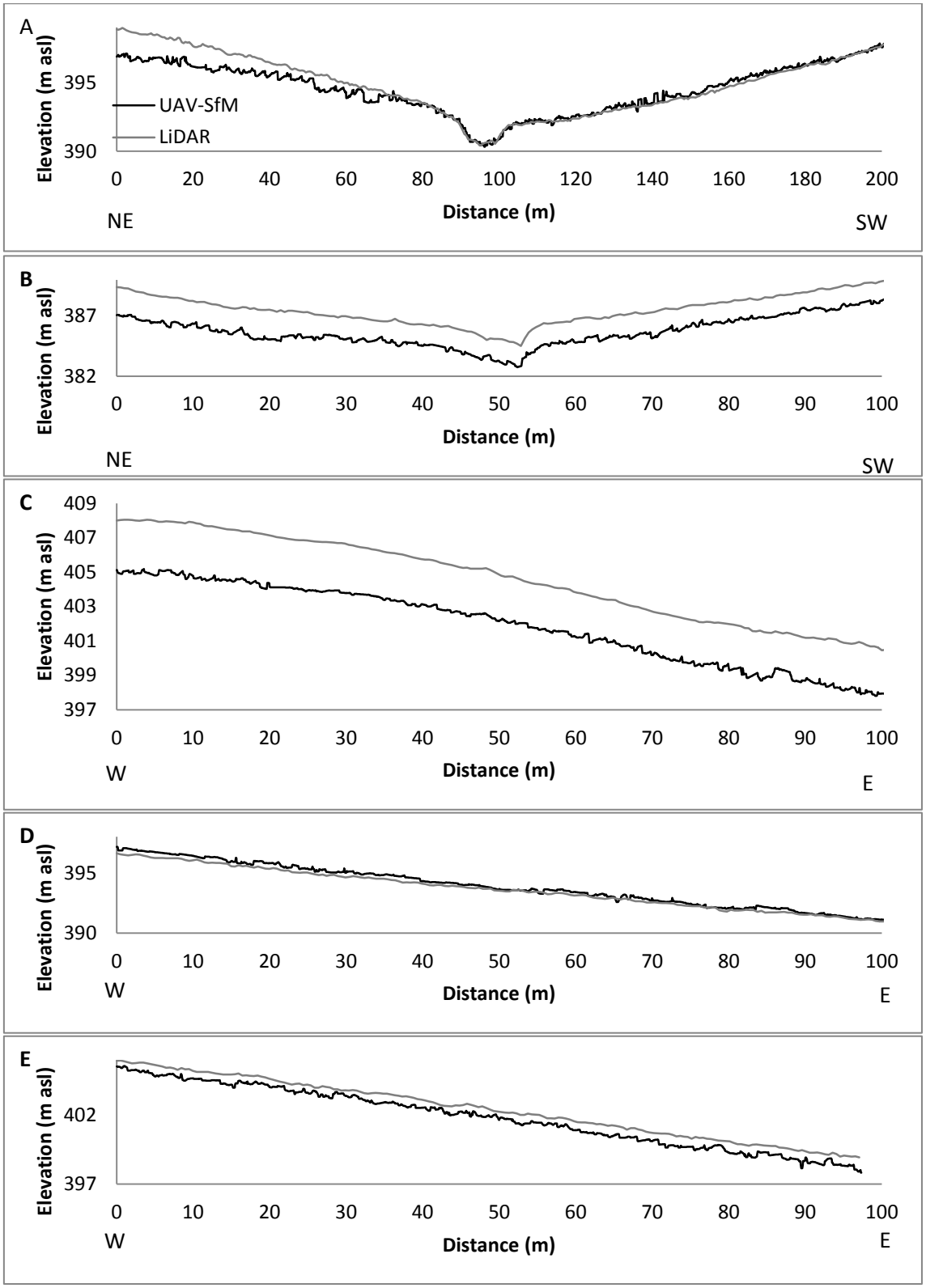

Figure 7.11 Cross-sections of elevation along lines A, B, C, D & E (Figure 7.10) for UAV-based image VisualSfM digital surface model (DSM) (0.05 m resolution) and LiDAR DSM (0.5 m resolution). Note Line A is 200 m long whilst the others are 100 m long. Vertically exaggerated.

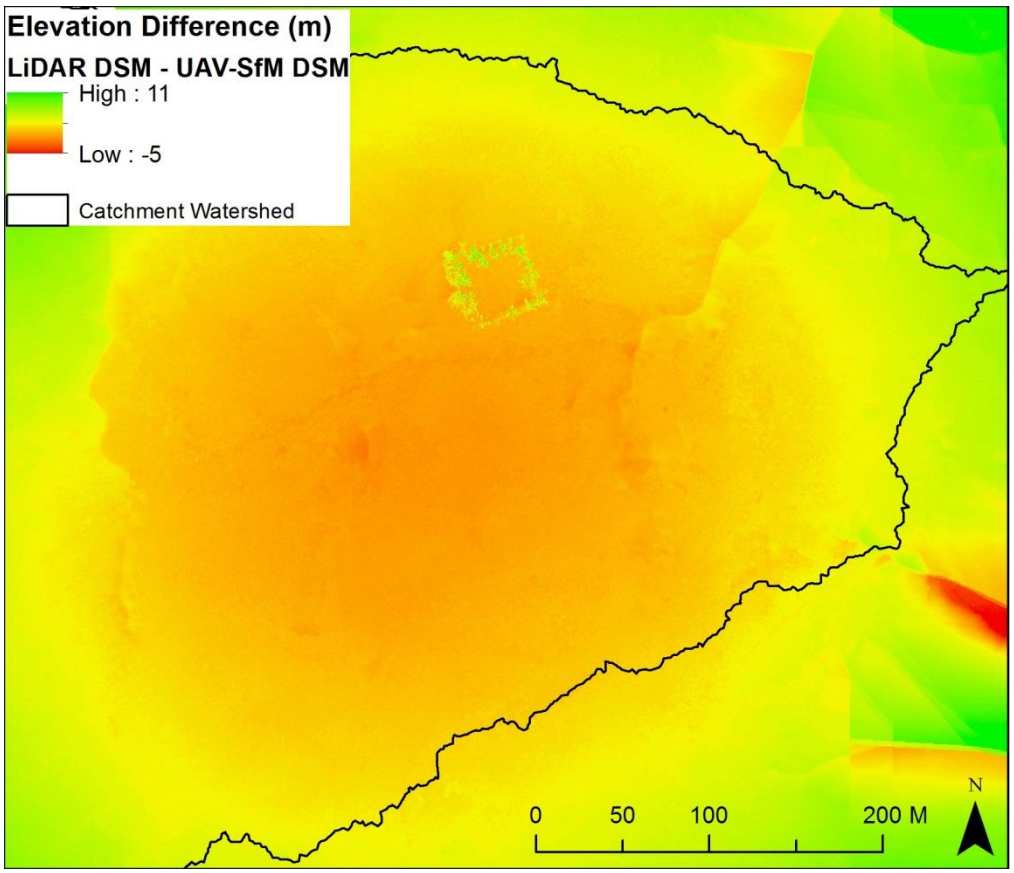

Figure 7.12 Difference in elevation (m) between LiDAR digital surface model (DSM) and UAV-based image VisualSfM DSM. The elevation of the LiDAR is greater than the UAV-SfM DSM in the green areas and lower in the red areas.

Georectification of the UAV-SfM point cloud had a RMSE of 0.12 m and mean absolute error of 0.13 m, reported by VisualSfM software. However, comparison between DGPS measured elevations within an area of interest and modelled elevation by the DSMs indicate between 0.17 and 0.30 m root mean square error in the z-axis (Table 7.3) for the UAV-SfM DSMs compared to 0.07 m for the LiDAR DSM.

LiDAR underestimated the elevation of all but five tussock tops (Figure 7.13). The UAV image derived DSMs all overestimated both the inter tussock areas and the tussock tops with the exception of two tussock tops in the 0.10 m grid and nine tussock tops in the 0.275 m grid. The smaller resolution grid size showed the greatest overestimation (Figure 7.13) and therefore the smaller grid size DSMs had the larger RMSEs (Table 7.3). Errors were greater when

estimating the elevation of inter tussock areas than the tussocks for all the UAV-SfM derived DSMs (Table 7.3) as the inter tussock areas displayed greater overestimation (Figure 7.13). RMSE was less for the inter tussock areas (0.06 m) than the tussock tops (0.011 m) for the LiDAR DSM.

Table 7.3 Root mean squared errors (RMSE), Pearson Correlation Coefficients and significance (p) between elevation (meters above sea level) measured using a DGPS and modelled using 0.5 m resolution LiDAR data, 0.02, 0.05, 0.10 and 0.275 m resolution DSMs derived from digital images using VisualSfM. A total of 71 tussock tops and 284 inter tussock locations were measured.

DSM Cell Resolution (m)		All			Tussock Tops			Inter Tussocks		
		RMSE (m)	r	p	RMSE (m)	r	p	RMSE (m)	r	p
UAV – SfM	0.02	0.30	0.64	0.000	0.22	0.71	0.000	0.32	0.69	0.000
	0.05	0.27	0.64	0.000	0.18	0.73	0.000	0.29	0.70	0.000
	0.10	0.23	0.23	0.000	0.14	0.77	0.000	0.25	0.79	0.000
	0.275	0.17	0.17	0.000	0.09	0.82	0.000	0.19	0.87	0.000
LiDAR	0.50	0.07	0.75	0.000	0.11	0.80	0.000	0.06	0.84	0.000

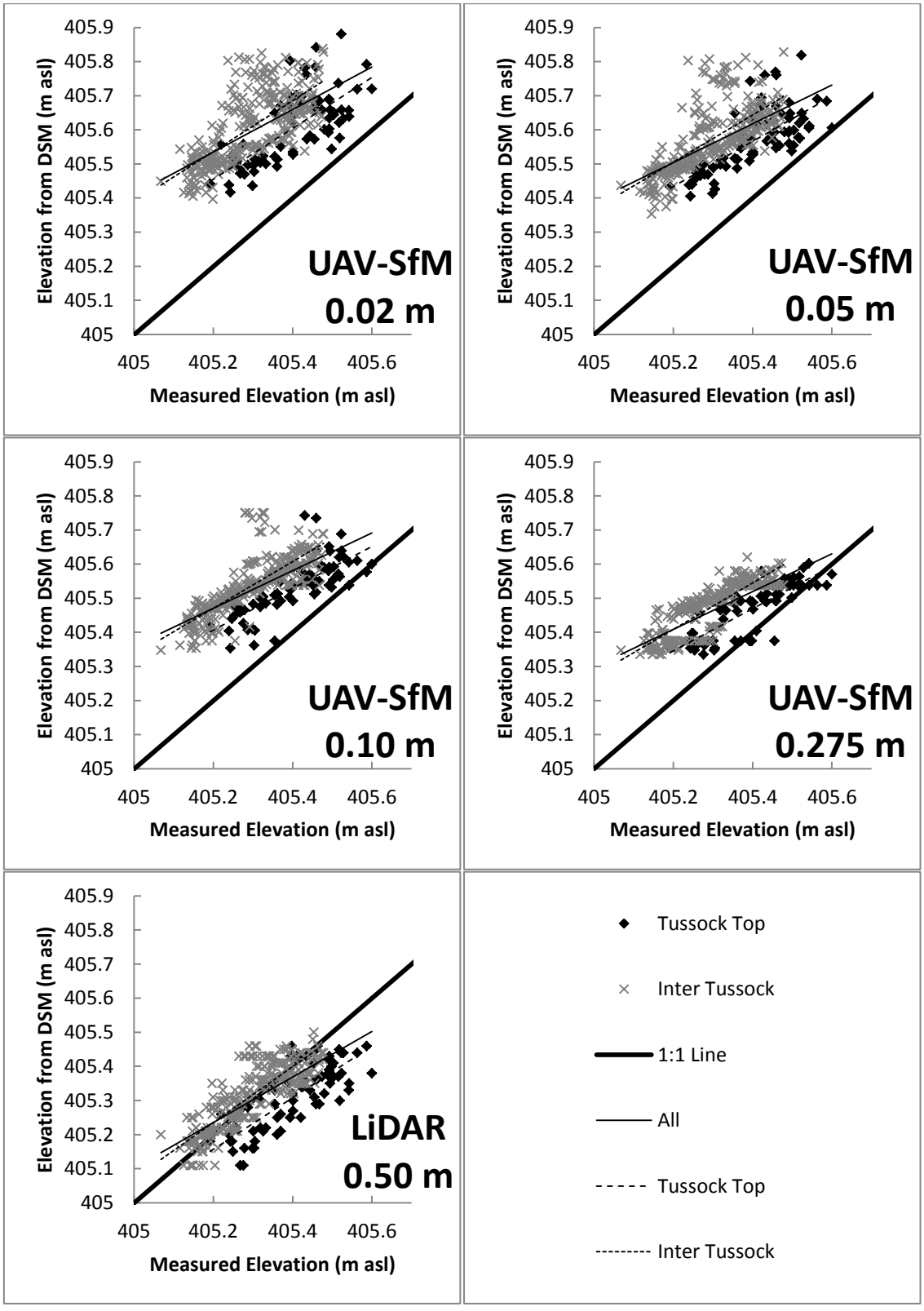

Figure 7.13 Relationship between tussock (black diamond) and inter tussock (grey cross) elevations (meters above sea level) as measured using DGPS and estimated from the digital surface models (DSMs) derived using LiDAR and digital images from a UAV at a range of grid sizes.

LiDAR showed the strongest correlation ($r=0.75$, $p<0.001$) with all the elevation data whilst 0.275 m resolution UAV-SfM derived DSM showed the strongest correlation with tussock tops and inter tussocks when assessed separately ($r=0.82$ and 0.87 $p<0.001$ respectively). For all grid sizes the UAV-SfM DSMs overestimated elevation with greater overestimation for the lower elevations and by the smaller resolution DSMs. The Pearson's correlation coefficient decreased as the grid size decreased (Table 7.3) to a minimum of 0.40 ($p<0.001$) for tussock tops by a 0.02 m grid size. Related to the increase in scatter observed within the estimated-measured elevation graph as the grid size decreased (Figure 7.13) due to a greater range of estimated elevations, 0.48 m for the 0.002 m DSM compared to 0.29 m for the 0.275 m UAV-SfM DSM. The LiDAR DSM and the larger resolution UAV-SfM derived DSMs (0.10 and 0.275 m) showed stronger correlations with measured elevation for the inter tussock areas compare to the tussock tops (Table 7.3). Conversely the smaller resolution UAV-SfM derived DSMs (0.02 and 0.05 m) showed stronger correlations with the tussock tops.

7.5.5 Structural Characteristics at a Landscape Extent Derived from UAV-Based Images

It was hypothesised that structural characteristics (tussock height, area and volume) can be derived across large spatial extents using SfM techniques on images collected from a camera mounted on a fixed-wing UAV. This hypothesis was tested using the DSMs at 0.02, 0.05, 0.10 and 0.27 m resolutions (e.g. Figure 7.10) derived for the area of interest where the ground validation measurements were collected.

Comparing tussock heights measured using the GPS to tussock height derived from the UAV images (Table 7.4) it can be seen that the VisualSfM method had a tendency to underestimate tussock height similar to at the plot scale (Figure 7.8a). The mean tussock height and standard deviation increased as the grid resolution decreased (Table 7.4) to a grid size of 0.05 m which still underestimated 45 % of tussocks. Even for the 0.05 m DSM, RMSE was over half the mean tussock height indicating comparatively large errors in tussock

height estimation. However, the mean tussock height estimated for the area of interest using the 0.05 m DSM (0.11 ± 0.06 m) was comparable to the average measured (0.11 ± 0.04 m) even though accuracy associated with the estimation of individual tussock heights was poor. Pearson's Correlation tests indicated there was a significant correlation between estimated and measured tussock heights for the 0.05 m DSM (r=0.268, p=0.024). For the other grid sizes the relationship was not significant as both over and underestimations occurred across the range of measured tussock heights.

Table 7.4 Comparison between mean tussock height (m), standard deviation from mean (Stdev) (m) and root mean square error (RMSE) between tussock heights derived from UAV digital images at 0.02, 0.05, 0.1 and 0.275 m grid resolution and measured tussock heights. Percentage of tussocks where the height was overestimated, Pearson's Correlation coefficient and significance (p). n=71.

		Average Tussock Height (m)	Stdev (m)	Tussocks Overestimated (%)	RMSE (m)	Pearson's Correlation	p
Validation Data		0.11	0.04				
DSM resolution (m)	0.02	0.09	0.05	39	0.07	0.075	0.536
	0.05	0.11	0.06	45	0.06	0.268	0.024
	0.1	0.05	0.04	14	0.09	-0.003	0.979
	0.275	0.01	0.02	1	0.11	-0.065	0.592

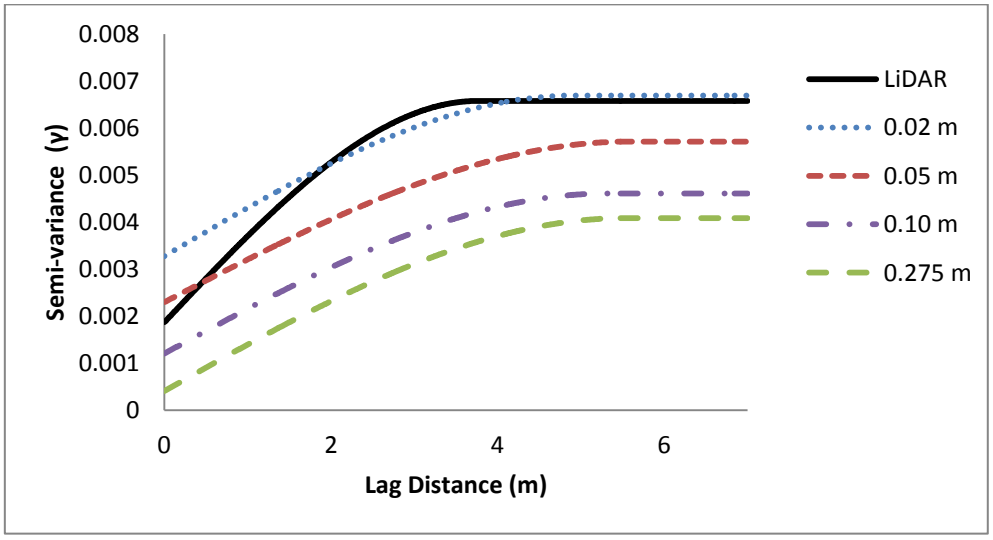

Figure 7.14 Semi-variograms of UAV image and LiDAR derived digital surface models for a 14 x 14 m area of interest.

The semi-variogram analysis indicates the error and fine scale variability (less than 0.5 m across) was greatest (0.003) for the 0.02 m DSM, indicated by the greater intercept on the y-axis (Figure 7.14). The total variation in height (semi-variance value at 7 m) was similar for the 0.02 m DSM and the LiDAR (0.006). The spread of estimated elevations for the tussock tops and inter-tussock areas (Figure 7.13) were greater for the LiDAR and 0.02 m UAV-DSM. The total variation in height and the nugget (y- axis intercept) (Figure 7.14) as well as the range of estimated elevations (Figure 7.13) decreased as UAV-SfM DSM cell resolution increased.

The horizontal length scale of spatial features (indicated by the distance at which the curve flattened) was less for the LiDAR (3.8 m) than for 0.02 m DSM (4.9 m). This indicates for the UAV derived DSMs the distance over which patterns are auto-correlated was greater than for the LiDAR.

7.5.6 Relationship Between Vegetation Structure and Environmental Conditions

It was hypothesised that if there were significant relationships between structural characteristics of *Molinia caerulea* and environmental conditions (e.g. water table depth) both measured at a plot scale; and those same structural characteristics could be measured across a landscape extent; then these relationships could be used to derive spatially distributed estimates of the environmental conditions across a landscape extent.

Firstly, relationships between structural characteristics and environmental conditions, vegetation composition and CO_2 fluxes at a plot scale were tested. There were significant correlations between tussock height ($r=0.67$ $p=0.009$ mean threshold; $r=0.60$ $p=0.024$ natural break threshold) and area ($r=-0.55$ $p=0.041$ mean threshold; $r=-0.66$ $p=0.011$ natural break threshold) and ecosystem respiration the strongest correlation occurred with tussock height derived using the mean threshold. Ecosystem respiration was greater where tussock height was greater (Figure 7.15g) and tussock area smaller (not shown). Figure 7.15g indicates that where *M. caerulea* does not form tussocks

(height of 0 cm), the ecosystem respiration falls to between 9 and 10 µgC m^{-2} s^{-1}). The strongest but non-significant correlation (r=0.51, p=0.062) occurred between mean water table depth and tussock volume using the natural break threshold (Figure 7.15a). Tussocks were taller where the water table was deeper. The y-axis intercept suggests there would be no tussocks if the mean depth to water table was 5.7 cm. Using the natural breaks threshold species richness (r=-0.54, p=0.044) showed a correlation with tussock height. Where tussocks were taller species richness was lower (Figure 7.15b).

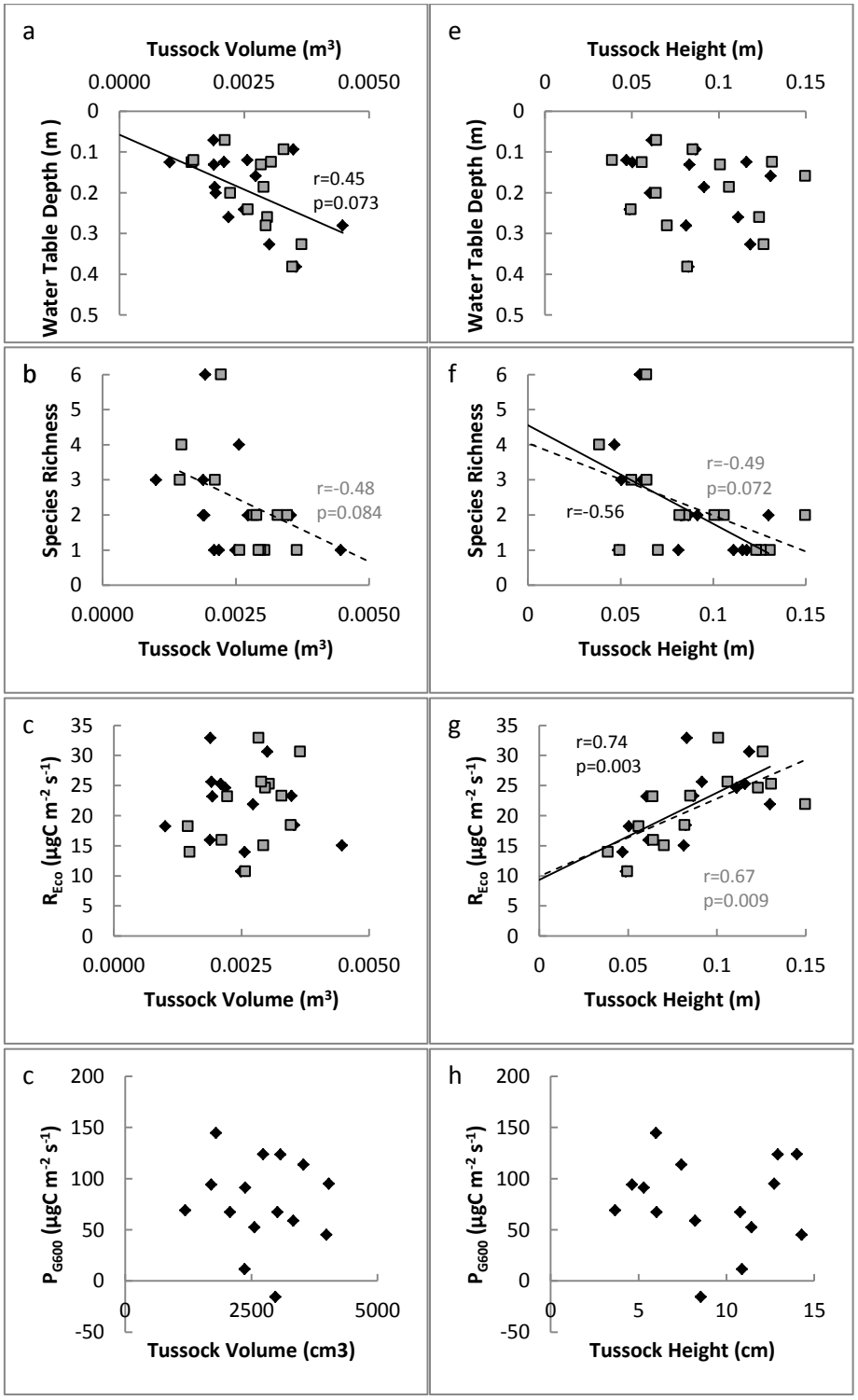

Figure 7.15 Variation in water table depth (m below ground surface) (a and e), species richness (b and f), ecosystem respiration (R_{Eco}) (µgC m^{-2} s^{-1}) (c and g) and photosynthesis (P_{G600}) (µgC m^{-2} s^{-1}) (d and h) with tussock volume (m^3) (a, b, c and d) and maximum tussock height (m). R_{Eco} and P_{G600} derived from an empirical model) at a temperature of 12 °C, GEI of 60 and PAR of 600 (see section 6.5) based on flux chamber measurements. Tussock height and volume were derived using VisualSfM and the mean threshold (grey squares and dashed lines) and natural break threshold (black diamonds and solid lines). Pearson correlation coefficient (r) and significance (p) values are shown.

Table 7.5 Comparison between ecosystem respiration (µgC m^{-2} s^{-1}) estimated from tussock heights derived from UAV digital images at 0.02, 0.05, 0.10 and 0.275 m grid resolution and validation data modelled for a temperature of 12 °C based on empirically derived parameters. RMSE is the root mean square error.

		Ecosystem Respiration (µgC m^{-2} s^{-1})			
Plot		**S1R1**	**S1R2**	**S1R3**	**RMSE**
Validation Data		33.5	11.7	29.6	
DSM grid resolution (m)	**0.02**	18.0	17.0	21.5	10.6
	0.05	17.0	19.0	23.9	10.9
	0.10	11.5	17.3	17.3	14.9
	0.275	12.6	9.9	9.9	16.6

Secondly having determined structural characteristics (including tussock height) from DSMs (Table 7.4), derived using SfM and UAV-based images (Figure 7.10), using the relationship between tussock height and ecosystem respiration (Figure 7.15g) an estimation of the spatial distribution of ecosystem respiration at a landscape extent was made. It can be seen that the range of ecosystem respiration values estimated from tussock height was smaller than the range of the validation data (Table 7.5). RMSE decreased as the grid resolution decreased and predicted tussock height increased. Errors were larger for 0.10 and 0.275 m grid resolution than the flux from S1R2.

7.6 DISCUSSION

7.6.1 Plot Scale Digital Surface Models Derived using Ground Based images and SfM

SfM techniques enabled the creation of plot scale point clouds (Figure 7.5) and DSMs (Figure 7.7) of dormant *Molinia caerulea* in a remote field site using only a consumer grade digital camera. From these it was possible to derive repeatable quantitative estimates of tussock height, area and cumulative volume for a 0.55 x 0.55 m plot (Figure 7.8) with no prior knowledge of the ground surface. This demonstrates this methods potential for extending its use beyond geomorphology (Castillo *et al.* 2012, Westoby *et al.* 2012) to use in monitoring plot scale changes to vegetation structures.

Other studies have found that the similar colouration of vegetation and inconsistent geometries has led to point clouds of vegetation that are more random and less uniform in spatial coverage (Dandois and Ellis 2010, Mathews and Jensen 2013) compared to other surfaces. Despite plots containing only vegetation, point cloud spatial coverage was sufficient in all but two locations (S1C1 and S2C2) to produce a 0.02 x 0.02 m DSM. The main control on the quality of DSMs produced was the prevailing conditions during image collection and the number of images collected. Where all images were collected under bright diffuse light, more images were used in the model and denser point clouds with better coverage were created (Table 7.2). Sparse, patchy point clouds were created when: a) insufficient images were collected and/or b) some of the images were collected in bright sunshine resulting in deep shadows with little texture and varying appearance with viewing direction (James and Robson 2012). When this occurred generally the images from bright sunshine were not selected by the software. As images were collected circulating the plot (Figure 7.2), this meant the distribution of images used in the model was restricted to one side of the plot resulting in increased occlusion. Generally point cloud density was lowest within hollows as these were often obscured in images by surrounding tussocks or leaf litter. These also had a tendency to deeper shade reducing feature differentiation (James and Robson 2012).

The number of images collected was also an important factor, generally denser point clouds were created where more images were collected. As keypoints must be present in at least three images, where there were more images there was more chance of a keypoint being identified. However, indiscriminately increasing the number of images collected dramatically increases the processing time and graphics card memory required (Figure 7.6a) but does not always increase the information content (Figure 7.6c ,d e & f). Increasing the number of images increases the number of keypoints identified and hence the size of intermediate results stored in the Graphics Processing Unit (GPU). It also increases the processing time as all previously identified keypoints are compared to each new image. However, much of the workflow required little

manual intervention so provided the GPU was sufficiently large (in this case 1 GB) this would have minimal impact.

The distance at which images were collected also influenced the resulting point cloud. Images collected further away from the plot were more likely to have captured distinct features, e.g. rucksack, wooden stakes, but at greater distance the pixel resolution and therefore accuracy was lower. Close ups of the plot, when included, greatly improved detail captured within the plot but were less likely to be included as the texture of the vegetation surface appears different close up, where individual leaves are resolved, compared to further away making the identification of keypoints difficult (James and Robson 2012). This may explain why run 5 (Figure 7.5 40 a) with 20 images from approximately 1 m and 20 images from approximately 2 m created a sparser point cloud than run 4 with all images from approximately 1 m. The difference in texture at the greater distance meant fewer keypoints were identified and therefore fewer images were used (27 compared to 36, Table 7.1). Where possible a range of distances should be used to provide a nested approach where features can be recognised in the scale above and below, linking the large and small scale textures. This would enable both fine details to be resolved but also include features required for georeferencing.

Georeferencing errors (0.008 to 0.038) were greater than measurement uncertainty reported for other plot scale methods, roller chain (0.005 m), pin-meter (0.002 m) and laser scanner (0.001 m) (Jester and Klik 2005) but the time required in the field was less than these methods (25 to 90 minutes).

7.6.2 Plot Scale Structural Characteristics Derived using SfM

Estimated tussock heights from the plot scale DSMs were shorter than those measured (Figure 7.8) and at the low end of the range previously reported 0.08-0.25 m (Jefferies 1915). When measuring tussock height the leaf litter was cleared away to help identify individual tussocks so heights measured were from the peat surface to the tussock top. It is unlikely that the dense leaf litter (Mathews and Jensen 2013) was penetrated by the camera, a passive sensor,

resulting in an underestimate of tussock height. Additionally as tussock area was overestimated and tussock height underestimated (Figure 7.8) it is likely that both of the data derived thresholds used were above the true soil surface. These thresholds were selected as they did not require prior knowledge of the elevation of the peat surface and could be derived from the DSM enabling the method to be extended to unknown areas. Ultimately this study aimed to link tussock structural characteristics to environmental variables, therefore the accuracy of tussock heights was less important than the ability to use the same soil-tussock threshold in both methods (ground-based and UAV-based). If estimating tussock height is the main aim then additional work is required to find a more appropriate threshold method to identify the soil surface.

Tussock height was the most sensitive to the threshold elevation and the distribution of tussocks within the plot. If the plot did not contain both tussock top and inter tussock area then difference between the maximum and threshold elevation would have been reduced, limiting the estimation of tussock height. To minimise this effect a moving window was used when determining tussock height from the UAV image derived DSM.

7.6.3 Landscape Extent Digital Surface Models Derived using UAV-based images and SfM

Again the quality of the resultant DSM was strongly dependent on the images collected. It can be seen that adding more images did not result in a better DSM for the area of interest (Figure 7.9). The number of keypoints that are used in feature matching between images is by default limited to 8192 (2^{13}) with features sorted by scale (Wu 2011). Therefore including images with larger scale features (e.g. field boundaries) prioritised these features over smaller ones. Images not containing the large scale features and therefore the prioritised keypoints, were not used to create the point cloud model. In this current study this resulted in images not containing field boundary, mining spoil or mowing patterns being excluded. The result of this was that all images for the area of interest were excluded from the model. By manually selecting images which did not include field boundaries or mowing patterns the features

used for feature matching were different, smaller scale features, present in the area of interest. When deriving a DSM for a large extent it may be better to create multiple point clouds of smaller areas with finer scale features and then mosaic these to obtain the coverage required.

DSMs created from digital images are more robust where overlap between images is greater (James and Robson 2014) however, wind direction restricted the amount of overlap possible between images as ideally a fixed wing UAV should fly into or with the wind. Additionally during the flight unexpected strong winds at altitude blew the UAV off course reducing the across track overlap (Figure 7.4). Gaps in the point cloud can be seen where overlap was insufficient (Figure 7.9b). Overlap could potentially have been increased by banking the aircraft to get oblique views as in Mathews and Jensen (2013) or by flying a gently curved overpass (James and Robson 2014), however, limited battery power prevented this. Mathews and Jensen (2013) deployed brightly coloured targets across the whole area to aid keypoint recognition, this may have improved keypoint identification and reduced processing time in a texturally monotonous landscape.

There is a pay off when selecting flight altitude; lower altitudes enable finer pixel resolution but greater ground speeds result in image blurring (Frankenberger *et al.* 2008). Another compromise occurred between extent covered and density of images possible, dependent on battery life and camera memory. The entire catchment (1100 m x 600 m) was flown as part of a wider study into the effects of ecological restoration on peatlands. This tested the ability of fixed-wing UAV derived images to produce a DSM at a catchment extent but as a result image density was lower than ideal and there were gaps between flight lines (Figure 7.9b). Limited battery prevented additional flights. The area of interest chosen for validation was near centre of the catchment where point density was greater, it can be seen that coverage becomes patchy towards the edge of the point cloud (Figure 7.9b). Due to the difficulties in getting sufficient overlap with a fixed-wing UAV, a rotor-wing UAV would be more appropriate where the

required resolution and spatial coverage are smaller (Anderson and Gaston 2013).

Comparing the landscape scale DSM derived using LiDAR and UAV based images (Figure 7.10) it can be seen that the both capture the fine scale topography of the catchment (Figure 7.11). Without the LiDAR for comparison the UAV-SfM DSM would appear realistic and could be used in error for example, to assess the slope, aspect and shaded relief as well as delineate flow paths and watershed boundaries (Jenson 1991), delineate the extent of erosion (Kincey and Challis 2010) or model parameters such as the topographic wetness index (Beven and Kirkby 1979). These would more than likely produce apparently accurate and realistic results. However, the UAV-SfM DSM is distorted compared to the LiDAR DSM (Figure 7.12), overestimating elevation towards the centre of the catchment and underestimating elevation at the edges. This is indicative of radial distortion resulting from insufficient non-parallel images causing a doming towards the centre of the point cloud, georectification would have scaled and oriented the model but not corrected for this distortion (James and Robson 2014). It had been hoped given the oblique flight path designed to prevent doming and the windy conditions resulting in pitch and roll, this would provide the necessary number of oblique images to prevent radial distortion. Keypoints present in two or more radially distorted parallel images converge short of the true distance to an object leading to an overestimation of elevation and therefore doming. If these images were at an oblique angle to one another, changes in the geometry of light passing through a lens mean the depth at which the keypoints converge would be accurate after corrections for the change in angle have been applied. This demonstrates both the need to include more oblique angles in the flight path at the planning stage and the requirement to cross-validate UAV-SfM DSMs created over large extents.

Within a limited area of interest it was expected that all the DSMs would underestimate tussock tops and overestimate inter-tussock areas resulting in a smoothing of the landscape (Luscombe *et al.* 2014b) with greater smoothing as

the grid size increased. It can be seen that the LiDAR DSM underestimated tussock tops and overestimated inter tussock areas but that image derived DSMs all overestimated both the inter tussock areas and the tussock tops (Table 7.3, Figure 7.13). Overestimation was greatest for the inter tussock areas particularly when the grid size was smaller. This may be because the camera, a passive sensor, did not penetrate the dense leaf litter between tussocks (Mathews and Jensen 2013), with the smaller grid resolution less likely to contain a point in the leaf litter resulting in greater overestimation. This may also explain why there was greater overestimation of lower elevation points (Figure 7.13). As both the inter tussocks and tussocks were overestimated it indicates a potential problem with georeferencing as in the UAV-SfM DSM (Figure 7.11).

VisualSfM software reported a georectification RMSE of 0.12 m for the point cloud, however, a root mean square error for accuracy in the z-axis of between 0.17 and 0.30 m (Table 7.3) occurred between the ground control points and DSMs and 0.07 m between the LiDAR and DSMs. This was less accurate than Mathews and Jensen (2013) who obtained a mean estimated error of 0.1083 m from a fixed-wing UAV flying at 100 to 200 m and Lucieer *et al.* (2014) who reported a RMSE of 0.042 m from a rotor-wing UAV at 50 m elevation. It was more accurate than Dandois and Ellis (2010) who used aerial photographs with 0.6 m horizontal accuracy to georectify their point cloud (<1.5 m). It is noted that the position of points used to assess the accuracy of the DSM, clustered in the centre, is not ideal but these were collected primarily to assess tussock height. Greater positioning error would be expected towards the edge of the point cloud (James and Robson 2012, Turner *et al.* 2012) so a greater spread of ground control points would be expected to increase the RMSE.

Comparing the Pearson's correlation coefficient between measured and estimated elevations, the LiDAR ($r=0.75$ $p<0.001$) then the 0.02 and 0.05 m resolution DSMs ($r=0.64$, $p<0.001$) showed the strongest correlations to all the data. The 0.275 m resolution DSM showed the strongest correlation with tussock tops and inter tussocks when assessed separately ($r=0.82$ and $r=0.87$

p<0.001 respectively) (Table 7.3, Figure 7.13). This indicates the finer DSMs were better able to distinguish between tussock tops and inter tussock areas whereas larger resolution DSMs smoothed the data. To capture the fine scale topography the moving window used to create the DSM (three times the grid resolution) had to be smaller than the tussock width (0.28 to 0.44 m measured) to minimise the number of mixed pixels. Knowing the required DSM resolution and extent would assist in flight planning (Salamí *et al.* 2014).

Figure 7.11 demonstrates that UAV images can be used to derive fine scale microtopographical details of a surface where the spatial resolution of LiDAR has previously made this impossible. Additionally the economic advantage of the UAV system should be noted. The cost of acquiring the data was in the order of £100,000 for the LiDAR (all of Exmoor National Park surveyed 192 km^2 coverage) but only £2,000 for the UAV. Once purchased the UAV system can be repeatedly deployed, either at the same location over time or at different locations, for limited additional costs.

7.6.4 Fine Scale Structural Characteristics at a Landscape Extent

In their comprehensive review of the use of UAVs in vegetated areas Salami *et al*. (2014) did not mention any Structure for Motion studies on vegetated areas. This may be because vegetated surfaces have been highlighted as likely to result in patchy point clouds where individual leaves and stems are visible (Castillo *et al.* 2012). However, structural elements of vegetation e.g. tree trunks, branches and grass tussocks show sufficient texture and lack of movement to enable VisualSfM reconstruction. In addition a whole canopy of leaves, but not individual leaves, has be successfully captured to derive a canopy surface model (Dandois and Ellis 2010) and tree height and crown width (Wallace *et al.* 2012). This study highlights the potential for deriving fine scale structural characteristics from digital images. Despite the complications of using SfM methods on vegetation these methods should not be rejected but rather further investigation should be carried out to discover what is possible given these constraints.

This study aimed to model the ground surface and bare tussocks rather than vegetation canopy. To facilitate this minimum elevation points were used to derive the DSM and the UAV was flown in late spring, when vegetation was dormant and leaf litter had been flattened over the winter. A second in-leaf flight could be carried out in the summer when the majority of points would be from the canopy surface. This could potentially provide a measure of canopy biomass (Bendig *et al.* 2014) or even LAI (Mathews and Jensen 2013). It would be expected that the canopy would produce a sparser point cloud as matching keypoints would be more difficult due to leaf gaps, repeated structures of the same colour and random geometries (Dandois and Ellis 2010, Mathews and Jensen 2013) and errors associated with a vegetated landscape would be larger (Westoby *et al.* 2012). However, the possibility to obtain spatially distributed measures of these key ecological parameters, potentially repeated over the season and for a fraction of the cost of LiDAR, is worth further investigation.

Using this method individual tussock heights were poorly captured by all but the 0.05 m DSM, as demonstrated by the insignificance of the Pearson's correlation between measured and modelled tussock heights (Table 7.4). As the pixel resolution increased the chance of having both tussock and inter-tussock areas within a single pixel increased. Within these mixed pixels the minimum elevation will be from the inter-tussock area. Tussock height, derived from these mixed pixels, will have been underestimated (Table 7.4) as the mean and maximum elevations will have both been from inter-tussock areas. Despite individual tussock heights being poorly estimated the mean tussock height estimated from the 0.05 x 0.05 m grid was only 0.002 m different from that measured and the standard deviation for tussock height from the DSM (0.057 m) was similar to that measured (0.043 m) indicating this method could be of more use in deriving average properties for an area of interest rather than properties of individual tussocks.

Comparison between semi-variograms for the LiDAR and UAV-SfM DSMs indicated the 0.02 m resolution DSM showed similar total variation in height

over the area of interest (Figure 7.14). The lag distance was selected to enable a fair comparison between LiDAR and UAV-SfM derived DSMs. As most tussocks were less than 0.5 m wide (Table 7.4) the elevation difference between tussocks and inter-tussock areas would be included with error in the nugget (y-axis intercept). This may explain why the nugget was greater for the 0.02 and 0.05 m resolution DSMs which estimated greater tussock heights (Table 7.4) than the larger grid sizes. When the lag size is too large, short range autocorrelation e.g. height over the width of a tussock will be masked. Having the capacity to reduce the resolution of the DSM may enable fine scale spatial patterning to be investigated. The LiDAR and UAV derived DSMs differed in their horizontal spatial patterning. LiDAR indicated autocorrelation occurred over a distance of 3.76 m whilst VisualSfM DSMs indicated autocorrelation occurred over a greater distance (4.92 to 5.58 m). None of these distances agree with obvious features in the landscape. The area of interest showed significant anisotropy perpendicular to the underlying topography (removed by a first order trend removal) which may be associated with drainage features. It is possible that the DSMs were identifying this spatial patterning which is masked by the presence of tussocks in the field.

7.6.5 Tussock Structure and its Environment

It was hypothesised that structural characteristics of the *M. caerulea* would co-vary with water level and therefore provide a means by which water level could be estimated across a *Molinia caerulea* dominated landscape. In this study structural characteristics varied non-significantly ($p>0.062$) with water table depth. This may be due to the limited sample size ($n=14$) or because tussock shape was in part controlled by other factors such as slope, peat thickness (Lindsay 2010), nutrient availability or fire history (Brys *et al.* 2005). A lack of significant relationships precludes the use of tussock structure to estimate the spatial distribution of water level. Rutter (1955) also found no relationship between tussock height and water table depth but proposed that water table depth limited tussock height; with taller tussocks restricted to areas where water tables were shallower. This is contrary to the findings of this study where

tussock volume was greater where water tables were deeper (Figure 7.15a). Differences may have occurred as Rutter (1955) measured *Molinia caerulea, Calluna vulgaris* and *Erica tetralix* tussocks so the effect of vegetation composition confounded any effect of water table depth. Luscombe *et al.* (2014a) also found wetter areas to have taller vegetation, again this study included other types of vegetation in particular comparatively tall and hydrophilic *Juncus effusus.* Figure 7.15g suggests raising the mean water table to a depth of 5 cm would change the form of the *Molinia caerulea* present from tussock forming to a continuous matt which may enable other species to grow, increasing the biodiversity present. In all these studies it has been assumed that water table depths control tussock structure however, tussock structure may feedback to water table depths by altering amongst other things evapotranspiration, interception and overland flow routing (Belyea and Baird 2006).

Species richness co-varied with tussock height and volume using the natural break threshold (Figure 7.15b & f), these were both less where tussocks were taller and larger. It is possible that taller and larger *M. caerulea* tussocks have a greater size-asymmetric competitive advantage (Bonan 1988) and can more effectively suppress the presence of other vegetation, thereby reducing species richness. Again the findings of this study contrasts with Rutter's study (1955) which found the proportion of *M. caerulea* to increase (at the expense of *Calluna vulgaris* and *Erica tetralix*) where tussocks were taller and water tables deeper. The difference may have occurred as he compared structure and water table depths between different plant assemblages (e.g. wet heath, *Molinietum* etc.) whilst this study focused on *M. caerulea* dominated locations (85±5 %) with neither *Calluna vulgaris* nor *Erica tetralix* present in the Exmoor study locations.

Photosynthesis co-varied spatially with water table depth (r^2=0.13, p=0.034) across a larger sample (n=36) (Table 6.5) but did not correlate with tussock volume (n=14) where water table depths did (Figure 7.15a & d) albeit non-significantly ()indicating no direct link between photosynthesis and tussock

volume; prohibiting the use of the structural characteristics measured to estimate the spatial distribution of photosynthesis. Conversely ecosystem respiration showed no significant spatial variation across a larger sample (n=36) (Table 6.3) and did not co-vary with any of the spatially distributed variables tested (including water table depth, coverage of non-*Molinia* species and species richness (Table 6.5) however, ecosystem respiration significantly co-varied with tussock height using the natural break threshold (r=0.56, p=0.039) which also co-varied with species richness (Figure 7.15f). Where tussocks were taller (but covered a smaller area), ecosystem respiration was greater and vegetation diversity lower (Figure 7.15f & g). The author is unaware of any studies investigating the effect of vegetation morphology on CO_2 fluxes in tussock grasses. This study is the first to suggest a link between a comparatively easily measured structural characteristic (tussock height) and a hugely important parameter for understanding the current state of the carbon stored within a peatlands (heterotrophic respiration) for which the current measurement methods are spatially restricted (plot scale).

The inability of the landscape scale DSM method to accurately estimate individual tussock heights (Table 7.4) and the weak relationship between tussock height and ecosystem respiration (Figure 7.15g) resulted in large RMSEs for estimated ecosystem respiration (Table 7.5). Despite estimated tussock heights ranging from 0 to 0.11 m ecosystem respiration estimates only ranged from 9.9 to 23.9 μgC m^{-2} s^{-1} whereas modelled ecosystem respiration at 12 °C ranged from 11.7 to 33.5 μgC m^{-2} s^{-1}. This small range in estimated ecosystem respiration indicated ecosystem respiration is dependent on factors additional to tussock height which need further investigation.

7.7 CONCLUSION

This study demonstrated digital camera images and SfM software can be used to derive quantitative structural measures (tussock height, area and volume) of *Molinia caerulea* tussocks at a plot scale. As both image quantity and content (e.g. scale of texture, shadow and overlap with other images) affected point

cloud density and processing time showed a quadratic increase (R^2=0.99, p<0.001) with number of images, where possible image content should be optimised to minimise the number of images required.

Unpiloted aerial vehicle (UAV) derived digital images (203) were processed to create 600 x 700 m DSMs. Despite oblique flight paths these DSMs exhibited radial distortion due to insufficient non-parallel image overlap. Allowing for this, both the 0.05 m resolution UAV-SfM DSM and the 0.50 m LiDAR DSM significantly (p<0.001) correlated with inter-tussock (n=284) and tussock top (n=71) elevation and (r=0.64 and r=0.75 respectively) with the finer resolution UAV-SfM DSMs better able to distinguish tussock tops from inter-tussock areas. The camera, a passive sensor, was unable to penetrate the leaf litter leading to an overestimation of elevation, particularly for smaller pixel sizes. Despite this the 0.05 m resolution UAV-SfM DSM accurately predicted average tussock height (0.11 ± 0.06 m) within an area of interest (0.11 ± 0.04 m measured) revealing the capability of this method to investigate microtope properties.

Plot scale tussock volume showed a non-significant correlation (r=0.51, p=0.062) with mean water table depth whilst tussock height showed a significant correlation with species richness (r=-0.54, p=0.044) and ecosystem respiration (r=0.67, p=0.009) but not photosynthesis, with greater respiration and lower species richness occurring where tussocks were taller. Poor individual tussock height prediction meant landscape-scale estimations of ecosystem respiration were inaccurate.

This study highlights the potential for deriving fine-scale vegetation structure in a spatially explicit, economical, robust and repeatable fashion at both the plot and landscape level in a remote area using SfM methods on ground and UAV based digital images. Structural characteristics of *M. caerulea* have the potential to reveal information about vegetation diversity and ecosystem respiration within *M. caerulea* dominated landscapes and tussock grasslands in general. The methods used provide a quantitative comparison of structural characteristics and inferred environmental conditions over time and/or space.

Repeated surveys would enable fine-scale shifts in vegetation structure, and therefore vegetation diversity and ecosystem respiration, to be monitored in response to changing environmental conditions driven by, for example, ecohydrological restoration or climate change.

7.8 ACKNOWLEDGEMENTS

The authors would like to thank the Exmoor Mires Project for their help with site access and Exmoor National Park for permission to work on the site. This research received financial support from South West Water and The University of Exeter (SK05284). The UAV was provided by the TSB and NERC funded Quest-Earth-Water project 2012-3 (101340).

8 SHORT-TERM EFFECTS OF ECOHYDROLOGICAL RESTORATION ON CO_2 FLUXES IN A DRAINED *MOLINIA CAERULEA* DOMINATED PEATLAND

8.1 ABSTRACT

Drained peatlands dominated by purple moor grass (*Molinia caerulea*) are widespread in the UK and western Europe. Although substantial carbon stores may be present in these peatlands, in this degraded state they are not currently acting as carbon sinks. Therefore, *M. caerulea* dominated peatlands have been identified as potential sites for ecohydrological restoration. However, at present little is known about whether ditch blocking can raise water tables and promote the recovery of bog plant species required to restore carbon sequestration in these peatlands.

Photosynthesis at 600 µmol Photons m^{-2} s^{-1} (P_{G600}), ecosystem respiration (R_{Eco}) and partitioned below-ground respiration were measured in two *Molinia caerulea* dominated shallow peatlands located in Exmoor National Park, southwest England. Measurements were made in two headwater catchments (Aclands and Spooners) at ⅛, ¼ and ½ of the distance between adjacent ditches at six control-restored paired sites, during the growing seasons pre- (2012) and post- (2013 & 2014) restoration.

Contrary to the goals of restoration, in both catchments water tables fell, proximal to the gas flux monitoring locations, following restoration due to drier climatic conditions. Allowing for the climatic variability by comparing the difference in water table depths between control and restored locations (DiffWTD) indicated restoration had no significant effect on average water tables. At Aclands, DiffWTD responded significantly differently ($p=0.020$) pre- and post-restoration, suggesting shallower water tables were maintained during dry conditions at the restored locations following restoration.

Temporal and spatial changes in P_{G600}, R_{Eco} and below-ground autotrophic respiration observed were most likely due to small differences in vegetation

composition between locations responding differently to climatic variation. At Aclands these changes may have been enhanced by restoration, with shallower water tables during dry periods limiting photosynthesis. Additionally at Aclands, heterotrophic respiration increased following restoration, possibly due to alleviation of moisture stress in the surface layer. This research illustrates that, at least in the short-term, restoration may not deliver significant enough increases in water table levels, to protect the existing peat store and promote the change in vegetation required to restore CO_2 sequestration. Further work is required to monitor over particularly wet years (as seen pre-restoration in 2012), in order to understand whether the short-term results persist or whether medium to long-term changes in CO_2 fluxes due to restoration are manifest.

8.2 KEYWORDS

Ditch blocking, Photosynthesis, Respiration, Heterotrophic, Autotrophic, Peat dams,

8.3 INTRODUCTION

Drainage of peatlands for agriculture and forestry has been widespread across Europe (Sjörs 1980). This has shifted the balance between primary productivity and decomposition, turning many of these peatlands from carbon sinks to carbon sources (Littlewood *et al.* 2010). In their natural state, peatlands provide a range of highly valuable ecosystem services, including carbon storage, river flow regulation, drinking water provision, biodiversity, food and fibre provision and cultural services, which, although currently vulnerable, may be secured by ecological restoration (Grand-Clement *et al.* 2013a). In light of this, restoration projects aimed at restoring ecohydrological functioning to peatlands were instigated in the UK (e.g. Lunt *et al.* 2010), continental Europe (e.g. Komulainen *et al.* 1999) and north America (e.g. Gorham and Rochefort 2003). Although a range of restoration techniques are used to ameliorate different forms of degradation (Parry *et al.* 2014), there are two main aims of bog restoration; 1, the re-establishment of near- or at-surface water tables and 2, the re-

colonisation of peat forming species especially *Sphagnum* (Holden *et al.* 2004). Re-establishing *Sphagnum*-rich vegetation communities is particularly important when carbon sequestration is a key aim of restoration (Lunt *et al.* 2010).

A combination of gas flux chambers and soil collars can be used to measure both ecosystem and partitioned below-ground fluxes at a scale that is attributable to processes (Tuittila *et al.* 1999) facilitating understanding of the temporal and spatial effects of restoration. Partitioning below-ground respiration enables the separation of the more variable autotrophic respiration, anticipated to respond slowly as vegetation composition changes, from heterotrophic respiration associated with decomposition of the peat store. At present very little is known about the short-term effects of restoration on below-ground heterotrophic respiration even though conserving the existing peat store is the first step towards reinstating carbon sequestration. Re-establishing a *Sphagnum*-rich vegetation community can take decades (Haapalehto *et al.* 2010) however, measuring photosynthesis, ecosystem respiration and below-ground autotrophic respiration should reveal the short-term (1-2 year) effects of restoration on *Molina caerulea* and the processes driving these changes. Research is needed to understand the direction of the response of CO_2 fluxes following restoration (Ballantyne *et al.* 2014) and to indicate if restoration weakens *Molinia caerulea*, a species adapted to live where water table depths fluctuate (Jefferies 1915), and therefore whether future vegetation change is probable in *Molinia caerulea* dominated peatlands.

Several studies have investigated the effect of re-wetting commercial peat cuttings on CO_2 fluxes (e.g. Waddington *et al.* 2010, Samaritani *et al.* 2011, Strack and Zuback 2013). Such work demonstrated that vegetation cover increased and the type of vegetation changed towards more typical bog species, in particular an increase in S*phagnum* cover was observed. Re-wetting and vegetation change altered the balance between photosynthesis and ecosystem respiration towards greater CO_2 sequestration, however, not all the restored peatlands became CO_2 sinks. These peatlands had the original mire

surface removed and frequently had bare peat at the surface. As such they represent a poor comparison to vegetated drained peatlands.

Where the effect of ditch blocking on CO_2 fluxes has been investigated in drained peatlands it has focused on areas representative of different microtopography and vegetation cover (Komulainen *et al.* 1999, Urbanová *et al.* 2012) rather than explicitly investigating a spatially distributed response with respect to the drainage features themselves. The response to restoration was therefore dependent on the conditions (water table depth and vegetation composition) prior to restoration. Urbanová *et al.* (2012) found no significant difference in plant community between drained and restored areas or any plant die-back in the restored areas 1-year after restoration. Komulainen *et al.* (1999) found raising the water table led to a decrease in *Cladonia* and increase in *Sphagnum balticum, Sphagnum fuscum* and *Polytrichum strictum.* Ecosystem respiration decreased in all nanotopes whilst photosynthesis decreased in the hollows, as *Calluna vulgaris* died back, but increased on the hummocks as the *Empetrum nigrum* cover increased.

The spatially distributed effect of gully blocking on CO_2 fluxes was investigated along a transect by Clay *et al.* (2012). Although there were no significant differences in net ecosystem exchange (NEE) across the transect, both photosynthesis and ecosystem respiration were greater in the gully floor, with vegetation composition the main control on CO_2 exchange (Clay *et al.* 2012). These gullies were much deeper and wider than those typically cut for drainage, had exposed bare peat prior to restoration and required different restoration techniques (e.g. seeding and liming, heather brash cover) therefore they provide a poor comparison with the work proposed here. Research is needed to understand the spatially distributed response of CO_2 fluxes to ditch blocking.

It is hypothesised that ecohydrological restoration will raise water tables and reduce all CO_2 fluxes measured (ecosystem respiration; gross photosynthesis; total below-ground respiration; heterotrophic respiration of soil organic matter

and below-ground autotrophic respiration including root respiration and microbial respiration of root exudates). More specifically it is hypothesised that:

1. Restoration will raise water tables with the greatest effect during dry conditions when water tables are expected to fall at the control locations but be maintained at the restored locations by pools upslope of the peat dams.
2. Restoration will reduce CO_2 fluxes with the greatest effect observed;
    a. during dry conditions when the difference in water table depth between control and restored locations will be greatest,
    b. on ecosystem respiration and below-ground heterotrophic restoration as raised water tables (temporal variation) will reduce decomposition rates, shifting the ecosystem towards carbon sequestration.
3. Restoration will raise water tables with the greatest effect observed;
    a. closest to the ditch nearer the pools formed upslope of the peat dams
    b. where peat is thicker and therefore the potential to prevent deeper water tables during dry conditions is greater.
4. Restoration will reduce CO_2 fluxes with the greatest effect observed;
    a. closest to the ditch, controlled by water table depth, primary productivity and vegetation composition,
    b. where peat is thickest, controlled by water table depth, primary productivity and vegetation composition,
    c. on ecosystem respiration and below-ground heterotrophic restoration as higher mean water tables will reduce decomposition rates, shifting the ecosystem towards carbon sequestration.

These hypotheses were tested in two drained, temperate maritime peatlands in the United Kingdom that had been widely affected by ditch blocking (Grand-

Clement *et al.* 2014, Luscombe *et al.* 2014a, Luscombe *et al.* 2014b, Luscombe *et al.* In prep, In Review).

8.4 METHOD

8.4.1 Study Sites

The study sites were located in Exmoor National Park in the southwest England in two *Molinia caerulea* dominated headwater catchments subject to drainage (Aclands 51°7’51.3N 3°48’44.4W) and Spooners (51°7’21.9N, 3°44’52.9W) catchments, Figure 8.1). These catchments were selected to be characteristic of the widespread drained peatland areas which are currently being restored across Exmoor using peat dams (Grand-Clement *et al.* 2015). Restoration occurred in March to April 2013 at Spooners and March 2014 at Aclands. For further details on the study sites see chapter 0 and section 6.4.

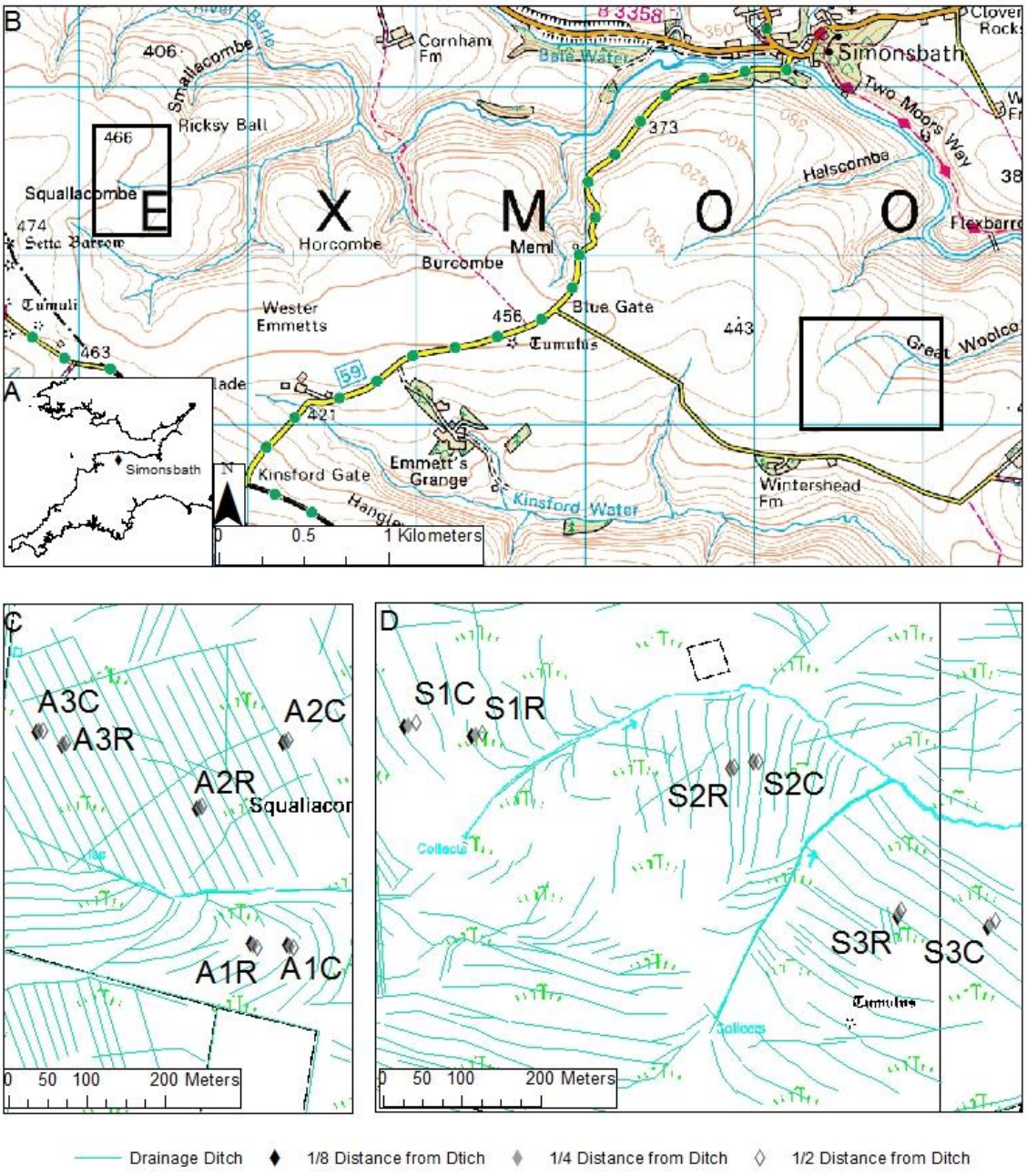

Figure 8.1 Location of Aclands and Spooners catchments (b) within the southwest of England (a). Location of control (C) and restored (R) study sites within Aclands (c) and Spooners (d) study catchments. The three plots within each study site were located ⅛, ¼ and ½ the distance between adjacent ditches. Coastline shapefile (Ordnance Survey 2008a), 1:50 000 Ordnance Survey Map (Ordnance Survey 2008e) 1:10 000 Ordnance Survey map (Ordnance Survey 2008b, c).

8.4.2 Experimental Design

Within each catchment, three pairs of sites were chosen to encompass the expected variation in altitude, aspect, slope, peat depth, ditch dimensions and

initial wetness, while minimising the variation between the paired replicates (Figure 5.1; for further details see chapter 0 and section 6.4). In each pair, one site remained unrestored to act as a control (C) whilst the other site was restored through ditch blocking (R). As ecosystem respiration exhibits significant climate driven inter-annual variability (Lafleur *et al.* 2003), comparison with control sites is essential for the effects of restoration to be quantified. Investigations into the effects of drainage ditches on water table depths commonly use transects perpendicular to the ditch (e.g. Wilson *et al.* 2010). As the ditches in these sites were largely unevenly spaced, plots were located ⅛, ¼, and ½ of the distance between the ditch being monitored and the adjacent ditch to evaluate the spatial effect of restoration on CO_2 fluxes (chapter 0 and section 6.4).

8.4.3 Measurements and Data Analysis

8.4.4 Gas Flux Measurements

8.4.4.1 Photosynthesis and Ecosystem Respiration

A 55 cm x 55 cm x 25 cm Perspex gas flux chamber was rested on permanently installed 50 cm tall legs with a plastic skirt weighted down to the soil surface (section 6.5.3). An EGM-4 infra-red gas analyser (PP Systems, Hitchin, UK) measured accumulated CO_2 every 10 seconds for 2 minutes concurrently with chamber temperature and photosynthetic active radiation (PAR) (Skye Instruments, Llandrindod Wells, UK).

Measurements were made approximately monthly at both catchments from May to September (Supplementary Material Table 11.1). Key respiratory and photosynthetic parameters were calculated from light response curves (full light, full dark and ~60% ~40%, ~10%) measured at each R and C site (each site having plots at three distances from the ditch) during 13 separate campaigns (Equation 8.1);

Equation 8.1 hyperbolic light response curve

$$\mathrm{NEE} = R_{\mathrm{Eco}} - \frac{P_{max}.\mathrm{I}}{k + \mathrm{I}}$$

where NEE is the net ecosystem exchange (μgC m^{-2} s^{-1}), P_{max} is the rate of light saturated photosynthesis (μgC m^{-2} s^{-1}), k is the half-saturation constant of photosynthesis (μmol Photons m^{-2} s^{-1}), I the incident PAR (μmol Photons m^{-2} s^{-1}) and R_{Eco} the ecosystem respiration (μgC m^{-2} s^{-1}). Photosynthesis at 600 μmol Photons m^{-2} s^{-1} was calculated for each growing season sample round (13 in total). To account for climatic variability (e.g. temperature, precipitation etc.) between the baseline year and subsequent years, P_{G600} and R_{Eco} at the restored locations were expressed as a proportion of P_{G600} or R_{Eco} at the equivalent control location ($PG_{R/C}$ and $REco_{R/C}$).

8.4.4.2 Soil CO_2 Efflux

At each location, four PVC collars (16 cm diameter, 8 cm height) were sealed to the peat using non-setting putty (Evo-Stik 'Plumbers Mait') in March 2012. All collars had above-ground vegetation removed by clipping so they measured below-ground fluxes only. In addition, circular 20 cm deep and 56 cm diameter trenches were dug around half the collars. Thus, live roots were excluded enabling below-ground heterotrophic respiration to be measured. The collars with only above-ground vegetation removed were used to measure total below-ground respiration (including autotrophic and heterotrophic components). At each plot, the two replicates of each treatment were averaged to produce a single value for total and heterotrophic respiration.

CO_2 measurements were taken in a semi-randomised pattern approximately every three weeks over the growing season (Supplementary Material Table 11.2) CO_2 flux was measured over 2 minutes using an EGM-4 infra-red gas analyser and a CPY-4 canopy assimilation chamber (PP Systems, Hitchin, UK). Autotrophic respiration was calculated from the difference between average total (n≤2) and average heterotrophic respiration (n≤2) measured at

each location for each sample round. Soil temperature at 5 cm was measured at the same time as CO_2 flux measurements.

Soil temperature has been shown to affect below-ground respiration strongly (Lloyd and Taylor 1994) varying over the duration of a sample round. To account for this, below-ground respiration rates were normalised to 10 °C (section 6.5.4) for control and restored sites separately using the seasonal $Q_{10,}$ (the increase in respiration rate for a 10 °C increase in temperature; Supplementary Material Table 10.7). Temperature corrected respiration at the restored locations was expressed as a proportion of temperature corrected respiration at the equivalent control location ($RTot_{R/C,}$ $RHet_{R/C}$ and $RAut_{R/C}$) to account for climatic variability.

8.4.5 Vegetation Measurements

8.4.5.1 Vegetation Phenology Proxy

A proxy for vegetation phenology was derived from the Moderate resolution Imaging Spectroradiometer (MODIS) MODIS9A1 surface reflectance product (500 x 500 m resolution) as in chapter 4. MODIS tiles h17 v3 (49 to 60°N, 0E to 20°WE) from March to October 2012-2014 were downloaded from USGS Earth Explorer (http://earthexplorer.usgs.gov). The normalised difference vegetation index (NDVI) was derived as follows; NDVI= (Band 2 – Band 1) / (Band 2 + Band 1). This product has been widely used to show changes in vegetation vigour (Mkhabela *et al.* 2011), phenology (Zhang *et al.* 2003) and biomass (Fensholt *et al.* 2004).

MODIS data quality labels and cloud cover data were extracted for the pixels of interest (two for each catchment). Poor quality data were given a weighting of 0 and all other data a weighting of 1. To minimise variation due to atmospheric conditions, illumination and observation geometry, a third order Fourier smoothing filter was applied. Points outside the 99 % confidence interval were excluded. All remaining points were then weighted equally and a Fourier third

order series fitted to form a continuous timeseries for each pixel. These values were then averaged to form a composite NDVI timeseries for each catchment.

8.4.5.2 Vegetation Composition and Annual Net Primary Productivity

Annual net primary productivity (ANPP) was measured in August 2012, 2013 and 2014 at Spooners and in August 2012 and late July 2014 at Aclands by destructive harvest of a 55 x 55 cm plot <4 m down-slope of each flux measurement plot (n=36).

Vegetation composition including leaf litter (% cover) of each NEE plot was estimated by visual inspection in August 2012. As several species occurred only at one location the percentage coverage of non-*Molinia* species was calculated. The number of species present at each location was counted to derive the species richness for each location. The Inverse Simpson Diversity Index (Equation 8.2), a second measure of ecological diversity, was also calculated. D increases from 1 to n as the number of species present and/or the proportional abundance of different species becomes more equal.

Equation 8.2 Inverse Simpson Diversity Index

$$D = {}^{1}\Big/\frac{\sum n(n-1)}{N(N-1)}$$

8.4.6 Ancillary Data

Water table depths were measured in dipwells installed to the base of the peat soil profile. Measurements were taken concurrently with both NEE and soil efflux measurements. Incomplete sample rounds i.e. those which covered only part of a catchment were excluded leaving 24 sample rounds at Aclands and 42 at Spooners. To allow for climatic variability the difference in water table depth between the control and restored locations (DiffWTD) was calculated.

Rainfall data were collected every 15 minutes using a 0.2 mm tipping bucket rain gauge and a NOMAD Portable Weather station (Casella, USA) in each

catchment. Rainfall was summed for the preceding 0, 7, 14 and 28 days to describe antecedent conditions prior to sampling.

Peat thickness, from the peat surface to the peat-mineral soil interface (cm), was measured using an auger and tape measure during dipwell installation.

8.4.7 Statistical Analysis

Locations where dipwells were dry on more than four occasions out of 44 were excluded from analysis (A2R2, A3R1, S1R1, S1R2 and S3R2). To test hypothesis 1, if linear regression relationships between water table depth at the control location (WTD_C) and the difference in water table depths between the control and restored locations (DiffWTD) were significantly different pre- and post- restoration, a sum-of-squares F-test was used. The sum-of-squares (adjusted for the degrees of freedom) for a global model, with a single slope for all the data but different intercepts for pre- and post-restoration, was compared against the sum-of-squares of a model with different slopes and intercepts for pre- and post-restoration.

To test hypothesis 2, a repeated measures ANOVA was carried out on $PG_{R/C}$ and $REco_{R/C}$ (based on light response curves by site) for each catchment with pre-restoration, one and two years post-restoration (at Spooners only) as the three within-subject factor levels. A two-way repeated measures ANOVA was carried out on $RTot_{R/C}$, $RHet_{R/C}$ and $RAut_{R/C}$ for each catchment with site as the between-subject factor and pre-restoration, one and two years post-restoration (at Spooners only) as within-subject factor levels. Outliers (> 3 standard deviations from the site average) were removed. All data were normal (Kolmogorov-Smirnov Test). To test for differences in the relationship between CO_2 fluxes and variables pre- and post- restoration a sum-of-squares F-test was carried out with WTD_C, DiffWTD, NDVI and total rainfall in the preceding 0, 7, 14 and 28 days as independent variables.

To test hypothesis 3, paired t-tests at Aclands and ANOVA at Spooners were used to compare DiffWTD averaged by site pre-, 1-year and 2-year post-

restoration at each proportional distance from the ditch. DiffWTD was normal (Kolmogorov-Smirnov Test). The relationship between average peat thickness and average DiffWTD for each pair of locations (excluding those locations which were dry on more than four occasions, n=11), was compared pre- and 1-year post-restoration using a sum-of-squares F-test. To test if the relationship between the difference in water table depths (DiffWTD) and the initial water table conditions (WTD_C) were different pre- and post-restoration a sum-of-squares F-test was carried out.

To test hypothesis 4, paired t-tests at Aclands and ANOVA at Spooners were used to compare $PG_{R/C}$ and $REco_{R/C}$ (light response curves by plot) pre-, 1-year and 2-year post-restoration at each proportional distance from the ditch. Paired t-tests at Aclands and ANOVA at Spooners were used to compare $RTot_{R/C}$, $RHet_{R/C}$ and $RAut_{R/C}$, averaged by site pre-, 1-year and 2-year post-restoration at each proportional distance from the ditch. Outliers (> 3 standard deviations from the plot average) were removed. All data were normal (Kolmogorov-Smirnov Test). All statistical analyses were performed with SPSS 19 (SPSS Inc., Chicago, Illinois, US).

8.5 RESULTS

Comparing the regional (southwest England) seasonal rainfall and mean air temperatures during this study (2012-2014) to the 100 year mean (Figure 8.2) it can be seen that the summer of 2012 was 226 mm wetter than the long-term average, whilst the summers of 2013 and 2014 were 69 and 12 mm drier respectively. The post-restoration summers were also 1.1 and 0.8 °C warmer than average for 2013 and 2014 respectively. Spring and autumn 2012 (pre-restoration) as well as autumn 2013 and spring 2014 (post-restoration) were wetter than average. Spring 2013 was notably cooler than average (1.6 °C) which may have an impact on the following growing season.

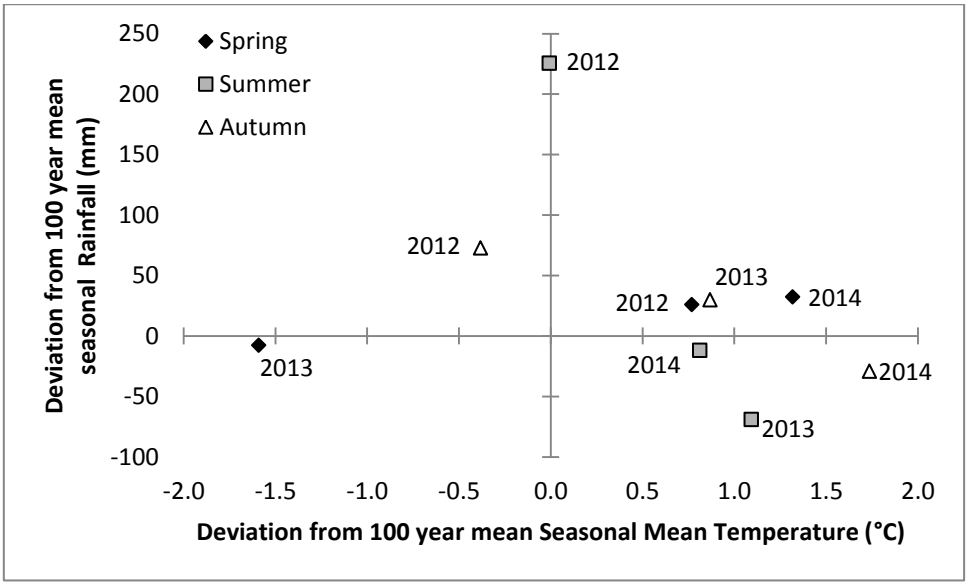

Figure 8.2 Deviation of the regional (Southwest England) seasonal rainfall (mm) and mean air temperatures (°C) during 2012, 2013 and 2014 from the 100 year mean (UK Meteorological Office 2015).

8.5.1 Hypothesis 1: The Effect of Restoration on Water Table Depths through Time

Due to climatic variation, a wet baseline year compared to dry post-restoration years (Figure 5.2, Figure 8.2), water tables fell at both the control and restored locations following restoration (Figure 8.3a). At Aclands It can be seen that the decrease was smaller at the restored locations compared to the control locations but separating the effect of restoration from the climatic variability is difficult.

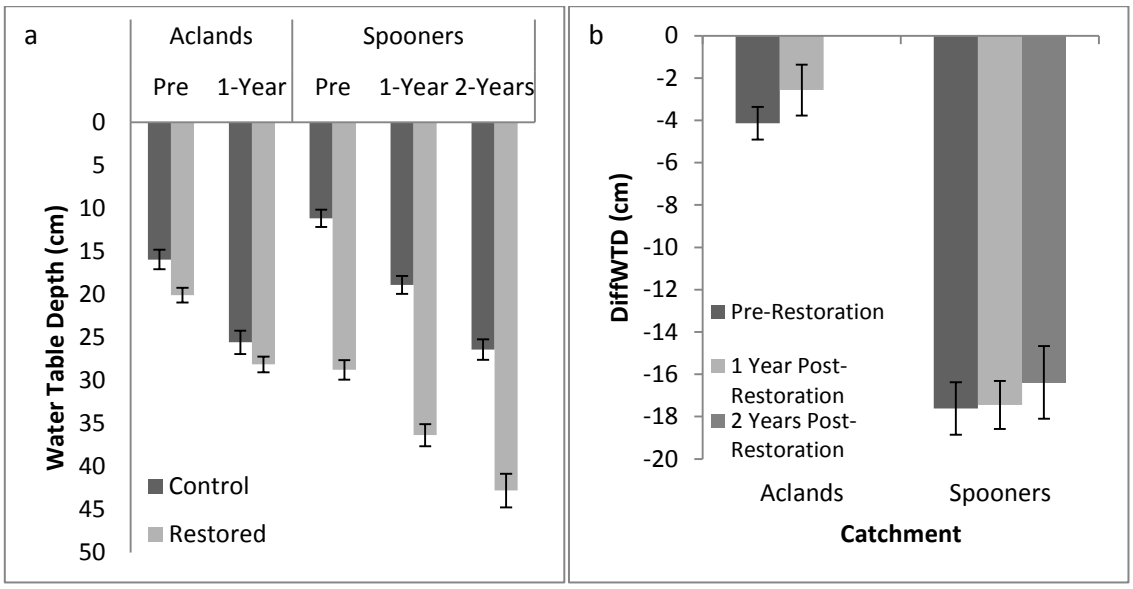

Figure 8.3 Average water table depth at the control and restored locations pre-, 1-year and 2-years post restoration (a). Difference in water table depth between the control and restored locations (DiffWTD) pre-, 1-year and 2-years post-restoration (b). Error bars are one standard error. n>36.

Comparing the difference in water table depths between the control and restored locations (DiffWTD) pre- and post-restoration (Figure 8.3b). It can be seen that there were no significant differences between pre- and post-restoration water tables.

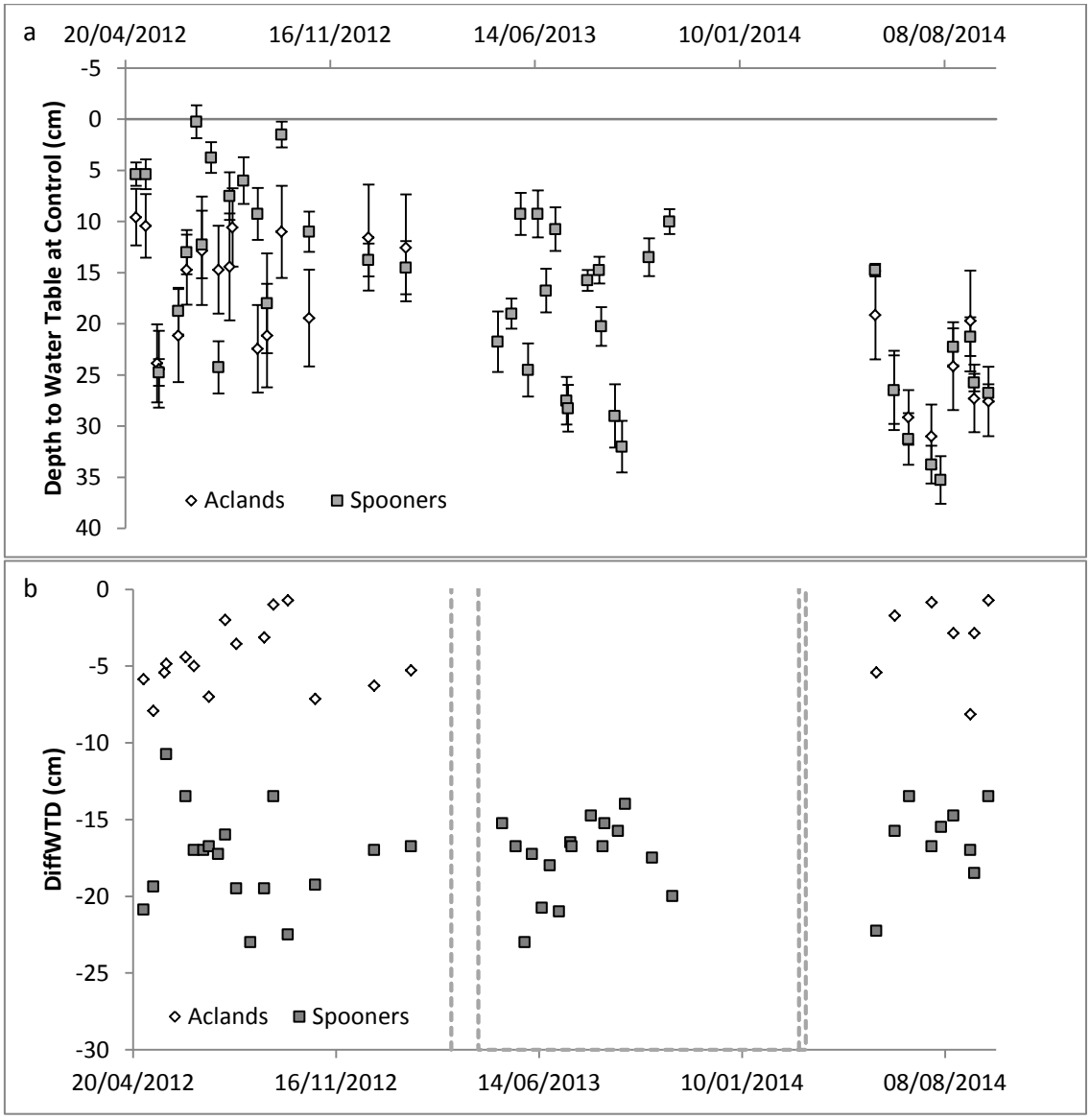

Figure 8.4 a, Depth to water table (cm) at the control location at Aclands (white diamonds) (n=7) and Spooners (grey squares) (n=4). Error bars are one standard error. b, Difference in water table depth between the control and restored locations at Aclands and Spooners . Vertical dashed lines indicate the start and finish of restoration at Spooners (March-April 2013) and Aclands (April 2014).

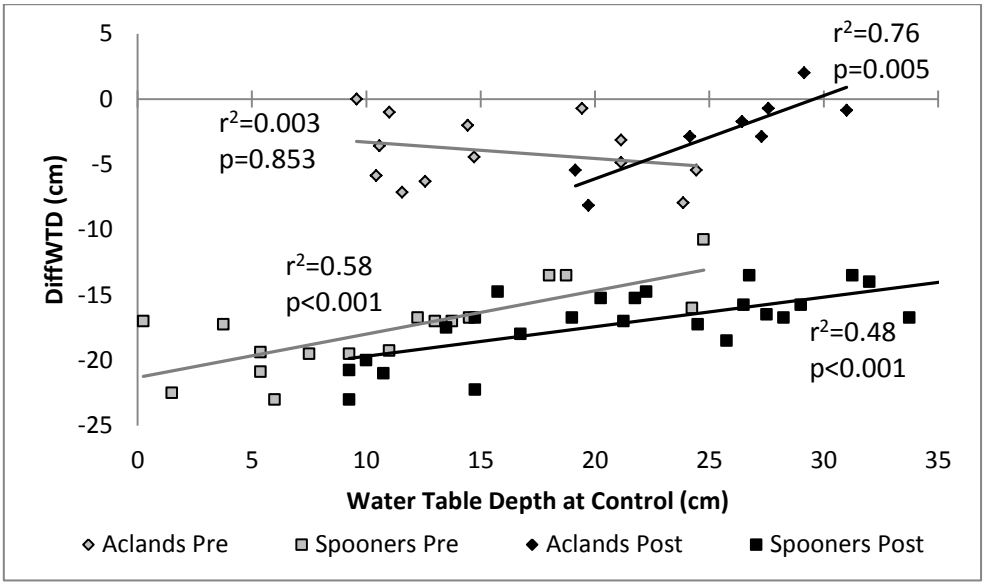

Figure 8.5 Variation in the difference in water table depth between the control and restored locations (DiffWTD) (cm) with variation in water table depth at the control locations (cm) at Aclands (diamonds) and Spooners (squares) catchments pre-(grey) and post-restoration (black).

2012 was the wettest year in the study and 2014 was the driest (Figure 8.4). Average water table depths were similar in both catchments during 2012 reaching a maximum depth of 24 and 25 cm respectively for Aclands and Spooners. Following restoration at Aclands it appeared that when water tables at the control locations (WTD_C) increased the difference in water table depth between the restored and control locations (DiffWTD) reduced. In Spooners catchment there was a significant relationship between WTD_C and DiffWTD both pre- and post-restoration (Figure 8.5). However, there was no significant difference (p=0.103) between the linear regressions pre- and post-restoration. At Aclands there was no relationship between WTD_C and DiffWTD pre-restoration but there was a significant relationship post-restoration (Figure 8.5). The WTD_C and DiffWTD relationships pre- and post-restoration were significantly different (p=0.020). It should be noted that there was limited overlap in water table depths measured pre- and post-restoration (19 to 24 cm) but the data available indicates that following restoration during dry conditions water table depths at the control and restored locations were more similar. Given the control locations were, on average, wetter this indicates water tables

remained higher during dry conditions. This finding suggests that following restoration either water tables at the restored locations rose less during wet conditions or fell less during dry conditions.

8.5.2 Hypothesis 2: The Effect of Restoration on CO_2 Fluxes through Time

8.5.2.1 Photosynthesis and Ecosystem Respiration

Post-restoration P_{G600} and R_{Eco} increased at both the control and restored locations in both catchments (Figure 8.6a & b) reflecting improved growing conditions. Similar to water table depths (Figure 8.3a), climatic variation i.e. the variation between years within the control locations, was larger than variation due to restoration. By expressing fluxes at the restored locations as a proportion of that measured at the control locations (e.g. $PG_{R/C}$) or the difference between fluxes measured at the control and restored locations climatic variation can be accounted for.

No significant differences in $REco_{R/C}$ or $PG_{R/C}$ occurred following restoration (Figure 8.6c & d) at either Aclands or Spooners.

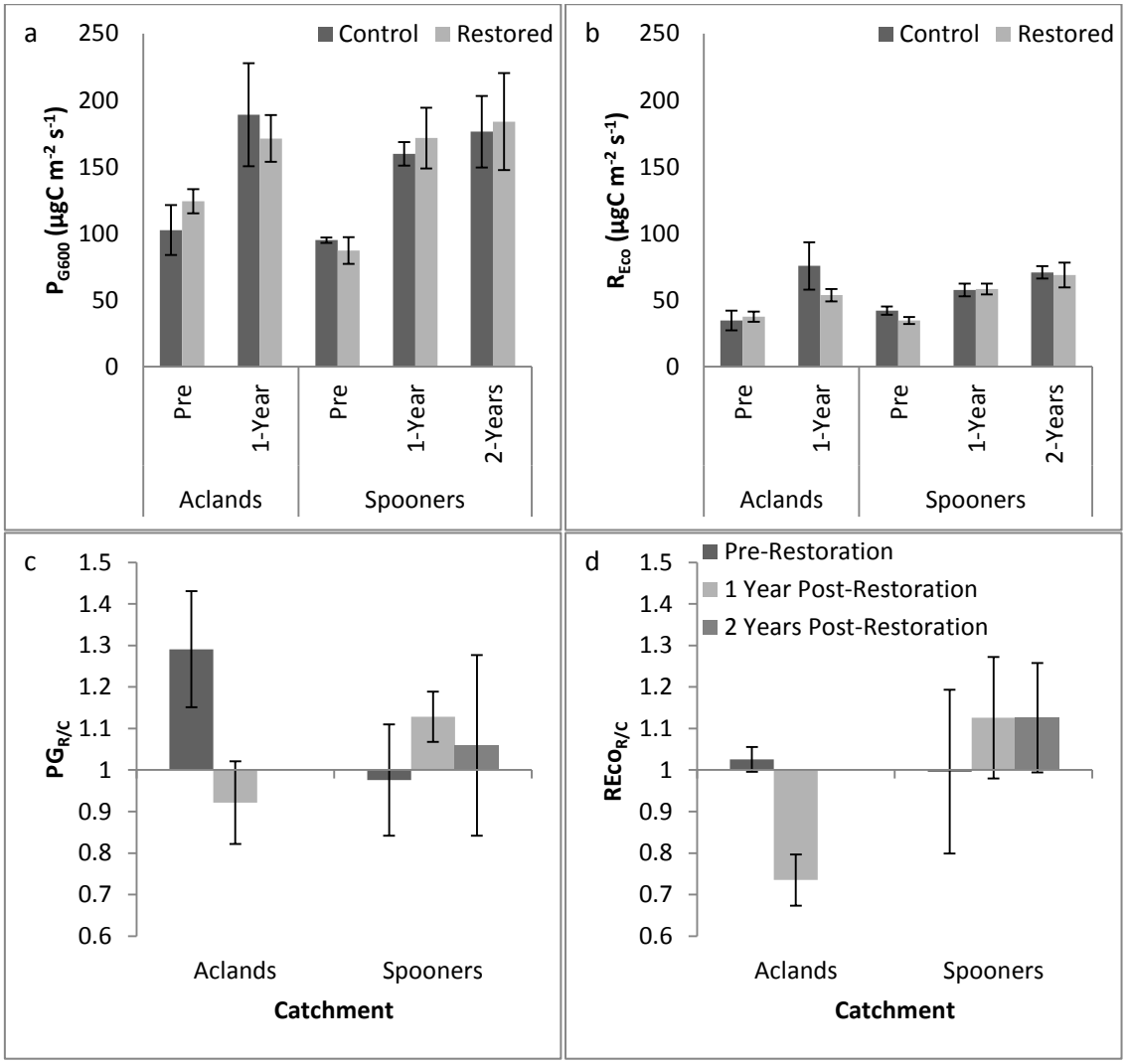

Figure 8.6 Average photosynthesis at 600 µmol Photons m^{-2} s^{-1} (a) and ecosystem respiration (b) at the control and restored locations pre-, 1-year and 2-years post-restoration (µgC m^{-2} s^{-1}). Average photosynthesis at 600 µmol Photons m^{-2} s^{-1} ($PG_{R/C}$) (c) and ecosystem respiration ($REco_{R/C}$) (d) at the restored location as a proportion of the variable at the controlled location pre-, 1-year and 2-years post- restoration. Error bars are one standard error.

Comparing the change in absolute CO_2 fluxes (Figure 8.7) it can be seen that there was considerable uncertainty in the measurements, as such no statistically significant changes were observed. Pre-restoration at Aclands and the first year post-restoration at Spooners, the restored locations took-up more CO_2 by photosynthesis than the control locations but also released more CO_2 by ecosystem respiration. Post-restoration at Aclands and pre-restoration at Spooners the reverse occurred, restored locations took-up less CO_2 by

photosynthesis but released less CO_2 by ecosystem respiration than the control locations. This finding demonstrates an inconsistent response to restoration between the two catchments.

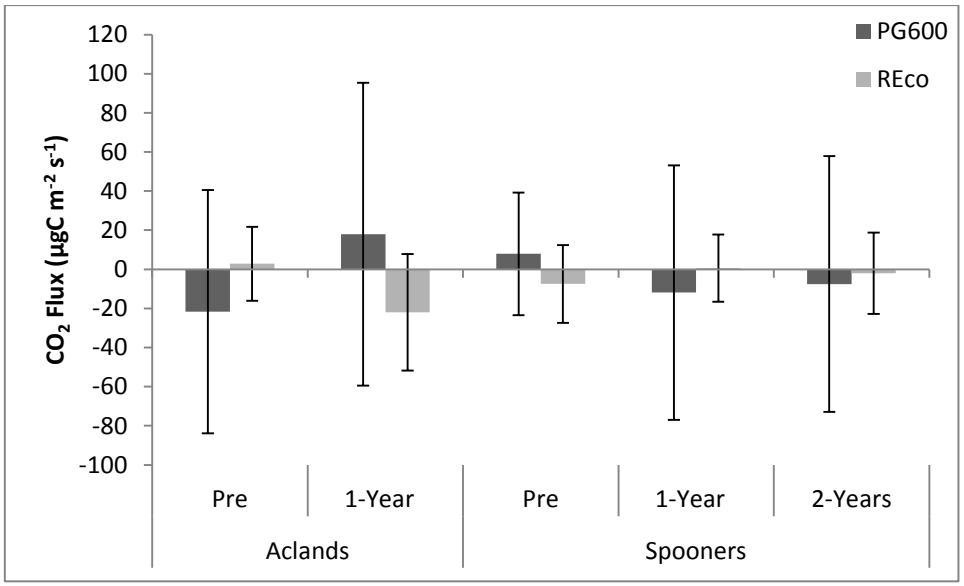

Figure 8.7 Average difference in photosynthesis at 600 µmol Photons m^{-2} s^{-1} (P_{G600}) and ecosystem respiration (R_{Eco}) (µgC m^{-2} s^{-1}) between control and restored locations pre-, 1-year and 2-years post-restoration at Aclands and Spooners catchments. A positive value indicates restored locations released more CO_2 i.e. more respiration or less photosynthesis. Error bars are one standard error.

It can be seen that both R_{Eco} and P_{G600} varied seasonally (Figure 8.8a &b) with greater fluxes in the summer but there was no consistent relationship between control and restored locations. There was also no obvious change in behaviour following restoration associated with restoration or time since restoration.

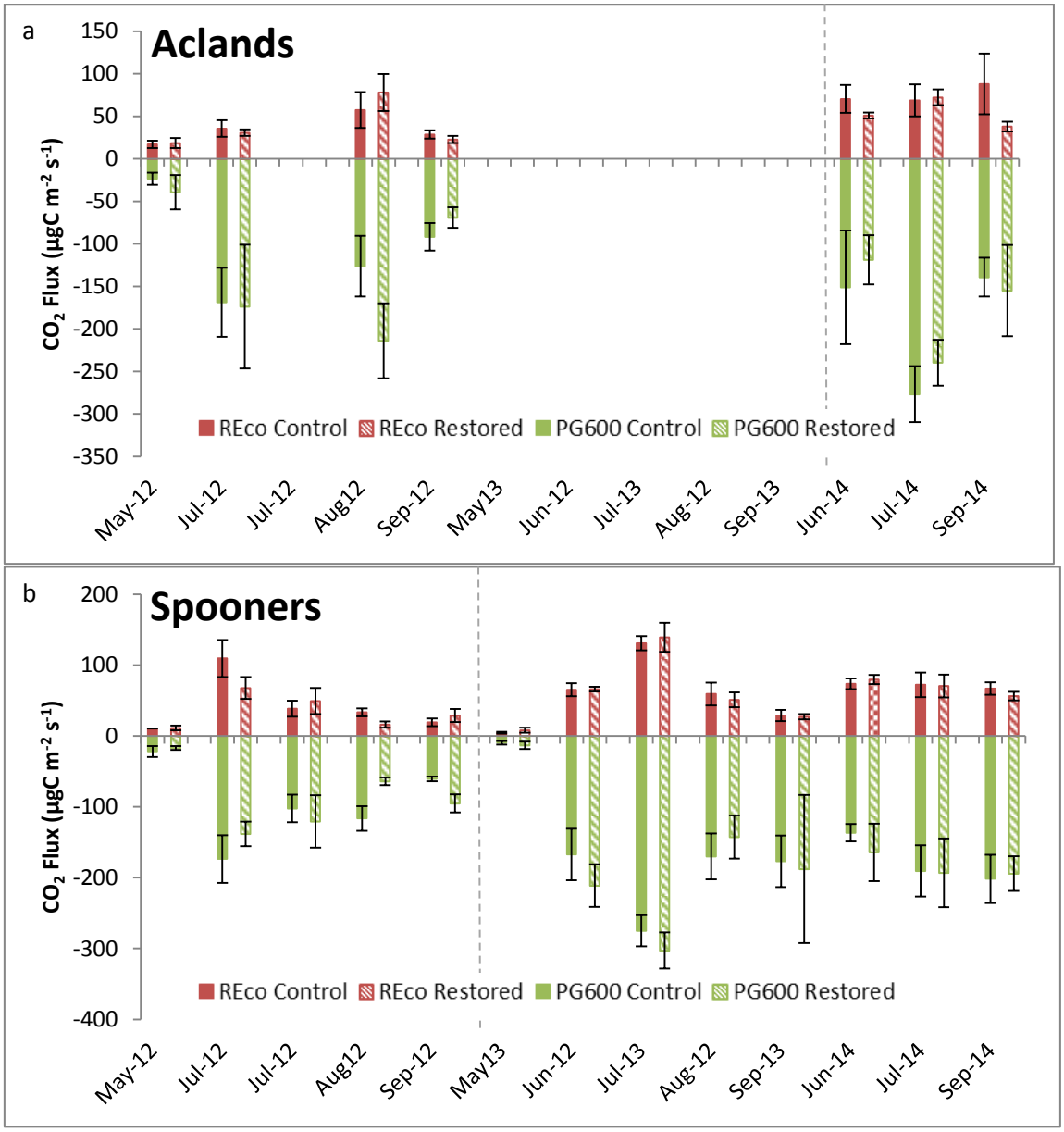

Figure 8.8 Temporal variation in photosynthesis at 600 µmol Photons m^{-2} s^{-1} (P_{G600}) and ecosystem respiration (R_{Eco}) at the control and restored locations (µgC m^{-2} s^{-1}) at Aclands (a) and Spooners (b). Vertical dashed line indicates timing of restoration. Error bars are one standard error.

Investigating other potential drivers of temporal variation, $PG_{R/C}$ and $REco_{R/C}$ showed no significant difference in their relationships with antecedent rainfall (0, 7, 14 or 28 days), T5 or NDVI pre- or post-restoration in either catchment (not shown).

8.5.2.2 Below-Ground Respiration

Total and heterotrophic respiration decreased in the first year following restoration in both catchments (Figure 8.9a) at both the control and restored locations. At Spooners total respiration then increased between the first and second years following restoration at both the control and restored locations. As both the control and restored locations responded similarly this indicates much of this change was due to inter-annual climatic variability. Heterotrophic respiration increased between the first and second years following restoration at the control location but decreased at the restored location, although these differences were within one standard error bar. Autotrophic respiration at both control and restored locations increased between 2012 and 2014 (1st year post at Aclands and 2nd year post at Spooners) with an intermediate decline at Spooners. At both Aclands and Spooners, $RTot_{R/C,}$ $RHet_{R/C}$ and $RAut_{R/C}$ (Figure 8.9b) showed no significant change following restoration.

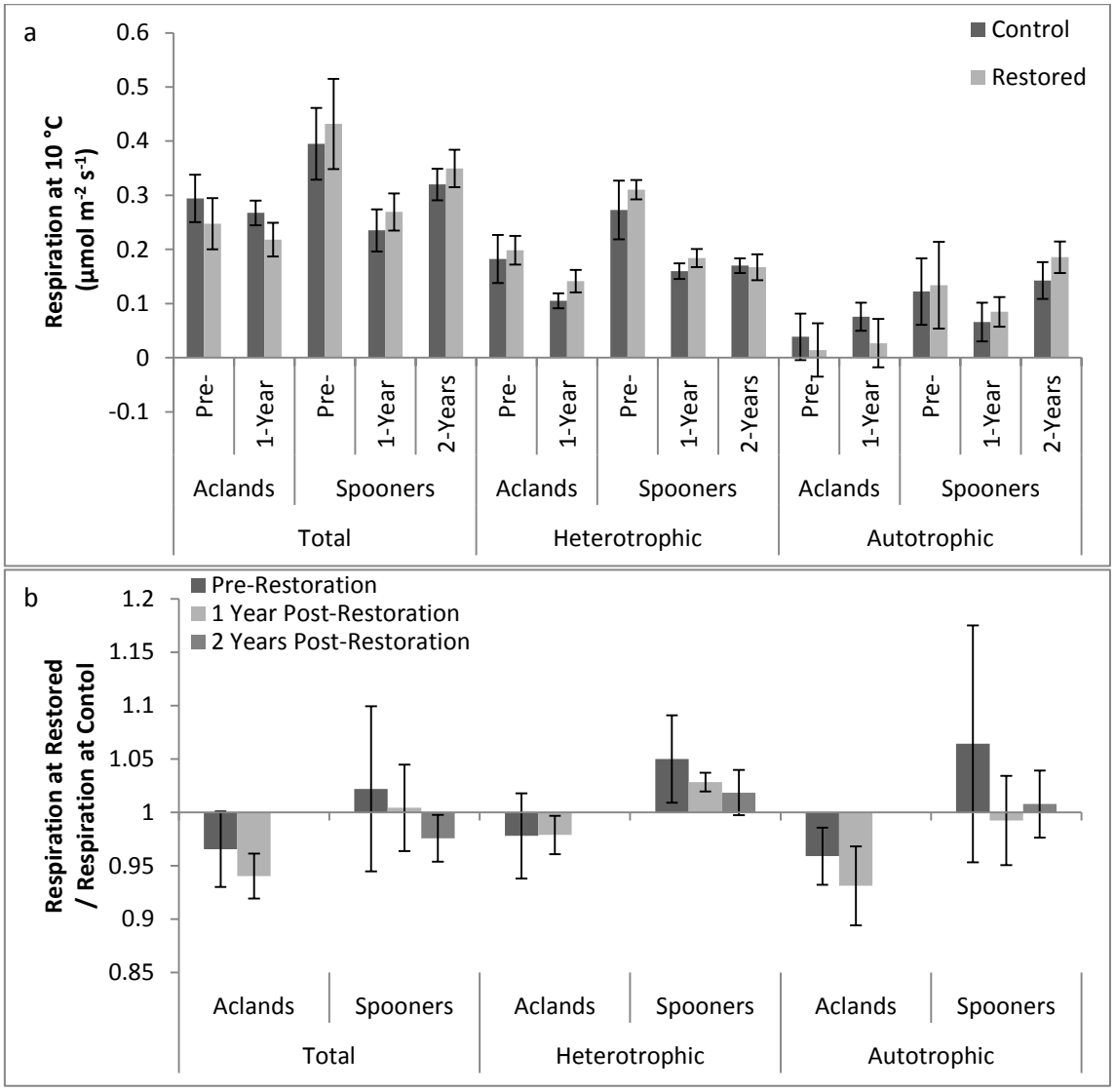

Figure 8.9 Average total, heterotrophic and autotrophic respiration at 10 °C at control and restored locations pre-, 1-year and 2-years post-restoration (a). Average total, heterotrophic and autotrophic respiration at the restored location as a proportion of respiration at the control location pre-, 1-year and 2-years post- restoration (b). Error bars are one standard error.

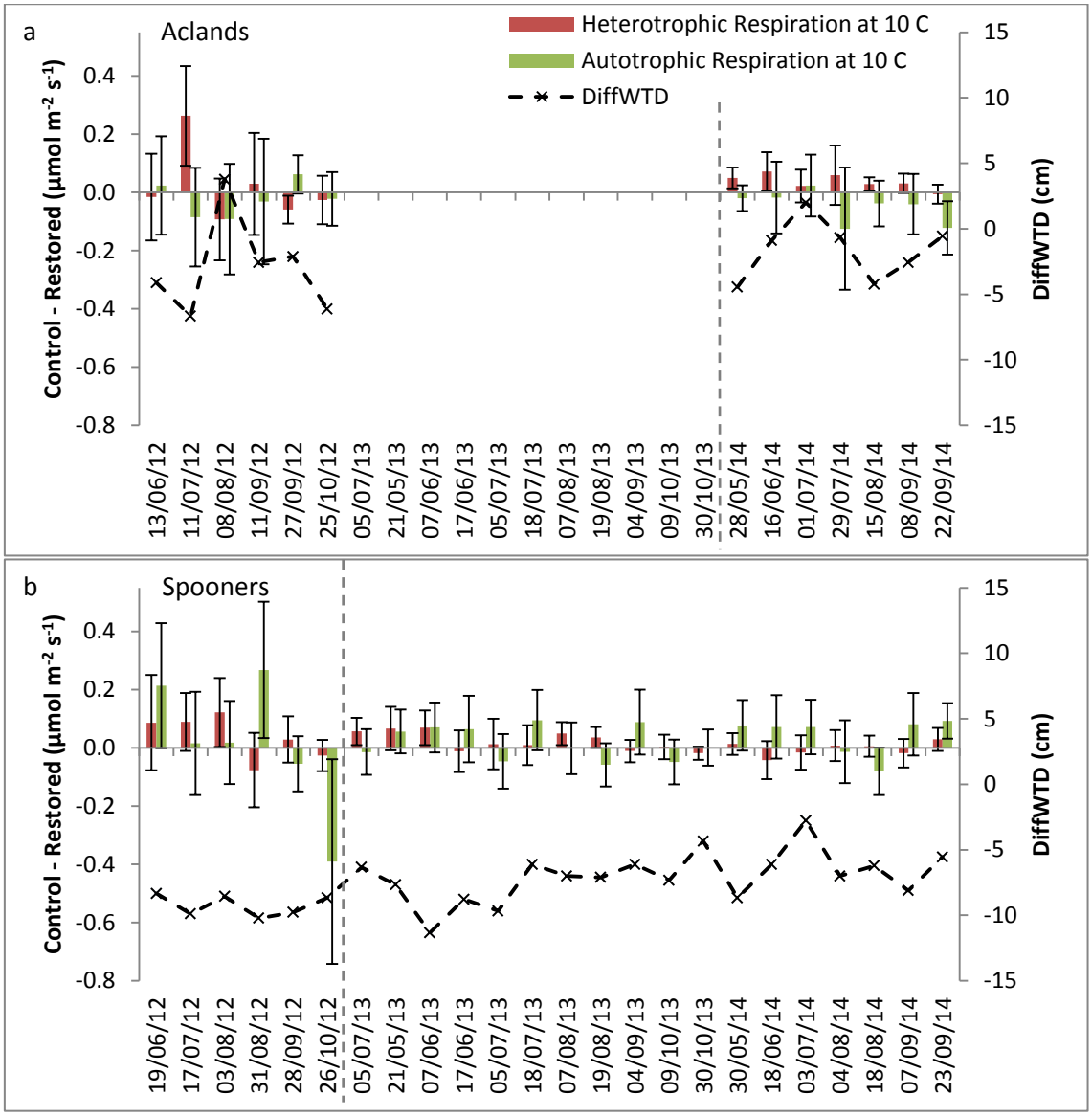

Figure 8.10 Temporal variation in the difference in water table depth (cm), heterotrophic and autotrophic respiration (µmol m^{-2} s^{-1}) between control and restored locations in Aclands (a) and Spooners (b) catchments. Vertical dashed line indicates timing of restoration. Error bars are one standard error.

Comparing the difference in heterotrophic and autotrophic respiration between the control and restored locations at Aclands, it can be seen that prior to restoration both control and restored locations had greater respiration rates on occasion (Figure 8.10a). Following restoration, heterotrophic respiration was consistently greater at the restored locations. Conversely, autotrophic respiration was generally less at the restored locations following restoration. At

Spooners heterotrophic respiration was initially greater at the restored locations but over time respiration became greater at the control locations (Figure 8.10b). The difference in water table depths generally increased over the same period. Autotrophic respiration had a tendency to be greater at the restored locations with no apparent temporal trends.

Comparing the response to temporal drivers pre- and post-restoration indicated that restoration did not affect the response of autotrophic or heterotrophic respiration in either catchment or total respiration in Spooners to WTD_C, DiffWTD, total rain in the preceding 0, 7, 14, and 28 days or NDVI, despite the apparent temporal trends in respiration (Figure 8.10). In Aclands $RTot_{R/C}$ responded significantly differently to rain on the sample day pre- and post-restoration ($p=0.037$). Pre-restoration, when the total rain increased $RTot_{R/C}$ decreased, indicative of reduced respiration at the restored location compared to the control locations during drier conditions. Post-restoration, when the total rain increased $RTot_{R/C}$ also increased indicative of comparatively greater respiration at the restored location during wetter conditions. It should be noted that there was a minimum of 0.2 mmm rainfall on each sample day pre-restoration but no rainfall on the sample day for 5/7 occasions post-restoration. Indicating post-restoration respiration is unlikely to be controlled by rainfall on the sample day.

8.5.3 Hypothesis 3: The Spatial Effect of Restoration on Water Table Depths

Water tables fell at all locations following restoration, due to warmer and drier conditions (Figure 8.3a). At Aclands ½-distance the difference in water table depths between control and restored locations (DiffWTD) significantly reduced following restoration (Figure 8.11). As the control locations were wetter than the restored locations this decrease is indicative of the restored locations becoming comparatively wetter following restoration. However, given the DiffWTD (Figure 8.5) decreased during drier conditions (deeper WTD_C). The decrease in DiffWTD observed may have resulted from drier weather in 2013 and 2014 compared to 2012 rather than an effect of restoration.

Closest to the ditch at Spooners and Aclands, where it was hypothesised that the greatest effect of restoration on water table depths would occur, DiffWTD showed no significant change following restoration (Figure 8.11a).

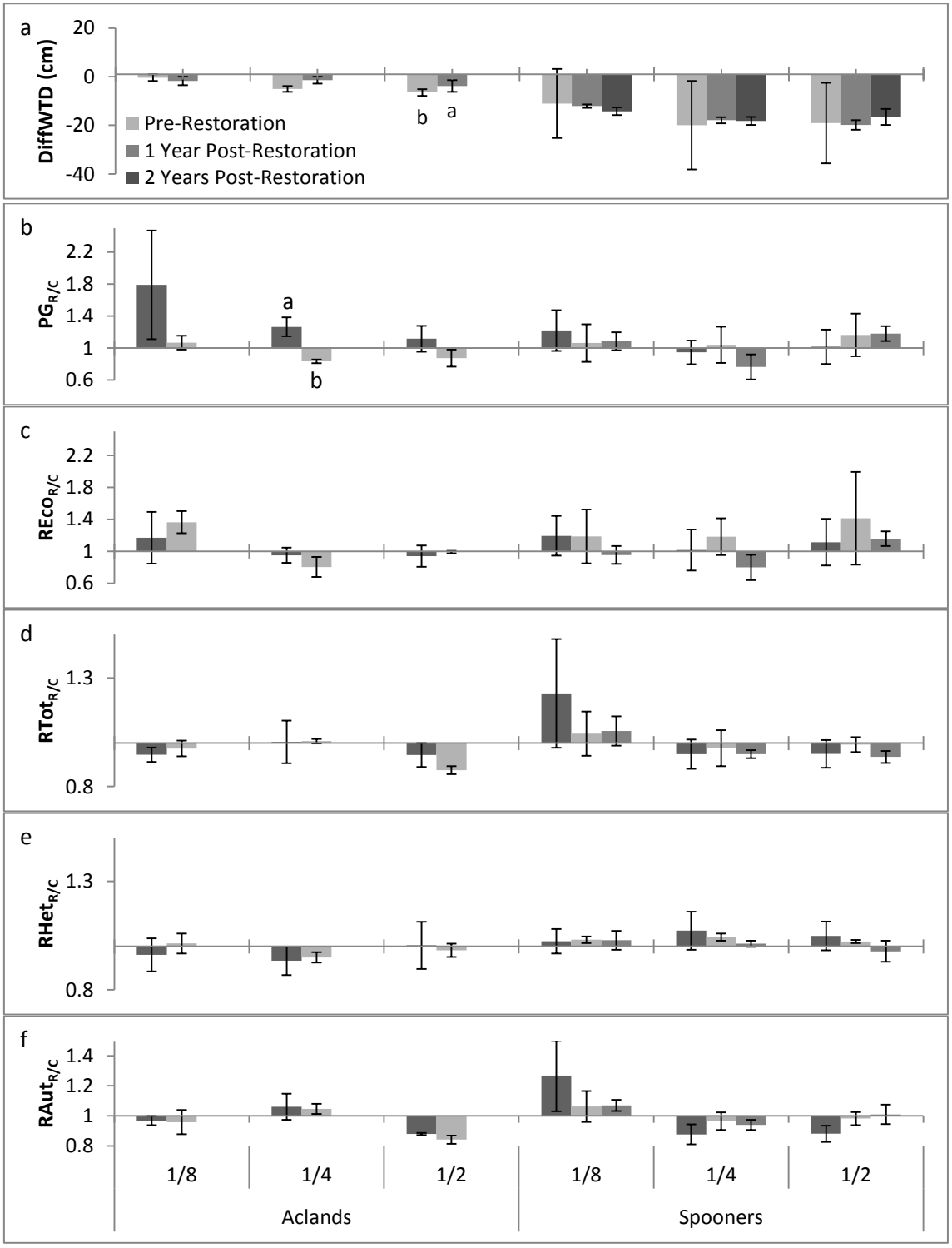

Figure 8.11 Spatial variation in a, difference in water table depth between control and restored locations (DiffWTD) (cm), b, photosynthesis at 600 µmol Photons m^{-2} s^{-1} ($PG_{R/C}$), c, ecosystem respiration ($REco_{R/C}$), and d, total ($RTot_{R/C}$), e, heterotrophic ($RHet_{R/C}$) and f, autotrophic below-ground respiration ($RAut_{R/C}$) at the restored location as a proportion of the variable at the controlled location at different proportional distances from the ditch at Aclands and Spooners, pre-(2012) and 1-year (2013 at Spooners, 2014 at Aclands) and 2-years (2014 at Spooners) post-restoration. Error bars are one standard error. Letters denote statistically significant groups ($p<0.050$). Higher values indicate depth to water table or CO_2 flux from restored location greater than depth to water table or flux from control location.

It was hypothesised that the greatest change in water tables would occur where peat was thicker. Across all locations where dipwells were not excluded (n=11) the relationship between peat thickness and DiffWTD was not significantly different pre- and post-restoration at either Aclands (p=0.889), Spooners (p=0.907) or both catchments together (p=0.730). The difference in water table depths between control and restored locations was greater where the peat was thicker (Figure 8.12 a) strongly controlled by the deeper peat at Spooners site 2. This finding suggests peat thickness did not influence the effect of restoration on water table depths.

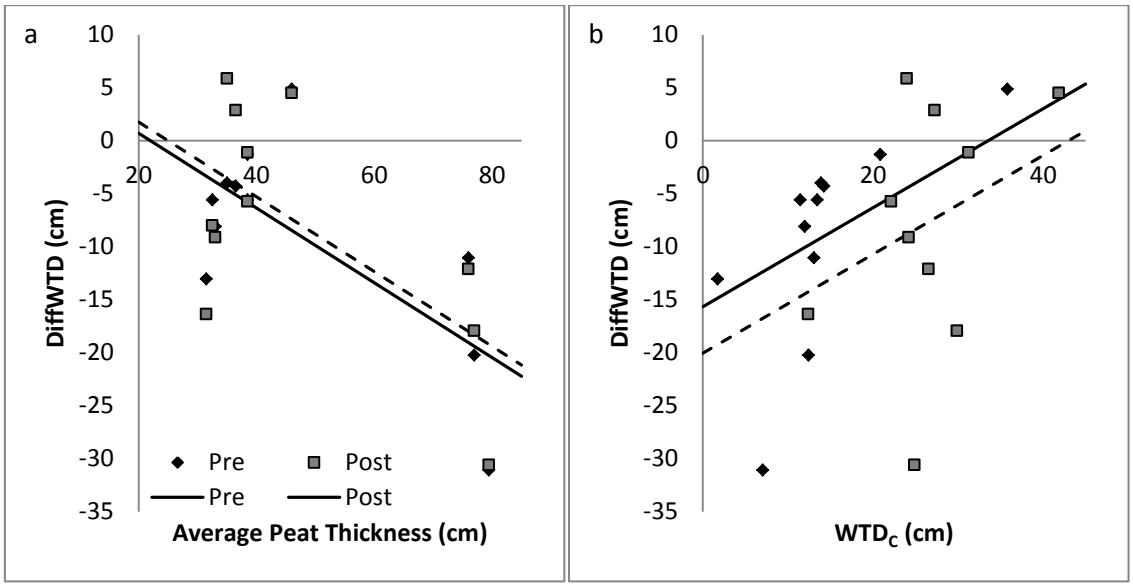

Figure 8.12 Spatial variation in the difference in water table depths between control and restored locations (DiffWTD) with average peat thickness of the control and restored pairs (cm) (a) and water table depth at the control location (WTD_C) (cm) (b) pre- and 1-year post restoration. Global models with the same slope but different intercepts drawn for pre- and post-restoration.

A sum-of-squares F-test was carried out to investigate if restoration altered the relationship between initial wetness conditions (WTD_C) and DiffWTD. There was no significant difference in the relationships pre- and post-restoration at Aclands (p=0.419), Spooners (p=0.143) or both catchments together (p=0.369). The difference in water table depths was greater where the initial conditions (WTD_C) were wetter (Figure 8.12b).

8.5.4 Hypothesis 4: The Spatial Effect of Restoration on CO_2 Fluxes

$PG_{R/C}$ significantly decreased at Aclands ¼-distance (Figure 8.11b, Table 8.1) indicating P_{G600} decreased at the restored locations compared to the control locations following restoration. The greatest difference between pre- and post-restoration average $PG_{R/C}$ occurred closest to the ditch (⅛-distance) but given the large standard error pre-restoration this change was not significant.

No other significant changes in gas fluxes were observed following restoration (Figure 8.11). $PG_{R/C}$ decreased at all distances from the ditch at Aclands between pre-restoration and 2-years after restoration at ⅛- and ¼-distances at Spooners but increased at ½-distance (Figure 8.11b, Table 8.1). $RAut_{R/C}$ showed a similar pattern (Figure 8.11b). $REco_{R/C}$ showed a much less clear pattern (Figure 8.11c) with no significant differences between years (Table 8.1). $REco_{R/C}$ increased at Aclands ⅛- and ½-distances but decreased at ¼-distance. At Spooners ⅛-distance decreased but ¼ and ½-distances showed an initial increase followed by a decrease. $RTot_{R/C}$ showed a similar pattern (Figure 8.11d) reflecting the combined effects of restoration on both heterotrophic and autotrophic respiration.

$RHet_{R/C}$ increased at Aclands ⅛- and ¼-distances and Spooners ⅛-distance but decreased at Aclands ½-distance and Spooners ¼- and ½-distances (Figure 8.11e) mirroring the effect of photosynthesis (Figure 8.11b). Generally, where photosynthesis increased following restoration, heterotrophic respiration decreased and *visa-versa*.

Table 8.1 Significance of T-tests between pre- and post-restoration at Aclands and ANOVA between pre-, 1 year post and 2 years post-restoration at Spooners within proportional distances (⅛, ¼, ½) from the ditch in each catchment. Shaded dark grey where p<0.050.

Variable	Distance	Aclands (T-test)	Spooners (ANOVA)
DiffWTD	1/8	0.735	0.146
	1/4	0.807	0.066
	1/2	0.023	0.365
$PG_{R/C}$	1/8	0.411	0.873
	1/4	0.029	0.664
	1/2	0.301	0.871
$REco_{R/C}$	1/8	0.366	0.837
	1/4	0.384	0.590
	1/2	0.751	0.864
$RTot_{R/C}$	1/8	0.718	0.424
	1/4	0.975	0.773
	1/2	0.222	0.339
$RHet_{R/C}$	1/8	0.227	0.891
	1/4	0.742	0.569
	1/2	0.816	0.570
$RAut_{R/C}$	1/8	0.882	0.426
	1/4	0.861	0.425
	1/2	0.248	0.149

Table 8.2 Average and standard error (in brackets) of species coverage (percent) by site and proportional distance from the ditch (plot). # coverage of 1 % at one location.

Catchment	Plot	Control or Restored	*Molinia caerulea*	*Non-Molinia*	Leaf Litter	*Potentilla erecta*	*Hypnum cupressiforme*	*Rhytidiadelphus quarrosus*	*Festuca sp.*	*Vaccinium myrtillus*	*Agrostis sp.*	*Liverwort*	*Galium saxatile*	*Pseudoscleropodium purum*	*Trichophorum cespitosum*	*Anthoxanthum odoratum*	*Narthecium ossifragum*	*Sphagnum fallax*	*Aulacomnium palustre*	*Carex echinata*	Species Richness
Aclands	1/8	C	80 (12)	4 (1)	90 (0)	1 (1)	1 (0)	1 (0)	.	#	#	.	.	#	.	.	.	.	#	.	4
		R	92 (2)	6 (4)	85 (3)	4 (3)	1 (1)	1 (0)	.	.	.	.	#	#	.	.	.	.	.	.	4
	1/4	C	73 (12)	6 (4)	90 (6)	#	2 (2)	.	#	1 (1)	#	#	.	1 (1)	1 (1)	.	.	1 (1)	.	.	5
		R	83 (7)	6 (2)	87 (3)	#	2 (2)	2 (1)	.		.	.	2 (2)	.	.	.	.	.	.	.	3
	1/2	C	92 (8)	5 (5)	83 (7)	1 (0)	#	.	3 (3)	.	#	#	.	.	#	.	.	.	.	.	3
		R	90 (6)	1 (0)	87 (3)	.	#	#	.	.	.	.	.	.	.	.	.	.	.	.	2
	Total	C	82 (6)	5 (2)	88 (3)	1 (0)	1 (1)	.	1 (1)	.	.	.	.	.	.	.	.	#	#	.	4
		R	88 (3)	4 (2)	86 (2)	1 (1)	1 (1)	1 (0)	.	.	.	.	1 (1)	.	.	.	.	.	.	.	3
Spooners	1/8	C	90 (10)	4 (4)	80 (15)	4 (3)	#	.	.	.	.	.	.	.	.	.	.	.	.	.	2
		R	100 (0)	1 (1)	93 (3)	1 (1)	.	.	.	.	.	.	.	.	.	#	.	.	.	.	1
	1/4	C	88 (7)	2 (2)	62 (20)	2 (2)	#	.	.	.	.	.	.	.	.	.	.	.	.	#	2
		R	80 (20)	15 (14)	90 (6)	1 (1)	1 (1)	1 (1)	10 (10)	2 (2)	.	.	.	.	.	1(0)	.	.	.	.	3
	1/2	C	83 (9)	21 (6)	87 (9)	5 (5)	1 (1)	.	4 (3)	.	.	1 (0)	.	.	.	.	10 (10)	.	.	.	3
		R	83 (9)	34 (17)	90 (6)	2 (2)	2(2)	.	18 (9)	3 (3)	8 (5)	#	#	.	.	.	.	.	.	.	5
	Total	C	87 (4)	9 (4)	76 (8)	4 (2)	.	.	1 (1)	.	.	.	.	.	.	.	3 (3)	.	.	.	2
		R	88 (7)	17 (8)	91 (3)	1 (0)	1 (1)	.	9 (5)	2 (1)	3 (2)	.	.	.	.	.	.	.	.	#	3

8.6 DISCUSSION

8.6.1 Hypothesis 1: The Effect of Restoration on Water Table Depths through Time

Due to a wet baseline year followed by two drier years (Figure 8.2) water tables fell following restoration at both the control and restored locations (Figure 8.3a). Allowing for this variability by comparing water table depths at control and restored, locations there was no significant change in the difference in water depth between the control and the restored locations following restoration (Figure 8.3b). Other studies investigating the effect of ditch blocking on water table depths (Komulainen *et al.* 1999, Jauhiainen *et al.* 2002, Wilson *et al.* 2010, Holden *et al.* 2011) have consistently found a rise in average water tables following ditch blocking. Where these studies have reported pre- and post-restoration conditions they had similar water table depths in their control locations pre- and post- restoration. Unlike Wilson *et al.* (2010) and Holden *et al.* (2011) who measured water table depths continuously, in this study water table depths were measured concurrently with gas flux monitoring. Consequently measurements were biased towards drier conditions, a change in water table depths may have been observed if wetter conditions were included.

At Aclands the change in relationship between WTD_C and DiffWTD (Figure 8.5) suggests that at Aclands restoration had an effect on water table depths, raising them less during wet conditions and/or maintaining them during dry conditions at the restored locations. Holden *et al*. (2011) found the response of water tables to rainfall to be reduced following restoration due to a reduction in the range of water table depths. Given water tables fell in this study following restoration (Figure 8.4), due to drier conditions, it is improbable that the potential response to rainfall was limited. Conversely Wilson *et al*. (2010) found water tables to increase in response to rainfall following restoration due to reduced overland flow. This may have been the case at the control locations, causing an increase in DiffWTD during wetter conditions (Figure 8.5) but WTD_C showed no change in response to rainfall pre- and post-restoration. Wilson *et*

al. (2010) also found water tables to be maintained at higher levels for longer during dry conditions, whilst Holden *et al*. (2011) found water tables at restored locations fell below those of drained locations during the driest conditions. As Holden *et al*. (2011) did not present baseline data for their sites it is not possible to know if this was amplified or diminished by restoration.

Schouwenaars (1993) argues that for water tables to rise following restoration of bog subject to peat cutting and cultivation, precipitation must be greater than seepage and evapotranspiration. It is likely in these shallow peats dominated by *Molinia caerulea*, that horizontal and vertical seepage and evapotranspiration (Nieveen and Jacobs 2002) rapidly diminished water stored during rainfall events in both the control and restored locations resulting in the drying out of pools, as observed in both 2013 and 2014. Despite this, the change in WTD_C-DiffWTD relationship (Figure 8.5) suggests restoration maintained shallower water tables during drier conditions in the restored locations at Aclands, possibly due to reduced seepage. However, this did not result in significant changes to average water tables following restoration.

8.6.2 Hypothesis 2: The Effect of Restoration on CO_2 Fluxes through Time

8.6.2.1 Photosynthesis and Ecosystem Respiration

Photosynthesis and ecosystem respiration increased in 2013 and 2014 reflecting the better growing conditions (Figure 8.6a & b). There were no significant changes in $PG_{R/C}$ or $REco_{R/C}$ (Figure 8.6c & d) following restoration reflecting no significant change to DiffWTD (Figure 8.3b). To initiate a return to a *Calluna vulgaris* dominated ecosystem containing *Sphagnum* (Rutter 1955), which was previously present on Exmoor (Chambers *et al.* 1999), it has been suggested that the water table must be maintained near the peat surface without great fluctuation (Schouwenaars 1993, Holden *et al.* 2004). Rutter (1955) suggested water tables must remain within 8 cm of the surface of a wet heath for *Calluna vulgaris* growth to occur. Even six years after restoration, water tables in restored peatlands may fluctuate to a greater extent than in

more pristine peatlands (Holden *et al.* 2011). Water table depths measured at the restored locations in this study still reached as deep as 71 cm post-restoration (at S2R3 on 21/07/2014 and S2R2 on 04/08/2014). If water tables are insufficiently high and stable following restoration it may be that *Molinia caerulea* adapts its morphology (root distribution and tussock height) to suit the new water table depth conditions (Rutter 1955) rather than being outcompeted by other species. An ecosystem dominated by *Molinia caerulea* (86 ±3 %) does not sequester carbon (chapter 5) so unless vegetation change occurs this peatland may continue to be a carbon source.

In other catchments within Exmoor National Park subject to ditch blocking, vegetation communities have been shown to change within three years of restoration to a community more rich in *Sphagnum* (Barrowclough 2014) (based on a three year sample frequency). Catchments with the same initial National Vegetation Classification class (NVC) (Rodwell 1991) as Aclands and Spooners, M25 (*Molinia caerulea – Potentilla erecta* mire), changed to vegetation more typical of a poor-fen following restoration, (NVC M6 *Carex echinata-Sphagnum recurvum/auriculatum* mire) (Barrowclough 2014). However, no *Sphagnum* cover has been noted during NEE measurements undertaken at the sites studied here, except at Aclands site 1 where *Sphagnum fallax* was present prior to restoration; evidence thus far suggests that neither Aclands nor Spooners have altered their vegetation species composition in response to restoration. A slower response may have occurred at these sites due to their exceptionally poor diversity prior to restoration, locally limiting the species available to recolonize, if conditions are altered.

Comparing these findings to other research it has been shown that in the short-term (1-2 years), artificially raising the water tables can have a range of effects – e.g. it has been shown to reduce gross carbon fixation in a *Lolium perenne* grassland (Best and Jacobs 1997) and significantly decrease photosynthesis and ecosystem respiration from a *Calluna vulgaris* dominated bog (Komulainen *et al.* 1999). This decrease in photosynthesis and ecosystem respiration has been shown to persist over longer timescales (80 years) in poor fens where no

apparent changes to vegetation occurred (Ballantyne *et al.* 2014). However, more often changes to water table depths result in subsequent changes to vegetation, observed up to 11 years post-restoration (Komulainen *et al.* 1999, Jauhiainen *et al.* 2002, Haapalehto *et al.* 2010, Bellamy *et al.* 2012), which further influences photosynthesis and ecosystem respiration. Ditch blocking at a Finnish bog raised water tables and increased *Eriophorum vaginatum* cover in the first year following restoration (Komulainen *et al.* 1999) and although this increased photosynthesis, ecosystem respiration reduced. In all these studies restoration significantly raised water tables which was not the case in this study. It is still unknown how *Molinia caerulea*, a species adapted to survive prolonged periods of waterlogging (Taylor *et al.* 2001) will respond in the longer-term if water tables are eventually raised.

Overall raising water tables has been found to have no significant effect on NEE comparing a drained site to a site 80 years after restoration in a poor fen, despite difference in P_G and R_{Eco} (Ballantyne *et al.* 2014) and increased seasonal CO_2 uptake in an ombrotrophic bog within 2 years of restoration with the greatest effect in the hollow sites colonised by mire vegetation including *Sphagnum rubellum* and *Sphagnum balticum*. (Komulainen *et al.* 1999). In this study, restoration did not consistently increase or decrease P_{G600} and R_{Eco} across both catchments (Figure 8.7), following restoration CO_2 uptake was greater at Spooners but less at Aclands. Therefore, it is currently unclear if and how restoration has affected NEE, and therefore whether restoration will increase carbon sequestration.

8.6.2.2 Below-Ground Respiration

The author is unaware of any studies reporting the effect of restoration on either heterotrophic or autotrophic below-ground respiration. Therefore, this study provides the first insight into the immediate effects of restoration on partitioned below-ground respiration rates. Heterotrophic respiration in both catchments and autotrophic respiration in Spooners were greater at the restored locations pre- and post-restoration (Figure 8.9a) with inter-annual variability greater than the difference between control and restored pairs. In both catchments there

was no significant change in total, heterotrophic or autotrophic respiration following restoration (Figure 8.9b). Examining how restoration affected below-ground respiration at different proportional distances from the ditch (Figure 8.11d, e & f) indicated that the response to restoration was not uniform. Ditch blocking has been found to have no effect on total below-ground respiration from a *Lolium perenne* grassland (Best and Jacobs 1997) or in the first year following restoration of a Finnish bog (Komulainen *et al.* 1999) but cause significant reductions in total respiration in the second year.

At Spooners, the difference in heterotrophic respiration between control and restored sites generally decreased over time (Figure 8.10b). This effect could be due to two main reasons. Firstly, assuming deeper water tables increase the volume of oxygenated peat and promote more aerobic respiration (Clymo 1983) then respiration would be expected to be greater at the drier restored locations. As the difference in water table depths between the control and restored locations decreased over the same period, primarily due to climatic conditions, the difference in respiration rates would be expected to decrease. However, heterotrophic respiration has shown no significant relationships with water table depth prior to restoration (Table 5.5) suggesting this is unlikely. Secondly, as leaf litter was cleared from the ground surface the locations with the greater initial respiration rates (restored locations) would be expected to degrade the available organic matter more rapidly thereby reducing the rate of respiration over time compared to the control locations. This finding suggests restoration had little impact on heterotrophic respiration at Spooners.

At Aclands heterotrophic respiration was consistently greater at the restored locations following restoration (Figure 8.10a). As restoration appears to have raised water tables during dry conditions (Figure 8.5), it is possible that restoration maintained wetter near surface conditions during the dry conditions of 2014 enhancing decomposition. Cellulose decomposition has been found to be limited at a depth of 10 cm compared to 30 cm in a drained peatland due to moisture availability despite a moisture content of 320 to 560 % by mass (Lieffers 1988). Similarly decomposition of Scots pine needles and fine roots in

the top 10 cm of a sedge pine fen was greater in a pristine site compared to a drained site suggesting moisture stress in the surface layers of the drained sites. Again it should be noted that no significant relationships between heterotrophic respiration and water table depth were found prior to restoration (Table 5.5) however, the very low hydraulic conductivity of peat means that changes in water level do not necessarily result in comparable changes to soil moisture at the surface. As reducing heterotrophic respiration and therefore conserving the existing peat store is the first stage in returning a system to carbon sequestration, a trend towards increased heterotrophic respiration raises concerns about the efficacy of ditch blocking as a means to protect the existing carbon store. It is possible there is a water table threshold, above which heterotrophic respiration is limited by saturation and therefore oxygen availability, but that due to the dry conditions post-restoration this was not observed.

8.6.3 Hypothesis 3: The Spatial Effect of Restoration on Water Table Depths

It was hypothesised that the response of water table depths to restoration would be greatest nearer the ditch. Instead, the only significant change occurred at Aclands ½-distance where DiffWTD significantly decreased indicating water table depths became more similar following restoration. It may be that as average water tables were deeper closer to the ditch prior to restoration (Figure 6.2a), and DiffWTD was less where the water table was deeper (Figure 8.13b) that there was limited scope to alter water table depths during dry conditions. Continuous monitoring of different ditches within the same catchments found locations with deeper water tables prior to restoration to show the greatest rise in average water tables post-restoration. Additionally some of the wetter areas become drier post-restoration (Luscombe *et al.* 2015) however, this study included both wet and dry conditions.

Water tables have been found to be deeper closer to drainage ditches (Wilson *et al.* 2010, Holden *et al.* 2011, Laine *et al.* 2011, Luscombe *et al.* In prep) and this gradient was removed (Laine *et al.* 2011), reduced (Wilson *et al.* 2010) or

remained (Holden *et al.* 2004) following restoration even through average water tables were raised by blocking in all three studies.

Wilson *et al.* (2010) found peat depth to influence water table depths more strongly post-restoration compared to pre-restoration, when drainage factors and rainfall on the preceding day were more important. No change in the response of DiffWTD to peat thickness was observed pre- and post-restoration in this study (Figure 8.13a), possibly due to the limited thickness (<46 cm) of the peat in the study sites with the exception of Spooners site 2. It may also be because unlike in their study water tables did not significantly rise in response to ditch blocking and therefore were more likely to be governed by the same processes pre- and post-restoration such as microtopography and rainfall (Luscombe 2014).

8.6.4 Hypothesis 4: The Spatial Effect of Restoration on CO_2 Fluxes

8.6.4.1 Photosynthesis and Ecosystem Respiration

Spatially, restoration non-significantly reduced photosynthesis in the restored locations compared to the control locations at all distances from the ditch at Aclands and at ⅛- and ¼- distances at Spooners (Figure 8.11b). The greatest, but not significant, change was closest to the ditch in both catchments, as hypothesised. However, this cannot be linked to an equivalent change in water table depths so is unlikely to be solely due to restoration.

In an unrestored state a greater coverage of non-*Molinia* species occurred where water table depths were closer to the surface (Table 6.5) indicating their competitive advantage over *M. caerulea* in wetter conditions Given that during dry conditions water tables were comparatively higher at the restored locations (Figure 8.5) post-restoration then climatic variability may have limited photosynthesis from *M. caerulea* resulting in a decrease in $PG_{R/C}$ observed at Aclands and Spooners ⅛ and ¼-distances (Figure 8.11b).

At Spooners the increase in $PG_{R/C}$ and $REco_{R/C}$ (Figure 8.11b & c) at ¼ and ½-distances may have occurred due to the different response of the vegetation

present (Table 8.2) to the climatic conditions. For example, Spooners ½-distance control location has on average 10±10 % *Narthecium ossifragum,* a water tolerant species, whereas the restored location had *Festuca sp., Vaccinium myrtillus* and *Agrostis sp.* species which prefer drier conditions. In a wetter year conditions would be better for the water tolerant species found at the control location and sub-optimum for the drier species resulting in lower $PG_{R/C}$ and $REco_{R/C}$ and *visa versa* in a drier year.

Post-restoration blocked gully floors have been found to have higher ecosystem respiration and photosynthesis compared to gully sides or interfluves (Clay *et al.* 2012) contradicting findings from this study, where the greater change was nearer the ditch. However, Clay *et al.* (2012) found that different positions along a transect were associated with differing vegetation communities. Komulainen *et al.* (1999) also found ecosystem respiration to be greater in plots further from the feeder ditch, again this was an effect associated with changing vegetation.

8.6.4.2 Below-Ground Respiration

Changes in $RAut_{R/C}$ mirrored changes in $PG_{R/C,}$ (Figure 8.11 b & f) reflecting the dependence of below-ground autotrophic respiration on photosynthetic activity (Subke *et al.* 2006). As discussed in section 8.6.4.1 this is most likely reflects small variation in vegetation communities responding differently to climatic variability.

The pattern in $RHet_{R/C}$ generally mirrored the pattern in $PG_{R/C}$ (Figure 8.11b & e). It may be that where locations were wetter (e.g. Aclands ¼-distance) this limited photosynthesis at the restored locations but enhanced heterotrophic respiration at restored locations by alleviating moisture stress. Again this suggests that restoration may have increased the decomposition of the existing peat store.

It may be that restoration would have had more impact had there been more rainfall for the peat dams to retain (Figure 8.2). A significant change in water tables may have resulted in more significant and possibly different changes in

CO_2 fluxes. In addition this study was short (3 years) compared to the timescales over which vegetation composition and peatland form and function change (Belyea and Baird 2006). Further measurements are required under a greater range of climatic conditions and over a longer time span to determine if the initial trends observed in this study are maintained.

8.7 CONCLUSION

Although carried out in usually dry conditions this study found ditch blocks in shallow peats did not raise water tables. However, at Aclands the relationship between climatic conditions and DiffWTD was significantly different pre- and post-restoration ($p=0.020$) suggesting shallower water tables were maintained during dry conditions at the restored locations as a result of restoration. This suggests ditch blocks had no significant effect during wet conditions and only had a significant effect in some areas during dry conditions

Non-significant changes in photosynthesis, ecosystem respiration and below-ground autotrophic respiration could be explained by variability in vegetation composition responding to climatic conditions. This may have been enhanced by restoration during dry conditions at Aclands, with wetter conditions limiting photosynthesis. This suggests that where and when restoration raised water tables, conditions became sub-optimum for *Molinia caerulea,* which may over time enable other species to successfully compete in this species-poor ecosystem.

Heterotrophic respiration of the peat store increased at Aclands following restoration, possibly due to the alleviation of moisture stress in the surface layer. This finding raises concerns about the ability of restoration to protect the existing peat store, a first step towards reinstating carbon sequestration. This study suggests a small rise in water tables may decrease photosynthesis and increase heterotrophic respiration shifting the peatland towards carbon release. It remains uncertain how *Molinia caerulea* will respond to changes in water table depths (if any) in the longer term and whether changes in water table depths will

be sufficient to promote the change in vegetation required to resume CO_2 sequestration.

8.8 ACKNOWLEDGMENTS

The authors would like to thank the Exmoor Mires Project for their help with site access, Exmoor National Park and the May family for permission to work on the sites. This research received financial support from South West Water and The University of Exeter (SK05284).

9 GENERAL DISCUSSION

This study aimed to determine the effect of peatland restoration on CO_2 exchange and potential for climate change mitigation. Although carbon markets may provide a potential funding source for peatland restoration (Bonn *et al.* 2014), there were no suitable emissions factors for drained *Molinia caerulea* dominated peatlands (Birkin *et al.* 2011), before this work began, revealing a need to quantify CO_2 fluxes in these ecosystems. This was particularly pertinent for Exmoor, where the study was located, as over 2000 hectares of drained, *M. caerulea* dominated blanket bog was earmarked for restoration at the start of the PhD project. In addition, studies on the effects of drainage on CO_2 fluxes (Oechel *et al.* 1998, Chimner and Cooper 2003, Strack *et al.* 2006, Jaatinen *et al.* 2007) and restoration (Silvola *et al.* 1996a, Komulainen *et al.* 1999, Urbanová *et al.* 2012) have been focussed on *Sphagnum* dominated peatlands so an evidence base for the function of *M. caerulea* dominated peatlands was required for both pre- and post-restoration conditions. The controls on CO_2 fluxes and the potential effects of restoration on *Molinia caerulea*, a plant evolved to tolerate waterlogging (Taylor *et al.* 2001), were unknown. This study firstly sought to quantify CO_2 fluxes from a shallow, drained *Molinia caerulea* dominated peatland and to understand the temporal and spatial controls on these fluxes. To support this work novel remote sensing techniques were developed which provided a daily resolution proxy for vegetation phenology and fine scale monitoring of vegetation structure across landscape extents. Having established a baseline understanding of function prior to restoration, the study then aimed to quantify the spatial and temporal effects of ditch blocking on water table depths and CO_2 fluxes in the first and second growing seasons following restoration. These three work packages provide a framework with which to evaluate how this study has advanced existing scientific understanding of these ecosystems.

9.1 REMOTE SENSING OF VEGETATION PHENOLOGY AND STRUCTURE

Prior to this work the use of digital images as measures of vegetation phenology had primarily been applied to forested ecosystems (e.g. Ahrends *et al.* 2008) employing advanced technologies such as computer controlled digital cameras. Chapter 4 demonstrated that an inexpensive, off-the-shelf time-lapse camera is capable of monitoring changes in vegetation phenology with a daily time-step in an isolated study area, and established the utility of these data to scale up local observations to globally available vegetation products monitored by Earth observing satellites. Due to its cost and ease of use, this method could have widespread applicability, particularly within citizen science (e.g. in schools) or where funding is limited (e.g. environmental charities).

Previous studies had demonstrated the potential for using Moderate resolution Imaging Spectroradiometer (MODIS) vegetation products to monitor both vegetation phenology (e.g. Ahl *et al.* 2006) and estimate CO_2 fluxes (e.g. Schubert *et al.* 2010, Kross *et al.* 2013) but again most previous work had demonstrated the application of this technique in ecosystems that are quite different from upland peatland systems such as the study catchments used in this PhD. The *in situ* digital camera images enabled the validation of a wider range of MODIS vegetation products to determine which was the most appropriate for these deciduous grass ecosystems. This work has provided a robust and repeatable method for assessing the phenology of *Molinia caerulea* at a regional scale using MODIS Normalised Difference Vegetation Index (NDVI). This method could be extended to unmonitored locations, in the first instance across Exmoor, but also to any deciduous grass dominated ecosystem. Deciduous grass ecosystems occur globally from the tussock grasses of the arctic and alpine tundra, pampas, steppe, prairies and altiplano to the warm grasses of the rangelands and savannahs. Drivers of seasonal variation vary between these ecosystems but the pattern of annual variability could be captured using the same method as outlined in this study for the deciduous grasses of Exmoor.

This method would allow a phenological timeseries to be estimated which could then be used in conjunction with meteorological observations to estimate CO_2 fluxes. Although the uncertainties associated with these CO_2 estimates would not be trivial, the cost and difficulty of monitoring in some locations means that upscaling from a few well-studied sites to calculate regional fluxes is unavoidable and the remote sensing methodology validated in this thesis could be extremely useful.

The MODIS historic database would allow NDVI-timeseries to be retrospectively compared to temporally variable CO_2 fluxes measured across a wider range of ecosystems to potentially extend its applicability. Being able to estimate inter- and intra-annual variability in regional vegetation phenology and consequently model CO_2 flux timeseries should be of interest to those assigning emissions factors to specific vegetation types, particularly in ecosystems such as these where annual net ecosystem exchange (NEE) appears to be largely driven by primary productivity. Primary productivity has been found to be the main control on annual NEE in alpine grasslands (Wohlfahrt *et al.* 2008), rangelands including; Great Plains grasslands, desert shrubland, desert grasslands and sagebrush stepp (Polley *et al.* 2010) as well as temperate Japanese oak and birch forests (Saigusa *et al.* 2005).

The presence of drainage features has obviously altered the ecohydrological functioning of these landscapes. Despite this, the explicit role of drainage features on CO_2 fluxes has not previously been investigated. This study is the first to suggest that spatial variation in photosynthesis within these species-poor ecosystems can be linked to water table depths even where a change in vegetation composition is not observed (Table 6.5). It also highlighted the insignificant relationship between proximity to a drainage ditch and water table depths. This demonstrates that despite their prominence within the landscape, these structural features are not the primary control on water table depths and therefore cannot be used to map water table depths (or photosynthesis) at a landscape scale. Chapter 7 addressed this by using structural characteristics of *M. caerulea* tussocks to determine the spatial distribution of water table depths

and CO_2 fluxes and showed that ecosystem respiration was correlated to tussock height (Figure 7.15g).

The remote sensing methods developed in chapter 4 enabled finer temporal resolution estimation of vegetation phenology than conventional manual techniques. In chapter 7 a method was developed which enabled these tussock grasslands to be represented at a fine spatial scale (5 cm resolution) across larger spatial extents than was previously possible. Novel remote sensing methods, in particular Unmanned Aerial Vehicle (UAV) based Structure from Motion derived surface models, have been tested in these tussock grasslands and show the potential for these low cost, high resolution methods to be used to estimate spatially distributed structural parameters at a landscape scale. Recently spectral classifiers have been applied to UAV images to upscale CO_2 fluxes from both chamber and eddy covariance (Vivoni *et al.* 2014) measurements but these use fluxes from distinct vegetation communities or microforms. Traditional remote sensing techniques using per-pixel landcover mapping overlook important functional relationships between vegetation structure and CO_2 fluxes. Using vegetation structure to estimate spatial distribution of CO_2 fluxes within a vegetation community is an innovative and potentially rewarding method of upscaling fluxes and worthy of further investigation.

Both the NDVI timeseries and UAV-based image derived digital surface models enabled upscaling of measurements collected during this study, one over time the other over space. Further work is required to determine which structural characteristic(s) of the *M. caerulea* tussock are most affected by changes in water table depths but this method shows promise as a means to estimate the spatial distribution of water tables. Future or repeated use of these methods may demonstrate changes in vegetation phenology (due to changes in vegetation composition) and structure (due to phenotypic plasticity) resulting from restoration. Both these methods enable robust and repeatable fine scale monitoring of remote and complex landscapes.

9.2 Spatial and Temporal Controls on CO_2 Fluxes in a Degraded Peatland

Of importance to this study, MODIS NDVI provided a finer temporal resolution (daily) dataset compared to more traditional *in situ* monitoring techniques. In conjunction with water table depth and temperature measurements this provided a foundation on which to assess the temporal controls on CO_2 fluxes. This study highlighted the strong seasonal variation in photosynthesis as well as ecosystem and below-ground respiration rates associated with vegetation phenology and soil temperature. Temporal variation in water table depths did not affect any of the CO_2 fluxes measured however, spatial variation in species richness and coverage of non-*Molinia* species were both related to seasonal water table depth. Additionally photosynthesis was lower where water tables were raised following restoration indicating the existing plant communities preferred drier conditions. This demonstrates how, over longer timescales, water table depths indirectly influence CO_2 fluxes through their control on vegetation composition.

It is believed that these are the first reported photosynthesis rates for *Molinia caerulea* at a fixed photosynthetically active radiation (PAR) (Figure 5.3). Therefore these are the first values that can be directly compared across ecosystems without the confounding influence of variable light conditions during data collection and so this is a unique outcome of this PhD project. Greater photosynthetic and ecosystem respiration rates resulting in a smaller (or negative) annual carbon uptake compared to a *Sphagnum* peatlands were anticipated (section 2.1.6). The work has also shown how heterotrophic, autotrophic and total below-ground respiration rates change seasonally and spatially and furthermore, these are believed to be the first reported for a *M. caerulea* dominated peatland and add to the small number of peatland studies which partitioned below-ground respiration rates (Figure 5.4). Notably higher photosynthetic rates, lower below-ground respiration rates and an inconsistent response to temporal variation in water table depths demonstrate

functional differences between these humified *M. caerulea* dominated peatlands and actively forming *Sphagnum* peatlands (Figure 9.1).

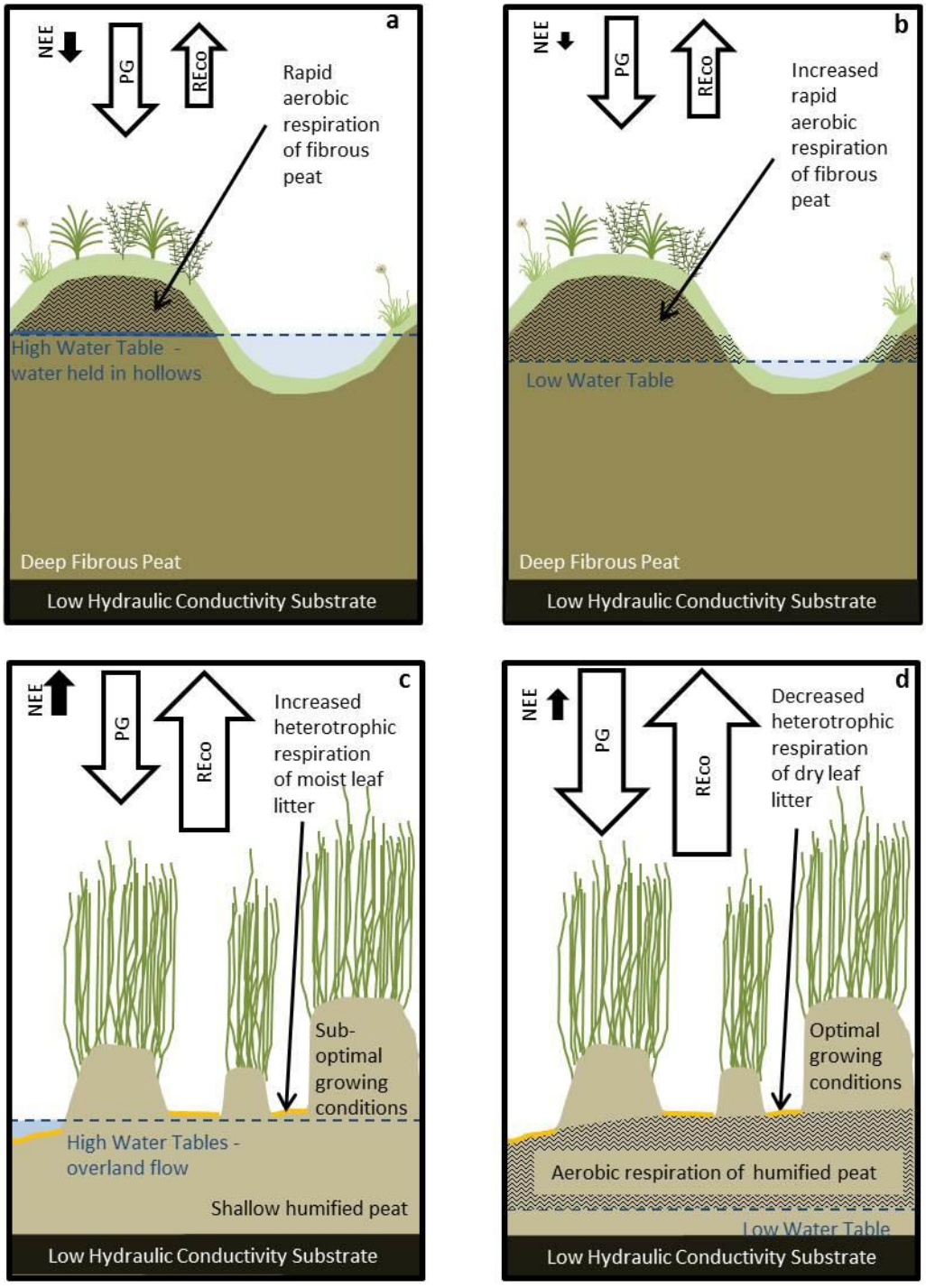

Figure 9.1 Functioning of a deep actively forming *Sphagnum* peatland (a & b) and a shallow degraded *Molinia caerulea*-dominated peatland (c & d) under high (a & c) and low (b & d) water tables.

Potential respiration rates (e.g. determined through incubation experiments) were not measured in this study but it is possible that the potential respiration rates would be greater in the leaf litter and in the upper millimetres of the peat compared to deeper in the humified peat (Lafleur *et al.* 2005). The insignificant response of heterotrophic respiration rates to water table depths may be due to these two sources of organic matter (Figure 9.1). It is suggested that under high water table conditions a reduction in oxygen availability reduces respiration from the peat but promotes respiration from the leaf litter by alleviating moisture stress. Conversely, under dry conditions respiration from the leaf litter is moisture limited, but aeration of the humified peat and greater root exudate production enhances respiration at depth.

This study has also highlighted the competitive nature of *Molinia caerulea* over a range of environmental conditions (e.g. aspect, altitude etc.) and in particular water table depth (Table 6.1 and Table 6.2). Although non-*Molinia* species and species richness were greater where the water table was shallower, the dominance of this species across the landscape raises concerns about the magnitude of environmental change required to promote a change in vegetation composition towards communities more associated with carbon sequestration.

Both *Sphagnum* and *Molinia caerulea* tussocks engineer the landscape to maintain optimum conditions for growth (Figure 9.1). In a *Sphagnum*-dominated peatland, capillary action draws water to the surface and the hummock and hollow microtopography holds water following rainfall to maintain high water tables. In a *Molinia caerulea* dominated-peatland, tussock formation results in areas of interconnected peat, which enable rapid overland flow following rainfall. *Molinia caerulea* can survive both water logging and periods of deeper water tables (due to its deep roots, >80 cm) but, by facilitating fluctuating water tables through rapid overland flow, *Molinia caerulea* maintains dominance in these landscapes. In addition, dense mats of leaf litter smother seedlings and rapid growth of large spreading leaves in the spring shades other vegetation. Furthermore, in the autumn, nutrients are translocated from the leaves to the root nodes (Taylor *et al.* 2001). By retaining nutrients within the

plant the *Molinia caerulea* is less likely to be nutrient limited resulting in a competitive advantage in these nutrient poor environments.

Due to these functional differences between deep *Sphagnum* peatlands and shallow *Molinia caerulea*-dominated peatlands, restoration techniques reported elsewhere may not be applicable to these environments (Grand-Clement *et al.* 2015). In addition, due to the substantial deviation in form and function from active *Sphagnum* peatlands it cannot be assumed that over the longer-term, restoration will have similar effects over a given timescale to those observed in other peatlands.

The findings arising from this research represent a significant contribution toward scientific understanding of the temporal and spatial controls on CO_2 fluxes in a drained *Molinia caerulea* peatland. The fluxes measured and modelled provide a baseline to which future change may be appraised. Estimation of annual net ecosystem exchange, although very uncertain indicate that in a drained condition these shallow *Molinia caerulea* peatlands are sources of CO_2. This highlights the need for ecohydrological restoration to prevent the loss of existing carbon stores. This demonstrates that these peatlands are not sustainable in their current condition, providing evidence which could be used to justify further investment in peatland restoration schemes.

The estimates provided by this study may prove to be useful for GEST (Greenhouse gas Emission Site Type) approaches to carbon markets. They are the best, most reliable estimates ever produced for this vegetation type and could be applied with a degree of confidence across Exmoor, and with increasing uncertainty be extended across all *Molinia caerulea* dominated peatlands. Data collected for this thesis (pre-restoration emission estimations) have already been used in a Peatland Code pilot project application.

9.3 EFFECT OF RESTORATION ON CO_2 FLUXES

Due to climatic variability and below average rainfall over the two growing seasons since restoration, it has been difficult to unequivocally identify the impacts of restoration and to be able to assess with any certainty whether trends observed are typical for restoration. If they are typical then it would appear that restoration does not always have a significant effect over the short timescales that can be measured in a PhD programme, as observed in Spooners catchment (section 8.5). In Aclands catchment restoration raised the water table during dry conditions (Figure 8.5) and photosynthesis reduced non-significantly (Figure 8.6). In an unrestored state temporal variation in CO_2 fluxes was not related to water table depth (section 5.4.3) but spatially, photosynthesis was greater in drier locations (Table 6.5) so it is not certain that the response in photosynthesis was due to raised water tables. Over the longer timescales now planned for continued monitoring of these variables it will be possible to see if these relationships change as restoration takes effect and water tables stabilise.

To date it appears that the disturbance due to restoration has been insufficient to promote vegetation change given the range of conditions over which *M. caerulea* is competitive. Spatial variation in water table depths and vegetation composition pre-restoration indicated that where water tables were closer to the surface other species were present even though *M. caerulea* was still dominant and that *M. caerulea* remained dominant over a range of conditions. This indicates a small change in seasonal water table depth may induce some change in vegetation composition but to diminish the presence of *M. caerulea* a greater change will be required.

Shallower water tables during dry periods may have alleviated moisture stress increasing heterotrophic respiration of the peat store. This suggests restoration failed to protect the existing carbon store and reduced photosynthesis moving the peatland towards being a greater carbon source (Figure 9.2). However, as previously stated the conditions over the post-restoration period were unusually

dry. Given wetter or more normal conditions the effect on water table depths may have been greater and sufficient to promote vegetation change and suppress respiration of the peat store. Further study is required under a greater range of conditions and over a longer timescale to understand if, when, how and under what conditions (e.g. wetter weather) restoration has a significant impact on water table depths and the resultant effect on CO_2 fluxes.

Figure 9.2 outlines the observed and theorised processes resulting from restoration, highlighting the need for a process shift in order to reduce net ecosystem release and promote carbon uptake. This shift may occur under sustained wetter conditions but it is more likely to occur with additional management as has been shown by Heffernan (2008) albeit in desert wetlands. An increase in flooding resulted in the replacement of desert riverine wetlands by vegetation free gravel beds. However, flood protection alone was insufficient to restore the wetlands, additional measures including the exclusion of cattle were required.

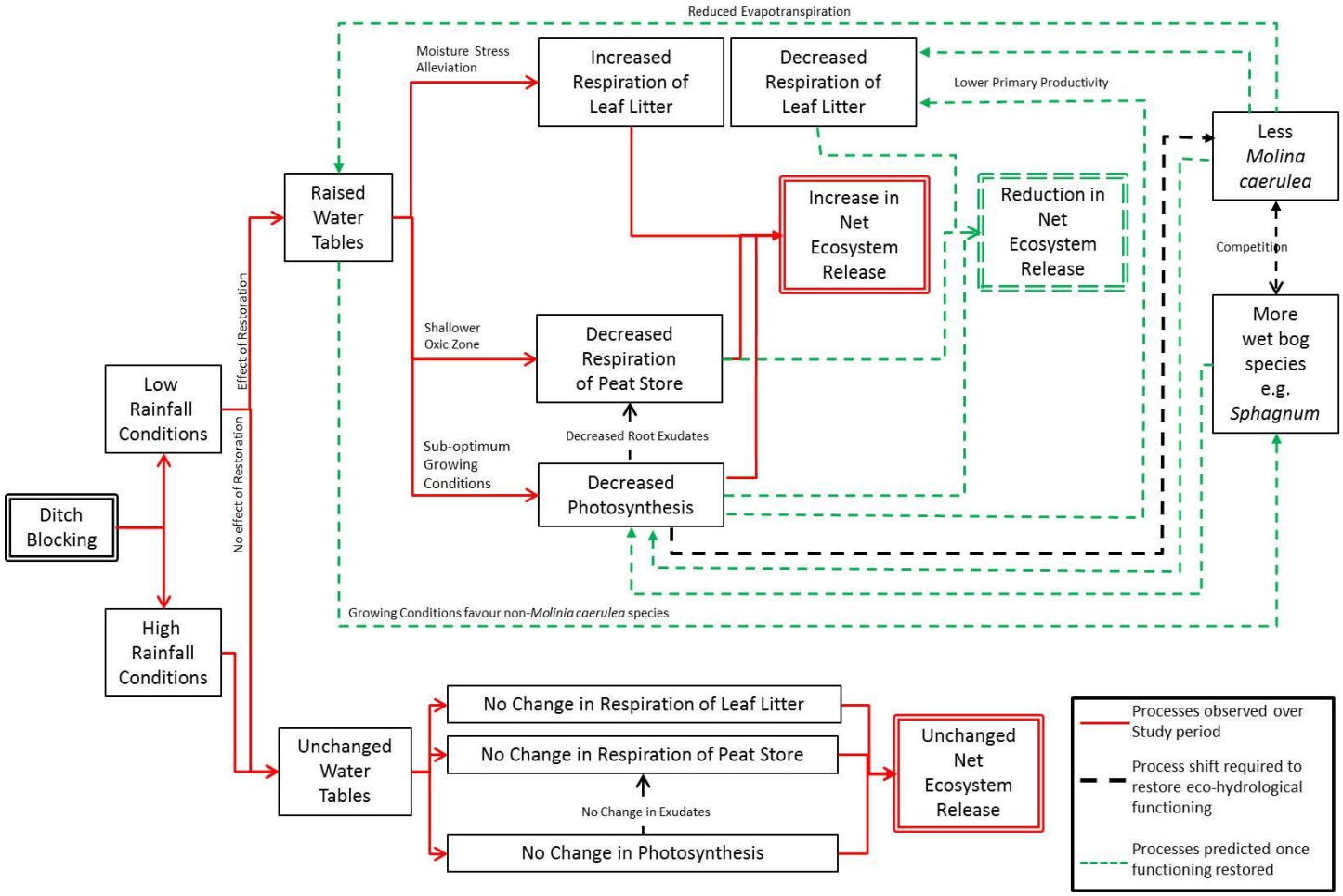

Figure 9.2 Processes observed (red) following restoration and predicted (green) should decreased photosynthesis bring about a dramatic change in vegetation composition.

9.4 LANDSCAPE MANAGEMENT IMPLICATIONS

Estimates of annual net ecosystem exchange indicate, if left unrestored, these damaged landscapes will continue to release carbon to the atmosphere (section 5.4.4). This finding highlights a need to re-establish ecological functioning in order to protect the existing stored carbon and potentially initiate future carbon sequestration. However, the immediate response of water tables to restoration has been minor and variable in time and space (sections 8.5.1 and 8.5.3). Given the dominance of *Molinia caerulea* across the landscape, and under a wide range of water table depths (section 6.6.2), it is unlikely that the observed changes in water tables following restoration will be sufficient to promote the change in vegetation community required to restore carbon sequestration. Additional ecological engineering measures may have to be considered.

Early trials to control *Molinia caerulea* on upland grouse moors focused on combinations of burning, grazing and herbicide application (Milligan *et al.* 1999, Ross *et al.* 2003, Marrs *et al.* 2004). Burning further increased the dominance of *Molinia caerulea* (Ross *et al.* 2003) and although glyphosate (Roundup) applications reduced *Molinia caerulea* (Marrs *et al.* 2004), because it is a non-selective herbicide it also reduced *Calluna vulgaris* growth (Milligan *et al.* 1999). Furthermore, widespread application of herbicides is contrary to one of the central aims of the Mires on the Moors project, that of improving downstream water quality.

Hakrová and Novotná (2011) found that mowing *Molinia caerulea*-encroached sub-alpine meadows annually in July, the peak of the vegetation season, increased the number of species present and decreased the abundance and biomass of *Molinia caerulea*. Hájková *et al*. (2009) recommended twice a year mowing (May and September) as an initial restoration measure in calcareous fens as it more strongly affected vascular plant species composition than annual mowing in September. However, Grant et al. (1996) demonstrated that the frequency (three times a year compared to once) and severity of defoliation (66

compared to 33 % removal) were more important than the timing of a single annual cut.

Although mowing has been shown to reduce the dominance of *Molinia caerulea* (Hájková *et al.* 2009, Hakrová and Novotná 2011) it is not economically sustainable in the long-term. On the other hand, changes to the grazing regime (stocking levels and livestock species) will be important in future management. The rapidity of growth and tallness of *M. caerulea* communities suggests these landscapes are most suited to summer grazing by cattle. Whilst sheep concentrate on *Agrostis-Fesuca* areas (Hunter 1962), cattle were found to consume *Molinia caerulea* preferentially*;* the repeated, within season defoliation reduced subsequent leaf production reducing competition for light. In addition, grazing transferred nutrients from the *M. caerulea* to other grasses leading to an increase in other broad leaved grasses (Grant *et al.* 1996).

Many bog species *(e.g. Sphagnum fallax, Eriophorum vaginatum, Calluna vulgaris* and *Erica tetralix)* were present within both catchments so, unlike restoration of bare peat areas, it may not be necessary to sow seed, spread *Sphagnum* encased within protective beads, or plant plug plants (Parry *et al.* 2014). However, seeding with *Calluna vulgaris* on disturbed soil (rotavated or trampled by cattle) increased *C. vulgaris* establishment even where seed was present in the soil (Mitchell *et al.* 2008) indicating seeding may accelerate recolonization.

The above management techniques can reduce the dominance *Molinia caerulea* and increased biodiversity so long as management continued. A combination of these techniques may be required to restore eco-hydrological function of these damaged, shallow bogs. Ditch blocking is necessary to increase the wetness of these peatlands so that changes in vegetation composition resulting from mowing and/or seeding are sufficient to be self-sustaining in the future in order to re-establish a functioning peat forming ecosystem.

9.5 LIMITATIONS

The experimental design using control restored pairs and pre- and post-restoration data enabled the controls on CO_2 fluxes to be understood and attempted to allow for inter-annual variability when assessing the impacts of restoration. The methods used, in particular the use of closed chamber techniques, were selected to enable CO_2 fluxes to be directly linked to processes. Using three pairs of sites in each catchment, each with three plots (⅛, ¼ and ½ -distances) enabled both temporal and spatial controls (by site or by proportional distance from the ditch) to be analysed with statistical robustness. However, the use of closed chamber techniques is labour intensive, limiting the number of temporal and spatial replicates possible.

Determining photosynthesis at the same photosynthetically active radiation meant that photosynthesis could be compared between sample rounds, locations or to other studies even though conditions during data collection varied. In order to do this CO_2 fluxes were collected under a range of light conditions rather than just full-light and full-dark. This increased the number of measurements required from a minimum of four to seven at each location so fewer locations could be measured per day (Table 11.1). Although fewer replicates could be collected, the ability to directly compare between sample rounds monitored under different light levels (e.g. overcast July 2012 compared to strong direct sun in July 2014) was vital to assess the impact of restoration when sampling conditions have varied so greatly.

To prevent fine roots being severed and changes to hydrological and micrometeorological conditions within the chamber, particularly between sampling, it was decided not to use a permanently installed collar but rather a removable plastic skirt and heavy chain following Street *et al.* (2007). A combination of collecting fluxes from a range of light conditions and not using a fixed collar made the method more time consuming restricting the temporal and spatial replicates that were feasible within the time-frame of a PhD research

programme, but nonetheless allowed spatial and temporal controls on photosynthesis and ecosystem respiration to be investigated successfully.

A maximum of 36 locations was considered feasible for a single researcher. It was decided to split these evenly between the two catchments and have restored-control pairs to account for climatic variability. A nested design of three sites with plots at three distances from the ditch was considered to maximise the amount of statistically valid data possible from these 36 locations, and to permit upscaling. One option was to space plots at discrete distances from the ditch e.g. 1, 2 and 3 m. However, this would leave all the areas more than 3 m away from the ditch unmeasured. Given ditch spacing is generally 10-40 m this would include most of the peatland. The other option was to space plots at proportional distances from the ditch (⅛, ¼ and ½ distances) this covers all the area of the peatland but meant within a proportional distance from the ditch group (e.g. ½-distance) there was a range of absolute distances from the ditch, potentially increasing variability in water table depths and vegetation compositions potentially obscuring spatially distributed relationships between water table depth and vegetation composition.

To estimate annual net ecosystem exchange an empirical model based on relationships with other variables (e.g. NDVI) was required. This used monthly net ecosystem exchange measurements collected during sunny, daytime conditions extrapolated across the whole year. As a result the estimate was subject to considerable uncertainty. Part of this uncertainty may have occurred as no spatially distributed measure of vegetation biomass was collected at a plot scale. The vegetation phenology timeseries (NDVI) provided a fine temporal resolution proxy for vegetation biomass but it has a spatial resolution of 500 m, as such it did not enable biomass to be compared between plots within this study. Initially it was intended to collect downward facing true colour photographs monthly from every location as a measure of leaf area index. However, this method proved to be too labour intensive, provided insufficient temporal resolution, showed poor correlation to measured leaf area index and ultimately, due to equipment failure, was abandoned in favour of a time-lapse

camera. A measure of biomass within the NEE plot e.g. vegetative green area or LAI may have provided better assessment of vegetation biomass and enabled a greater proportion of NEE to be explained through an empirical model. However, these measurements were considered too labour intensive to be practical at a remote field site.

In order to maximise the likelihood of observing a change in vegetation composition driven by restoration, locations were selected to be as similar as possible in terms of vegetation composition prior to restoration. This limits the applicability of CO_2 fluxes measured to areas with more diverse vegetation composition. It also restricted the likelihood of observing spatial variation between locations due to vegetation prior to restoration. However, this did allow for any effects of water table depth to be isolated and showed that photosynthesis varied spatially with water table depth (Table 6.5) even though a comparative change in vegetation composition was not observed.

The methods used were entirely objective but the quality of the results obtained can be strongly influenced by the researcher's skill. Protocols to collect the best quality data were revised to be more appropriate to the conditions encountered over the first growing season. The summer of 2012 also had the least favourable weather conditions meaning data was collected in sub-optimal conditions (variable or dull light levels, windy). Unfortunately this has resulted in greater uncertainty within the baseline data than in subsequent data sets.

The most obvious limitation to understanding the effect of restoration on *M. caerulea* dominated peatlands is the timescale of this study, restricted by the time available to a PhD project. Given CO_2 fluxes are strongly affected by vegetation composition which changes slowly, the possibility of observing a quantifiable response was small. However, this short-term study was designed to give an indication of the direction of response and indicate if restoration weakens *Molinia caerulea*, a species adapted to live where water table depths fluctuate (Jefferies 1915), and therefore whether future vegetation change is probable in *Molinia caerulea* dominated peatlands. Partitioning below-ground

respiration enabled the immediate effect of restoration on heterotrophic respiration of the peat store to be observed, monitoring if restoration promotes the conservation of the existing peat store, a first step towards reinstating carbon sequestration. In addition the baseline and control-restored pairs design allows for continued or intermittent future monitoring to establish the longer-term impacts of ditch blocking on CO_2 fluxes and vegetation composition.

Another major, but unavoidable limitation was the weather conditions; an exceptionally wet baseline year followed by two dry summers. With such limited rainfall it was difficult to observe any effect of the peat dams, and consequently restoration. Ongoing monitoring under more diverse meteorological conditions will hopefully indicate the effect of restoration during wetter conditions and enable a better comparison.

9.6 FURTHER WORK

Control locations have been maintained in both Spooners and Aclands catchments. These will continue to be monitored mainly to provide a reference against which to assess the impact of restoration over the longer term. However, in their own right they will continue to provide information about the functioning of a drained *Molinia caerulea* peatland under an increasing range of conditions, assuming that they have not been impacted by the surrounding restoration.

This study has focused on the most dominant vegetation present across Exmoor however, it would also be possible to monitor CO_2 fluxes from other vegetation types e.g. *Calluna vulgaris*, *Juncus effusus* etc. Using UAV derived images it would be possible to map the spatial extent of vegetation types from these images and estimate the net ecosystem exchange for a more heterogeneous landscape.

In order to assess the likely trajectory of restoration over the longer-term a space-for-time substitution could be made. Using historic vegetation monitoring, areas which used to be dominated by *Molinia caerulea* and have

undergone restoration between 1995 and 2013 could be selected. The effects on water table depth, vegetation composition and CO_2 fluxes could be monitored using the same techniques used in this study. It would also be desirable to monitor an area of eco-hydrologically functioning bog within Exmoor to provide a benchmark against which the progress of restoration could be assessed.

If the vegetation changes away from deciduous grass towards evergreen *Sphagnum* then the temporal patterns of vegetation phenology may change. Temporal patterns in NDVI have been used to automatically assess land-cover change (forest, grassland, wetland, agriculture, water and urban) in the Albemarle–Pamlico estuary system, US (Lunetta *et al.* 2006). Given the historical vegetation surveys and MODIS database it may be possible to identify change in vegetation cover through changes in the spectral signal of the vegetation at particular times of the year. This could provide an index of restoration success against which all the peatlands of Exmoor could be assessed to target restoration towards the most damaged areas in the future.

Given the difficulties of understanding the controls on heterotrophic respiration in the field, an incubation experiment might provide insight into the potential rates of respiration from the leaf litter and deeper peats as well as the effects of soil moisture and temperature on these different organic matter sources. This may help in understanding the source/depth/age of carbon being respired from the carbon store and reveal the conditions required to prevent further carbon loss.

The use of methods developed for the *M. caerulea* dominated peatlands of Exmoor have already been extended onto the deeper peats of Dartmoor, this could be used locally within the upland peatlands Bodmin Moor, the lowland peatlands of the Somerset Levels or the tussocky Culm grasslands. A method which enables the measurement of CO_2 fluxes at a scale attributable to processes allows the spatial and/or temporal controls on CO_2 fluxes to be investigated. Monitoring at this scale, particularly with control locations would

enable the direct effect of management such as ditch-blocking, burning, shrub clearance etc. to be investigated. Understanding the consequences of management decisions on water table depths, vegetation composition and CO_2 is increasingly important as a wider range of ecosystem services are being expected from these landscapes.

CONCLUSION

Remote sensing techniques have been developed which provide a daily resolution proxy for vegetation phenology and cm resolution measures of tussock structure across a landscape extent. These methods were developed to enable temporal and spatial upscaling of measurements collected during this study but are applicable to a range of ecosystems.

Uniquely this study has investigated spatial controls on CO_2 fluxes from *Molinia caerulea* dominated peatland, highlighting the competitive nature of this species over a range of environmental conditions. In particular it is the first to investigate the control of drainage ditches on CO_2 fluxes from peatlands despite their prominence within these landscapes.

The fluxes reported for photosynthesis at a set photosynthetically active light level are believed to be the first reported for *Molinia caerulea* allowing direct comparison across ecosystems without the confounding influence of variable light conditions during data collection. The partitioned (total, autotrophic and heterotrophic) below-ground respiration rates add to a very limited number of studies reporting below-ground respiration rates particularly from maritime peatlands. Findings arising from this research represent a significant contribution toward understanding the temporal and spatial controls on these fluxes.

This study adds to scarce few others investigating the effect of ditch blocking on CO_2 fluxes, mainly in *Sphagnum* dominated peatlands. Even rarer are studies with both baseline conditions and control-restored pairs making this study exceptional in its robust experimental design. Data collected to date has demonstrated inconsistent impacts of restoration over the short-term in dry conditions. However, the experimental design allows for future monitoring to determine the longer-term impacts of ditch blocking on CO_2 fluxes and vegetation composition under a greater range of conditions.

10 SUPPLEMENTARY MATERIAL

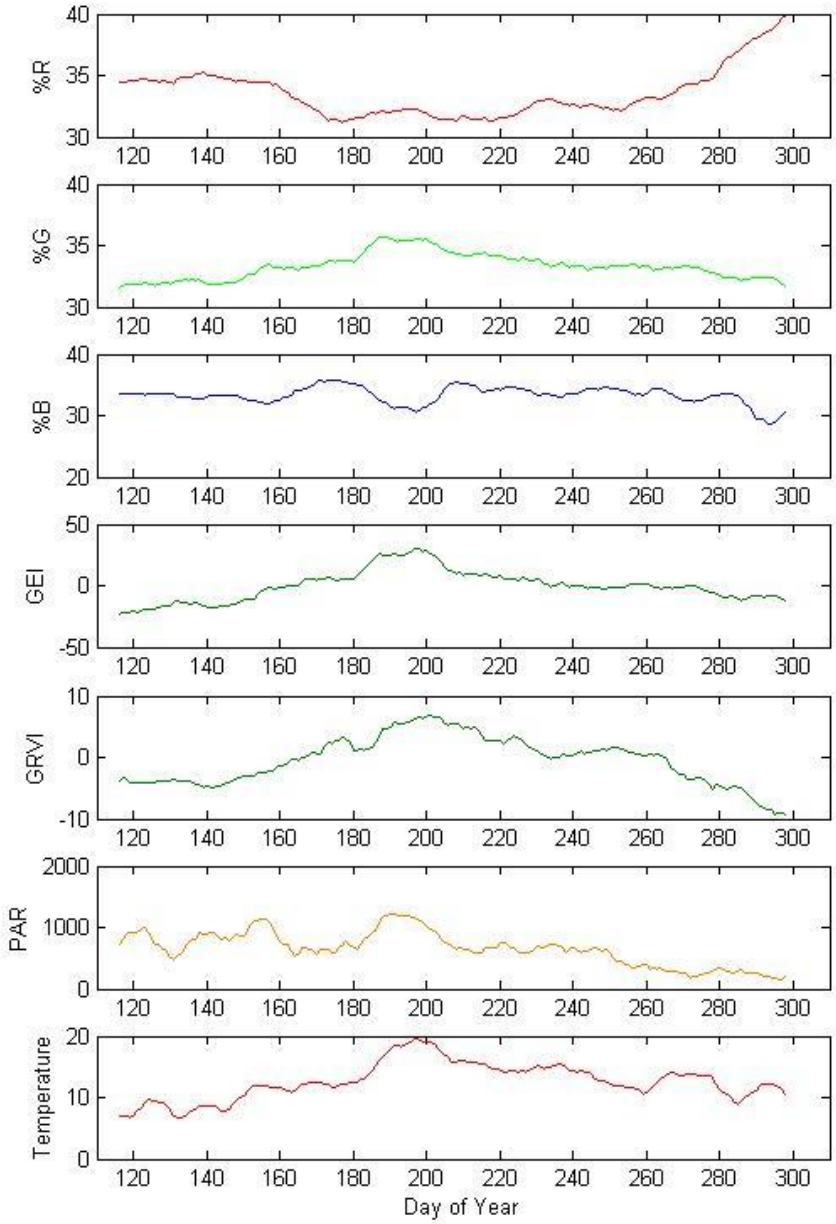

Figure 10.1 Time series of an 8-day moving average relative brightness (Error! Reference source not found.**) of (a) red, (b) green and (c) blue for the 2013 growing season. Time series of and 8-day moving average (d) greenness excess index (**Error! Reference source not found.**) and (e) green-red vegetation index (**Error! Reference source not found.**), (f) photosynthetically active radiation (PAR) (µmol.Photons.m^{-2}s^{-1}) and (g) air temperature (°C) for the 2013 growing season.**

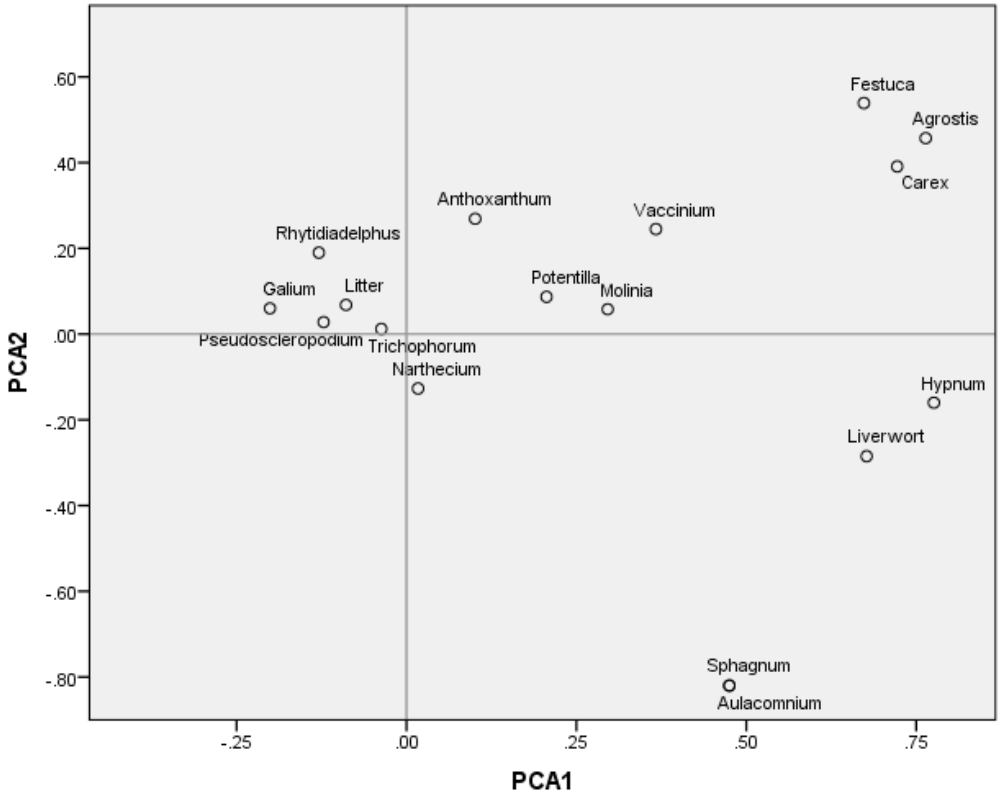

Figure 10.2 Factor weightings for the first (PCA1) and second (PCA2) principal axis from principal component analysis of species present in vegetation composition analysis

Table 10.1 Number of sample locations and number of net ecosystem exchange measurements collected in dark and light (full and shaded) condition at Aclands and Spooners on a given date and sample round. # Excluded as only three out of nine locations sampled. * excluded when focussing on growing season.

Date	Round	Aclands						Spooners					
		Control			Restored			Control			Restored		
		Location	Dar	Ligh	Location	Dar	Ligh	Location	Dar	Ligh	Location	Dar	Ligh
16/05/201	1							3	6	20	3	8	16
17/05/201	1							3	6	7	7	15	16
18/05/201	1							1	2	7	2	2	10
22/05/201	1	3	6	12	5	10	18						
23/05/201	1	6	12	24	4	9	17						
05/07/201	2							3	6	6	1	2	2
06/07/201	2							6	12	13	8	16	17
09/07/201	2	6	13	11	5	10	10						
10/07/201	2	3	6	9	4	9	12						
26/07/201	3							3	6	14	6	12	29
27/07/201	3							6	12	30	3	6	15
09/08/201	4	3	6	14	5	10	22						
10/08/201	4	3	6	13	3	6	15						
16/08/201	4							3	6	13	3	6	14
20/08/201	4							6	10	27	3	6	13
22/08/201	4	3	7	14	1	4	4					7	13
05/09/201	5	6	13	25	3	6	12						
06/09/201	5	3	5	12	6	12	27						
07/09/201	5							5	10	22	3	6	12
19/09/201	5							4	8	17	3	13	25
15/01/201	*	3	6	6	6	12	12						
16/01/201	*	6	12	13	3	6	6						
19/02/201	*							9	18	18	6	18	18
20/05/201	#							3	7	5	9	13	16
30/05/201	7							6	9	7	3	6	6
31/05/201	7							3	4	13	6	7	12
25/06/201	8							5	10	23	3	11	27
26/06/201	8							4	8	19	6	6	16
16/07/201	9							3	6	15	3	10	28
17/07/201	9							6	10	29	6	6	14
20/08/201	10							3	6	15	3	12	28
22/08/201	10							6	12	30	6	5	16
10/09/201	11							3	5	12	3		
11/09/201	11							3	6	15	9	21	37
12/09/201	11							3	6	12	1	2	5
12/06/201	12							5	10	24	5	9	25
13/06/201	12							4	8	18	4	7	19
14/06/201	12	5	10	26	5	10	25						
17/06/201	12	4	8	21	4	8	19						
17/07/201	13	5	10	26	5	10	25						
21/07/201	13							5	11	22	5	10	24
23/07/201	13							4	8	21	4	7	20
18/08/201	13	4	8	17	4	9	20						
02/09/201	14	5			5	26	10						
03/09/201	14	4			4	20	8						
04/09/201	14							5			5	10	25
05/09/201	14							4			4	8	20

Table 10.2 Number of sample locations where clipped (2 replicates) and clipped and trenched (2 replicates) measurements were collected at Aclands and Spooners on a given date and sample round. # data excluded as treatment effects apparent. *Data excluded as levels of detection less than uncertainty within a plot.

		Aclands		Spooners	
Date	Round	Control	Restored	Control	Restored
16/04/2012	#				3
27/04/2012	#	6	6		
02/05/2012	#	3	3	3	3
04/05/2012	#			6	6
24/05/2012	#	9	9		
25/05/2012	#			9	9
13/06/2012	1	9	9		
19/06/2012	1			9	9
25/06/2012	2	6	3		
17/07/2012	2			9	9
19/07/2012	2	6	6		
03/08/2012	3			9	9
08/08/2012	3	9	9		
31/08/2012	4			9	9
10/09/2012	4	6	6		
13/09/2012	4	3	3		
27/09/2012	5	9	9	3	
28/09/2012	5			6	9
25/10/2012	6	9	9		
26/10/2012	6			9	9
11/12/2012	*			9	7
09/01/2013	*	9	9		
11/01/2013	*				3
07/05/2013	7			9	9
21/05/2013	8			9	9
07/06/2013	9			9	9
17/06/2013	10			9	9
05/07/2013	11			9	9
18/07/2013	12			9	9
07/08/2013	13			9	9
19/08/2013	14			9	9
04/09/2013	15			9	9
09/10/2013	16			9	9
30/10/2013	17			9	9
28/05/2014	18	9	9		
30/05/2014	118			9	9
16/06/2014	19	9	9		
18/06/2014	19			9	9
01/07/2014	20	9	9		
03/07/2014	20			9	9
29/07/2014	21	9	9		
04/08/2014	21			9	9
15/08/2014	22	9	9		
18/08/2014	22			9	9
07/09/2014	23			9	9
08/09/2014	23	9	9		
22/09/2014	24	9	9		
23/09/2014	24			9	9

Table 10.3 Reported photosynthesis and ecosystem respiration values (µgC m^{-2} s^{-1}). Results from this study are shaded grey. CC closed chamber, EC eddy covariance

Flux	Flux (µgC m^{-2} s^{-1})	Mire Type	Dominant Vegetation	Peat Thickness (m)	Method	Location	Study
Summer Photosynthesis							
Summer PG (min)	10	**Upland blanket bog**	***Molinia caerulea***	0.23 - 0.56	CC	Exmoor, England, UK	This study
Summer PG	19	Appa mire	*Carex-Scorpidium wet flarks*	?	CC	Kaamanen, northern Finland	(Maanavilja *et al.* 2011)
Summer Pmax	37	Ombrotrophic bog	*Sphagnum sp., Chamaedaphn cealyculata*	2-6 m	EC	Ottawa, Canada	(Bubier *et al.* 2003)
Summer Pmax	38	Ombrotrophic bog	*Sphagnum sp., Chamaedaphn cealyculata*	2-6 m	EC	Ottawa, Canada	(Bubier *et al.* 2003)
Summer PG	48	Appa mire	*Trichophorum flarks*	?	CC	Kaamanen, northern Finland	(Maanavilja *et al.* 2011)
Summer Pmax	48	Blanket Bog	***Molinia caerulea**, Schoenus nigricans*	?	EC	County Kerry, Ireland	(Laine *et al.* 2006)
Summer Pmax	50	Blanket Bog	*Sphagnum sp., Racomitrium lanuginosum, Calluna vulgaris, Erica tetralix and* ***Molinia caerulea***	?	EC	County Kerry, Ireland	(Laine *et al.* 2006)
Summer PG	57	Appa mire	*Betula-Sphagnum string margins*	?	CC	Kaamanen, northern Finland	(Maanavilja *et al.* 2011)
Summer PG	62	Appa mire	*Ericales-Pleurozium string tops*	?	CC	Kaamanen, northern Finland	(Maanavilja *et al.* 2011)
Summer PG	76	**Upland ombrotrophic bog**	***Molinia caerulea***	?	CC	Bohemian Forest, Czech Republic	(Urbanová *et al.* 2012)
Summer PG (max)	82	Ombrotrophic bog	*Sphagnum angustifolium pine bog*	~2 m	EC	Ust-Pojeg, Komi, Russia	(Schneider *et al.* 2012)
Summer PG	87	**Upland ombrotrophic bog**	***Molinia caerulea***	?	CC	Bohemian Forest, Czech Republic	(Urbanová *et al.* 2012)
Summer PG (max)	93	Upland blanket bog	*Calluna vulgaris*	1 to 1.5 m	EC	North Pennines, England, UK	(Lloyd 2010)
Summer PG	139	**Upland blanket bog**	***Molinia caerulea***	0.23 - 0.56	CC	Exmoor, England, UK	This study
Summer PG (max)	224	Appa Mire (Fen)	*Betula nana, Menyanthes triforliata*	<3 m	EC	Lompolojankka, Northwest Finland	(Aurela *et al.* 2009)
Summer PG (max)	277	**Upland blanket bog**	***Molinia caerulea***	0.23 - 0.56	CC	Exmoor, England, UK	This study
Winter Photosynthesis							
Winter PG (min)	2	**Upland blanket bog**	***Molinia caerulea***	0.23 - 0.56	CC	Exmoor, England, UK	This study
Winter PG (max)	6	Upland blanket bog	*Calluna vulgaris*	1 to 1.5 m	EC	North Pennines, England, UK	(Lloyd 2010)
Winter PG (max)	7	Ombrotrophic bog	*Sphagnum angustifolium pine bog*	~2 m	EC	Ust-Pojeg, Komi, Russia	(Schneider *et al.* 2012)
Winter PG (max)	9	**Upland blanket bog**	***Molinia caerulea***	0.23 - 0.56	CC	Exmoor, England, UK	This study

Flux	Flux ($\mu gC\ m^{-2}\ s^{-1}$)	Mire Type	Dominant Vegetation	Peat Thickness (m)	Method	Location	Study
Summer Ecosystem Respiration							
Summer REco (min)	5	**Upland blanket bog**	***Molinia caerulea***	0.23 - 0.56	CC	Exmoor, England, UK	This study
Summer REco (min)	7	Ombrotrophic bog	*Sphagnum sp., Chamaedaphne calyculata*	2-6 m	EC	Ottawa, Canada	(Lafleur *et al.* 2005)
Summer REco	12	Appa mire	*Carex-Scorpidium wet flarks*	?	CC	Kaamanen, northern Finland	(Maanavilja *et al.* 2011)
Summer REco	13	**Upland blanket bog**	*Calluna vulgaris*	< 4 m	CC	North Pennines, England, UK	(McNamara *et al.* 2008)
Summer REco	14	Ombrotrophic bog	*Sphagnum sp., Chamaedaphn cealyculata*	2-6 m	EC	Ottawa, Canada	(Bubier *et al.* 2003)
Summer REco (max)	17	Fen	*Agrostis canina, Agrostis stolonifera,*	?	EC	Schloppner Brunnen, Germany	(Otieno *et al.* 2009)
Summer REco (max)	17	Ombrotrophic bog	*Sphagnum sp., Chamaedaphn cealyculata*	2-6 m	EC	Ottawa, Canada	(Lafleur *et al.* 2005)
Summer REco	18	Ombrotrophic bog	*Sphagnum sp., Chamaedaphn cealyculata*	2-6 m	EC	Ottawa, Canada	(Bubier *et al.* 2003)
Summer REco	26	**Upland blanket bog**	*Sphagnum sp.*	< 4 m	CC	North Pennines, England, UK	(McNamara *et al.* 2008)
Summer REco	26	**Upland blanket bog**	***Mixed grasses***	< 4 m	CC	North Pennines, England, UK	(McNamara *et al.* 2008)
Summer REco (mean)	27	Lowland raised bog	***Molinia caerulea***	0-2.5 m	EC	Netherlands	(Nieveen *et al.* 1998)
Summer REco	34	Appa mire	*Trichophorum flarks*	?	CC	Kaamanen, northern Finland	(Maanavilja *et al.* 2011)
Summer REco	40	**Upland blanket bog**	*Sphagnum sp., C. vulgaris, E. vaginatum*	1 - 2 m	CC	North Pennines, England, UK	(Hardie *et al.* 2009)
Summer REco (max)	46	**Upland blanket bog**	*Calluna vulgaris*	1 to 1.5 m	EC	North Pennines, England, UK	(Lloyd 2010)
Summer REco (max)	47	**Upland blanket bog**	*Calluna vulgaris*	0.5 - 2 m	CC	Grampians, Scotland, UK	(Chapman and Thurlow 1996)
Summer REco	47	**Upland blanket bog**	*Sphagnum sp., C. vulgaris, E. vaginatum*	1 - 2 m	CC	North Pennines, England, UK	(Hardie *et al.* 2009)
Summer REco	49	**Upland blanket bog**	*Eriophorum vaginatum*	< 4 m	CC	North Pennines, England, UK	(McNamara *et al.* 2008)
Summer REco	53	Appa mire	*Betula-Sphagnum string margins*	?	CC	Kaamanen, northern Finland	(Maanavilja *et al.* 2011)
Summer REco	54	**Upland blanket bog**	***Molinia caerulea***	0.23 - 0.56	CC	Exmoor, England, UK	This study
Summer REco	55	Ombrotrophic bog	*Sphagnum angustifolium pine bog*	~2 m	EC	Ust-Pojeg, Komi, Russia	(Schneider *et al.* 2012)
Summer REco	59	**Upland ombrotrophic bog**	***Molinia caerulea***	?	CC	Bohemian Forest, Czech Republic	(Urbanová *et al.* 2012)
Summer REco	62	**Upland ombrotrophic bog**	***Molinia caerulea***	?	CC	Bohemian Forest, Czech Republic	(Urbanová *et al.* 2012)
Summer REco	73	Appa mire	*Ericales-Pleurozium string tops*	?	CC	Kaamanen, northern Finland	(Maanavilja *et al.* 2011)
Summer REco	112	Appa Mire (Fen)	*Betula nana, Menyanthes triforliata*	<3 m	EC	Lompolojankka, Northwest Finland	(Aurela *et al.* 2009)
Summer REco (max)	123	Lowland raised bog	***Molinia caerulea***	0 - 2.5 m	EC	Netherlands	(Nieveen *et al.* 1998)
Summer REco (max)	131	**Upland blanket bog**	***Molinia caerulea***	0.23 - 0.56	CC	Exmoor, England, UK	This study
Winter Ecosystem Respiration							
Winter REco (min)	1	**Upland blanket bog**	***Molinia caerulea***	0.23 - 0.56	CC	Exmoor, England, UK	This study
Winter REco (min)	2	**Upland blanket bog**	*Calluna vulgaris*	0.5 - 2 m	CC	Grampians, Scotland, UK	(Chapman and Thurlow 1996)
Winter REco (min)	3	Lowland raised bog	***Molinia caerulea***	0 - 2.5 m	EC	Netherlands	(Nieveen *et al.* 1998)
Winter REco (max)	5	**Upland blanket bog**	***Molinia caerulea***	0.23 - 0.56	CC	Exmoor, England, UK	This study
Winter REco	6	Ombrotrophic bog	*Sphagnum fuscum*	< 3.9 m	CC	Ilomantsi, Finland	(Alm *et al.* 1999a)
Winter REco	7	Ombrotrophic bog	*Sphagnum angustifolium pine bog*	~2 m	EC	Ust-Pojeg, Komi, Russia	(Schneider *et al.* 2012)

Table 10.4 Reported total and heterotrophic below-ground respiration rates (µmol m^{-2} s^{-1}). Results from this study are shaded grey.

Flux	Flux (µmol m^{-2} s^{-1})	Mire Type	Dominant Vegetation	Peat Thickness (m)	Location	Study
Total Below-Ground Respiration						
Summer(min)	0.00	Ombrotrophic Bog	*Sphagnum sp., Empetrum hermaphoditum, Eriophorum vaginatum*	?	Sweden	(Svensson 1980)
Summer (min)	0.12	**Upland blanket bog**	***Molinia caerulea***	0.23 - 0.56	Exmoor, England, UK	This study
Annual mean	0.34	Pastureland (Drainage Ditch)	*Lepidium latifolium, Hordenum murinum*	< 3 m	Sherman Island, California, USA	(Teh *et al.* 2011)
Summer (mean)	0.45	**Upland blanket bog**	***Molinia caerulea***	0.23 - 0.56	Exmoor, England, UK	This study
Study Mean	0.50	**Upland blanket bog**	*Calluna vulgaris*	1 to 1.5 m	North Pennines, England, UK	(Lloyd 2010)
Annual mean	0.90	Pastureland (Hummock/hollow)	*Lepidium latifolium, Hordenum murinum*	< 3 m	Sherman Island, California, USA	(Teh *et al.* 2011)
Summer (max)	0.95	**Upland blanket bog**	***Molinia caerulea***	0.23 - 0.56	Exmoor, England, UK	This study
Summer (min)	0.98	**Upland blanket bog**	*Sphagnum sp., C. vulgaris, E. vaginatum*	1 - 2 m	North Pennines, England, UK	(Hardie *et al.* 2009)
Summer (October)	1.15	**Upland blanket bog**	*Sphagnum sp., C. vulgaris, E. vaginatum*	1 – 2 m	North Pennines, England, UK	(Heinemeyer *et al.* 2011)
Summer (max)	1.60	**Upland blanket bog**	*Sphagnum sp., C. vulgaris, E. vaginatum*	1 - 2 m	North Pennines, England, UK	(Hardie *et al.* 2009)
Summer (July)	1.70	**Upland blanket bog**	*Sphagnum sp., C. vulgaris, E. vaginatum*	1 - 2 m	North Pennines, England, UK	(Heinemeyer *et al.* 2011)
Annual mean	1.90	Ombrotrophic bog - drained	*Pinus sylvestris, Cladotiia species, Sphagnum sp.,*	?	southern Finland	(Komulainen *et al.* 1999)
Summer(max)	2.07	Ombrotrophic Bog	*Sphagnum sp., Empetrum hermaphoditum, Eriophorum vaginatum*	?	Sweden	(Svensson 1980)
Summer (max)	2.50	Ombrotrophic bog - drained	*Empetrum nigrum, Andromeda polifolia, Betula nana*	?	Ilomantsi, southern Finland	(Silvola *et al.* 1996b)
Summer (max)	2.50	Ombrotrophic bog - drained	*Eriophorum vaginatum, Empetrum nigrum, Sphagnum russowii*	?	Lakkasuo, eastern Finland	(Silvola *et al.* 1996b)
Annual mean	2.80	Ombrotrophic bog - rewetted	*Cladotiia species, Sphagnum sp., Andromieda polifolia, Empetrum nigrum*	?	southern Finland	(Komulainen *et al.* 1999)
Summer (max)	2.90	Ombrotrophic bog - drained	*Eriophorum vaginatum, Vaccinium uliginosum, Rubus chamaemorus*	?	Lakkasuo, eastern Finland	(Silvola *et al.* 1996b)
Annual mean	3.10	Minerotrophic fen -drained	*Pinus sylvestris, Vaccinium myrtillis, Pleurozi schreberi*	?	southern Finland	(Komulainen *et al.* 1999)
Annual mean	4.90	Minerotrophic fen - rewetted	*Vaccinium myrtillis, Pleurozi schreberi, Eriophorum vaginatum*	?	southern Finland	(Komulainen *et al.* 1999)

Flux	Flux (µmol $m^{-2} s^{-1}$)	Mire Type	Dominant Vegetation	Peat Thickness (m)	Location	Study
Below-Ground Heterotrophic Respiration						
Summer (min)	0.04	**Upland blanket bog**	***Molinia caerulea***	0.23 - 0.56	Exmoor, England, UK	This study
Summer (July)	0.10	**Upland blanket bog**	*Sphagnum sp., Calluna vulgaris, Eriophorum vaginatum*	1 - 2 m	North Pennines, England, UK	(Heinemeyer *et al.* 2011)
Summer (mean)	0.24	**Upland blanket bog**	***Molinia caerulea***	0.23 - 0.56	Exmoor, England, UK	This study
Annual mean	0.37	Ombrotrophic bog - drained	Drained ombrotrophic pine bog	3.4 m	Ilomantsi, southern Finland	(Silvola *et al.* 1996a)
Summer (max)	0.42	**Upland blanket bog**	***Molinia caerulea***	0.23 - 0.56	Exmoor, England, UK	This study
Annual mean	0.47	Ombrotrophic bog - drained	Drained ombrotrophic pine bog	3.4 m	Ilomantsi, southern Finland	(Silvola *et al.* 1996a)
Summer (October)	0.52	**Upland blanket bog**	*Sphagnum sp., Calluna vulgaris, Eriophorum vaginatum*	1 - 2 m	North Pennines, England, UK	(Heinemeyer *et al.* 2011)
Annual mean	0.72	Ombrotrophic bog - drained	Drained Ombrotrophic bog	2 - 2.5 m	Lakkasuo, eastern Finland	(Silvola *et al.* 1996a)
Annual mean	0.75	Ombrotrophic bog - drained	Drained dwarf Shrub pin bog	2.8 m	Lakkasuo, eastern Finland	(Silvola *et al.* 1996a)
Annual mean	0.77	Ombrotrophic bog - drained	Drained dwarf Shrub pin bog	2.8 m	Lakkasuo, eastern Finland	(Silvola *et al.* 1996a)
Annual mean	0.90	Ombrotrophic bog - drained	Drained ombrotrophic pine bog	1.8 - 2 m	Ilomantsi, southern Finland	(Silvola *et al.* 1996a)
Annual mean	1.00	Ombrotrophic bog - drained	Drained ombrotrophic pine bog	1.8 - 2 m	Ilomantsi, southern Finland	(Silvola *et al.* 1996a)
Annual mean	1.04	Ombrotrophic bog - drained	Drained Ombrotrophic bog	2 - 2.5 m	Lakkasuo, eastern Finland	(Silvola *et al.* 1996a)
Summer (max)	1.70	Ombrotrophic bog - drained	*Empetrum nigrum, Andromeda polifolia, Betula nana*	?	Ilomantsi, southern Finland	(Silvola *et al.* 1996b)
Summer (max)	2.20	Ombrotrophic bog - drained	*Eriophorum vaginatum, Vaccinium uliginosum, Rubus chamaemorus*	?	Lakkasuo, eastern Finland	(Silvola *et al.* 1996b)
Summer (max)	2.30	Ombrotrophic bog - drained	*Eriophorum vaginatum, Empetrum nigrum, Sphagnum russowii*	?	Lakkasuo, eastern Finland	(Silvola *et al.* 1996b)

Table 10.5 Reported net ecosystem exchange values (tonnes ha^{-1} yr^{-1}), positive values indicate a source of CO_2 to the atmosphere, negative values a sink. Results from this study are shaded grey

NEE (tonnes ha-1 a-1)	Uncertainty (tonnes ha-1 a-1)	Mire Type	Community	Peat Depth		Sample Period	Location	Source
0.97		Drained Raised Bog	***Molinia caerulea***	0-2.5 m	Annual Mean	Nov 1994 - Nov 1995	Netherlands	(Nieveen *et al.* 1998)
0.88	-2.07 to 3.86	**Blanket Bog**	***Molinia caerulea***	generally < 50 cm	Annual Mean	May 2012 - Apr 2013	Exmoor (Aclands and Spooners)	This Study
0.82	± 0.13	**Blanket Bog**	Bare Soil Gully	2 to 3 m	Study Mean	Jan 2007 - Dec 2011	Peak District, UK	(Dixon *et al.* 2013)
0.62	± 0.13	**Blanket Bog**	Flat	2 to 3 m	Study Mean	Jan 2007 - Dec 2011	Peak District, UK	(Dixon *et al.* 2013)
0.26		Drained ombrotrophic bog	***Molinia caerulea***		Study Mean	May 2010 to Oct 2010	southern Czech Republic	(Urbanová *et al.* 2013)
0.17		Drained ombrotrophic bog	***Molinia caerulea***		Study Mean	May 2009 to Oct 2009	southern Czech Republic	(Urbanová *et al.* 2013)
0.16	-3.19 to 3.88	**Blanket Bog**	***Molinia caerulea***	generally < 50 cm	Annual Mean	May 2013 - Apr 2014	Exmoor (Aclands and Spooners)	
0.14		Ombrotrophic Bog	*Sphagnum sp., Chamaedaphne calyculata, Ledum groenlandicum,*	<3 to 6 m	6 Year Minimum	1998 - 2004	Mer Blue, Canada	(Roulet *et al.* 2007)
-0.04		Appa Mire (Fen)	*Betula nana, Menyanthes triforliata, Salix lapponum, Carex sp.*	<3 m	Annual Mean	2006	Northern Finland	(Aurela *et al.* 2009)
-0.04	± 0.01	**Blanket Bog**	*Sphagnum sp., Racomitrium lanuginosum, Calluna vulgaris,*	0.5 to 5 m	Annual Mean	2006	County Kerry, Ireland	(Koehler *et al.* 2011)
-0.04	± 0.01	**Blanket Bog**	*Sphagnum sp., Racomitrium lanuginosum, Calluna vulgaris,*	0.5 to 5 m	Annual Mean	2007	County Kerry, Ireland	(Koehler *et al.* 2011)
-0.04	-.08 to -.01	Appa Mire (Mesotrophic Fen)	*Carex sp., mosses, Ledum palustre,*	?	Annual Mean	1997	Kaamanen, Northern Finland	(Aurela *et al.* 2004)
-0.05	± 0.28	**Blanket Bog**	Natural Channel	2 to 3 m	Study Mean	Jan 2007 - Dec 2011	Peak District, UK	(Dixon *et al.* 2013)
-0.06	-0.9 to -0.05	Appa Mire (Mesotrophic Fen)	*Carex sp.,* mosses, *Ledum palustre,*	?	Annual Mean	2000	Kaamanen, Northern Finland	(Aurela *et al.* 2004)
-0.08	-0.12 to -0.06	Appa Mire (Mesotrophic Fen)	*Carex sp.,* mosses, *Ledum palustre,*	?	Annual Mean	1999	Kaamanen, Northern Finland	(Aurela *et al.* 2004)
-0.10	± 0.59	**Blanket Bog**	Naturally Revegetating Gully	2 to 3 m	Study Mean	Jan 2007 - Dec 2011	Peak District, UK	(Dixon *et al.* 2013)
-0.11	± 0.14	Ombrotrophic Bog	*Sphagnum sp., Chamaedaphne calyculata, Ledum groenlandicum*	2-6 m	Annual Mean	2001 - 2002	Ottawa, Canada	(Lafleur *et al.* 2003)
-0.13	± 0.01	**Blanket Bog**	*Sphagnum sp., Racomitrium lanuginosum, Calluna vulgaris*	0.5 to 5 m	Annual Mean	2008	County Kerry, Ireland	(Koehler *et al.* 2011)
-0.14		Minerotrophic Mire	*S. majus, Eriophorum vaginatum, Trichoporum cespitosum*	3 to 4 m	Annual Mean	2001	Degero Stormyr, Northern Sweden	(Sagerfors *et al.* 2008)

NEE (tonnes ha-1 a-1)	Uncertainty (tonnes ha-1 a-1)	Mire Type	Community	Peat Depth		Sample Period	Location	Source
-0.16		Minerotrophic Mire	*S. majus, Eriophorum vaginatum, Trichoporum cespitosum*	3 to 4 m	Annual Mean	2003	Degero Stormyr, Northern Sweden	(Sagerfors *et al.* 2008)
-0.18		Minerotrophic Mire	*S. majus, Eriophorum vaginatum, Trichoporum cespitosum*	3 to 4 m	Annual Mean	2002	Degero Stormyr, Northern Sweden	(Sagerfors *et al.* 2008)
-0.20	± 0.02	**Blanket Bog**	*Sphagnum sp., Racomitrium lanuginosum, Calluna vulgaris*	0.5 to M	Annual Mean	2003	County Kerry, Ireland	(Koehler *et al.* 2011)
-0.20	± 0.01	**Blanket Bog**	*Sphagnum sp., Racomitrium lanuginosum, Calluna vulgaris*	0.5 to M	Annual Mean	2004	County Kerry, Ireland	(Koehler *et al.* 2011)
-0.2	± 0.03	Minerotrophic Mire	*Sphagnum Sp., E. vaginatum, Trichoporum cespitosum*	3 to 4 m	Annual Mean	2005	Degero Stormyr, Northern Sweden	(Nilsson et al. 2008
-0.21	-0.27 to -0.17	Appa Mire (Mesotrophic Fen)	*Carex sp., mosses, Ledum palustre*	?	Annual Mean	1998	Kaamanen, Northern Finland	(Aurela *et al.* 2004)
-0.21		Fen	*Sphagnum sp., Scheuchzeria palustris, Carex rostrata*	2 to 4 m	Growing Season Mean	Jun 2005 -Sep 2005	Southern Finland	(Riutta *et al.* 2007)
-0.23	±0.0.06	Eccentric Bog	*Calluna vulgaris, Erica tetralix, Sphagnum sp., E. vaginatum*	4 to 5 m		Aug 2005 - Jul 2006	Fajemyr, Southern Sweden	(Lund *et al.* 2007)
-0.25	± 0.01	**Blanket Bog**	*Sphagnum sp., Racomitrium lanuginosum, Calluna vulgaris*	0.5 to M	Annual Mean	2005	County Kerry, Ireland	(Koehler *et al.* 2011)
-0.25		**Blanket Bog**	*Sphagnum sp. Deschampsia flexuosa, E. vaginatum, Juncus effusus*	<0.5 to >5 m	Study Mean	1995 - 1996	Auchencorth Moss, Southeast Scotland	(Hargreaves *et al.* 2003)
-0.27	± 0.03	Minerotrophic Mire	*S. majus, Eriophorum vaginatum, Trichoporum cespitosum*	3 to 4 m	Annual Mean	2004	Degero Stormyr, Northern Sweden	(Nilsson *et al.* 2008)
-0.36		Appa Mire (Fen)	*Betula nana, Menyanthes triforliata, Salix lapponum, Carex sp.*	<3 m	Annual Mean	2007	Northern Finland	(Aurela *et al.* 2009)
-0.37	-0.41 to -0.34	Appa Mire (Mesotrophic Fen)	*Carex sp., mosses, Ledum palustre*	?	Annual Mean	2001	Kaamanen, Northern Finland	(Aurela *et al.* 2004)
-0.38		Wet Tussock Grassland	*Calamagrostis, Carex appendiculata, E. angustifolium*	?	Growing Season Mean	2003	Kolyma River, Northeast Siberia	(Corradi *et al.* 2005)
-0.4	± 0.41	Ombrotrophic Bog	*S. capillifolium, S. magellanicum, Chamaedaphne calyculata*	<3 to 6 m	6 Year Mean	1998 - 2004	Mer Blue, Canada	(Roulet *et al.* 2007)
-0.49		**Blanket Bog**	*Sphagnum sp., Racomitrium lanuginosum, Calluna vulgaris*	0.5 to 5 m	Annual Mean	2003	Glencar, Southwest Ireland	(Sottocornola and Kiely 2005)
-0.53	-0.56 to -0.50	Appa Mire (Mesotrophic Fen)	*Carex sp., mosses, Ledum palustre*	?	Annual Mean	2002	Kaamanen, Northern Finland	(Aurela *et al.* 2004)
-0.56	± 0.23	**Blanket Bog**	Flat Seeded and Limed	2 to 3 m	Study Mean	Jan 2007 - Dec 2011	Peak District, UK	(Dixon *et al.* 2013)
-0.61		**Blanket Bog**	*Sphagnum sp., Racomitrium lanuginosum, Calluna vulgaris*	0.5 to 5 m	Annual Mean	2004	Glencar, Southwest Ireland	(Sottocornola and Kiely 2005)

NEE (tonnes ha-1 a-1)	Uncertainty (tonnes ha-1 a-1)	Mire Type	Community	Peat Depth		Sample Period	Location	Source
-0.63		Appa Mire (Fen)	*Betula nana, Menyanthes triforliata, Salix lapponum, Carex sp.*	<3 m	Annual Mean	2008	Northern Finland	(Aurela *et al.* 2009)
-0.74	± 0.36	Ombrotrophic Bog	*Sphagnum sp., Chamaedaphne calyculata, Ledum groenlandicum*	2-6 m	Annual Mean	2000-2001	Ottawa, Canada	(Lafleur *et al.* 2003)
-0.742		**Blanket Bog**	*Sphagnum sp. Deschampsia flexuosa, E. vaginatum, Juncus effusus*	<0.5 to >5 m		2003-2008	Auchencorth Moss, Scotland	(Dinsmore *et al.* 2010)
-0.74	± 0.44	Ombrotrophic Bog	*Sphagnum sp., Chamaedaphne calyculata, Ledum groenlandicum*	2-6 m	Annual Mean	1999-2000	Ottawa, Canada	(Lafleur *et al.* 2003)
-0.81	± 0.14	Ombrotrophic Bog	*Sphagnum sp., Chamaedaphne calyculata, Ledum groenlandicum*	2-6 m	Annual Mean	1998-1999	Ottawa, Canada	(Lafleur *et al.* 2003)
-0.89		Ombrotrophic Bog	*S. capillifolium, S. magellanicum, Chamaedaphne calyculata*	<3 to 6 m	6 Year Maximum	1998-2004	Mer Blue, Canada	(Roulet *et al.* 2007)
-0.935		**Blanket Bog**	*Sphagnum sp. Deschampsia flexuosa, E. vaginatum, Juncus effusus*	<0.5 to >5 m		2008	Auchencorth Moss, Scotland	(Dinsmore *et al.* 2010)
-1.12	± 0.11	Temperate Heath	*Calluna vulgaris , moss and Deschampsia flexuosa*	On mineral soil	Annual Mean	Sep 2004 - Sep 2005	Mols Bjerge, Denmark	(Larsen *et al.* 2007)
-1.31	± 0.54	**Blanket Bog**	Gully - Seeded, limed and gully blocked	2 to 3 m	Study Mean	Jan 2007 - Dec 2011	Bleaklow Plateau, Peak District	(Dixon *et al.* 2013)
-1.36		**Blanket Bog**	*Sphagnum sp. Deschampsia flexuosa, E. vaginatum, Juncus effusus*	<0.5 to >5 m		2007	Auchencorth Moss, Scotland	(Dinsmore *et al.* 2010)
-1.44	± 1.92	Appa Mire	Betula-Sphagnum string margins	?	Growing Season Mean	Jun 2007 - Sep 2007	Northern Finland	(Maanavilja *et al.* 2011)
-1.44	± 0.51	**Blanket Bog**	Gully - Seeded, limed and heather brash	2 to 3 m	Study Mean	Jan 2007 - Dec 2011	Bleaklow Plateau, Peak District	(Dixon *et al.* 2013)
-1.73	±0.078	**Blanket Bog**	*Calluna vulgaris, E. vaginatum, Sphagnum sp.*	1 to 1.5 m	Annual Mean	Jul 2006 -Jun 2007	Moor House England	(Lloyd 2010)
-1.85		Raised Bog	*Sporadanthus traversii, Empodisma*	<15 m	Annual Mean	1999	Moanatuatua, New Zealand	(Smith 2003)
-1.90		Fen	*Carex lasiocarpa, Betula nana, Andromeda polifolia*	2 to 4 m	Growing Season Mean	Jun 2005 -Sep 2005	Southern Finland	(Riutta *et al.* 2007)
-2.00	± 0.26	**Blanket Bog**	Gully - Seeded, limed and geojute	2 to 3 m	Study Mean	Jan 2007 - Dec 2011	Peak District, UK	(Dixon *et al.* 2013)
-2.1		Raised Bog	*Sporadanthus traversii, Empodisma*	<15 m	Annual Mean	2000	Moanatuatua, New Zealand	(Smith 2003)
-2.15	± 1.03	Appa Mire	*Carex-Scorpidium* wet flarks	?	Growing Season Mean	Jun 2007 - Sep 2007	Northern Finland	(Maanavilja *et al.* 2011)
-3.93	± 1.85	Appa Mire	*Ericales-Pleurozium* string tops	?	Growing Season Mean	Jun 2007 - Sep 2007	Northern Finland	(Maanavilja *et al.* 2011)
-4.82	± 1.18	Appa Mire	*Trichophorum* flarks	?	Growing Season Mean	Jun 2007 - Sep 2007	Northern Finland	(Maanavilja *et al.* 2011)

Table 10.6 Location specific empirically derived coefficients for R_{Eco} and P_{G600} models. Regression coefficient (r^2), number of data points (n) parameters: P1 (µgC m^{-2} s^{-1}), K1 (µmol Photons m^{-2} s^{-1}), a (dimensionless), b ($°C^{-1}$), c (dimensionless), d ($°C^{-1}$), e (dimensionless), T_{Opt} (°C) and T_{Tol} (°C).

Location	Photosynthesis Model						Ecosystem Respiration Model						
	r^2	n	P_1	K_1	a	b	r^2	n	c	d	e	T_{Opt}	T_{Tol}
A1C1	0.94	15	-4	709	-58	381	0.69	10	85	27	72	13	
A1C2	0.76	19	-3	457	-13656	98	0.38	12	68	811	70932888	78	12
A1C3	0.76	15	-33	6316	-107639	100	0.98	8	111	22	520	12	
A1R1	0.57	16	-3	938	-135786	102	0.84	9	53	726	549947913	30	-3
A1R2	0.67	15	-3	3253	-15614	71	0.86	13		-14	54	15	-2
A1R3	0.76	19	-5	365	-20677	85	0.80	8	3690	62	-1227	-48718	671
A2C1	0.95	16	-4	209	0	-77	0.88	10	610	66	72	16	2
A2C2	0.97	17	-4	182	-10	5	0.40	9		-120	99	15	
A2C3	0.91	19	-4	238	-21	3	0.04	9	121	898	7083	239	70
A2R1	0.84	17	-3	247	0	-176	0.68	9	30	6	24	12	
A2R2	0.99	15	-8	1088	-18	10	0.20	12	72	803	345046	184	39
A2R3	0.90	13	-2	46	0	-11	0.95	8	59	898	661	20	3
A3C1	0.77	15	-2	51	285	486	0.15	13	22	1	10	-39	2
A3C2	0.86	17	-2	187	-31	11	0.62	11	30	5	11	127	-9
A3C3	0.82	15	-6	1256	-918	425	0.54	11	33	7	7	179	1
A3R1	0.50	17	-2	100	-53	6	0.74	10	76	792	34	12	4
A3R2	0.89	15	-4	313	-1003	64	0.38	13	54	9	11	252	-29
A3R3	0.89	19	-3	111	-11	4	0.76	10	92	500	34	13	5

Location	Photosynthesis Model						Ecosystem Respiration Model						
	r^2	n	P_1	K_1	a	b	r^2	n	c	d	e	T_{Opt}	T_{Tol}
S1C1	0.93	17	-3	425	0	-46	0.25	15	33	7	3	340	-38
S1C2	0.91	21	-4	3728	-4807	55	0.56	16	609	39	64	6	1
S1C3	0.89	18	-11	4470	-284	18	0.84	15	5587	62	62	1064	123
S1R1	0.86	23	-2	270	-100	15	0.80	11	1052	97	2533	52	-14
S1R2	0.92	22	-3	207	-3	-1	0.87	15	-13578	58	925	23	5
S1R3	0.88	20	-9	4495	-48	4	0.61	15	828225759	275	30	11	4
S2C1	0.80	16	-2	202	-111	14	0.67	12	223	43	35	13	2
S2C2	0.76	22	-3	403	0	-39	0.66	13	65	522	809389	187	38
S2C3	0.61	17	-1	120	-1	-11	0.55	13	151	27	6	251	-31
S2R1	0.88	16	-2	57	5349	83	0.77	12	619	49	27	13	
S2R2	0.62	20	-1	98	-15	0	0.54	13	1	-7	29	12	2
S2R3	0.73	22	-3	546	-28	4	0.30	11	35	8	42	18	1
S3C1	0.86	22	-3	192	0	-49	0.33	12	58	10	10	239	5
S3C2	0.92	21	-3	285	0	-64	0.60	14	43	8	9	15	1
S3C3	0.65	21	-2	452	0	-143	0.13	14	21	5	11	141	12
S3R1	0.78	21	-3	178	-74	18	0.72	17	902	49	963	13	
S3R2	0.51	22	-2	64	-17221	81	0.51	9	65	891	7326792	94	16
S3R3	0.88	25	-3	311	2455	71	0.47	17	53	10	28	17	1

Table 10.7 Seasonal Q_{10} and mean respiration at 10 °C (R_{10}) values for total, heterotrophic and autotrophic respiration at each site. Regression coefficient (r_2) and significance (p) of exponential relationships between soil temperature at 5 cm (°C) and total, heterotrophic and autotrophic respiration at each site. n is the number of sample days.

Respiration Source		Site		Q_{10}	R_{10}	n	r^2	p
Total	Aclands	1	C	2.7	0.34	13	0.67	0.001
			R	1.9	0.22	13	0.65	0.001
		2	C	1.4	0.22	14	0.40	0.009
			R	2.0	0.26	14	0.48	0.010
		3	C	1.5	0.26	13	0.35	0.031
			R	2.1	0.24	11	0.48	0.018
	Spooners	1	C	2.5	0.40	23	0.86	0.000
			R	2.0	0.32	23	0.67	0.000
		2	C	1.6	0.17	23	0.53	0.000
			R	2.0	0.29	23	0.67	0.000
		3	C	2.1	0.23	22	0.67	0.000
			R	2.0	0.30	23	0.66	0.000
Heterotrophic	Aclands	1	C	1.9	1.17	12	0.45	0.017
			R	1.6	1.11	13	0.55	0.030
		2	C	1.7	1.07	12	0.61	0.003
			R	1.4	1.17	12	0.37	0.036
		3	C	1.3	1.18	11	0.42	0.027
			R	1.7	1.19	13	0.49	0.006
	Spooners	1	C	1.4	1.23	23	0.33	0.003
			R	1.4	1.21	23	0.63	0.000
		2	C	1.4	1.13	23	0.58	0.000
			R	1.4	1.18	23	0.61	0.000
		3	C	1.3	1.15	23	0.43	0.001
			R	1.3	1.17	23	0.40	0.001
Autotrophic	Aclands	1	C	2.6	1.13	12	0.52	0.009
			R	1.5	1.09	12	0.45	0.170
		2	C	1.4	1.03	12	0.42	0.020
			R	1.9	1.05	13	0.64	0.001
		3	C	1.4	1.05	12	0.58	0.004
			R	2.0	1.01	11	0.42	0.034
	Spooners	1	C	2.2	1.18	23	0.71	0.000
			R	1.5	1.11	23	0.35	0.001
		2	C	1.3	1.00	21	0.35	0.005
			R	1.6	1.10	23	0.50	0.000
		3	C	1.7	1.09	22	0.35	0.003
			R	1.7	1.13	23	0.40	0.002

Table 10.8 Average vegetation composition (% coverage) and standard errors (in brackets) by proportional distance from the ditch and site. Overall mean, minimum (min), maximum (max) and number of occurrences (n). # cover of 1 % at a single location

	Proportional Distance from the Ditch			Site						Total			
	1/8	1/4	1/2	A1	A2	A3	S1	S2	S3	Mean	Min	Max	n
Molinia caerulea	90 (4)	81 (20)	87 (13)	88 (5)	83 (7)	83 (6)	88 (6)	78 (9)	97 (3)	86 (3)	40	100	36
Leaf Litter	87 (4)	82 (20)	87 (10)	87 (2)	89 (3)	85 (3)	80 (7)	100 (0)	71 (9)	85 (3)	35	100	36
Potentilla erecta	2 (1)	1 (1)	2 (1)	1 (0)	2 (2)	#	4 (1)	#	3 (2)	2 (1)	0	15	15
Hypnum cupressiforme	1 (0)	1 (1)	1 (0)	1 (1)	1 (0)	1 (1)	2 (1)	.	#	1 (0)	0	5	14
Rhytidiadelphus squarrosus	1 (0)	1 (0)	#	1 (1)	1 (0)	1 (0)	#	.	.	0 (0)	0	3	10
Eriophorum vaginatum	.	3 (3)	7 (3)	.	.	2 (2)	11 (6)	.	6 (5)	3 (1)	0	30	6
Vaccinium myrtillus	#	1 (0)	1 (1)	1 (0)	.	#	1 (1)	.	2 (2)	1 (0)	0	10	5
Agrostis sp.	#	#	1 (0)	.	.	1 (0)	1 (1)	.	1 (1)	0 (0)	0	5	5
Liverwort	.	#	#	#	.	#	#	#	#	0 (0)	0	1	5
Galium saxatile	#	#	#	1 (1)	.	.	.	#	.	0 (0)	0	5	3
Pseudoscleropodium purum	#	#	.	.	#	1 (0)	.	.	.	0 (0)	0	2	3
Trichophorum cespitosum	.	#	#	.	.	1 (0)	.	.	.	0 (0)	0	2	2
Anthoxanthum odoratum	.	#	.	.	.	.	#	.	#	0 (0)	0	1	2
Narthecium ossifragum	.	.	3 (3)	.	.	.	.	5 (5)	.	1 (1)	0	30	1
Nardus stricta	.	.	1 (1)	.	.	.	3 (3)	.	.	0 (0)	0	15	1
Sphagnum fallax	.	#	.	#	.	.	.	.	.	0 (0)	0	2	1
Festuca sp.	.	#	.	#	.	.	.	.	.	0 (0)	0	1	1
Aulacomnium palustre	.	#	.	#	.	.	.	.	.	0 (0)	0	1	1
Carex echinata	.	.	#	.	.	.	#	.	.	0 (0)	0	1	1

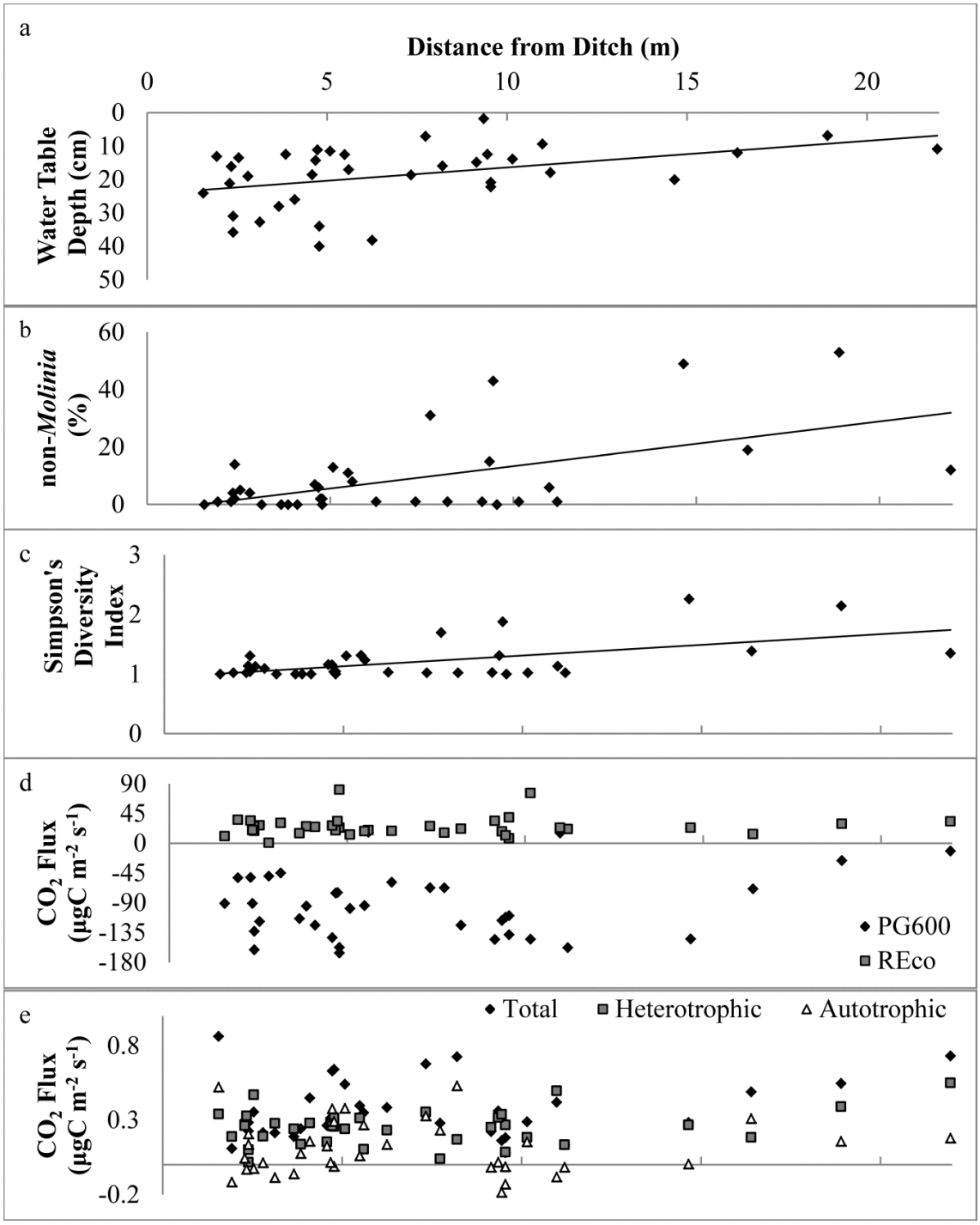

Figure 10.3 Variation in a, water table depth (cm), b, percentage coverage of non-*Molinia* species, c, Inverse Simpson Diversity Index, d, modelled photosynthesis (P_{G600}) (µgC m^{-2} s^{-1}) and ecosystem respiration (R_{Eco}) (µgC m^{-2} s^{-1}) and e, total, heterotrophic and autotrophic respiration at 10 °C (µmol m^{-2} s^{-1})

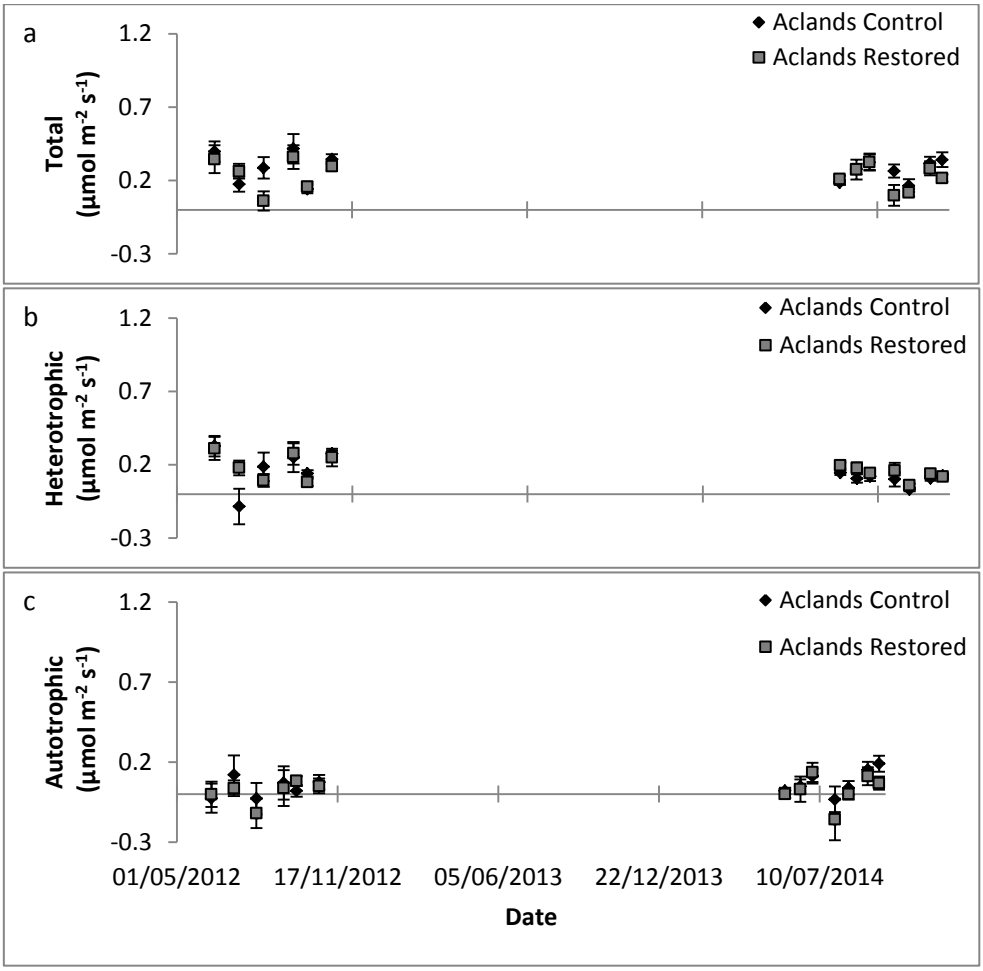

Figure 10.4 Temporal variation in total (a), heterotrophic (b) and autotrophic (c) respiration (µmol m^{-2} s^{-1}) at 10 °C at control and restored locations within Aclands catchment. Error bars are one standard error.

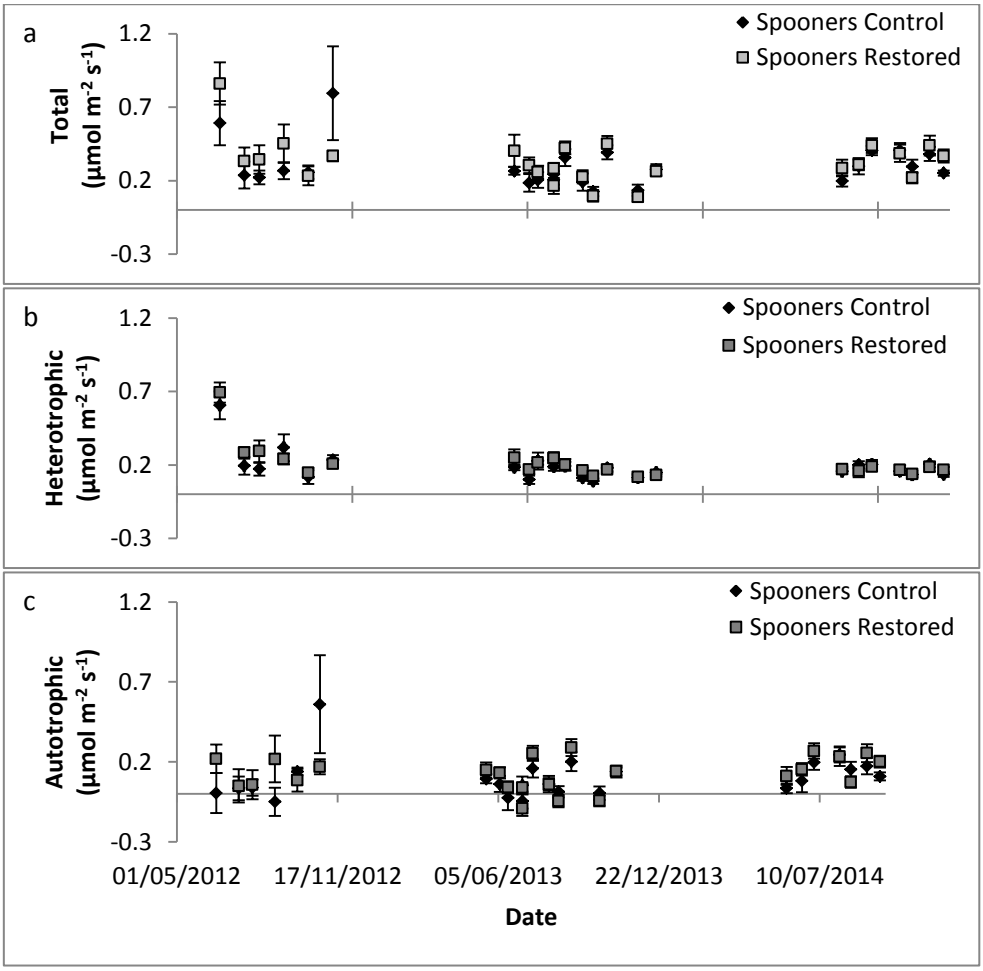

Figure 10.5 Temporal variation in total (a), heterotrophic (b) and autotrophic (c) respiration (µmol m^{-2} s^{-1}) at 10 °C at control and restored locations within Spooners catchment. Error bars are one standard error.

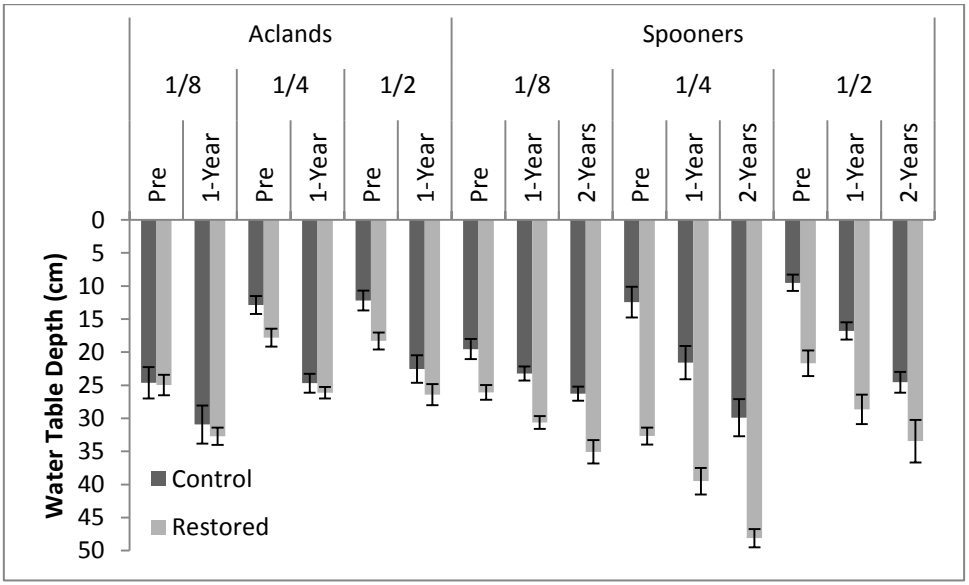

Figure 10.6 Water table depth (cm) at the control and restored locations averaged by proportional distance from the ditch within each catchment, pre- 1-year and 2-years post-restoration. Error bars are one standard error.

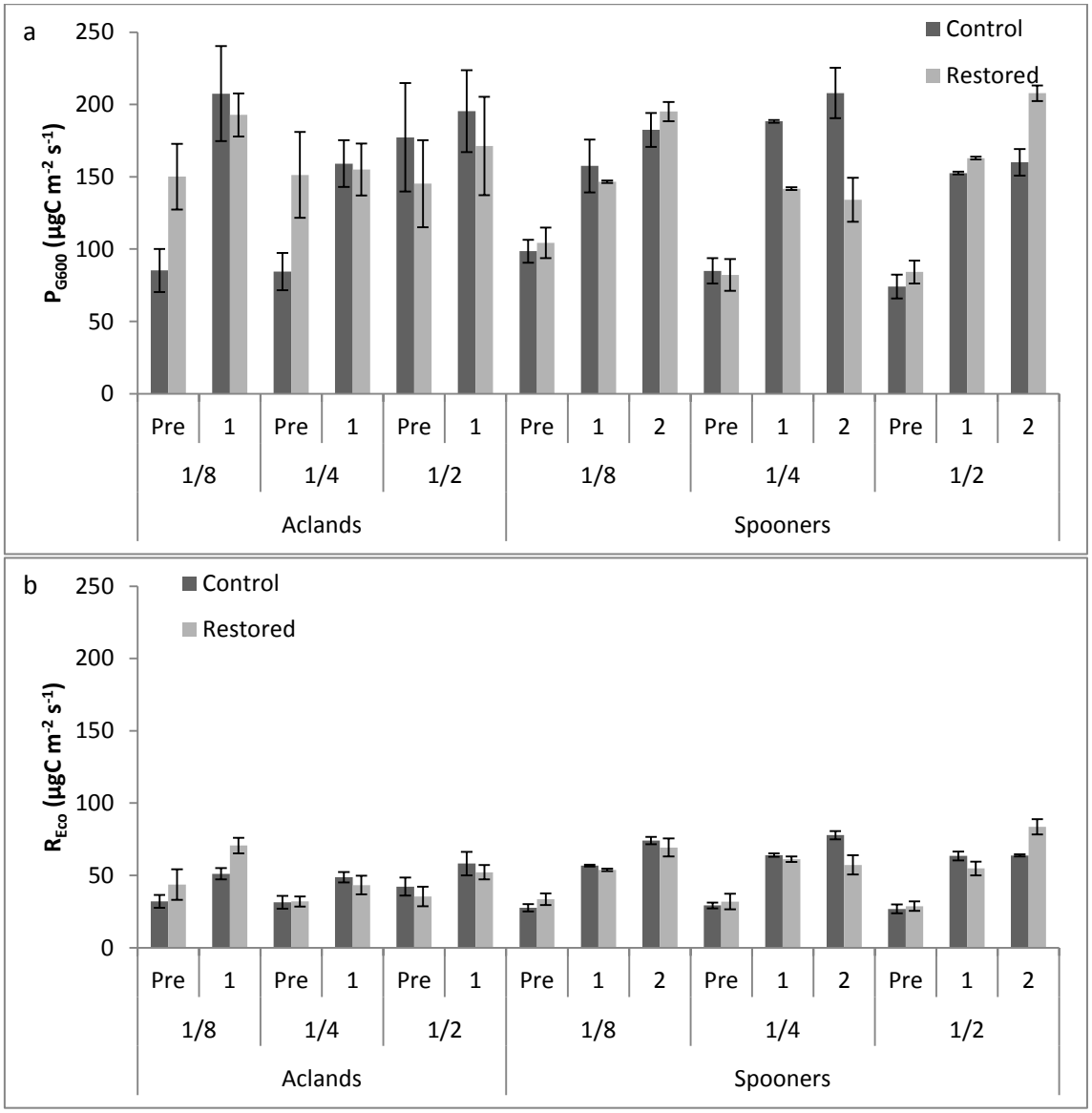

Figure 10.7 Photosynthesis at 600 µmol Photons m^{-2} s^{-1} (a) and ecosystem respiration (b) at the control and restored locations pre-, 1-year and 2-years post restoration (µgC m^{-2} s^{-1}). Error bars are one standard error.

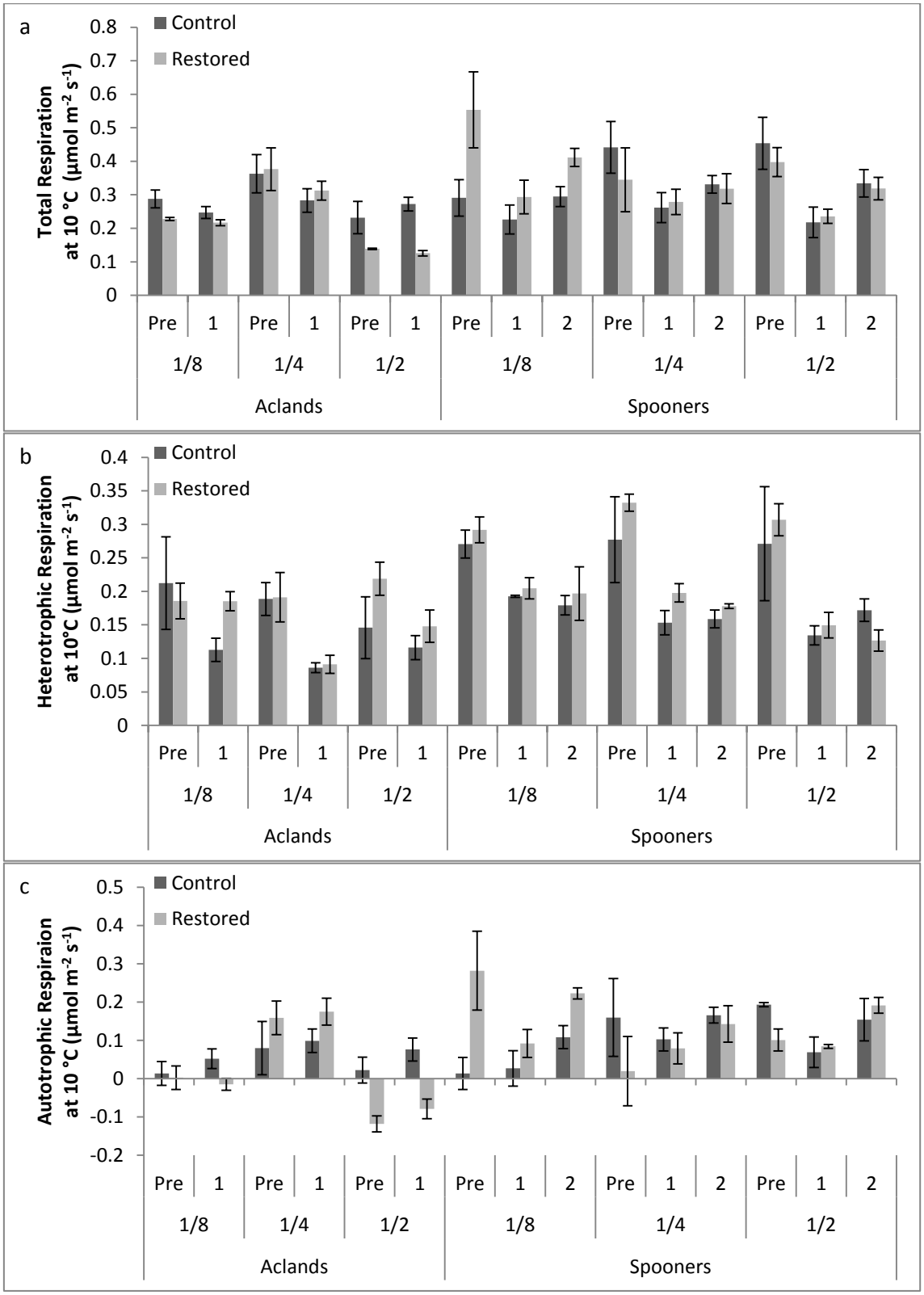

Figure 10.8 Total (a), heterotrophic (b) and autotrophic (c) respiration at 10 °C at the control and restored locations pre-, 1-year and 2-years post restoration (µmol m^{-2} s^{-1}). Error bars are one standard error.

11 BIBLIOGRAPHY

Aerts, R. 1990. Nutrient use efficiency in evergreen and deciduous species from heathlands. Oecologia **84**:391-397.

Aerts, R. and F. Berendse. 1988. The effect of increased nutrient availability on vegetation dynamics in wet heathlands. Vegetatio **76**:63-69.

Ahl, D. E., S. T. Gower, S. N. Burrows, N. V. Shabanov, R. B. Myneni, and Y. Knyazikhin. 2006. Monitoring spring canopy phenology of a deciduous broadleaf forest using MODIS. Remote Sensing of Environment **104**:88-95.

Ahrends, H. E., R. Brugger, R. Stockli, J. Schenk, P. Michna, F. Jeanneret, H. Wanner, and W. Eugster. 2008. Quantitative phenological observations of a mixed beech forest in northern Switzerland with digital photography. Journal of Geophysical Research-Atmospheres **113**:G04004.

Alberton, B., J. Almeida, R. Helm, R. D. Torres, A. Menzel, and L. P. C. Morellato. 2014. Using phenological cameras to track the green up in a cerrado savanna and its on-the-ground validation. Ecological Informatics **19**:62-70.

Alm, J., S. Saarnio, H. Nykänen, J. Silvola, and P. Martikainen. 1999a. Winter CO_2, CH_4 and N_2O fluxes on some natural and drained boreal peatlands. Biogeochemistry **44**:163-186.

Alm, J., S. Saarnio, H. Nykanen, J. Silvola, P. Martikainen, and C. Winter. 1999b. Appendix 3A. 3 Wetlands Remaining Wetlands: Basis for Future Methodological Development. LUCF SECTOR GOOD PRACTICE GUIDANCE **11**:310.

Anderson, K., J. Bennie, and A. Wetherelt. 2010. Laser scanning of fine scale pattern along a hydrological gradient in a peatland ecosystem. Landscape Ecology **25**:477-492.

Anderson, K. and K. J. Gaston. 2013. Lightweight unmanned aerial vehicles will revolutionize spatial ecology. Frontiers in Ecology and the Environment **11**:138-146.

Anderson, P., P. Worrall, S. Ross, G. Hammond, and A. Keen. 2011. Restoring Drained, Burned and Grazed Moorlands. Penny Anderson Associates Limited, Derbyshire.

Armstrong, A., J. Holden, P. Kay, B. Francis, M. Foulger, S. Gledhill, A. T. McDonald, and A. Walker. 2010. The impact of peatland drain-blocking on dissolved organic carbon loss and discolouration of water; results from a national survey. Journal of Hydrology **381**:112-120.

Arrhenius, S. 1898. Uber die Reaktionsgeschwindigkeit bei der Inversion von Rohrzucker durch Sauren. Zeitschrift fur Physik Chemique **4**:226-248.

Atkin, O. K. and M. G. Tjoelker. 2003. Thermal acclimation and the dynamic response of plant respiration to temperature. Trends in Plant Science **8**:343-351.

Aurela, M., T. Laurila, and J.-P. Tuovinen. 2004. The timing of snow melt controls the annual CO2 balance in a subarctic fen. Geophysical Research Letters **31**:L16119.

Aurela, M., A. Lohila, J.-P. Tuovinen, J. Hatakka, T. Riutta, and T. Laurila. 2009. Carbon dioxide exchange on a northern boreal fen. Boreal Environment Research **14**:699-710.

Avery, B. W. 1990. Soils of the British Isles. CAB International.

Bain, C. G., Bonn, A., Stoneman, R., Chapman, S., Coupar, A., Evans, M., Gearey, B., Howat, M., Joosten, H., Keenleyside, C., Labadz, J., Lindsay, R., Littlewood, N., Lunt, P., Miller, C.J., Moxey, A., Orr, H., Reed, M., Smith, P., Swales, V., Thompson, D.B.A., Thompson, P.S., Van de Noort, R., Wilson, J.D. & Worrall,

F. 2011. IUCN UK Commission of Inquiry on Peatlands. IUCN UK Peatland Programme, Edinburgh.

Baldocchi, D., E. Falge, L. Gu, R. Olson, D. Hollinger, S. Running, P. Anthoni, C. Bernhofer, K. Davis, and R. Evans. 2001. FLUXNET: A new tool to study the temporal and spatial variability of ecosystem-scale carbon dioxide, water vapor, and energy flux densities. Bulletin of the American Meteorological Society **82**:2415-2434.

Baldocchi, D. D. 2003. Assessing the eddy covariance technique for evaluating carbon dioxide exchange rates of ecosystems: past, present and future. Global Change Biology **9**:479-492.

Ballantyne, D. M., J. A. Hribljan, T. G. Pypker, and R. A. Chimner. 2014. Long-term water table manipulations alter peatland gaseous carbon fluxes in Northern Michigan. Wetlands Ecology and Management **22**:35-47.

Barrowclough, C. 2014. Exmoor Mires Project Botanical Data Analysis 2013 First Ecology.

Becker, T., L. Kutzbach, I. Forbrich, J. Schneider, D. Jager, B. Thees, and M. Wilmking. 2008. Do we miss the hot spots? - The use of very high resolution aerial photographs to quantify carbon fluxes in peatlands. Biogeosciences **5**:1387-1393.

Bellamy, P. E., L. Stephen, I. S. Maclean, and M. C. Grant. 2012. Response of blanket bog vegetation to drain-blocking. Applied Vegetation Science **15**:129-135.

Belyea, L. R. and A. J. Baird. 2006. Beyond "The Limits to Peat Bog Growth": Cross-scale Feedback in Peatland Development. Ecological Monographs **76**:229-322.

Bendig, J., A. Bolten, S. Bennertz, J. Broscheit, S. Eichfuss, and G. Bareth. 2014. Estimating Biomass of Barley Using Crop Surface Models (CSMs) Derived from UAV-Based RGB Imaging. Remote Sensing **6**:10395-10412.

Benner, P., P. Sabel, and A. Wild. 1988. Photosynthesis and transpiration of healthy and diseased spruce trees in the course of three vegetation periods. Trees **2**:223-232.

Bennie, J., K. Anderson, and A. Wetherelt. 2011. Measuring biodiversity across spatial scales in a raised bog using a novel paired-sample diversity index. Journal of Ecology **99**:482-490.

Berendse, F. 1998. Effects of Dominant Plant Species on Soils during Succession in Nutrient-poor Ecosystems. Biogeochemistry **42**:73-88.

Bernacchi, C. J., E. L. Singsaas, C. Pimentel, A. R. Portis Jr, and S. P. Long. 2001. Improved temperature response functions for models of Rubisco-limited photosynthesis. Plant, Cell & Environment **24**:253-259.

Best, E. P. H. and F. H. H. Jacobs. 1997. The influence of raised water table levels on carbon dioxide and methane production in ditch-dissected peat grasslands in the Netherlands. Ecological Engineering **8**:129-144.

Beven, K. and M. Kirkby. 1979. A physically based, variable contributing area model of basin hydrology. Hydrological Sciences Journal **24**:43-69.

Birkin, L. J., S. Bailey, F. E. Brewis, P. Bruneau, I. Crosher, K. Dobbie, C. Hill, S. Johnson, P. Jones, M. J. Shepherd, J. Skate, and L. Way. 2011. The requirement for improving greenhouse gases flux estimates for peatlands in the UK. Joint Nature Conservation Committee, Peterborough.

Bliss, L. and N. Matveyeva. 1992. Circumpolar arctic vegetation. Arctic ecosystems in a changing climate: an ecophysiological perspective:59-89.

Blodau, C. and T. R. Moore. 2003a. Experimental response of peatland carbon dynamics to a water table fluctuation. Aquatic Sciences - Research Across Boundaries **65**:47-62.

Blodau, C. and T. R. Moore. 2003b. Micro-scale CO_2 and CH_4 dynamics in a peat soil during a water fluctuation and sulfate pulse. Soil Biology and Biochemistry **35**:535-547.

Blodau, C., N. T. Roulet, T. Heitmann, H. Stewart, J. Beer, P. Lafleur, and T. R. Moore. 2007. Belowground carbon turnover in a temperate ombrotrophic bog. Global Biogeochem. Cycles **21**:GB1021.

Bonan, G. B. 1988. The size structure of theoretical plant populations: spatial patterns and neighborhood effects. Ecology:1721-1730.

Bond-Lamberty, B., D. Bronson, E. Bladyka, and S. T. Gower. 2011. A comparison of trenched plot techniques for partitioning soil respiration. Soil Biology and Biochemistry **43**:2108-2114.

Bond-Lamberty, B., C. Wang, and S. T. Gower. 2004. A global relationship between the heterotrophic and autotrophic components of soil respiration? Global Change Biology **10**:1756-1766.

Bonn, A., M. S. Reed, C. D. Evans, H. Joosten, C. Bain, J. Farmer, I. Emmer, J. Couwenberg, A. Moxey, R. Artz, F. Tanneberger, M. von Unger, M.-A. Smyth, and D. Birnie. 2014. Investing in nature: Developing ecosystem service markets for peatland restoration. Ecosystem Services **9**:54-65.

Bowes, A. C. 2006. Exmoor Blanket bog Inventory and restoration plan for English Nature. University of Calgary, Calgary.

Breda, N. J. 2003. Ground-based measurements of leaf area index: a review of methods, instruments and current controversies. Journal of Experimental Botany **54**:2403-2417.

Bridgham, S. D. and C. J. Richardson. 1992. Mechanisms controlling soil respiration (CO_2 and CH_4) in southern peatlands. Soil Biology and Biochemistry **24**:1089-1099.

Brys, R., H. Jacquemyn, and G. De Blust. 2005. Fire increases aboveground biomass, seed production and recruitment success of Molinia caerulea in dry heathland. Acta Oecologica **28**:299-305.

Bubier, J. L., G. Bhatia, T. R. Moore, N. T. Roulet, and P. M. Lafleur. 2003. Spatial and temporal variability in growing-season net ecosystem carbon dioxide exchange at a large peatland in Ontario, Canada. Ecosystems **6**:353-367.

Bunce, R. G. H. and C. J. Barr. 1988. The extent of land under different management regimes in the uplands and the potential for change. Pages 415-426 *in* M. B. Usher and D. B. A. Thompson, editors. Ecological Change in the Uplands, Special Publication no. 7 of the British Ecological Society. Blackwell Scientific Publications, Oxford, UK.

Cannell, M. G. R., R. C. Dewar, and D. G. PYATT. 1993. Conifer Plantations on Drained Peatlands in Britain: a Net Gain or Loss of Carbon? Forestry **66**:353-369.

Carey, C. 2015. Geoarchaeological investigation on Exmoor; reconstructing the human-environmental dynamic of Early Holocene Exmoor.*in* Exmoor Mires Project Conference, Dulverton.

Castillo, C., R. Pérez, M. R. James, J. N. Quinton, E. V. Taguas, and J. A. Gómez. 2012. Comparing the accuracy of several field methods for measuring gully erosion. Soil Science Society of America **14**.

Chabot, D. and D. M. Bird. 2013. Small unmanned aircraft: precise and convenient new tools for surveying wetlands. Journal of Unmanned Vehicle Systems **01**:15-24.

Chambers, F. M., D. Mauquoy, and P. A. Todd. 1999. Recent rise to dominance of Molinia caerulea in environmentally sensitive areas: new perspectives from palaeoecological data. Journal of Applied Ecology **36**:719-733.

Chapman, S. and M. Thurlow. 1998. Peat respiration at low temperatures. Soil Biology and Biochemistry **30**:1013-1021.

Chapman, S. J. and M. Thurlow. 1996. The influence of climate on CO_2 and CH_4 emissions from organic soils. Agricultural and Forest Meteorology **79**:205-217.

Charman, D. 2002. Peatlands and Environmental Change. John Wiley & Sons Ltd, Chichester.

Chassereau, J. E., J. M. Bell, and R. Torres. 2011. A comparison of GPS and lidar salt marsh DEMs. Earth Surface Processes and Landforms **36**:1770-1775.

Chen, X., C. Xu, and Z. Tan. 2001. An analysis of relationships among plant community phenology and seasonal metrics of Normalized Difference Vegetation Index in the northern part of the monsoon region of China. International Journal of Biometeorology **45**:170-177.

Chimner, R. A. and D. J. Cooper. 2003. Influence of water table levels on CO_2 emissions in a Colorado subalpine fen: an in situ microcosm study. Soil Biology and Biochemistry **35**:345-351.

Clark, J. M., A. V. Gallego-Sala, T. E. H. Allott, S. J. Chapman, T. Farewell, C. Freeman, J. I. House, H. G. Orr, I. C. Prentice, and P. Smith. 2010. Assessing the vulnerability of blanket peat to climate change using an ensemble of statistical bioclimatic envelope models. Climate Research **45**:131-U462.

Clay, G. D., S. Dixon, M. G. Evans, J. G. Rowson, and F. Worrall. 2012. Carbon dioxide fluxes and DOC concentrations of eroding blanket peat gullies. Earth Surface Processes and Landforms **37**:562-571.

Clymo, R. 1984. The limits to peat bog growth. Philosophical Transactions of the Royal Society of London B: Biological Sciences **303**:605-654.

Clymo, R. S. 1983. Peat. Pages 159-224 *in* A. J. P. Gore, editor. Mires, Swamp, Fen and Moor. General Studies. Ecosystems of the World 4a. Elsevier Scientific, Amsterdam.

Clymo, R. S. 1992. Models of peat growth. Suo **43**:127-136.

Cook, B. D., P. V. Bolstad, E. Næsset, R. S. Anderson, S. Garrigues, J. T. Morisette, J. Nickeson, and K. J. Davis. 2009. Using LiDAR and quickbird data to model plant production and quantify uncertainties associated with wetland detection and land cover generalizations. Remote Sensing of Environment **113**:2366-2379.

Cooper, M. D. A., C. D. Evans, P. Zielinski, P. E. Levy, A. Gray, M. Peacock, D. Norris, N. Fenner, and C. Freeman. 2014. Infilled Ditches are Hotspots of Landscape Methane Flux Following Peatland Re-wetting. Ecosystems **17**:1227-1241.

Coops, N. C., T. Hilker, C. W. Bater, M. A. Wulder, S. E. Nielsen, G. McDermid, and G. Stenhouse. 2011. Linking ground-based to satellite-derived phenological metrics in support of habitat assessment. Remote Sensing Letters **3**:191-200.

Corradi, C., O. Kolle, K. Walter, S. Zimov, and E. D. Schulze. 2005. Carbon dioxide and methane exchange of a north-east Siberian tussock tundra. Global Change Biology **11**:1910-1925.

Coulson, J. C. and J. Butterfield. 1978. An Investigation of the Biotic Factors Determining the Rates of Plant Decomposition on Blanket Bog. Journal of Ecology **66**:631-650.

Coulson, J. C., J. E. L. Butterfield, and E. Henderson. 1990. The Effect of Open Drainage Ditches on the Plant and Invertebrate Communities of Moorland and on the Decomposition of Peat. Journal of Applied Ecology **27**:549-561.

Couwenberg, J. 2005. A simulation model of mire patterning – revisited. Ecography **28**:653-661.

Couwenberg, J., A. Thiele, F. Tanneberger, J. Augustin, S. Barisch, D. Dubovik, N. Liashchynskaya, D. Michaelis, M. Minke, A. Skuratovich, and H. Joosten. 2011.

Assessing greenhouse gas emissions from peatlands using vegetation as a proxy. Hydrobiologia **674**:67-89.
Cruickshank, M. and R. Tomlinson. 1990. Peatland in Northern Ireland: inventory and prospect. Irish Geography **23**:17-30.
Curiel Yuste, J., I. A. Janssens, A. Carrara, and R. Ceulemans. 2004. Annual Q10 of soil respiration reflects plant phenological patterns as well as temperature sensitivity. Global Change Biology **10**:161-169.
Dandois, J. P. and E. C. Ellis. 2010. Remote Sensing of Vegetation Structure Using Computer Vision. Remote Sensing **2**:1157-1176.
Dandois, J. P. and E. C. Ellis. 2013. High spatial resolution three-dimensional mapping of vegetation spectral dynamics using computer vision. Remote Sensing of Environment **136**:259-276.
Davis, K. J., P. S. Bakwin, C. Yi, B. W. Berger, C. Zhao, R. M. Teclaw, and J. G. Isebrands. 2003. The annual cycles of CO_2 and H_2O exchange over a northern mixed forest as observed from a very tall tower. Global Change Biology **9**:1278-1293.
Demarez, V., S. Duthoit, F. Baret, M. Weiss, and G. Dedieu. 2008. Estimation of leaf area and clumping indexes of crops with hemispherical photographs. Agricultural and Forest Meteorology **148**:644-655.
Dinsmore, K. J., M. F. Billett, U. M. Skiba, R. M. Rees, J. Drewer, and C. Helfter. 2010. Role of the aquatic pathway in the carbon and greenhouse gas budgets of a peatland catchment. Global Change Biology **16**:2750-2762.
Dixon, S. D., S. M. Qassim, J. G. Rowson, F. Worrall, M. G. Evans, I. M. Boothroyd, and A. Bonn. 2013. Restoration effects on water table depths and CO_2 fluxes from climatically marginal blanket bog. Biogeochemistry:1-18.
Dixon, S. D., F. Worrall, J. G. Rowson, and M. G. Evans. 2015. Calluna vulgaris canopy height and blanket peat CO_2 flux: Implications for management. Ecological Engineering **75**:497-505.
Dowling, T. J., A. M. Read, and J. C. Gallant. 2009. Very high resolution DEM acquisition at low cost using a digital camera and free software. 18th World IMACS / MODSIM Congress, Cairns, Australia.
Ducke, B., D. Score, and J. Reeves. 2011. Multiview 3D reconstruction of the archaeological site at Weymouth from image series. Computers & Graphics **35**:375-382.
Dunn, C. and C. Freeman. 2011. Peatlands: our greatest source of carbon credits? Carbon Management **2**:289-301.
Evans, C., F. Worrall, J. Holden, P. Chapman, P. Smith, and R. Artz. 2011. A programme to address evidence gaps in greenhouse gas and carbon fluxes from UK peatlands, Report No. 443. JNCC, Peterborough.
Evans, C. D., A. Bonn, J. Holden, M. S. Reed, M. G. Evans, F. Worrall, J. Couwenberg, and M. Parnell. 2014. Relationships between anthropogenic pressures and ecosystem functions in UK blanket bogs: Linking process understanding to ecosystem service valuation. Ecosystem Services **9**:5-19.
Fenner, N. and C. Freeman. 2011. Drought-induced carbon loss in peatlands. Nature Geoscience **4**.
Fensholt, R., I. Sandholt, and M. S. Rasmussen. 2004. Evaluation of MODIS LAI, fAPAR and the relation between fAPAR and NDVI in a semi-arid environment using in situ measurements. Remote Sensing of Environment **91**:490-507.
Fisher, J. I. and J. F. Mustard. 2007. Cross-scalar satellite phenology from ground, Landsat, and MODIS data. Remote Sensing of Environment **109**:261-273.

Fisher, J. I., J. F. Mustard, and M. A. Vadeboncoeur. 2006. Green leaf phenology at Landsat resolution: Scaling from the field to the satellite. Remote Sensing of Environment **100**:265-279.

Flanagan, L. B. and B. G. Johnson. 2005. Interacting effects of temperature, soil moisture and plant biomass production on ecosystem respiration in a northern temperate grassland. Agricultural and Forest Meteorology **130**:237-253.

Fontaine, S., S. Barot, P. Barre, N. Bdioui, B. Mary, and C. Rumpel. 2007. Stability of organic carbon in deep soil layers controlled by fresh carbon supply. Nature **450**:277-280.

Fontana, F., C. Rixen, T. Jonas, G. Aberegg, and S. Wunderle. 2008. Alpine Grassland Phenology as Seen in AVHRR, VEGETATION, and MODIS NDVI Time Series - a Comparison with In Situ Measurements. Sensors **8**:2833-2853.

Frankenberger, J. R., C. Huang, and K. Nouwakpo. 2008. Low-Altitude Digital Photogrammetry Technique to Assess Ephemeral Gully Erosion. Pages IV - 117-IV - 120 *in* Geoscience and Remote Sensing Symposium, 2008. IGARSS 2008. IEEE International.

Freeman, C., J. Ostle, N. Fenner, and H. Kang. 2004. A regulatory role for phenol oxidase during decomposition in peatlands. Soil Biology and Biochemistry **36**:1663-1667.

Freeman, C., J. Ostle, and H. Kang. 2001. An enzymic 'latch' on a global carbon store. Nature **409**.

Fyfe, R., P. Anderson, R. Barnett, W. Blake, T. Daley, K. Head, A. MacLeod, I. Matthews, and D. Smith. 2014. Vegetation and climate change on Exmoor over the last millennium: detailed analysis of Ricksy Ball. Plymouth University, Plymouth.

Fyfe, R. M., P. Anderson, T. Daley, M. Gehrels, and D. Smith. 2012. Environmental change over the last millennium at Spooners and Ricksy Ball, Exmoor Stage 1 report. Prepared for Exmoor National Park Authority.

Gamon, J. A., C. B. Field, M. L. Goulden, K. L. Griffin, A. E. Hartley, G. Joel, J. Peñuelas, and R. Valentini. 1995. Relationships Between NDVI, Canopy Structure, and Photosynthesis in Three Californian Vegetation Types. Ecological Applications **5**:28-41.

Gamon, J. A., L. Serrano, and J. S. Surfus. 1997. The photochemical reflectance index: an optical indicator of photosynthetic radiation use efficiency across species, functional types, and nutrient levels. Oecologia **112**:492-501.

Garrigues, S., N. V. Shabanov, K. Swanson, J. T. Morisette, F. Baret, and R. B. Myneni. 2008. Intercomparison and sensitivity analysis of Leaf Area Index retrievals from LAI-2000, AccuPAR, and digital hemispherical photography over croplands. Agricultural and Forest Meteorology **148**:1193-1209.

Glaser, P. H. 1987. The development of streamlined bog islands in the continental interior of North America. Arctic and Alpine Research:402-413.

Gogo, S., F. Laggoun-Dafarge, F. Delarue, and N. Lottier. 2011. Invasion of a Sphagnum-peatland by Betula spp and Molinia caerulea; impacts organic matter biochemistry. Implications for carbon and nutrient cycling. Biogeochemistry **106**:53-69.

Goldhammer, T. and C. Blodau. 2008. Desiccation and product accumulation constrain heterotrophic anaerobic respiration in peats of an ombrotrophic temperate bog. Soil Biology and Biochemistry **40**:2007-2015.

Gore, A. J. P. and C. Urquhart. 1966. The Effects of Waterlogging on the Growth of Molinia Caerulea and Eriophorum Vaginatum. Journal of Ecology **54**:617-633.

Gorham, E. 1991. Northern Peatlands - Role in the Carbon-Cycle and Probable Responses to Climatic Warming. Ecological Applications **1**:182-195.

Gorham, E. and L. Rochefort. 2003. Peatland restoration: a brief assessment with special reference to Sphagnum bogs. Wetlands Ecology and Managagment **11**:109-119.

Goulden, M. L., J. W. Munger, S.-M. Fan, B. C. Daube, and S. C. Wofsy. 1996. Measurements of carbon sequestration by long-term eddy covariance: Methods and a critical evaluation of accuracy. Global Change Biology **2**:169-182.

Grand-Clement, E., K. Anderson, D. Smith, M. Angus, D. J. Luscombe, N. Gatis, L. S. Bray, and R. E. Brazier. 2015. New Approaches to the Restoration of Shallow Marginal Peatlands. Journal of Environmental Management, doi.org/10.1016/j.jenvman.2015.06.023.

Grand-Clement, E., K. Anderson, D. Smith, D. Luscombe, N. Gatis, M. Ross, and R. Brazier. 2013a. Evaluating ecosystem goods and services after restoration of marginal upland peatlands in south-west England. Journal of Applied Ecology **50**:324-334.

Grand-Clement, E., K. Anderson, D. Smith, D. Luscombe, N. Gatis, M. Ross, and R. E. Brazier. 2013b. Evaluating ecosystem goods and services after restoration of marginal upland peatlands in South-West England. Journal of Applied Ecology **50**:324-334.

Grand-Clement, E., D. J. Luscombe, K. Anderson, N. Gatis, P. Benaud, and R. E. Brazier. 2014. Antecedent conditions control carbon loss and downstream water quality from shallow, damaged peatlands. Science of The Total Environment **493**:961-973.

Grand-Clement, E., M. Ross, D. Smith, K. Anderson, D. J. Luscombe, N. Le Feuvre, and R. E. Brazier. 2012. " Upstream Thinking": the catchment management approach of a water provider. . Page 4238 EGU General Assembly, Vienna, Austria.

Grant, S. A., L. Torvell, T. Common, E. M. Sim, and J. Small. 1996. Controlled grazing studies on Molinia grassland: effects of different seasonal patterns and levels of defoliation on Molinia growth and responses of swards to controlled grazing by cattle. Journal of Applied Ecology:1267-1280.

Haapalehto, T. O., H. Vasander, S. Jauhiainen, T. Tahvanainen, and J. S. Kotiaho. 2010. The Effects of Peatland Restoration on Water-Table Depth, Elemental Concentrations, and Vegetation:10 Years of Changes. Restoration Ecology **19**:12.

Hájková, P., M. Hájek, and K. Kintrová. 2009. How can we effectively restore species richness and natural composition of a Molinia-invaded fen? Journal of Applied Ecology **46**:417-425.

Hakrová, P. and K. Novotná. 2011. Changes in the species composition and vegetation structure of species-poor grasslands after restoration of a mowing regime. Journal of Landscape Studies **4**:117-129.

Hardie, S. M. L., M. H. Garnett, A. E. Fallick, N. J. Ostle, and A. P. Rowland. 2009. Bomb-C-14 analysis of ecosystem respiration reveals that peatland vegetation facilitates release of old carbon. Geoderma **153**:393-401.

Hargreaves, K., R. Milne, and M. Cannell. 2003. Carbon balance of afforested peatland in Scotland. Forestry **76**:299-317.

Harris, A., R. G. Bryant, and A. J. Baird. 2005. Detecting near-surface moisture stress in Sphagnum spp. Remote Sensing of Environment **97**:371-381.

Harwin, S. and A. Lucieer. 2012. Assessing the Accuracy of Georeferenced Point Clouds Produced via Multi-View Stereopsis from Unmanned Aerial Vehicle (UAV) Imagery. Remote Sensing **4**:1573-1599.

Hearn, S. M., J. R. Healey, M. A. McDonald, A. J. Turner, J. L. G. Wong, and G. B. Stewart. 2011. The repeatability of vegetation classification and mapping. Journal of Environmental Management **92**:1174-1184.

Heffernan, J. B. 2008. Wetlands as an alternative stable state in desert streams. Ecology **89**:1261-1271.

Hegarty, C. and K. Toms. 2009. Exmoor National Park National Mapping Programme Managment and Summary Report. Exmoor National Park Authority, Dulverton.

Heinemeyer, A., C. Di Bene, A. R. Lloyd, D. Tortorella, R. Baxter, B. Huntley, A. Gelsomino, and P. Ineson. 2011. Soil respiration: implications of the plant-soil continuum and respiration chamber collar-insertion depth on measurement and modelling of soil CO_2 efflux rates in three ecosystems. European Journal of Soil Science **62**:82-94.

Heinemeyer, A., D. Tortorella, B. Petrovicova, and A. Gelsomino. 2012. Partitioning of soil CO_2 flux components in a temperate grassland ecosystem. European Journal of Soil Science **63**:249-260.

Helfter, C., C. Campbell, K. J. Dinsmore, J. Drewer, M. Coyle, M. Anderson, U. Skiba, E. Nemitz, M. F. Billett, and M. A. Sutton. 2015. Drivers of long-term variability in CO2 net ecosystem exchange in a temperate peatland. Biogeosciences **12**:1799-1811.

Hengl, T. 2006. Finding the right pixel size. Computers & Geosciences **32**:1283-1298.

Henneken, R., V. Dose, C. Schleip, and A. Menzel. 2013. Detecting plant seasonality from webcams using Bayesian multiple change point analysis. Agricultural and Forest Meteorology **168**:177-185.

Hill, M. O., J. O. Mountford, D. B. Roy, and R. G. H. Bunce. 1999. Factors controlling biodiversity in the British countryside (ECOFACT), Volume 2: Technical Annex – Ellenberg's indicator values for British plants. Institute of Terrestrial Ecology, Huntingdon.

Hobbs, N. B. 1986. Mire morphology and the properties and behaviour of some British and foreign peats. Quarterly Journal of Engineering Geology and Hydrogeology **19**:7-80.

Holden, J., P. J. Chapman, and J. C. Labadz. 2004. Artificial drainage of peatlands: hydrological and hydrochemical process and wetland restoration. Progress in Physical Geography **28**:95–123.

Holden, J., Z. E. Wallage, S. N. Lane, and A. T. McDonald. 2011. Water table dynamics in undisturbed, drained and restored blanket peat. Journal of Hydrology **402**:103-114.

Hopkinson, C., K. Lim, L. E. Chasmer, P. Treitz, I. F. Creed, and C. Gynand. 2004. Wetland grass to plantation forest - estimating vegetation height from the standard deviation of lidar frequency distributions. **36**.

Hornibrook, E. 2015. Greenhouse gas overview and carbon storage in mires.*in* Exmoor Mires Project Conference, Dulverton.

Hornibrook, E., A. McAleer, J. Tian, and B. Middleton. 2012. Exmoor Mires Project, University of Bristol - Year 2 Report Actions and Achievements 2011-2012. University of Bristol, Bristol.

Hufkens, K., M. Friedl, O. Sonnentag, B. H. Braswell, T. Milliman, and A. D. Richardson. 2012. Linking near-surface and satellite remote sensing measurements of deciduous broadleaf forest phenology. Remote Sensing of Environment **117**:307-321.

Hunter, R. 1962. Hill sheep and their pasture: a study of sheep-grazing in south-east Scotland. The Journal of Ecology:651-680.

Ide, R. and H. Oguma. 2010. Use of digital cameras for phenological observations. Ecological Informatics **5**:339-347.

Ingram, H. 1978. Soil layers in mires: function and terminology. Journal of Soil Science **29**:224-227.

IPCC. 2014. 2013 Supplement to the 2006 IPCC Guidelines for National Greenhouse Gas Inventories: Wetlands.*in* T. Hiraishi, T. Krug, K. Tanabe, N. Srivastava, J. Baasansuren, M. Fukuda, and T. G. Troxler, editors. IPCC, Switzerland.

Ivanov, K. E. 1981. Water movement in mirelands. Translated from Russian by Thompson, A., and Ingram, H. A. P. Academic Press, London.

Jaatinen, K., H. Fritze, J. Laine, and R. Laiho. 2007. Effects of short-and long-term water-level drawdown on the populations and activity of aerobic decomposers in a boreal peatland. Global Change Biology **13**:491-510.

Jaatinen, K., R. Laiho, A. Vuorenmaa, U. Del Castillo, K. Minkkinen, T. Pennanen, T. Penttilä, and H. Fritze. 2008. Responses of aerobic microbial communities and soil respiration to water-level drawdown in a northern boreal fen. Environmental Microbiology **10**:339-353.

James, M. R. and S. Robson. 2012. Straightforward reconstruction of 3D surfaces and topography with a camera: Accuracy and geoscience application. Journal of Geophysical Research - Earth Surface **117**.

James, M. R. and S. Robson. 2014. Mitigating systematic error in topographic models derived from UAVand ground-based image networks. Earth Surface Processes and Landforms **39**:1413-1420.

Jauhiainen, S., R. Laiho, and H. Vasander. 2002. Ecohydrological and vegetational changes in a restored bog and fen. Annales Botanici Fennici **39**:185-199.

Jefferies, T. A. 1915. Ecology of the Purple Heath Grass (Molinia Caerulea). Journal of Ecology **3**:93-109.

Jenkins, G., J. Murphy, D. Sexton, J. Lowe, P. Jones, and C. Kilsby. 2009. UK climate projections: briefing report. MET Office Hadley Centre, Exeter.

Jenson, S. K. 1991. Applications of hydrologic information automatically extracted from digital elevation models. Hydrological Processes **5**:31-44.

Jester, W. and A. Klik. 2005. Soil surface roughness measurement - methods, applicability, and surface representation. CATENA **64**:174-192.

JNCC. 2011. Towards and assessment of the state of UK Peatlands, JNCC report No. 445.

Jolly, W. M., R. Nemani, and S. W. Running. 2005. A generalized, bioclimatic index to predict foliar phenology in response to climate. Global Change Biology **11**:619-632.

Jonsson, P. and L. Eklundh. 2002. Seasonality extraction by function fitting to time-series of satellite sensor data. Geoscience and Remote Sensing, IEEE Transactions on **40**:1824-1832.

Joosten, H. and D. Clarke. 2002. Wise Use of Mires and Peatlands. International Mire Conversation Group and International Peat Society, Totnes.

Juszczak, R., E. Humphreys, M. Acosta, M. Michalak-Galczewska, D. Kayzer, and J. Olejnik. 2013. Ecosystem respiration in a heterogeneous temperate peatland and its sensitivity to peat temperature and water table depth. Plant and Soil **366**:505-520.

Karu, H., M. Pensa, E. I. Room, A. Portsmuth, and T. Triisberg. 2014. Carbon fluxes in forested bog margins along a human impact gradient: could vegetation structure be used as an indicator of peat carbon emissions? Wetlands Ecology and Management **22**:399-417.

Keenan, T. F., B. Darby, E. Felts, O. Sonnentag, M. A. Friedl, K. Hufkens, J. O'Keefe, S. Klosterman, J. W. Munger, M. Toomey, and A. D. Richardson. 2014. Tracking forest phenology and seasonal physiology using digital repeat photography: a critical assessment. Ecological Applications **24**:1478-1489.

Keenan, T. F., D. Y. Hollinger, G. Bohrer, D. Dragoni, J. W. Munger, H. P. Schmid, and A. D. Richardson. 2013. Increase in forest water-use efficiency as atmospheric carbon dioxide concentrations rise. Nature **499**:324-327.

Kennedy, K. and P. Addison. 1987. Some considerations for the use of visual estimates of plant cover in biomonitoring. The Journal of Ecology:151-157.

Kincey, M. and K. Challis. 2010. Monitoring fragile upland landscapes: The application of airborne lidar. Journal for Nature Conservation **18**:126-134.

Knorr, K.-H., G. Lischeid, and C. Blodau. 2009. Dynamics of redox processes in a minerotrophic fen exposed to a water table manipulation. Geoderma **153**:379-392.

Knoth, C., B. Klein, T. Prinz, and T. Kleinebecker. 2013. Unmanned aerial vehicles as innovative remote sensing platforms for high-resolution infrared imagery to support restoration monitoring in cut-over bogs. Applied Vegetation Science **16**:509-517.

Koehler, A. K., M. Sottocornola, and G. Kiely. 2011. How strong is the current carbon sequestration of an Atlantic blanket bog? Global Change Biology **17**:309-319.

Komulainen, V.-M., H. Nykänen, P. J. Martikainen, and J. Laine. 1998. Short-term effect of restoration on vegetation change and methane emissions from peatlands drained for forestry in southern Finland. Canadian Journal of Forest Research **28**:402-411.

Komulainen, V. M., E. S. Tuittila, H. Vasander, and J. Laine. 1999. Restoration of drained peatlands in southern Finland: initial effects on vegetation change and CO_2 balance. Journal of Applied Ecology **36**:634-648.

Korpela, I., M. Koskinen, H. Vasander, M. Holopainen, and K. Minkkinen. 2009. Airborne small-footprint discrete-return LiDAR data in the assessment of boreal mire surface patterns, vegetation, and habitats. Forest Ecology and Management **258**:1549-1566.

Kross, A., J. W. Seaquist, N. T. Roulet, R. Fernandes, and O. Sonnentag. 2013. Estimating carbon dioxide exchange rates at contrasting northern peatlands using MODIS satellite data. Remote Sensing of Environment **137**:234-243.

Kutsch, W. L., A. Staack, J. Wötzel, U. Middelhoff, and L. Kappen. 2001. Field measurements of root respiration and total soil respiration in an alder forest. New Phytologist **150**:157-168.

Kuzyakov, Y. and A. A. Larionova. 2005. Root and rhizomicrobial respiration: A review of approaches to estimate respiration by autotrophic and heterotrophic organisms in soil. Journal of plant nutrition and soil science **168**:503-520.

Lafleur, P. M., T. R. Moore, N. T. Roulet, and S. Frolking. 2005. Ecosystem respiration in a cool temperate bog depends on peat temperature but not water table. Ecosystems **8**:619-629.

Lafleur, P. M., N. T. Roulet, J. L. Bubier, S. Frolking, and T. R. Moore. 2003. Interannual variability in the peatland-atmosphere carbon dioxide exchange at an ombrotrophic bog. Global Biogeochemical Cycles **17**:14.

Laine, A., K. A. Byrne, G. Kiely, and E.-S. Tuittila. 2007. Patterns in vegetation and CO_2 dynamics along a water level gradient in a lowland blanket bog. Ecosystems **10**:890-905.

Laine, A., T. Riutta, S. Juutinen, M. Valiranta, and E. S. Tuittila. 2009. Acknowledging the spatial heterogeneity in modelling/reconstructing carbon dioxide exchange in a northern aapa mire. Ecological Modelling **220**:2646-2655.

Laine, A., M. Sottocornola, G. Kiely, K. A. Byrne, D. Wilson, and E.-S. Tuittila. 2006. Estimating net ecosystem exchange in a patterned ecosystem: Example from blanket bog. Agricultural and Forest Meteorology **138**:231-243.

Laine, A. M., M. Leppälä, O. Tarvainen, M. L. Päätalo, R. Seppänen, and A. Tolvanen. 2011. Restoration of managed pine fens: effect on hydrology and vegetation. Applied Vegetation Science **14**:340-349.

Laliberte, A. S. and A. Rango. 2009. Texture and Scale in Object-Based Analysis of Subdecimeter Resolution Unmanned Aerial Vehicle (UAV) Imagery. Geoscience and Remote Sensing, IEEE Transactions on **47**:761-770.

Lappalainen, E. 1996. Global peat resources. International Peat Society Jyskä.

Larsen, K. S., A. Ibrom, C. Beier, S. Jonasson, and A. Michelsen. 2007. Ecosystem respiration depends strongly on photosynthesis in a temperate heath. Biogeochemistry **85**:201-213.

Lashof, D. A. and D. R. Ahuja. 1990. Relative contributions of greenhouse gas emissions to global warming. Nature **334**:529-531.

Lee, M.-s., K. Nakane, T. Nakatsubo, and H. Koizumi. 2003. Seasonal changes in the contribution of root respiration to total soil respiration in a cool-temperate deciduous forest. Pages 311-318 *in* J. Abe, editor. Roots: The Dynamic Interface between Plants and the Earth. Springer Netherlands.

Lefsky, M. A., W. B. Cohen, S. A. Acker, G. G. Parker, T. A. Spies, and D. Harding. 1999. Lidar Remote Sensing of the Canopy Structure and Biophysical Properties of Douglas-Fir Western Hemlock Forests. Remote Sensing of Environment **70**:339-361.

Lelong, C. C., P. Burger, G. Jubelin, B. Roux, S. Labbé, and F. Baret. 2008. Assessment of unmanned aerial vehicles imagery for quantitative monitoring of wheat crop in small plots. Sensors **8**:3557-3585.

Lerma, J. L. and C. Muir. 2014. Evaluating the 3D documentation of an early Christian upright stone with carvings from Scotland with multiples images. Journal of Archaeological Science **46**:311-318.

Lieffers, V. 1988. Sphagnum and cellulose decomposition in drained and natural areas of an Alberta peatland. Canadian Journal of Soil Science **68**:755-761.

Lindsay, R. 1995. Ecology, classification and conservation of ombrotrophic mires. Scottish Natural Heritage Edinburgh.

Lindsay, R. A. 2010. Peatbogs and carbon: a critical synthesis to inform policy development in oceanic peat bog conservation and restoration in the context of climate change. University of East London, London.

Lindsay, R. A., D. J. Charman, F. Everingham, R. M. O'Reilly, M. A. Palmer, T. A. Rowell, and D. A. Stroud. 1988. Part I Peatland Ecology. Pages 9-32 *in* D. A. Ratcliffe and P. H. Oswald, editors. The Flow Country - The peatlands of Caithness and Sutherland. Nature Conservation Committee.

Lindsay, R. A., Rigall, J. and Burd, F. 1985. The use of small-scale surface patterns in the classification of British Peatlands. Aquilo Seria Botanica **21**:67-79.

Littlewood, N., P. Anderson, R. Artz, O. Bragg, P. Lunt, and R. Marrs. 2010. Peatland biodiversity. IUCN UK Peatland Programme, Edinburgh.

Lloyd, A. R. 2010. Carbon fluxes at an upland blanket bog in the north Pennines. Durham University, Durham.

Lloyd, J. and J. A. Taylor. 1994. On the Temperature Dependence of Soil Respiration. Functional Ecology **8**:315-323.

Lucieer, A., D. Turner, D. H. King, and S. A. Robinson. 2014. Using an Unmanned Aerial Vehicle (UAV) to capture micro-topography of Antarctic moss beds. International Journal of Applied Earth Observation and Geoinformation **27, Part A**:53-62.

Lund, M., J. Bjerke, B. Drake, O. Engelsen, G. Hansen, F. Parmentier, T. Powell, H. Silvennoinen, M. Sottocornola, and H. Tømmervik. 2015. Low impact of dry

conditions on the CO_2 exchange of a Northern-Norwegian blanket bog. Environmental Research Letters **10**:025004.
Lund, M., A. Lindroth, T. R. Christensen, and L. Strom. 2007. Annual CO_2 balance of a temperate bog. Tellus B **59**:804-811.
Lunetta, R. S., J. F. Knight, J. Ediriwickrema, J. G. Lyon, and L. D. Worthy. 2006. Land-cover change detection using multi-temporal MODIS NDVI data. Remote Sensing of Environment **105**:142-154.
Lunt, P., T. Allot, P. Anderson, M. Buckler, A. Coupar, P. Jones, J. Labadz, P. Worrall, and M. Evans. 2010. Impacts of peatland restoration. Draft Scientific Review for the IUCN UK Peatland Programme's Comission of Inquiry into Peatland Restoration.
Luscombe, D. J. 2014. Understanding the ecohydrology of shallow, drained and marginal blanket peatlands. University of Exeter, Exeter.
Luscombe, D. J., K. Anderson, N. Gatis, E. Grand-Clement, and R. E. Brazier. 2014a. Using thermal airborne imagery to measure near surface hydrology in upland ecosystems. Hydrological Processes.
Luscombe, D. J., K. Anderson, N. Gatis, A. Wetherelt, E. Grand-Clement, and R. E. Brazier. 2014b. What does airborne LiDAR really measure in upland ecosystems? Ecohydrology **DOI: 10.1002/eco.1527**.
Luscombe, D. J., K. Anderson, E. Grand-Clement, N. Gatis, J. Ashe, P. Benaud, D. Smith, and R. E. Brazier. In prep. Understanding the hydrology of shallow drained and marginal peatlands: Spatial Variability.
Luscombe, D. J., K. Anderson, E. Grand-Clement, N. Gatis, J. Ashe, P. Benaud, D. Smith, and R. E. Brazier. In Review. Understanding the hydrology of shallow drained and marginal peatlands: Temporal Variability. Hydrological Processes.
Luscombe, D. J., E. Grand-Clement, N. Gatis, P. Benaud, J. Ashe, K. Anderson, D. Smith, and R. E. Brazier. 2015. Understanding the ecohydrology of Exmoor's peatlands before and after restoration.*in* Exmoor Mires Project Conference, Dulverton.
Maanavilja, L., T. Riutta, M. Aurela, M. Pulkkinen, T. Laurila, and E. S. Tuittila. 2011. Spatial variation in CO_2 exchange at a northern aapa mire. Biogeochemistry **104**:325-345.
Macfarlane, C. and G. N. Ogden. 2011. Automated estimation of foliage cover in forest understorey from digital nadir images. Methods in Ecology and Evolution **3**:405-415.
Makiranta, P., K. Minkkinen, J. Hytonen, and J. Laine. 2008. Factors causing temporal and spatial variation in heterotrophic and rhizospheric components of soil respiration in afforested organic soil croplands in Finland. Soil Biology and Biochemistry **40**:1592-1600.
Malmer, N., T. Johansson, M. Olsrud, and T. R. Christensen. 2005. Vegetation, climatic changes and net carbon sequestration in a North-Scandinavian subarctic mire over 30 years. Global Change Biology **11**:1895-1909.
Marrs, R., J. Phillips, P. Todd, J. Ghorbani, and M. Le Duc. 2004. Control of Molinia caerulea on upland moors. Journal of Applied Ecology **41**:398-411.
Martikainen, P. J., H. Nykänen, J. Alm, and J. Silvola. 1995. Change in fluxes of carbon dioxide, methane and nitrous oxide due to forest drainage of mire sites of different trophy. Plant and Soil **168**:571-577.
Mathews, A. and J. Jensen. 2013. Visualizing and Quantifying Vineyard Canopy LAI Using an Unmanned Aerial Vehicle (UAV) Collected High Density Structure from Motion Point Cloud. Remote Sensing **5**:2164-2183.

McNamara, N. P., T. Plant, S. Oakley, S. Ward, C. Wood, and N. Ostle. 2008. Gully hotspot contribution to landscape methane (CH_4) and carbon dioxide (CO_2) fluxes in a northern peatland. Science of The Total Environment **404**:354-360.

Merryfield, D. L. 1977. Palynological and Stratigraphical studies on Exmoor. Unpublished. Kings College, London.

Metcalfe, D. B., R. A. Fisher, and D. A. Wardle. 2011. Plant communities as drivers of soil respiration: pathways, mechanisms, and significance for global change. Biogeosciences **8**:2047-2061.

Migliavacca, M., M. Galvagno, E. Cremonese, M. Rossini, M. Meroni, O. Sonnentag, S. Cogliati, G. Manca, F. Diotri, L. Busetto, A. Cescatti, R. Colombo, F. Fava, U. Morra di Cella, E. Pari, C. Siniscalco, and A. D. Richardson. 2011. Using digital repeat photography and eddy covariance data to model grassland phenology and photosynthetic CO_2 uptake. Agricultural and Forest Meteorology **151**:1325-1337.

Milligan, A. L., P. D. Putwain, and R. H. Marrs. 1999. A laboratory assessment of the relative susceptibility of Molinia caerulea (L.) Moench and Calluna vulgaris (L.) Hull to a range of herbicides. Annals of Applied Biology **135**:503-508.

Mills, J., C. Short, J. Ingram, B. Griffiths, J. Dwyer, L. McEwen, F. Chambers, and G. Kirkham. 2010. Review of the Exmoor Mires Restoration Project. Countryside and Community Research Institute.

Minkkinen, K., J. Laine, H. Nykänen, and P. J. Martikainen. 1997. Importance of drainage ditches in emissions of methane from mires drained for forestry. Canadian Journal of Forest Research **27**:949-952.

Mitchell, R. J., R. J. Rose, and S. C. F. Palmer. 2008. Restoration of Calluna vulgaris on grass-dominated moorlands: The importance of disturbance, grazing and seeding. Biological Conservation **141**:2100-2111.

Mizunuma, T., M. Wilkinson, E. L. Eaton, M. Mencuccini, J. I. L. Morison, and J. Grace. 2013. The relationship between carbon dioxide uptake and canopy colour from two camera systems in a deciduous forest in southern England. Functional Ecology **27**:196-207.

Mkhabela, M. S., P. Bullock, S. Raj, S. Wang, and Y. Yang. 2011. Crop yield forecasting on the Canadian Prairies using MODIS NDVI data. Agricultural and Forest Meteorology **151**:385-393.

Moore, P. D. 1987. Ecological and hydrological aspects of peat formation. Geological Society, London, Special Publications **32**:7-15.

Moore, T. R., P. M. Lafleur, D. M. I. Poon, B. W. Heumann, J. W. Seaquist, and N. T. Roulet. 2006. Spring photosynthesis in a cool temperate bog. Global Change Biology **12**:2323-2335.

Morgan, J. L., S. E. Gergel, and N. C. Coops. 2010. Aerial Photography: A Rapidly Evolving Tool for Ecological Management. BioScience **60**:47-59.

Morsdorf, F., B. Koetz, E. Meier, K. Itten, and B. Allgöwer. 2006. Estimation of LAI and Fractional Cover from Small Footprint Airborne Laser Scanning Data Based on Gap Fraction. Remote Sensing of Environment **104**:50-61.

Motohka, T., K. N. Nasahara, H. Oguma, and S. Tsuchida. 2010. Applicability of Green-Red Vegetation Index for Remote Sensing of Vegetation Phenology. Remote Sensing **2**:2369-2387.

Muraoka, H. and H. Koizumi. 2005. Photosynthetic and structural characteristics of canopy and shrub trees in a cool-temperate deciduous broadleaved forest: Implication to the ecosystem carbon gain. Agricultural and Forest Meteorology **134**:39-59.

Murphy, M. and T. Moore. 2010. Linking root production to aboveground plant characteristics and water table in a temperate bog. Plant and Soil **336**:219-231.

Murray, K. J., P. C. Harley, J. Beyers, H. Walz, and J. D. Tenhunen. 1989. Water content effects on photosynthetic response of Sphagnum mosses from the foothills of the Philip Smith Mountains, Alaska. Oecologia **79**:244-250.

NASA. 2012. MODIS Land Team Validation. NASA Goddard Space Flight Center.

Natural England. 2010. Englands Peatlands, Carbon storage and greenhouse gasses. Natural England, London.

Nieveen, J. P. and A. F. G. Jacobs. 2002. Behaviour of carbon dioxide and water vapour flux densities from a disturbed raised peat bog. International Journal of Climatology **22**:1543-1556.

Nieveen, J. P., C. M. J. Jacobs, and A. F. G. Jacobs. 1998. Diurnal and seasonal variation of carbon dioxide exchange from a former true raised bog. Global Change Biology **4**:823-833.

Nilsson, M., J. Sagerfors, I. Buffam, H. Laudon, T. Eriksson, A. Grelle, L. Klemedtsson, P. Weslien, and A. Lindroth. 2008. Contemporary carbon accumulation in a boreal oligotrophic minerogenic mire–A significant sink after accounting for all C-fluxes. Global Change Biology **14**:2317-2332.

Norman, J., C. Kucharik, S. Gower, D. Baldocchi, P. Crill, M. Rayment, K. Savage, and R. Striegl. 1997. A comparison of six methods for measuring soil surface carbon dioxide fluxes. Journal of Geophysical Research: Atmospheres (1984–2012) **102**:28771-28777.

Oechel, W. C., G. L. Vourlitis, S. J. Hastings, R. P. Ault, and P. Bryant. 1998. The effects of water table manipulation and elevated temperature on the net CO_2 flux of wet sedge tundra ecosystems. Global Change Biology **4**:77-90.

Ordnance Survey. 2008a. Coastline [Shapefile geospatial data], Coverage Great Britain. EDINA Digimap, Ordnance Survey Service.

Ordnance Survey. 2008b. OS Meridian 2 [NTF geospatial data], Scale: 1:10,000, Tile: SS73ne, . EDINA Digimap Ordnance Survey Service, Edinburgh.

Ordnance Survey. 2008c. OS Meridian 2 [NTF geospatial data], Scale: 1:10,000, Tile: SS73nw, . EDINA Digimap Ordnance Survey Service, Edinburgh.

Ordnance Survey. 2008d. OS Meridian 2 [NTF geospatial data], Scale: 1:25,000, Tile: SS73. EDINA Digimap Ordnance Survey Service, Edinburgh.

Ordnance Survey. 2008e. OS Meridian 2 [NTF geospatial data], Scale: 1:50,000, Tile: SS62ne, . EDINA Digimap Ordnance Survey Service, Edinburgh.

Otieno, D. O., M. Wartinger, A. Nishiwaki, M. Z. Hussain, J. Muhr, W. Borken, and G. Lischeid. 2009. Responses of CO_2 Exchange and Primary Production of the Ecosystem Components to Environmental Changes in a Mountain Peatland. Ecosystems **12**:590-603.

Parihar, S., S. Goroshi, R. P. Singh, N. S. R. Krishnayya, M. B. Sirsayya, A. Kumar, L. S. Rawat, and A. Sonakia. 2013. Observation of forest phenology using field-based digital photography and satellite data. Current Science **105**:1740-1747.

Parry, L. E., J. Holden, and P. J. Chapman. 2014. Restoration of blanket peatlands. Journal of Environmental Management **133**:193-205.

Peacock, M., T. G. Jones, B. Airey, A. Johncock, C. D. Evans, I. Lebron, N. Fenner, and C. Freeman. 2015. The effect of peatland drainage and rewetting (ditch blocking) on extracellular enzyme activities and water chemistry. Soil Use and Management **31**:67-76.

Pellerin, S., L.-A. Lagneau, M. Lavoie, and M. Larocque. 2009. Environmental factors explaining the vegetation patterns in a temperate peatland. Comptes Rendus Biologies **332**:720-731.

Pezeshki, S. R. 2001. Wetland plant responses to soil flooding. Environmental and Experimental Botany **46**:299-312.

Piao, S., J. Fang, P. Ciais, P. Peylin, Y. Huang, S. Sitch, and T. Wang. 2009. The carbon balance of terrestrial ecosystems in China. Nature **458**:1009-1013.

Polley, H. W., W. Emmerich, J. A. Bradford, P. L. Sims, D. A. Johnson, N. Z. Saliendra, T. Svejcar, R. Angell, A. B. Frank, R. L. Phillips, K. A. Snyder, and J. A. Morgan. 2010. Physiological and environmental regulation of interannual variability in CO_2 exchange on rangelands in the western United States. Global Change Biology **16**:990-1002.

Pumpanen, J., P. Kolari, H. Ilvesniemi, K. Minkkinen, T. Vesala, S. Niinisto, A. Lohila, T. Larmola, M. Morero, M. Pihlatie, I. Janssens, J. C. Yuste, J. M. Grunzweig, S. Reth, J. A. Subke, K. Savage, W. Kutsch, G. Ostreng, W. Ziegler, P. Anthoni, A. Lindroth, and P. Hari. 2004. Comparison of different chamber techniques for measuring soil CO_2 efflux. Agricultural and Forest Meteorology **123**:159-176.

Raich, J. and W. H. Schlesinger. 1992. The global carbon dioxide flux in soil respiration and its relationship to vegetation and climate. Tellus B **44**:81-99.

Ramírez, D. A., F. Valladares, A. Blasco, and J. Bellot. 2006. Assessing transpiration in the tussock grass Stipa tenacissima L.: the crucial role of the interplay between morphology and physiology. Acta Oecologica **30**:386-398.

Ramsar Convention. 1971. Strategic Framework and guidelines for the future development of the List of Wetlands of International Importance of the Convention on Wetlands (Ramsar, Iran, 1971) - paragraph 136. http://archive.ramsar.org/cda/en/ramsar-documents-guidelines-strategic-framework-and/main/ramsar/1-31-105%5E20823_4000_0 [Acessed 11/02/2015].

Ratcliffe, D. and P. Oswald. 1988. The flow country; the peatlands of Caithness and Sutherland. Nature Conservancy Council, Peterborough.

Reed, M. S., A. Bonn, C. D. Evans, H. Joosten, C. Bain, J. Farmer, I. Emmer, J. Couwenberg, A. Moxey, R. R. E. Artz, F. Tanneberger, M. VonUnger, M. Smyth, R. Birnie, I. Inman, S. Smith, T. Quick, C. Cowap, and S. Prior. 2013. Peatland Code research project. Final Report., DEFRA, London.

Reichstein, M., E. Falge, D. Baldocchi, D. Papale, M. Aubinet, P. Berbigier, C. Bernhofer, N. Buchmann, T. Gilmanov, and A. Granier. 2005. On the separation of net ecosystem exchange into assimilation and ecosystem respiration: review and improved algorithm. Global Change Biology **11**:1424-1439.

Richardson, A. D., J. P. Jenkins, B. H. Braswell, D. Y. Hollinger, S. V. Ollinger, and M.-L. Smith. 2007. Use of digital webcam images to track spring green-up in a deciduous broadleaf forest. Oecologia **152**:323-334.

Richardson, A. D., T. F. Keenan, M. Migliavacca, Y. Ryu, O. Sonnentag, and M. Toomey. 2013. Climate change, phenology, and phenological control of vegetation feedbacks to the climate system. Agricultural and Forest Meteorology **169**:156-173.

Rietkerk, M. and J. van de Koppel. 2008. Regular pattern formation in real ecosystems. Trends in Ecology & Evolution **23**:169-175.

Riutta, T., J. Laine, M. Aurela, J. Rinne, T. Vesala, T. Laurila, S. Haapanala, M. Pihlatie, and E. S. Tuittila. 2007. Spatial variation in plant community functions regulates carbon gas dynamics in a boreal fen ecosystem. Tellus Series B-Chemical and Physical Meteorology **59**:838-852.

Rodwell, J. 1991. British Plant Communities: Mires and heaths. 2nd edition. Cambridge University Press, Cambridge.

Ross, S., H. Adamson, and A. Moon. 2003. Evaluating management techniques for controlling Molinia caerulea and enhancing Calluna vulgaris on upland wet heathland in northern England, UK. Agriculture, Ecosystems & Environment **97**:39-49.

Rossini, M., S. Cogliati, M. Meroni, M. Migliavacca, M. Galvagno, L. Busetto, E. Cremonese, T. Julitta, C. Siniscalco, U. Morra di Cella, and R. Colombo. 2012. Remote sensing-based estimation of gross primary production in a subalpine grassland. Biogeosciences **9**:2565-2584.

Rosso, P. H., S. L. Ustin, and A. Hastings. 2003. Use of lidar to produce high resolution marsh vegetation and terrain maps.*in* Three Dimensional Mapping from InSAR and LIDAR Workshop, International Society for Photogrammetry and Remote Sensing, Portland, Oregon.

Roulet, N. T., P. M. Lafleur, P. J. H. Richard, T. R. Moore, E. R. Humphreys, and J. Bubier. 2007. Contemporary carbon balance and late Holocene carbon accumulation in a northern peatland. Global Change Biology **13**:397-411.

Rowson, J. G., H. S. Gibson, F. Worrall, N. Ostle, T. P. Burt, and J. K. Adamson. 2010. The complete carbon budget of a drained peat catchment. Soil Use and Management **26**:261-273.

Rowson, J. G., F. Worrall, and M. G. Evans. 2013. Predicting soil respiration from peatlands. Science of The Total Environment **442**:397-404.

Rutter, A. J. 1955. The Composition of Wet-Heath Vegetation in Relation to the Water-Table. Journal of Ecology **43**:507-543.

Sagerfors, J., A. Lindroth, A. Grelle, L. Klemedtsson, P. Weslien, and M. Nilsson. 2008. Annual CO_2 exchange between a nutrient-poor, minerotrophic, boreal mire and the atmosphere. Journal of Geophysical Research: Biogeosciences (2005–2012) **113**.

Saigusa, N., S. Yamamoto, S. Murayama, and H. Kondo. 2005. Inter-annual variability of carbon budget components in an AsiaFlux forest site estimated by long-term flux measurements. Agricultural and Forest Meteorology **134**:4-16.

Saitoh, T. M., S. Nagai, N. Saigusa, H. Kobayashi, R. Suzuki, K. N. Nasahara, and H. Muraoka. 2012. Assessing the use of camera-based indices for characterizing canopy phenology in relation to gross primary production in a deciduous broad-leaved and an evergreen coniferous forest in Japan. Ecological Informatics **11**:45-54.

Salamí, E., C. Barrado, and E. Pastor. 2014. UAV Flight Experiments Applied to the Remote Sensing of Vegetated Areas. Remote Sensing **6**:11051-11081.

Samaritani, E., A. Siegenthaler, M. Yli-Petays, A. Buttler, P. A. Christin, and E. A. D. Mitchell. 2011. Seasonal Net Ecosystem Carbon Exchange of a Regenerating Cutaway Bog: How Long Does it Take to Restore the C-Sequestration Function? Restoration Ecology **19**:480-489.

Schneider, J., L. Kutzbach, and M. Wilmking. 2012. Carbon dioxide exchange fluxes of a boreal peatland over a complete growing season, Komi Republic, NW Russia. Biogeochemistry **111**:485-513.

Schouwenaars, J. M. 1993. Hydrological Differences Between Bogs and Bog-Relicts and Consequences for Bog Restoration. Hydrobiologia **265**:217-224.

Schubert, P., L. Eklundh, M. Lund, and M. Nilsson. 2010. Estimating northern peatland CO_2 exchange from MODIS time series data. Remote Sensing of Environment **114**:1178-1189.

Shaver, G. R., L. E. Street, E. B. Rastetter, M. T. Van Wijk, and M. Williams. 2007. Functional convergence in regulation of net CO_2 flux in heterogeneous tundra landscapes in Alaska and Sweden. Journal of Ecology **95**:802-817.

Silvola, J., J. Alm, U. Ahlholm, H. Nykanen, and P. J. Martikainen. 1996a. CO_2 fluxes from peat in boreal mires under varying temperature and moisture conditions. Journal of Ecology **84**:219-228.

Silvola, J., J. Alm, U. Ahlholm, H. Nykanen, and P. J. Martikainen. 1996b. The contribution of plant roots to CO_2 fluxes from organic soils. Biology and Fertility of Soils **23**:126-131.

Sjörs, H. 1980. Peat on Earth: Multiple Use or Conservation? Ambio **9**:303-308.

Sjöström, M., J. Ardö, A. Arneth, N. Boulain, B. Cappelaere, L. Eklundh, A. de Grandcourt, W. L. Kutsch, L. Merbold, Y. Nouvellon, R. J. Scholes, P. Schubert, J. Seaquist, and E. M. Veenendaal. 2011. Exploring the potential of MODIS EVI for modeling gross primary production across African ecosystems. Remote Sensing of Environment **115**:1081-1089.

Smith, J. 2003. Fluxes of carbon dioxide and water vapour at a Waikato peat bog. University of Waikato.

Snavely, N., D. Seitz, and R. Szeliski. 2008. Modelling the world from internet photo collections. International Journal of Computer Vision **80**:189-210.

Soini, P., T. Riutta, M. Yli-Petays, and H. Vasander. 2010. Comparison of Vegetation and CO_2 Dynamics Between a Restored Cut-Away Peatland and a Pristine Fen: Evaluation of the Restoration Success. Restoration Ecology **18**:894-903.

Sonnentag, O., K. Hufkens, C. Teshera-Sterne, A. M. Young, M. Friedl, B. H. Braswell, T. Milliman, J. O'Keefe, and A. D. Richardson. 2012. Digital repeat photography for phenological research in forest ecosystems. Agricultural and Forest Meteorology **152**:159-177.

Sottocornola, M. and G. Kiely. 2005. An Atlantic blanket bog is a modest CO_2 sink. Geophysical Research Letters **32**:L23804.

Sottocornola, M. and G. Kiely. 2010. Hydro-meteorological controls on the CO_2 exchange variation in an Irish blanket bog. Agricultural and Forest Meteorology **150**:287-297.

Spieksma, J. F. M., E. J. Moors, A. J. Dolman, and J. M. Schouwenaars. 1997. Modelling evaporation from a drained and rewetted peatland. Journal of Hydrology **199**:252-271.

Stewart, A. J. A. and A. N. Lance. 1983. Moor-Draining - A Review of Impacts on Land-Use. Journal of Environmental Management **17**:81-99.

Straatsma, M. and H. Middelkoop. 2007. Extracting structural characteristics of herbaceous floodplain vegetation under leaf-off conditions using airborne laser scanner data. International Journal of Remote Sensing **28**:2447-2467.

Strack, M., J. Waddington, L. Rochefort, and E. S. Tuittila. 2006. Response of vegetation and net ecosystem carbon dioxide exchange at different peatland microforms following water table drawdown. Journal of Geophysical Research: Biogeosciences (2005–2012) **111**.

Strack, M. and Y. Zuback. 2013. Annual carbon balance of a peatland 10 yr following restoration. Biogeosciences **10**:2885-2896.

Straková, P., R. M. Niemi, C. Freeman, K. Peltoniemi, H. Toberman, I. Heiskanen, H. Fritze, and R. Laiho. 2011a. Litter type affects the activity of aerobic decomposers in a boreal peatland more than site nutrient and water table regimes. Biogeosciences **8**:2741-2755.

Straková, P., T. Penttilä, J. Laine, and R. Laiho. 2011b. Disentangling direct and indirect effects of water table drawdown on above- and belowground plant litter decomposition: consequences for accumulation of organic matter in boreal peatlands. Global Change Biology **18**:322-335.

Street, L. E., G. R. Shaver, M. Williams, and M. T. Van Wijk. 2007. What is the relationship between changes in canopy leaf area and changes in photosynthetic CO_2 flux in arctic ecosystems? Journal of Ecology **95**:139-150.

Studer, S., R. Stöckli, C. Appenzeller, and P. Vidale. 2007. A comparative study of satellite and ground-based phenology. International Journal of Biometeorology **51**:405-414.

Subke, J.-A., I. Inglima, and M. F. Cotrufo. 2006. Trends and methodological impacts in soil CO_2 efflux partitioning: A metaanalytical review. Global Change Biology **12**:921-943.

Svensson, B. H. 1980. Carbon Dioxide and Methane Fluxes from the Ombrotrophic Parts of a Subarctic Mire. Ecological Bulletins:235-250.

Tallis, J. 1997. The southern Pennine experience: an overview of blanket mire degradation. Pages 7-15 *in* J. Tallis, R. Meade, and P. D. Hulme, editors. Blanket Mire Degradation-Causes, Consequences and Challenges. Proceedings of a conference at University of Manchester, 9-11 April, 1979. The Macaulay Land Use Research Institute on behalf of the Mires Research Group., Aberdeen.

Tarvainen, O., A. M. Laine, M. Peltonen, and A. Tolvanen. 2013. Mineralization and Decomposition Rates in Restored Pine Fens. Restoration Ecology **21**:592-599.

Taylor, K., A. P. Rowland, and H. E. Jones. 2001. Molinia caerulea (L.) Moench. Journal of Ecology **89**:126-144.

Teh, Y. A., W. Silver, O. Sonnentag, M. Detto, M. Kelly, and D. Baldocchi. 2011. Large Greenhouse Gas Emissions from a Temperate Peatland Pasture. Ecosystems **14**:311-325.

Testa, S., E. C. B. Mondino, and C. Pedroli. 2014. Correcting MODIS 16-day composite NDVI time-series with actual acquisition dates. European Journal of Remote Sensing **47**:285-305.

Thormann, M. N., A. R. Szumigalski, and S. E. Bayley. 1999. Aboveground peat and carbon accumulation potentials along a bog-fen-marsh wetland gradient in southern boreal Alberta, Canada. Wetlands **19**:305-317.

Tomlinson, R. W. 2010. Changes in the extent of peat extraction in Northern Ireland 1990–2008 and associated changes in carbon loss. Applied Geography **30**:294-301.

Tucker, C. J. 1979. Red and photographic infrared linear combinations for monitoring vegetation. Remote Sensing of Environment **8**:127-150.

Tucker, G. 2003. Review of the Impacts of Heather and Grassland Burning in the Uplands on Soils, Hydrology and Biodiversity. English Nature.

Tuittila, E. S., V. M. Komulainen, H. Vasander, and J. Laine. 1999. Restored cut-away peatland as a sink for atmospheric CO_2. Oecologia **120**:563-574.

Turner, D., A. Lucieer, and C. Watson. 2012. An Automated Technique for Generating Georectified Mosaics from Ultra-High Resolution Unmanned Aerial Vehicle (UAV) Imagery, Based on Structure from Motion (SfM) Point Clouds. Remote Sensing **4**:1392-1410.

Turner, M. G. 1989. Landscape ecology: the effect of pattern on process. Annual review of ecology and systematics:171-197.

UK Meteorological Office. 2012. Met Office Integrated Data Archive System (MIDAS) Land and Marine Surface Stations Data (1853-current). NCAS British Atmospheric Data Centre.

UK Meteorological Office. 2015. Meteorological Office Climate Summaries for Southwest England and South Wales. UK Meteorological Office.

Updegraff, K., S. D. Bridgham, J. Pastor, P. Weishampel, and C. Harth. 2001. Response of CO_2 and CH_4 emissions from peatlands to warming and water table manipulation. Ecological Applications **11**:311-326.

Updegraff, K., J. Pastor, S. D. Bridgham, and C. A. Johnston. 1995. Environmental and substrate controls over carbon and nitrogen mineralization in northern wetlands. Ecological Applications **5**:151-163.

Urbanová, Z., T. Picek, T. Hájek, I. Bufková, and E.-S. Tuittila. 2012. Vegetation and carbon gas dynamics under a changed hydrological regime in central European peatlands. Plant Ecology & Diversity **5**:89-103.

Urbanová, Z., T. Picek, and E. Tuittila. 2013. Sensitivity of carbon gas fluxes to weather variability on pristine, drained and rewetted temperate bogs. Mires and Peat **11**:4.

Vermote, E. F. and A. Vermeulen. 1999. Algorithm Technical Background Document; Atmospheric Correction Algorithm:Spectral Reflectances (MOD09). NASA contract NAS5-96062. Version 4.0. University of Maryland, Department of Geography, Maryland.

Vierling, K. T., L. A. Vierling, W. A. Gould, S. Martinuzzi, and R. M. Clawges. 2008. Lidar: shedding new light on habitat characterization and modeling. Frontiers in Ecology and the Environment **6**:90-98.

Vivoni, E. R., A. Rango, C. A. Anderson, N. A. Pierini, A. P. Schreiner-McGraw, S. Saripalli, and A. S. Laliberte. 2014. Ecohydrology with unmanned aerial vehicles. Ecosphere **5**:art130.

Waddington, J. M., P. J. Morris, N. Kettridge, G. Granath, D. K. Thompson, and P. A. Moore. 2015. Hydrological feedbacks in northern peatlands. Ecohydrology **8**:113-127.

Waddington, J. M., M. Strack, and M. J. Greenwood. 2010. Toward restoring the net carbon sink function of degraded peatlands: Short-term response in CO_2 exchange to ecosystem-scale restoration. Journal of Geophysical Research: Biogeosciences **115**:G01008.

Wallace, L., A. Lucieer, C. Watson, and D. Turner. 2012. Development of a UAV-LiDAR system with application to forest inventory. Remote Sensing **4**:1519-1543.

Wallen, B. 1993. Methods for studying below-ground production in mire ecosystems. Suo (Helsinki) **43**:155-162.

Wang, C., M. Meneti, M.-P. Stoll, A. Feola, E. Belluco, and M. Marani. 2009. Separation of Ground and Low Vegetation Signatures in LiDAR Measurements of Salt-Marsh Environments. Institute of Electrical and Electronics Engineers, New York, USA.

Wang, T., L. Yan, and P. Mooney. 2011. Dense point cloud extraction from UAV captured images in forest area. Pages 389-392 *in* Spatial Data Mining and Geographical Knowledge Services (ICSDM), 2011 IEEE International Conference on.

Ward, S. E., R. D. Bardgett, N. P. McNamara, and N. J. Ostle. 2009. Plant functional group identity influences short-term peatland ecosystem carbon flux: evidence from a plant removal experiment. Functional Ecology **23**:454-462.

Weiss, M. 2010. CAN-EYE V6.2.*in* I. n. d. l. r. agronomique, editor. Institut national de la recherche agronomique.

Westergaard-Nielsen, A., M. Lund, B. U. Hansen, and M. P. Tamstorf. 2013. Camera derived vegetation greenness index as proxy for gross primary production in a low Arctic wetland area. ISPRS Journal of Photogrammetry and Remote Sensing **86**:89-99.

Westoby, M. J., J. Brasington, N. F. Glasser, M. J. Hambrey, and J. M. Reynolds. 2012. 'Structure-from-Motion' photogrammetry: A low-cost, effective tool for geoscience applications. Geomorphology **179**:300-314.

Wilson, D., J. Alm, T. Riutta, J. Laine, and K. A. Byrne. 2007. A high resolution green area index for modelling the seasonal dynamics of CO_2 exchange in peatland vascular plant communities. Plant Ecology **190**:37-51.

Wilson, L., J. Wilson, J. Holden, I. Johnstone, A. Armstrong, and M. Morris. 2010. Recovery of water tables in Welsh blanket bog after drain blocking: Discharge rates, time scales and the influence of local conditions. Journal of Hydrology **391**:377-386.

Wilson, L., J. Wilson, J. Holden, I. Johnstone, A. Armstrong, and M. Morris. 2011. Ditch blocking, water chemistry and organic carbon flux: Evidence that blanket bog restoration reduces erosion and fluvial carbon loss. Science of The Total Environment **409**:2010-2018.

Wohlfahrt, G., A. Hammerle, A. Haslwanter, M. Bahn, U. Tappeiner, and A. Cernusca. 2008. Seasonal and inter-annual variability of the net ecosystem CO_2 exchange of a temperate mountain grassland: Effects of weather and management. Journal of Geophysical Research: Atmospheres **113**:n/a-n/a.

Worrall, F., T. P. Burt, J. G. Rowson, J. Warburton, and J. K. Adamson. 2009. The multi-annual carbon budget of a peat-covered catchment. Science of The Total Environment **407**:4084-4094.

Wu, C. 2007. SiftGPU: A GPU implementation of Scale Invaraint Feature Transform (SIFT)", http://cs.unc.edu/~ccwu/siftgpu, Acessed 19/02/2013.

Wu, C. 2011. Visualsfm: A visual structure from motion system, http://ccwu.me/vsfm/, Acessed 19/02/2013.

Wu, C., S. Agarwal, B. Curless, and S. M. Seitz. 2011. Multicore Bundle Adjustment, CVPR 2011.

Yallop, A. R., J. I. Thacker, G. Thomas, M. Stephens, B. Clutterbuck, T. Brewer, and C. A. D. Sannier. 2006. The extent and intensity of management burning in the English uplands. Journal of Applied Ecology **43**:1138-1148.

Yu, Z., J. Loisel, D. P. Brosseau, D. W. Beilman, and S. J. Hunt. 2010. Global peatland dynamics since the Last Glacial Maximum. Geophysical Research Letters **37**:L13402.

Zhang, X., M. A. Friedl, and C. B. Schaaf. 2009. Sensitivity of vegetation phenology detection to the temporal resolution of satellite data. International Journal of Remote Sensing **30**:2061-2074.

Zhang, X., M. A. Friedl, C. B. Schaaf, A. H. Strahler, J. C. F. Hodges, F. Gao, B. C. Reed, and A. Huete. 2003. Monitoring vegetation phenology using MODIS. Remote Sensing of Environment **84**:471-475.

Zhou, L., H.-l. He, X.-m. Sun, L. Zhang, G.-r. Yu, X.-l. Ren, J.-y. Wang, and F.-h. Zhao. 2013. Modeling winter wheat phenology and carbon dioxide fluxes at the ecosystem scale based on digital photography and eddy covariance data. Ecological Informatics **18**:69-78.